AIX-MARSEILLE UNIVERSITÉ

THÈSE

présentée pour obtenir le grade de

DOCTEUR AIX MARSEILLE UNIVERSITÉ
délivré par l'Université de Provence

Spécialité : Mathématiques

par

Sébastien Benzekry

sous la direction de Dominique BARBOLOSI, Assia BENABDALLAH et Florence HUBERT

Titre :

Modélisation et analyse mathématique de thérapies anti-cancéreuses pour les cancers métastatiques

---

soutenue publiquement le 10 novembre 2011

JURY

Nicolas ANDRÉ	CHU - Timone	Examinateur
Dominique BARBOLOSI	Université Paul Cézanne	Directeur
Assia BENABDALLAH	Université de Provence	Directrice
Daniel BENNEQUIN	Université Pierre et Marie Curie	Examinateur
Gilles FREYER	Université Lyon 1	Rapporteur
Emmanuel GRENIER	ENS Lyon	Examinateur
Philip HAHNFELDT	CCSB - St Elizabeth's Medical Center	Rapporteur
Florence HUBERT	Université de Provence	Directrice
Benoît PERTHAME	Université Pierre et Marie Curie	Rapporteur

Remerciements

Je voudrais remercier en premier lieu mes trois directeurs Dominique Barbolosi, Assia Benabdallah et Florence Hubert pour tout ce qu'ils m'ont apporté durant ces trois années. Ce fut un réel bonheur d'être sous leur direction. Grâce à eux j'ai pu apprendre beaucoup dans plusieurs domaines scientifiques et bénéficier d'un sujet de thèse passionnant. Je tiens particulièrement à les remercier pour leurs grandes qualités humaines, m'offrant continuellement un soutien indéfectible qui m'a permis d'être un thésard épanoui.

Je tiens ensuite à remercier Benoît Perthame qui m'a fait l'honneur de rapporter sur ma thèse. Il a été présent durant toute ma formation mathématique et je suis très heureux qu'il le soit encore alors que celle-ci s'achève, d'autant plus que mon orientation vers les mathématiques appliquées à la biologie lui doit beaucoup. Merci aussi à Philip Hahnfeldt pour avoir rédigé un rapport sur ma thèse et pour l'intérêt qu'il porte à mes travaux. Mon sujet de thèse lui est redevable car il est basé en grande partie sur ses travaux. Merci enfin à Gilles Freyer d'avoir accepté de rapporter sur ma thèse bien qu'une grande partie ne lui soit pas familière. Je tiens à remercier ces trois rapporteurs pour les remarques pertinentes qu'ils ont formulées dans leurs rapports.

Mes remerciements se portent ensuite vers Nicolas André, Daniel Bennequin, Thierry Colin et Emmanuel Grenier qui me font l'honneur de faire partie du jury.

Merci aussi à Franck Boyer pour ses remarques, commentaires ainsi que pour sa disponibilité à répondre à toute question. Merci aussi à Benjamin Ribba et Olivier Saut. Je souhaite aussi remercier Joseph Ciccolini du laboratoire de pharmacocinétique pour son aide et ses orientations précieuses en matière de pharmacologie.

Merci à mes parents, sans qui je ne serais rien. Merci pour m'avoir amené dans ce monde et merci pour votre amour. Cette thèse n'existerait pas si vous ne m'aviez pas transmis la curiosité et le goût de la connaissance. Je remercie aussi mon frère pour son intelligence et son talent.

Gracias a vos Matí por tu amistad y por todo lo que me apprendiste matemáticamente. Las pruebas de esta tesis te agradecen mucho ! Gracias por tu vision de las matemáticas y por haberme iniciado un poquito a la belleza de la geometria. Merci à toi Fédé, qui m'accueillit et m'introduisit à la vie marseillaise avec beaucoup de générosité. Merci à tous les doctorants du LATP avec qui j'ai passé tant de repas gastronomiques au resto U et qui ont supporté trois ans durant mes coups de gueule politiques et mes épanchements sur mes étudiant(e)s. Merci à Clément, Ismaël, Lionel, François, Thomas, Mamadou et Boubakar. Je garderai gravées en moi à jamais les heures glorieuses du CMI foot ! Et merci à Flore d'être récemment venue apporter un peu de féminité à la troupe. Merci aussi à Valérie pour sa gentillesse, sa compétence et son efficacité.

Je souhaite aussi remercier les doctorants en maths-bio croisés un peu partout de par le monde et qui permirent de rendre les échanges au cours des congrès et autres conférences un peu moins formels. Merci Pierre, avec le souhait qu'un jour nous travaillions ensemble, Floriane, Erwan, Sepideh, Alexis, Pietro et tous ceux pour lesquels ma mémoire fait défaut. Grâce à vous, j'ai pu apprendre beaucoup de maths sous un angle moins académique.

Merci à toi Marseille ! Pour ton âme, ton coeur et ton soleil. Et merci aux marseillais et marseillaises de m'avoir trimbalé partout dans cette ville et dans la région. Cela fut aussi important

Enfin, merci à toi lecteur d'avoir ouvert cette thèse. En espérant que la lecture te sera agréable, je te souhaite un bon voyage !

All models are wrong, but some are useful.
George E. P. Box

S'il n'y avait pas la science [...] combien d'entre nous pourraient profiter de leur cancer pendant plus de cinq ans ?
P. Desproges

Contents

Partie II   Analyse mathématique et numérique   **69**

Chapter 3

Study of the space $W^p_{\mathrm{div}}(\Omega)$

Chapter 4

Autonomous case. Model without treatment

Journal of Evolution Equations, Vol. 11 No. 1 (2011)**, [Ben11a]**

Chapter 5

Non autonomous case. Theoretical and numerical analysis

to appear in *Mathematical Modeling and Numerical Analysis***, [Ben11b]**

Chapter 6

2D-1D Limit

to appear in *Journal of Biological Dynamics***, [Ben11c]**

Partie III   Applications médicales   155

Chapter 7

Simulation results

to appear in *Mathematical Modeling of Natural Phenomena*, **[BAB⁺11]**

Chapter 8

An optimal control problem for the metastases

in preparation, **[BB11]**

List of Figures

List of Tables

Introduction

En France, le cancer est devenu la première cause de mortalité. Malgré les efforts déployés, le taux de survie à 5 ans après diagnostic tous cancers confondus est de 52%[2], ce qui témoigne de l'importance d'améliorer les thérapies anti-cancéreuses existantes (ce chiffre cache cependant une grande disparité selon le type de cancer). Une explication de la difficulté à traiter le cancer est donnée par R. Weinberg dans [Wei07] : "Les métastases sont la cause de décès principale d'une maladie cancéreuse" (traduit de l'anglais). La classification duale du cancer en tant que maladie localisée ou métastatique est un des points clé dans l'élaboration de la thérapie pour un patient donné. Néanmoins, plusieurs études révèlent qu'une partie des pathologies diagnostiquées localisées sont en fait déjà métastatiques. Il y a probablement un *continuum* entre ces deux états.

L'arsenal classique du clinicien dans sa lutte contre le cancer s'oriente principalement autour de trois axes : chirurgie, chimiothérapie et radiothérapie. Suite à la découverte de l'angiogénèse tumorale par J. Folkman dans les années 1970, processus par lequel une tumeur est capable de stimuler le développement du réseau vasculaire environnant, une quatrième voie thérapeutique s'est ajoutée : cibler l'angiogénèse pour priver la tumeur d'accès aux nutriments et ainsi l'étouffer. Ce n'est cependant qu'au début du siècle actuel que sont arrivées les premières molécules anti-angiogéniques. Malgré l'espoir que ces nouvelles thérapies (dites "ciblées") suscitèrent, notamment dû à leur faible toxicité comparée à celle des chimiothérapies, les résultats ne sont pas à la hauteur et ces médicaments ne sont administrés qu'en combinaison avec un cytotoxique classique. Notre conviction est qu'une meilleure conception des protocoles temporels d'administration des traitements peut améliorer cette situation.

Face à ces constats, la modélisation mathématique peut apporter des éléments d'aide au diagnostic ainsi qu'à la décision thérapeutique. En effet, l'évolution d'un cancer est un processus dynamique qu'une bonne description mathématique peut permettre d'aider à contrôler. Un modèle mathématique peut permettre d'individualiser la thérapie en prenant en compte la variabilité pharmacocinétique, pharmacodynamique et pharmacogénomique au sein de la population. Par ailleurs, la modélisation mathématique peut permettre de mieux comprendre la répartition spatiale du réseau vasculaire et ses interactions avec les différents agents thérapeutiques, par

---

[2]rapport d'avril 2010 de l'Institut National du Cancer, disponible à l'adresse http ://www.e-cancer.fr/component/docman/doc_download/4890-survie-attendue-des-patients-atteints-de-cancers-en-france–etat-des-lieux

exemple dans le cadre des effets complexes de combinaison des anti-angiogéniques et des chimiothérapies. La modélisation en cancérologie est un domaine important des mathématiques appliquées à l'heure actuelle au sein duquel on peut distinguer deux types d'approches, répondant à deux problématiques différentes. L'approche mécanistique s'attache à décrire en détail le cancer de manière à mieux comprendre la biologie de ce système complexe, faisant souvent intervenir plusieurs échelles (moléculaire, cellulaire, tissulaire,...). L'approche phénoménologique quant à elle cherche avant tout à décrire le phénomène à l'échelle globale de la tumeur, voire du cancer. Son but est le contrôle de la maladie et elle est plus proche de la médecine et de la clinique. Bien entendu, ces deux approches vont de pair et se nourrissent l'une de l'autre. En 2000, Iwata & al. proposèrent un modèle phénoménologique décrivant l'évolution métastatique traduisant cette idée de *continuum* entre cancer localisé et métastatique. Ce modèle a ensuite été repris et étudié dans [BBHV09, Ver10, DGL09], notamment en y intégrant l'effet d'un traitement par chimiothérapie. Parallèlement, Hahnfeldt & al. proposèrent dans [HPFH99] un modèle simple décrivant la croissance tumorale sous contrôle angiogénique. La présente thèse résulte de la combinaison de ces deux modèles de manière à avoir un outil mathématique s'intéressant à l'évolution métastatique capable de prendre en compte l'effet des deux principales thérapies chimiques disponibles : cytotoxiques et anti-angiogéniques.

Notre modèle est une équation aux dérivées partielles de type transport munie d'une condition aux limites non-locale, vérifiée par la densité ρ de métastases. Il s'écrit (voir chapitre 1 pour les détails de la modélisation ainsi que les notations et l'expression des coefficients)

$$\begin{cases} \partial_t \rho + \mathrm{div}(\rho G) = 0 &]0, T[\times \Omega \\ -G \cdot \nu(t, \sigma)\rho(t, \sigma) = N(\sigma)\left\{ \int_\Omega \beta(X)\rho(t, X)dX + \beta(X_p(t)) \right\} &]0, T[\times \partial\Omega \\ \rho(0) = \rho^0 & \Omega \end{cases} \quad (1)$$

Ce type de problème s'inscrit dans le domaine de la dynamique des populations structurées et le type particulier d'équation tel que (1) est parfois nommé équation de renouvellement. La variable de structure est ici bidimensionnelle $X = (x, \theta)$, x représentant la taille et θ la vascularisation d'une tumeur donnée. La dynamique globale de la solution de (1) résulte de deux phénomènes : croissance, représentée par le terme de transport avec vitesse G dans l'équation, et émission (naissance) de nouvelles tumeurs, caractérisée par le coefficient β et la condition aux limites faisant intervenir l'intégrale de la solution sur tout le domaine.

Dans le cas sans traitement, le champ G est autonome et s'annule en un coin de Ω, qui est un carré. Ce fait entraîne des difficultés techniques dans l'analyse de l'équation, notamment pour l'existence de trace pour une solution. La régularité naturelle de l'équation invite à considérer l'espace

$$W_{\mathrm{div}}(\Omega) = \left\{ V \in L^1(\Omega);\ \mathrm{div}(GV) \in L^1(\Omega) \right\}$$

dont une étude est faite au chapitre 3. Celle-ci repose principalement sur le redressement des trajectoires du champ G de manière à formaliser le fait que $G \cdot \nabla V$ représente la dérivation le long de ces trajectoires. Nous prouvons un théorème de conjugaison de $W_{\mathrm{div}}(\Omega)$ et de $W^{1,1}(]0, +\infty[; L^1(\partial\Omega))$ exprimant ce fait.

L'analyse fonctionnelle du chapitre 3 donne les bases nécessaires pour envisager le problème (1) (sans le terme source dans la condition aux limites) comme un problème d'évolution de la forme

$$\begin{cases} \frac{d}{dt}\rho = A\rho \\ \rho(0) = \rho^0 \end{cases}$$

lié à un opérateur $(A, D(A))$ dont nous effectuons une étude systématique au chapitre 4. Nous prouvons que $(A, D(A))$ engendre un semigroupe ce qui permet d'établir l'existence et l'unicité de la solution au problème (1), ainsi que d'en préciser la régularité. Les propriétés spectrales de $(A, D(A))$ sont aussi analysées et permettent de montrer que le comportement asymptotique de la solution de (1) est donné par

$$\rho(t) \sim_\Psi m_0 e^{\lambda_0 t} V \tag{2}$$

dans le cas sans source (le comportement asymptotique du cas avec source est aussi établi). Les fonctions V et Ψ sont respectivement les vecteurs propres direct et adjoint associés à la première valeur propre $\lambda_0 > 0$ de $(A, D(A))$, appelée paramètre de Malthus. Le comportement asymptotique se prouve naturellement dans l'espace $L^1(\Omega)$ muni du poids Ψ ce qui est traduit dans (2) par le symbole $\sim_\Psi$.

Dans le cas non-autonome (avec traitement), la même idée de redressement des caractéristiques est appliquée pour discrétiser le problème (1). Le schéma numérique qui en résulte, de type lagrangien car lié aux caractéristiques, est analysé au chapitre 5. Le passage à la limite sur les pas de discrétisation permet d'établir l'existence de solutions au problème (1) dans le cas non-autonome. Des estimations d'erreur établissent la précision du schéma.

Sous l'hypothèse biologique que toutes les métastases naissent avec la même vascularisation, le terme N de (1) est une mesure de Dirac. Au chapitre 6, nous montrons que les solutions ρ^ε associées à des données $N^\varepsilon \in L^1(\partial\Omega)$ convergent vers la solution mesure de (1) avec donnée $N = \delta_{\sigma=\sigma_0}$, lorsque ε tend vers 0 et $N_\varepsilon \xrightarrow[\varepsilon\to 0]{} \delta_{\sigma=\sigma_0}$.

Le potentiel du modèle en terme d'applications cliniques est illustré par des simulations numériques au chapitre 7. En particulier, notre attention se focalise sur l'effet de différents protocoles temporels d'administration pour les thérapies anti-cancéreuses, notamment dans le cas des thérapies anti-angiogéniques, seules ou bien en combinaison avec une chimiothérapie. Nous comparons les effets des thérapies sur la tumeur primaire et sur les métastases. Le phénomène récemment mis en évidence d'accélération métastatique après traitement anti-angiogénique est étudié en utilisant le modèle. Une approche thérapeutique apparue récemment, les chimiothérapies métronomiques, consistant à administrer de faibles doses de la manière la plus dense possible, est testée *in silico*.

Afin de donner des réponses effectives aux problématiques cliniques envisagées au chapitre précédent, le chapitre 8 définit un problème de contrôle optimal intégrant la dynamique métastatique. Une étude théorique de ce problème établit l'existence d'un minimiseur et dérive un système d'optimalité du premier ordre vérifié par celui-ci. Le problème est ensuite étudié numériquement dans un cas plus simple, mettant en lumière une différence entre la stratégie optimale de réduction de la tumeur primaire et celle assurant le meilleur contrôle des métastases.

Le chapitre 2, un peu excentré par rapport au barycentre de cette thèse (les métastases), présente l'adaptation d'un modèle mécanisitique de croissance tumorale vasculaire, dans le but d'étudier les interactions complexes entre anti-angiogéniques et cytotoxiques. Ce modèle multi-échelle est composé d'un assez grand nombre d'équations aux dérivées partielles dont la simulation permet de faire émerger des hypothèses quand aux possibles synergies entre les traitements.

Part I

Modélisation

Despite the large amount of biological and clinical data about cancer published every year, as noted by [GM03] : "Clinical oncologists and tumor biologists possess virtually no comprehensive model to serve as a framework for understanding, organizing and applying their data". But as cited by [AM04] from [KSKK98] : "experimentalists and clinicians are becoming increasingly aware of the role of mathematical modeling as a new way forward, recognizing that current medical techniques and experimental approaches are often unable to distinguish between various possible mechanisms underlying important aspects of tumor growth".

Two approaches can be distinguished in cancer modeling : the *mechanistic* approach and the *descriptive* (or phenomenological) one. The former develops relatively mathematically complex models often comprising a large number of parameters and aims at integrating a lot of phenomenons taking place at various scales, from the intra-cellular one to the cell population one. It often describes the spatial evolution of cancer growth and invasion. The models are often too complex to support mathematical analysis and suffer from a large number of parameters limiting their clinical applicability. The second approach intends to establish models as simple as possible, with a few parameters, in order to reproduce empirical observations, without taking care of a thorough integration of all the relevant phenomenons, although without abandoning all biological relevance. The objectives of both approaches are different : while the first one aims at giving insights on the understanding of the complex *biology* of cancer by identifying crucial parameters and providing insights in the understanding of complex processes, the second one has for objective a direct *clinical* application, for instance in using the model to optimize the administration of anti-cancerous treatments. The major part of this thesis is devoted to a model belonging to the phenomenological approach, though the chapter 2 presents some work using a mechanistic model.

Chapter 1

Phenomenological modeling

This chapter is organized as follows : in the first section we give a few elements on clinical oncology, with a focus on the actual open clinical problems. The second section presents a brief state of the art of mechanistic modeling for tumoral growth and then describes some phenomenological models. The third section describes the tumoral growth model including angiogenesis from [HPFH99] which is the tumoral basis model of this thesis. Section 1.4 describes the modeling of the therapy and introduces basics of pharmacokinetics. The model of metastatic evolution, derived from [IKN00, BBHV09, DGL09] is described in the section 1.5.

1 A few elements of clinical oncology

1.1 Cancer biology

The cancer. What is a cancer[34]? It is a disease characterized by abnormal proliferation of
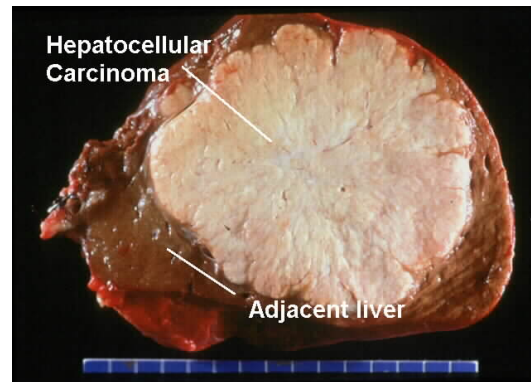
Figure 1: A hepatocellular carcinoma (liver cancer).

cells within a normal tissue. Distinction is made between solid cancers : carcinomas (epithelium cancers, i.e. of a tissue uniquely composed of cells) or sarcomas (cancer of a connective tissue, like bones) and liquid cancers as blood cancers (leukemia). This abnormal proliferation is due to one or more healthy cells which, after several successive genetic mutations, acquire various specific characteristics and loses cellular cycle control mechanisms. Benign tumors (which remain under the organism control) have to be distinguished from malign tumors. To do so, Hanahan and Weinberg proposed in [HW00] the following six phenotypes to qualify a malign cancer cell :

1. Self sufficiency in growth signals ("accelerator is blocked")

2. Insensitivity to anti-growth signals ("brakes don't work")

3. Evading apoptosis (= programmed cell death)

4. Limitless reproductive potential (infinite number of progeny)

5. Ability to provoke angiogenesis (see next paragraph)

6. Tissue invasion and metastasis

These mechanisms are regulated by various genes which are mutated in a cancerous cell : oncogenes, which are positive regulators of cellular proliferation, tumor suppressor genes, which are negative regulators of cellular proliferation (the "brakes") and other genes able to detect and repair DNA lesions affecting oncogenes or tumor suppressor genes.

---

[3]The word cancer comes from the latin *cancer* which means crab (by analogy with the fact that when a cancer seized an organ, it doesn't release it) itself derived from the greek καρκίνος, karkinos (crayfish) which gave the word carcinoma

[4]Various of the following comes from wikipedia

Tumoral angiogenesis.   Tumoral growth is limited by access to nutrients (oxygen, glucose,...) provided by the vascular network (blood vessels). This one becomes rapidly insufficient and without constant development, a tumor can not grow beyond a diameter of 2-3 mm. In the 1970's, thanks to the seminal work of Judah Folkman [Fol72], discovery is made that a tumor is able to stimulate neo-angiogenesis. It is able to promote formation of a proper vascular network providing supply of nutrients and ways of migration of cells outside of the tumor which can then form metastases. The cancerous cells emit molecules such as Vascular Endothelial Growth Factor (VEGF) which, by binding on specific receptors of surrounding endothelial cells (cells composing blood vessels), induce their proliferation as well as migration toward the tumor (see Figure 4).

Metastasis   Cells can detach from the tumor and migrate in the organism through the vascular network. They can settle in another organ and form secondary tumors called metastases (see Figure 2). The metastatic process can be divided into various stages (see Figure 3) :

Figure 2: Liver metastases coming from a pancreatic adenocarcinoma.

1. Cells dissociate by losing cadherins ("Calcium dependent adhesions") which are proteins involved in cell-cell adhesion.

2. Migration inside the tumor and invasion of the surrounding tissue, in particular using metalloproteinases attacking the basal lamina (the "barrier" surrounding the tissue)

3. Intravasation : entry in a blood vessel or lymphatic duct

4. Extravasation : exit from the blood vessel or lymphatic duct

5. Dormant phase

6. Avascular micrometastasis

7. Angiogenesis

We refer to [GM06] for a more detailed description of the metastatic process and to [CNM11] for recent novel insights on metastasis.
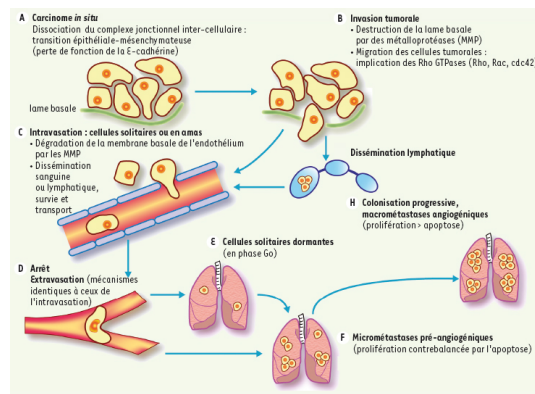
Figure 3: The metastatic process

1.2 Open clinical problems

In this section, we describe a few actual problematics in clinical oncology for which mathematical modeling could yield answers. The present thesis is devoted to development of such a model.

Classical cancer therapy is mainly achieved by three means : primary tumor surgery, chemotherapy and radiotherapy. We will not consider radiotherapy in this thesis although it represents a non-negligible part of the treatments used in the clinic. Chemotherapy consists in administration of cytotoxic agents which target dividing cells hence cancerous cells but not only, which makes it very toxic. Beside loosing hair for example (which are proliferating cells), chemotherapy present severe hematopoietic toxicities (i.e. on blood cells) which induce weakening of the patient's immunity system and can be lethal. Another major drawback of chemotherapies is development of resistances due to genetic instability of cancerous cells which mutate more than healthy ones.

Micrometastases In the case of a solid cancer, for instance breast cancer, the first therapy is surgery of the primary tumor. After it, in general the clinician doesn't see any lesion at imagery. However, metastases have been emitted, partly from the primary tumor before excision but also during the surgical operation which occasioned hemorrhages offering access to the central blood system to the cancerous cells. This is why neo-adjuvant therapy is performed (adjuvant therapy being the one performed before surgery). But the physician is blind since he doesn't have data on the state of the patient, a tumor being visible at imagery only when its size is bigger than 10^7 - 10^8 cells. Each patient being different therapy should be adapted as well as its duration so as not to treat too much in order to avoid heavy toxicities, but sufficiently to avoid relapse.

Clinical problem 1.1. *Predict the metastatic evolution of a given patient, especially the micrometastatic one (tumors of size $\leq 10^7$), with and without treatment .*

Anti-angiogenic (AA) treatments. Discovery of tumoral angiogenesis opened a new therapeutic way [Fol72] : target the tumoral vasculature development in order to suffocate the tumor by depriving it of access to nutrients. Biological research have been performed in order

to elaborate AA molecules and lead to elaboration of two classes of them : monoclonal anti-bodies which fix to molecules as VEGF and inactivate them and Tyrosine Kinase Inhibitors (TKI) which, by binding on VEGF endothelial cells receptors avoid activation of intracellular pathways of proliferation and migration. Encouraging preclinical studies (i.e. *in vivo* experiments on animals such as mice) were performed and gave rise to great hope for this new kind of therapies, named targeted therapies. In particular, the following arguments were advanced : a) expected low toxicity of these treatments comparatively to chemotherapies, b) less resistances since the targeted endothelial cells are genetically more stable. We had to wait until 2004 to see a monoclonal antibody, bevacizumab (commercial name : Avastin) be recognized as having anti-tumoral efficacy (see [GLFT05] for a synthesis of results of AA drugs). But efficacy is not proven in monotherapy and bevacizumab is administrated in combination with chemotherapy in the following cancers : colorectal, lung, breast and metastatic renal.

The results are quite disappointing : for example, results of a phase II[5] trial given in [DFH00] show an increase of only 10% of the response rate and of 3 months of progression free survival. Other phase II results are gathered in Table 1.

Reference	Cancer	Previous therapy	Treatment	n	Result
Miller et al., 2005 [MCH$^+$05]	Breast	yes	BV + capecitabine	462	RR : 19,8% VS 9,1% PFS : 4,86 m VS 4,17 m OS : 15,1 m VS 14,5 m
Hurwitz et al., 2004 [HFN$^+$04]	Colorectal	non	BV + IFL	813	RR : 44,8% VS 34,8% PFS : 10,6 m VS 6,2 m OS : 20,3 m VS 15,6 m
Robert et al., 2009 [RDG$^+$11]	Breast	yes	BV + capecitabine	615	RR : 23.6% VS 35.4% PFS : 5.7 m VS 8.6 m OS : 21.2 m VS 29 m

Table 1: Two phase II studies for bevacizumab in combination with chemotherapy (partially reproduced from [JDCL05]. BV = Bevacizumab. IFL : Irinotecan, 5-fluorouracil et leucovorin (chemotherapy). n = number of patients. RR : Response Rate[7]. PFS : Progression Free Survival[7]. OS : Overall Survival[7].

---

[5]Clinical trials are divided into four phases. Phase I determines the toxicity of the treatment on small groups (20-100) of patients. Phase II evaluates efficacy on larger groups (20-300) in order to define the optimal dose. Phase III is realized on wider groups of patients (300-3000) and aims at definitively assessing efficacy of the treatment and its advantages on existing ones. If this phases positively concludes the drug is approved by regulation agencies such as the EMA in Europe or the FDA in the United States. Phase IV consists in a security vigilance on long term.

[7]Two criteria are principally used to assess the results of a clinical trial : survival and response rate. Survival decompose into median Progression Free Survival and median overall survival. Since 2000, another criteria for progression of the disease called RECIST (Response Evaluation Criteria in Solid Tumors) has been established and is now used in all the trials. It is based on the sum of the biggest diameters of the patient's lesions for which progression is qualified in one of the four following class : CR (Complete Response) = disappearance of all the lesions, PR (Partial Response) = decrease of at least 30%, SD (Stable Disease) = decrease of less than 30% or increase of less than 20%, PD (Progressive Disease) = increase of at least 20%. The criterion Response Rate (RR), also named Objective Response (OR or ORR) corresponds to the sum of CR and PR.

Experimental studies [ELCM$^+$09, PRAH$^+$09] even obtained paradoxical results after AA therapy. In [ELCM$^+$09], the authors evidence metastatic acceleration after Sunitinib therapy on mice. Despite a positive effect on the primary tumor, on metastases the treatment is deleterious. Moreover, the temporal repartition of administration of the drug seems to play a role in the anti-tumor efficacy. In the chapter 7 we shall study this phenomenon more precisely.

The matter of the *scheduling* of anti-cancerous therapies seems of prior importance, in particular for AA drugs for which it is an open question, as mentioned by [GLFT05] and confirmed by [Rey10] in studying the Dose-Response curve of various AA drugs. This leads us to define the following clinical problem.

Clinical problem 1.2. *What is the best temporal administration protocol for AA drugs in monotherapy?*

Complex effects are expected in the combination between AA drugs and chemotherapies (CT). For example a negative effect of the AA on the CT is that, by reducing vascular support, the AA induces lower delivery of the CT. Besides, it has been discovered that AA would have a normalization effect on the vasculature [Jai01], thus improving its quality and the CT supply, which goes on the opposite direction than the previous argument. In a press review of January 2009, named "Tyrosin kinase inhibitors and chemotherapy : what if it was only a matter of scheduling?" (translated from french), B. You[8] gives another rational to explain the failure of TKIs in association with CT in non small cells lung cancers (see Table 2 for some clinical studies of combination of CT and TKIs in the case of this cancer) : "preclinical data suggest that simultaneous administration of TKI and chemotherapy would be deleterious since TKIs would stop cells in G1 phase, whereas chemotherapies would induce apoptosis preferentially in phase G2 or M" (translated from french). This argument enhances the importance of the way of

Reference	Treatment	n	% RR	OS
Giaccone,	Gemcitabin + cisplatin + gefitinib	365	50	9.9 m
2004 [GHM$^+$04]	Gemcitabin + cisplatin + placebo	365	47	10.9 m
Herbst,	Paclitaxel + carboplatine + gefitinib	347	30	8.7 m
2004 [HPH$^+$04]	Paclitaxel + carboplatine + placebo	345	28.7	9.9 m
Herbst,	Carboplatine + Paclitaxel	540	19.3	10.5 m
2005 [HGS$^+$05]	Carboplatine + Paclitaxel + erlotinib	539	21.5	10.6 m
Scagliotti,	Carboplatine + paclitaxel + sorafenib	464	27	10.7 m
2010 [SNV$^+$10]	Carboplatine + paclitaxel + placebo	462	24	10.6 m

Table 2: A few randomized trials testing combination of a chemotherapy and a tyrosine kinase inhibitor (TKI) in non small cells lung cancers. n = Number of patients. RR : Response Rate. OS : Overall survival. Gemcitabin, cisplatin, paclitaxel and carboplatin : cytotoxic agents. Molecules with "inib" : TKIs.

administrating AA in combination with CT. In Riely et al. [RRK$^+$09], the authors assay three combination protocols of CT (carboplatin, AUC (Area Under the Curve) =6) and paclitaxel (200 mg/m^{-2}) administrated every 3 weeks and erlotinib. The three protocols are :

---

[8]Medical oncology service, Hospital center of Lyon-Sud

1. Erlotinib 150 mg/d at D1 and D2 (day 1 and day 2) then CT at D3

2. Erlotinib 1500 mg/d at D1 and D2 then CT at D3

3. CT at D1 then Erlotinib 1500 mg/d at D2 and D3

The results obtained show that the second protocol is more efficient than the others. Indeed, the respective response rates are 18%, 34 % and 28 % and median survival are 10, 15 and 10 months. This proves the importance of the scheduling and that it should be rationally designed. However, the current approach in clinical oncology is to determine an efficient and non-toxic dose but few attention is given to determination of the optimal temporal administration protocol.

Clinical problem 1.3. *What is the best scheduling for combination of CT and AA therapy?*

Metronomic chemotherapies.   Recently, a novel way of using CTs is being explored. The classical way of administrating the CT is to give the Maximum Tolerate Dose (MTD), i.e. the strongest possible dose which respects the toxicity constraints, at the beginning of the therapy cycle (which lasts three weeks in general), and then let the patient recover during the rest of the cycle. Since about ten years, a new approach consists in giving a much weaker dose than the MTD, but in a more regular and continuous way, for example every day of the cycle. The feasibility of this kind of protocols, named *metronomic*, has been studied in several preliminary studies in children [ARC⁺08, BDH⁺06, KTR⁺05]. It seems that this way of giving the drug is more efficient and one of the possible explanation would be an anti-angiogenic action of cytotoxic agents [KK04]. Indeed, since the CT kills proliferative cells it also kills dividing endothelial cells participating to angiogenesis. But these cells present the advantage that they are more genetically stable than the cancerous ones and thus develop less resistances. Hence, even if less malignant cells are directly killed by the treatment, on long term the effect is more important since regression of the tumoral vasculature implies tumor suffocation, comprising eradication of resistant cancerous cells. But then, why is this AA effect not present in classical MTD protocols? The advanced argument is that the vasculature would recover rather quickly from the assault, stimulated by angiogenesis. A rest time of more than two weeks in a MTD protocol would give it time to reconstruct before the next assault. Another argument, supported by a mathematical model is proposed in [HFH03] : the heterogeneity of the cancer cell population, with subpopulations having different "resensibilization" rates to the treatment, would imply the superiority of an evenly distributed protocol.

However, if the dose is too weak, then the therapy is not efficient anymore. Determine what is the best repartition of doses in the framework of metronomic CTs is still an open problem.

Clinical problem 1.4. *What is the optimal temporal administration protocol for metronomic chemotherapies?*

2   A few descriptive models of tumoral growth

The principle of descriptive models of tumoral growth is the following : denoting $x(t)$ the number of cancer cells, modeled as a continuous function of the time t, we write the following conservation law :

$$x(t + dt) = x(t) + (\text{new cells per time unit} - \text{dead cells per time unit}) * dt$$

and then let dt go to zero to obtain :

$$\dot{x}(t) = \text{new cells per time unit} - \text{dead cells per time unit}.$$

Remark 1.1 (Number of cells and volume). *We will constantly do the amalgam between number of cancerous cells and tumoral volume, assuming that all cells have the same volume which is constant in time. We use the following proportionality conversion :*

$$1\,mm^3 = 10^6\ cells.$$

Malthusian growth. The simplest model of population growth is due to Malthus (1766-1834) and assumes that in a given population (in our case a cell population) the number of newborns and the number of deaths are proportional to the number of individuals in the population. Denoting respectively λ and μ these two proportionality rates we get

$$\dot{x}(t) = \lambda x(t) - \mu x(t).$$

The parameter λ stands thus for the number of newborns per individual per unit time, its unit as well as the one of μ is thus in $time^{-1}$. One can interpret μdt as the probability for a given individual to die during a small time dt. This model exhibits a very simple behavior : either exponential growth or exponential decreasing depending on the sign of $\lambda - \mu$ and this scared Malthus a lot when he applied this model to human population growth by arguing that the resources growth is only arithmetic. He concluded predicting inevitable demographic disasters. The doubling time (or dividing by half time) of the population is given by $\frac{\ln 2}{|\lambda - \mu|}$ and is a useful quantity for clinicians.

Logistic growth. To take into account the fact that resources are limited which tends to slow the growth of a population *via* competition of the individuals for these, the Belgian mathematician Verhulst (1804- 1849) introduced in [Ver45] the logistic model which says that the population growth rate $\frac{\dot{x}(t)}{x(t)}$ is not constant but rather depends on the size of the population in a non-increasing way and vanishing when the population reaches the maximal capacity of the environment, the so-called carrying capacity. The easiest way to do this is to take this rate equal to $a(1 - \frac{x(t)}{\theta})$ with a a parameter controlling the velocity of the growth and θ the carrying capacity. The equation writes

$$\dot{x}(t) = ax(t)\left(1 - \frac{x(t)}{\theta}\right). \tag{1}$$

This is a nonlinear ordinary differential equation which is used in a wide range of applications, for example in ecology. The mathematical analysis reveals an unstable equilibrium state in 0 and a globally stable one in θ. The number of individuals goes to this carrying capacity θ for large times. An explicit formula for the solution of (1) is given by :

$$x(t) = \frac{x_0 \theta}{(\theta - x_0)e^{-at} + x_0}.$$

Gompertzian growth   The model of Gompertz (1779-1865), dating from 1825 can be derived from the logistic one in the following way. To introduce an additional degree of freedom in order to obtain better fits to data, we consider the following model that we will call "logistic power" :

$$\dot{x}(t) = \frac{a}{\nu}x(t)\left(1 - \left(\frac{x(t)}{\theta}\right)^{\nu}\right).$$

This model reveals particularly adequate for describing tumoral growth, for example in the context of breast cancer [Ske86, SMS96] with $\nu = 1/4$. In the limit $\nu \to 0$ (see figure 4) we obtain the model of Gompertz given by

$$\dot{x}(t) = ax(t)\ln\left(\frac{\theta}{x(t)}\right). \tag{2}$$

This model is commonly used in the medical literature for describing tumoral growth where it
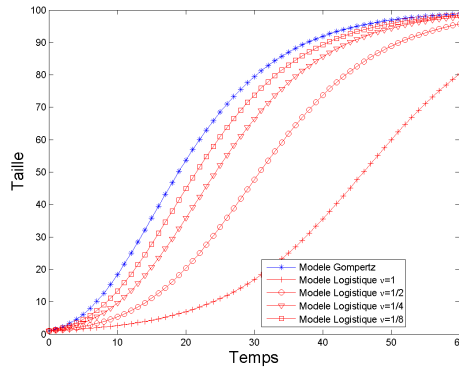
Figure 4: Convergence of the logistic power model toward the gompertzian one when $\nu \to 0$. Values of the parameters (chosen for illustrative purpose) : $a = 0.1$, $\theta = 100$.

was first introduced in [Lai64](where it fits well several data) and we shall use it as a basis for tumoral growth in this thesis. The equation can be solved explicitly :

$$x(t) = \theta e^{\ln\left(\frac{x_0}{\theta}\right)e^{-at}}$$

with x_0 the initial size of the population. Benjamin Gompertz in [Gom25] invented this model in the context of insurances and his idea was that the growth rate should decrease exponentially in time. Indeed if we set $\lambda = a\ln\frac{\theta}{x_0}$, one can compute that we have

$$\dot{x}(t) = \lambda e^{-at}x(t). \tag{3}$$

It is also possible to calculate the doubling time of the population which is an increasing function and is given by $\tau(t) = -\frac{1}{a}\ln\left(1 + Ae^{at}\right)$ where $A = \frac{\ln(2)}{\ln\left(\frac{x_0}{\theta}\right)} < 0$ if $x_0 < \theta$. One of the critics to the gompertzian model is that the growth rate tends to infinity when the size goes to zero (which can be viewed in (2)) and it is hard to imagine a little tumor having an infinite growth rate because it is bounded by the total cell cycle duration. However, this model is largely accepted

to describe the tumoral growth because it is experimentally observed [Lai64] that the growth rate of a tumor slows down as the size increases, which gives rise to curves well approached by sigmoïdal (or S-shaped) functions as the one resulting from the Gompertz or the logistic equation.

If we want to do the analogy between the logistic equation (1) and the Gompertz equation (2), there are two possible ways to proceed : either we want the same growth rates when the population is small and then we set $a_{log} \simeq a_{gom} \ln(\theta)$, where we denote a_{log} the parameter a in the logistic equation and a_{gomp} in the Gompertz one. This gives a very large a_{log} if we think that θ is big because it is the maximal reachable size. On the opposite, if we want to have the same exponential decrease of the asymptotic growth rate, we calculate for the logistic equation that :

$$\frac{\dot{x}(t)}{x(t)} = \frac{(\theta - 1)a_{log}e^{-at}}{1 + e^{-a_{log}t}(\theta - 1)} \underset{t \to \infty}{\sim} (\theta - 1)a_{log}e^{-a_{log}t}.$$

For the Gompertz, we get from (3) that the decrease of the growth rate is governed by a_{gom} and we are thus driven to take $a_{log} = a_{gom}$, which gives a slower initial growth for the logistic model. The figure 5 illustrates the three growth models : malthusian, logistic and Gompertz. We chose an intermediate situation for a_{log} regarding to the preceding analysis and took the same value for the carrying capacity θ.
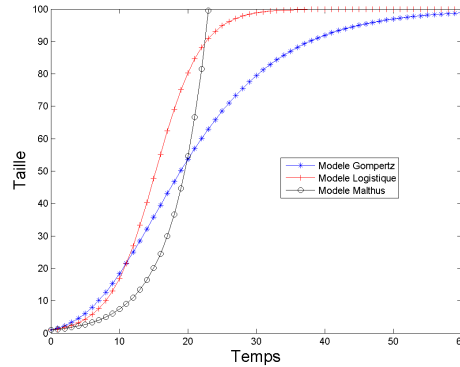
Figure 5: Three tumoral growth models. Values of the parameters : $a_{gom} = 0.1$, $a_{log} = 0.2$, $\theta = 100$. Malthus : $\lambda = 0.2$, $\mu = 0$.

From a mathematical point of view, the equation (2) presents a singularity in 0. Indeed, the function $g(x) = ax \ln\left(\frac{\theta}{x}\right)$ is continuous at 0 but not locally Lipschitz. We thus cannot apply the Cauchy-Lipschitz theorem to obtain the uniqueness of solutions passing through 0. However, there is uniqueness because the time that would spend a solution being in 0 at time t_0 to reach a point $x > 0$ is given by $\int_0^x \frac{dy}{g(y)} = +\infty$. In other words, a solution which passes by 0 doesn't get out in finite time . Thus the only solution passing by 0 is the constant function equal to 0.

Proposition 1.2 (Uniqueness in 0 for the Gompertz equation). *The unique solution of the equation* (2) *which cancels is the constant solution equal to zero for all time.*

Proof. Let $t \mapsto x(t)$ be a solution of (2) which cancels, say in t_0 and let t_1 be a time such that

$0 < x(t) < \theta$ for all $t_0 < t \leq t_1$. Then $x'(t) = g(x(t)) > 0$ on this interval and $t \mapsto x(t)$ is thus a $\mathcal{C}^1$-diffeomorphism there. One can do the following change of variables

$$+\infty > t_1 - t_0 = \int_{t_0}^{t_1} \frac{\dot{x}(s)}{g(x(s))} ds = \int_0^{x(t_1)} \frac{dy}{g(y)} = +\infty$$

which gives a contradiction. $\square$

Remark 1.3.

- *The previous proof shows that is $x(t)$ is a trajectory of the equation $\dot{x}(t) = g(x(t))$, with constant sign, then the time needed to go from x_1 to x_2 is $\int_{x_1}^{x_2} \frac{dy}{g(y)}$, that is : if $x(t_1) = x_1$ and $x(t_2) = x_2$, then $t_2 - t_1 = \int_{x_1}^{x_2} \frac{dy}{g(y)}$. This can also be viewed by saying that the travel time is the inverse function of the trajectory : if we denote by $t(y)$ the travel time between x_0 and y, then $x(t(y)) = y$ with $x(t)$ being the solution of the differential equation being in x_0 at time $t = 0$. We then get $\dot{t}(y) = \frac{1}{g(y)}$.*

- *In the classical case of $\dot{x}(t) = \sqrt{x(t)}$, then $\int_0^x \frac{dy}{\sqrt{y}} < +\infty$ for all $x > 0$, a solution can reach 0 in finite time and there is not uniqueness of the solution passing by 0.*

Explanation of tumoral growth by quiescence : the model of Gyllenberg-Webb [GW89]   In an attempt to explain the slowdown of the tumoral growth rate empirically observed and modeled by the logistic or Gompertz equations, Gyllenberg and Webb propose in [GW89] a model dividing the cancerous population between two compartments : the proliferative cells, that is the ones in phase S, G2 or M, denoted by $P(t)$ and contributing to the overall growth of the population, and the quiescent cells, that is in the G0 phase of the cell cycle, which don't divide. We denote $N(t) = P(t) + Q(t)$ the total number of malignant cells. The fact that proliferative cells go to quiescence is a reported phenomenon due to various causes, for example to overcrowd. Hence, the authors suppose that proliferative cells divide with a rate b and become quiescent with a rate $r_0(N)$ depending on the total number of cells. The resulting equations are

$$\begin{cases} \dot{P}(t) = (b - r_0(N(t)))P(t) \\ \dot{Q}(t) = r_0(N(t))Q(t). \end{cases} \tag{4}$$

The authors recover either the logistic equation or the Gompertz one depending on particular shapes of $r_0(N)$: a linear rate $r_0(N) = N$ gives the logistic model while a logarithmic rate $r_0(N) = 1 + \ln(N)$ gives the Gompertz model. We detail here the argument.

- Logisitic case : we take $b = 2$, $r_0(N) = N$ et $P(0) = Q(0) = 1$. Then we get the following system on N and P

$$\begin{cases} \dot{N} = \dot{P} + \dot{Q} = 2P \\ \dot{P} = (2 - N)P = \dot{N} - NP. \end{cases}$$

  We deduce that $\dot{P} = \dot{N} - \frac{1}{2}N\dot{N} = \widehat{(N - \frac{1}{4}N^2)}$, thus $P = N - \frac{1}{4}N^2 + P(0) - (N(0) - \frac{1}{4}N(0)^2) = N - \frac{1}{4}N^2$. Replacing in the first line if the preceding system, we obtain that N solves

$$\dot{N} = 2N - \frac{1}{2}N^2$$

  that is the logistic equation (1) with $a = 2$ and $\theta = 4$.

- Gompertz case : with the same type of argument, in the case $b = 1$, $P(0) = 1$, $Q(0) = 0$ we obtain that N solves

$$\dot{N} = (1 - \ln(N))N$$

which is the Gompertz equation (2) with $a = 1$ and $\theta = e$.

In their article [GW89], the authors build a more complex model, authorizing for example the quiescent cells to reintegrate the cellular cycle or to die, which we do not describe here.

The model of Simeoni et al. [SMC$^+$04] In conclusion, all these phenomenological models exhibit the same qualitative behavior : a slowdown of the tumora growth rate leading to saturation of the growth and a plateau. This gives this S-shape to the resulting curves (sigmoïdal curves). Noticing that the plateau inherent to the logistic and Gompertz models has never been observed in practical situations, Simeoni et al. introduce in [SMC$^+$04] a model fitting remarkably well to the experimental data of the article. Considering that tumoral growth can be divided between two phases : first exponential then linear, the authors consider that we must have

$$\dot{x}(t) = \lambda_0 x(t), \quad x(t) \le x_{th}$$
$$\dot{x}(t) = \lambda_1, \qquad x(t) > x_{th}$$

with λ_0 and λ_1 the respective parameters of exponential and linear growth and x_{th} a critical size for which the growth goes from exponential to linear. Expressing the continuity of the solution, we must have $x_{th} = \frac{\lambda_1}{\lambda_0}$. Following these considerations, the authors propose the following equation :

$$\dot{x}(t) = \frac{\lambda_0 x(t)}{\left[1 + \left(\frac{\lambda_0}{\lambda_1} x(t)\right)^\psi\right]^{1/\psi}}$$

which gives rise to the desired dynamic for a large value of ψ by noticing that if $x(t) \ll x_{th}$ then the growth rate is about $\lambda_0 x(t)$ while if $x(t) \gg x_{th}$ we have $\dot{x}(t) \simeq \lambda_1$. The authors take then the therapy into account via pharmacokinetics and the resulting model fits very well their data, reproducing with precision various therapies corresponding to various drugs administrated according to various temporal schemes. They confront predictions of the model with data and obtain a good accuracy. They thus conclude by recommending the use of their model in the elaboration of performing therapeutic schedules in the clinic.

3 Tumoral growth under angiogenic control

3.1 The model of Hahnfeldt et al.

We describe now the tumoral growth model that will be used in the major part of this thesis. It was introduced by P. Hahnfeldt, D. Panigraphy, J. Folkman and L. Hlatky in [HPFH99] and consists in extending the Gompertz model and integrates the vasculature of the tumor and the angiogenic process. Indeed, it is necessary to have a modelling of the evolution of the vascular support in order to model the effect of anti-angiogenic drugs. The principal idea of Hahnfeldt et al. is to consider the carrying capacity θ from the Gompertz equation (2) no more as a constant

parameter but rather as a dynamic variable representing the vasculature of the tumor, since it is defined as the maximal reachable size by the tumor limited by the nutrient's supply from the vasculature. We will use the term "vascular capacity" or "angiogenic capacity" to denote it. The equation on the size x of the tumor is identical to the Gompertz equation

$$\dot{x}(t) = ax(t)\ln\left(\frac{\theta(t)}{x(t)}\right). \tag{5}$$

For the θ dynamics, three phenomenons are taken into account : natural vascular loss due to natural endothelial cells death, stimulation by the tumor *via* molecules such as VEGF and inhibition of the vasculature by the tumor. The parameter for vascular loss is *a posteriori* estimated to zero in [HPFH99] by fitting the parameters to experimental data and we thus will neglect this aspect. The equation on θ is

$$\dot{\theta}(t) = cS(x,\theta) - dI(x,\theta)$$

where $S(x,\theta)$ and $I(x,\theta)$ stand respectively for the stimulating and inhibiting effects and will now be determined. The authors make the following assumptions, based on experimental data (quoted here from [dG04]) : (i) the tumor is a spheroid, (ii) the secretion rates of the different molecules are constant in space and time, (iii) the movement of molecules is due to diffusion only (and diffusion is quasi-stationary), (iv) the elimination rate of inhibitor molecules is much smaller than $\frac{D}{r_0^2}$, D being the diffusion coefficient and r_0 the tumoral radius and (v) the elimination rate of the stimulating molecules is much bigger than $\frac{D}{r_0^2}$. The two last hypotheses are the more important and the authors derive the expressions for S and I based on them. They mean that the inhibitor agents have much higher persistance than the stimulator ones. Denoting by n the agent concentration (stimulator or inhibitor), s the secretion rate of the molecule (equal to s_0 inside the tumor and null at the exterior) and c its elimination rate, the authors write the following reaction diffusion equation on the spatial evolution of n

$$\partial_t n - D^2\Delta n = s - cn.$$

Considering the equation at a quasi-stationary state, making the polar coordinates change of variable and using the spherical symmetry we get

$$n''(r) + \frac{2n'(r)}{r} - \frac{cn}{D^2} + \frac{s}{D^2} = 0$$

(remark that there is a 2 in the expression of the laplacian operator in polar coordinates since we place ourselves in dimension 3). Doing the change of variables $u = \frac{\sqrt{c}}{D}r$ and $\overline{z}(u) = (n(r) - \frac{s}{c})$ we find

$$\overline{z}'' + \frac{2\overline{z}'}{u} - \overline{z} = 0$$

then, setting $z(u) = u^{1/2}\overline{z}(u)$ (and not $r^{1/2}\overline{z}$ as written in [HPFH99], as it seems) we find that z solves the following modified Bessel equation

$$u^2 z''(u) + u z'(u) - (u^2 + \frac{1}{4})z = 0$$

for which we can check that two independent solutions are given by the functions $z_1(u) = \frac{\sinh(u)}{\sqrt{u}}$ and $z_2(u) = \frac{e^{-u}}{\sqrt{u}}$. Remarking that $\frac{z_2(u)}{\sqrt{u}}\Big|_{u=0} = +\infty$, the component in z_2 is null for the

concentration inside the tumor, denoted by n_{inside}. In the same way, since $\frac{z_1(u)}{\sqrt{u}}\Big|_{u=+\infty} = +\infty$ there can't have any z_1 component in the external concentration denoted by $n_{outside}$. Thus there exists two constants C_1 and C_2 such that

$$n_{inside}(r) = \frac{s_0}{c} + C_1 \frac{z_1(u)}{\sqrt{u}}$$

$$n_{outside}(r) = C_2 \frac{z_2(u)}{\sqrt{u}}$$

Writing the equality of n_{inside} and $n_{outside}$ in r_0 as well as for their derivatives to preserve continuous derivability of the solution allows to determine the values of C_1 and C_2 and we get

$$n_{inside}(r) = \frac{s_0}{c} \left[1 - (1 + u_0)e^{-u_0} \frac{\sinh(u)}{u} \right]$$

$$n_{outside}(r) = \frac{s_0}{c} \left[u_0 \cosh(u_0) - \sinh(u_0) \right] \frac{e^{-u}}{u}$$

Now we consider two different cases fort the elimination rate, traducing hypotheses (iv) and (v). For small c (inhibitor case), that is for $c \ll \frac{D^2}{r_0}$, that is $u_0 \ll 1$ a limited development gives

$$n_{inside}(r, c \text{ small}) \simeq \frac{s_0}{6D^2} \left[3r_0^2 - r^2 \right], \quad n_{outside}(r, c \text{ petit}) \simeq \frac{s_0 r_0^3}{3D^2 r}$$

whereas for large c (stimulator case) we have

$$n_{inside}(r, c \text{ big}) \simeq \frac{s_0}{c}, \quad n_{outside}(r, c \text{ grand}) \simeq 0.$$

From this analysis we deduce that the inhibitor concentration is proportional to the radius of the tumor to the square, that is to the volume at the power $2/3$ whereas the stimulator concentration is independent from the tumoral volume. This suggests to take $I(x, \theta) = x^{2/3}\theta$. For the stimulatory term, a natural choice following the previous analysis would be $S(x, \theta) = \theta$ but the authors rather choose $S(x, \theta) = x$ which in the end shouldn't influence too much the qualitative behavior of the system since x and θ tend to move together, as illustrated in [dG04] from which we reproduce the figure 1 on the figure 7. Eventually, we obtain the following ODE system

$$\begin{cases} \dot{x}(t) = ax(t) \ln\left(\frac{\theta(t)}{x(t)}\right) \\ \dot{\theta}(t) = cx(t) - dx(t)^{2/3}\theta(t). \end{cases} \tag{6}$$

Hahnfeldt et al. then fix the values of the parameters by fitting the model to experimental mice data whom was transplanted a lung tumor. They find that the model is able to describe quite precisely the tumoral dynamic, at least in mice and for this kind of tumor. The figure 3A from [HPFH99] is reproduced here through a simulation, on the figure 6. We observe a sigmoïdal shape of the curve, thus with the same qualitative behavior as the Gompertz model.

3.2 Qualitative analysis of the ODE system

We study now a few properties of the behavior of the ODE system (6) such as the well-posedness and asymptotic behavior of the solutions. Let us mention that a similar study
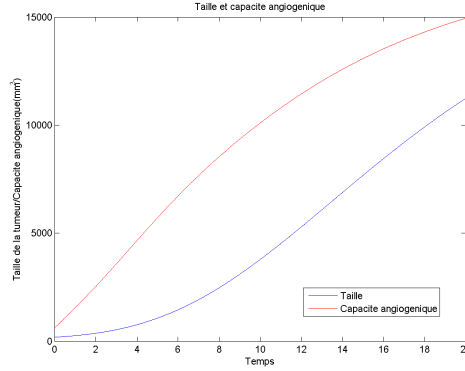
Figure 6: Simulation of the system (6). Parameter values are from [HPFH99] : $a = 0.192\ day^{-1}$, $c = 5.85\ day^{-1}$, $d = 0.00873\ day^{-1}mm^{-2}$. Initial conditions $x_0 = 200\ mm^3$, $\theta_0 = 625\ mm^3$.
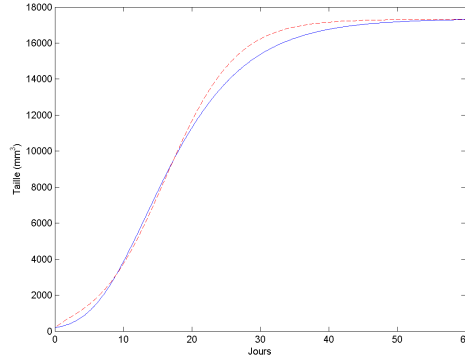
Figure 7: Comparison of tumoral growth for two modeling of $S(x, \theta)$. Solid line : $S(x, \theta) = x$, parameter values and initial condition from [HPFH99]. Broken line : $S(x, \theta) = \theta$, parameter values from [dG04] $a = 1.08\ day^{-1}$, $c = 0.243\ day^{-1}$, $d = 3.63 \cdot 10^{-4}\ mm^{-2}$, same initial condition.

has been performed by A. d'Onofrio and A. Gandolfi in [dG04]. Let $X(t) = \begin{pmatrix} x(t) \\ \theta(t) \end{pmatrix}$ and $G(X) = \begin{pmatrix} ax \ln\left(\frac{\theta}{x}\right) \\ cx - dx^{2/3}\theta \end{pmatrix}$, then the system endowed with initial condition becomes

$$\begin{cases} \frac{dX}{dt} = G(X) \\ X(t_0) = \begin{pmatrix} x_0 \\ \theta_0 \end{pmatrix} \end{cases} \tag{7}$$

We define

$$b = \left(\frac{c}{d}\right)^{\frac{3}{2}}, \quad 0 < x_{min} \le b \le x_{max}, \quad \Omega =]x_{min}, x_{max}[\times]x_{min}, x_{max}[.$$

Global existence of trajectories

Proposition 1.4 (Existence, uniqueness and boundedness of the solutions of (1))**.** *The system* (1) *has a unique solution for all initial condition* $x_0 > 0$, $\theta_0 > 0$, *defined for all* $t \in \mathbb{R}$. *Moreover this solution verifies* $x(t)$, $\theta(t) \in \overline{\Omega}$ *for all* $t \geq 0$ *if* $(x_0, \theta_0) \in \overline{\Omega}$.

Proof. The function G is $\mathcal{C}^1$ in $\mathbb{R}_+ \times \mathbb{R}_+$ so we can apply the Cauchy-Lipschitz theorem ensuring local existence and uniqueness of solutions. We use then the following lemma to have bounds on the solutions.

Lemma 1.5. *Let* $(x(t), \theta(t))$ *be a maximal solution of* (1) *such that* $(x_0, \theta_0) \in \overline{\Omega}$. *Then* $(x(t), \theta(t)) \in \overline{\Omega}$ *for all* $t \geq t_0$.

Proof. Let us show only that $x(t) \geq x_{min}$ and $\theta(t) \geq \theta_{min}$ for all $t \geq t_0$ since the other parts of the demonstration can be proven in the same way.

* **Step 1: There exists $t^* \geq t_0$ such that $x(t^*) > x_{min}$ and $\theta(t^*) > x_{min}$**
  If $x_0 > x_{min}$ and $\theta_0 > x_{min}$, there is no problem. Else, three cases can happen :

  – Either $x_0 = x_{min}$ and $\theta_0 > x_{min}$. Then $G_1(x_0, \theta_0) = ax_0 \ln\left(\frac{\theta_0}{x_{min}}\right) > 0$ so by continuity G_1 remains positive in a neighborhood V of (x_0, θ_0). By continuity again, the trajectory remains in this neighborhood for small times, say $X(t) \in V$, $\forall 0 \leq t \leq t^*$ and then $x(t^*) = x_{min} + \int_0^{t^*} G_1(x(s), \theta(s))ds > x_{min}$. Taking a smaller V if needed, we also have $\theta(t^*) > x_{min}$.

  – Either $\theta_0 = x_{min}$ and $x_0 > x_{min}$. The same argument can be applied for θ since $G_2(x_0, x_{min}) = cx_0 - dx_0^{2/3}x_{min} > x_0^{2/3}(cx_{min}^{1/3} - dx_{min}) \geq 0$ because $x_{min} \leq \left(\frac{c}{d}\right)^{\frac{3}{2}}$.

  – Either $x_0 = x_{min}$ and $\theta_0 = x_{min}$. Then we have $G_1(x_{min}, x_{min}) = 0$ and we cannot apply the same argument. Since $G_2(x_{min}, x_{min}) = cx_{min} - dx_{min}^{5/3} > 0$ if $x_{min} < \left(\frac{c}{d}\right)^{3/2} = b$, then by the previous argument, there exists $\eta > 0$ such that $\theta(t) > x_{min}$ for all $0 < t < \eta$. Suppose that $x(t) \leq x_{min}$ $\forall 0 < t < \eta$, then $G_1(x(t), \theta(t)) = ax(t) \ln\left(\frac{\theta(t)}{x(t)}\right) > 0$, $\forall 0 < t < \eta$ which implies $x(t) > x_{min}$, $\forall 0 < t < \eta$ and a contradiction. It remains he case $x_{min} = b$, $x_0 = \theta_0 = b$ for which $G(b, b) = (0, 0)$, but then the solution is constant equal to (b, b) so $x(t) \geq x_{min}$.

* **Step 2: For all $t \geq t^*$, $x(t) > x_{min}$ and $\theta(t) > \theta_{min}$**
  By contradiction. We define $\Omega^+ = \{(x, \theta) \in \mathbb{R}^2; \ x > x_{min} \text{ and } \theta > \theta_{min}\}$. Suppose that their exists $t > t^*$ such that $X(t) \notin \Omega^+$ and let $t_1 = \inf\{t > t^*; X(t) \notin \Omega^+\}$. Then $X(t_1) \in \partial\Omega^+$, so $x(t_1) = x_{min}$ or $\theta(t_1) = \theta_{min}$.

  – If $x(t_1) = x_{min}$ and $\theta(t_1) > \theta_{min}$, then $G_1(x_{min}, \theta(t_1)) > 0$. Let U be a neighborhood of $(x_{min}, \theta(t_1))$ such that G_1 be positive. There exists an interval $I = [t_1^*, t_1]$ such that : $\forall t \in I, (x(t), \theta(t)) \in U$, by continuity of the trajectories. The function $t \mapsto x(t)$ is non-decreasing on this interval since G_1 is positive in I but $x(t_1^*) > x_{min}$ because t_1 is the first reaching time of x_{min}, and $x(t_1) = x_{min}$. Contradiction.

  – If $\theta(t_1) = x_{min}$ and $x(t_1) \geq x_{min}$, then $G_2(x(t_1), \theta_{min}) > 0$ and the same argument holds.

To end the proof of the lemma, it remains to show that $\theta(t) \leq x_{max}$ and $x(t) \leq x_{max}$. For that, let us study the sign of G_2 on the straight line $\theta = x_{max}$ and the sign of G_1 along the straight line $x = x_{max}$. A sign study shows that $G_2(x, x_{max}) < 0$ and $G_1(x_{max}, x) > 0$ except for $x_{max} = x = b$, case for which the solution is stationary. $\qquad\square$

Remark 1.6.
• *This lemma shows quite fastidiously what is easily understood visually by noticing that the field G points inward all along the boundary of $\overline{\Omega}$.*
• *The proof shows that actually for $(x_0, \theta_0) \in \overline{\Omega} \setminus (b, b)$, $(x(t), \theta(t)) \in \Omega$ for all $t > 0$.*

To show that the solution doesn't explode in finite time it suffices now to remark that the trajectory are bounded thanks to the lemma. This implies global existence. $\qquad\square$

Remark 1.7 (Uniqueness along the line $x = 0$)**.** *Following the proposition 1.2 for the Gompertz equation, it is natural to rise the question of uniqueness of the solutions going through a point $(0, \theta_0)$ with $\theta_0 > 0$ since the function G is then continuous but not locally Lipschitz. The function G is not continuous in $(0, 0)$ as a function defined in $\mathbb{R}_+ \times \mathbb{R}_+$, however if we restrict ourselves to the open set $\{(x, \theta); \theta > x\}$ there is a limit for G in $(0, 0)$ which is 0 and permits to give a sense to the differential equation (6). The following argument shows that there is indeed uniqueness. Let $X(t)$ be a solution passing through (x_0, θ_0) at t_0 with $x_0 > 0$ and $\theta_0 \leq x_{max}$. We write*

$$\frac{dx}{dt} = ax \ln\left(\frac{\theta}{x}\right) \leq ax \ln\left(\frac{x_{max}}{x}\right)$$

so that

$$\frac{dx}{ax \ln(x_{max}) - ax \ln(x)} \leq dt$$

which gives after integration

$$\int_{x_0}^{x(t)} \frac{dy}{ay \ln(x_{max}) - ay \ln(y)} dy = -\frac{1}{a} \ln\left(\frac{\ln(x_{max})}{\ln(x(t))}\right) + \frac{1}{a} \ln\left(\frac{\ln(x_{max})}{\ln(x_0)}\right) \leq t - t_0.$$

Now, since the left hand side of this inequality tends to $+\infty$ when x_0 goes to 0, we see that it is not possible for a solution coming from a point $(0, \theta_0)$ to reach a point with positive first component in finite time. Moreover, since $G(0, \theta) = (0, 0)$, the only solution is the stationary solution.

Asymptotic behavior

The following proposition concerns the qualitative behavior of the system illustrated in the figure 8 where we observe global convergence to an equilibrium point.

Proposition 1.8. *The system (1) possesses a unique critical point globally asymptotically stable in $\overline{\Omega}$*

$$X^* = \begin{pmatrix} \left(\frac{c}{d}\right)^{\frac{3}{2}} \\ \left(\frac{c}{d}\right)^{\frac{3}{2}} \end{pmatrix}$$
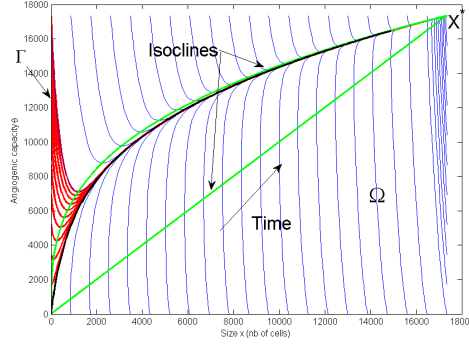
Figure 8: Phase plan of the system (6). The parameter values are the ones of [HPFH99].

Proof. Resolving the equation $G(x, \theta) = 0$ we get a unique solution $X^* = \begin{pmatrix} (\frac{c}{d})^{\frac{3}{2}} \\ (\frac{c}{d})^{\frac{3}{2}} \end{pmatrix}$.

• *Local stability* The fixed point X^* is locally asymptotically exponentially stable. Indeed, calculating the jacobian matrix of G in X^* gives $\begin{pmatrix} -a & a \\ \frac{c}{3} & -c \end{pmatrix}$ whose eigenvalues are $\alpha_1 = \frac{-(c+a)+\sqrt{\Delta}}{2}$ and $\alpha_2 = \frac{-(c+a)-\sqrt{\Delta}}{2}$, with $\Delta = c^2 + a^2 - \frac{2}{3}ac$ and are both real since $\Delta > (c-a)^2 \geq 0$ and negative. The linearisation Lyapunov theorem implies that the point X^* is locally asymptotically exponentially stable.

• *Global stability.* We use successively two theorems : first the Poincaré-Bendixson theorem which restrains the possibilities for the asymptotic behavior and then the Dulac criterion which eliminates the other possibilities than a critical point for the ω-limit set. We state the theorems here for the sake of completeness. They can be found in the book of Perko [Per01] and require the following definitions, where we denote Φ the flow of an ODE equation defined in $\mathbb{R}^2$:

$$\Gamma_{x_0} = \{\Phi_t(x_0); \ t \in \mathbb{R}\}, \ \Gamma_{x_0}^+ = \{\Phi_t(x_0); \ t \geq 0\}$$

$$\omega(\Gamma_{x_0}) = \{p \in \mathbb{R}^2, \ \exists t_n \to +\infty, \ \Phi_{t_n}(x_0) \to p\}.$$

Theorem 1.9 (Poincaré-Bendixson theorem ([Per01] p.245))**.** *Let $\dot{X} = f(X)$ a system of differential equations with $f \in \mathcal{C}^1(E)$, E being an open set of $\mathbb{R}^2$, which has a trajectory Γ such that Γ^+ is contained in a compact set of E, and with a finite number of critical points. Then the limit set $\omega(\Gamma)$ is either a critical point, either a periodic orbit, either the union of a finite number of critical points $p_1, ..., p_m$ and of a countable number of orbits joining a point p_i to a point p_j.*

From the theorem 1.4 the positive half trajectories of the system (1) are contained in the compact $\overline{\Omega}$. We can apply Poincaré-Bendixson theorem and the only possibilities for the asymptotic behavior of the system are thus convergence to the unique fix point X^*, a limit cycle, or a homoclinic orbit (i.e. an orbit starting and ending at the same point) starting and ending in X^*. The Dulac criterion eliminates the two last possibilities.

Theorem 1.10 (Dulac criterion ([Per01] p.265))**.** *Let $f \in \mathcal{C}^1(E)$ with E being simply connected.*

If the divergence of f is not identically zero and does not change sign in E, then the system $\dot{X} = f(X)$ has no closed non-punctual orbit contained in E and no homoclinic orbit.

In our case we cannot apply this theorem directly since $\partial_x G_1 = a(\ln(\frac{\theta}{x}) - 1)$, $\partial_\theta G_2 = -dx^{\frac{2}{3}}$, and thus

$$\mathrm{div}G = a \ln\left(\frac{\theta}{x}\right) - a - dx^{\frac{2}{3}},$$

which changes sign in $\overline{\Omega}$. To deal with this, we apply the following transformation to the system (1), taken from [dG04] :

$$\overline{t} = at, \ (\overline{c}, \overline{d}) = \frac{1}{a}(c, d), \ \overline{x} = \ln\left(\frac{x}{b}\right), \ \overline{\theta} = \ln\left(\frac{\theta}{b}\right)$$

and we get the following system (still denoting x for $\overline{x}$ and θ for $\overline{\theta}$)

$$\begin{cases} \frac{dx}{dt} = -x + \theta \\ \frac{d\theta}{dt} = \overline{c}(e^{x-\theta} - e^{\frac{2}{3}x}) \end{cases} . \tag{8}$$

The trajectories associated to this system are homeomorphic to the ones of system (1) but now the divergence of the field is

$$-1 - \overline{c}e^{x-\theta} < 0$$

We can thus apply the Dulac criterion which concludes to the impossibility of a limit cycle or a homoclinic orbit. The only left possibility is convergence to the unique equilibrium point of the system X^*. $\square$

Slow fast dynamic.

Observing the phase plan of Figure 8 drawn for $\Omega =]1, b[\times]1, b[$ with $b = \left(\frac{c}{d}\right)^{3/2}$ we have the feeling that the trajectories concentrate on the nullcline $G_2(x, \theta) = 0$. Let us study more in details the global aspect of the phase plan depending on the values of the parameters : what are the parameters which govern the shape of the phase plan? What is the role of each parameter?

The equilibrium point is given by $X^* = \left(\left(\frac{c}{d}\right)^{3/2}, \left(\frac{c}{d}\right)^{3/2}\right)$ thus it doesn't depend on the value of a. Moreover, augmenting d makes it closer to $(0, 0)$ and the opposite holds for c. What controls the slope of the trajectories? Calculating $\frac{d\theta}{dx} = \frac{G_1(x,\theta)}{G_2(x,\theta)} = \frac{ax\ln\left(\frac{\theta}{x}\right)}{cx - dx^{2/3}\theta}$ doesn't concludes. On the other side, if we renormalize to place ourselves at the scale of b we have the idea of the following change of variables :

$$\overline{x} = \frac{x}{b}, \ \overline{\theta} = \frac{\theta}{b}$$

which transforms the system (6) into

$$\begin{cases} \frac{d\overline{x}}{dt} = a\overline{x}\ln\left(\frac{\overline{\theta}}{\overline{x}}\right) \\ \frac{d\overline{\theta}}{dt} = c\left[\overline{x} - \overline{\theta}\overline{x}^{2/3}\right] \end{cases} \tag{9}$$

In this system, the slope of the tangent vector to a trajectory is given by $\frac{d\overline{\theta}}{d\overline{x}} = \frac{a}{c}\frac{\overline{x}\ln\left(\frac{\overline{\theta}}{\overline{x}}\right)}{\overline{x} - \overline{\theta}\overline{x}^{2/3}}$ and thus is governed by the ratio $\frac{a}{c}$. The parameter d doesn't appear anymore and we see that this

parameter of the endogenous inhibition of the vasculature only impacts on the asymptotic value b but not on the shape of the phase plan. This is illustrated in the figures 9.A and 9.B where we only change d between both. We observe that the two phase plans are homotheticals.

$$a = 10, \quad c = 10, \quad d = 1 \qquad\qquad a = 10, \quad c = 10, \quad d = 0.01$$

A

B

$$a = 10, \quad c = 100, \quad d = 1 \qquad\qquad a = 100, \quad c = 1, \quad d = 1$$
$$\frac{a}{c} \ll 1 \qquad\qquad\qquad\qquad \frac{a}{c} \gg 1$$

C

D
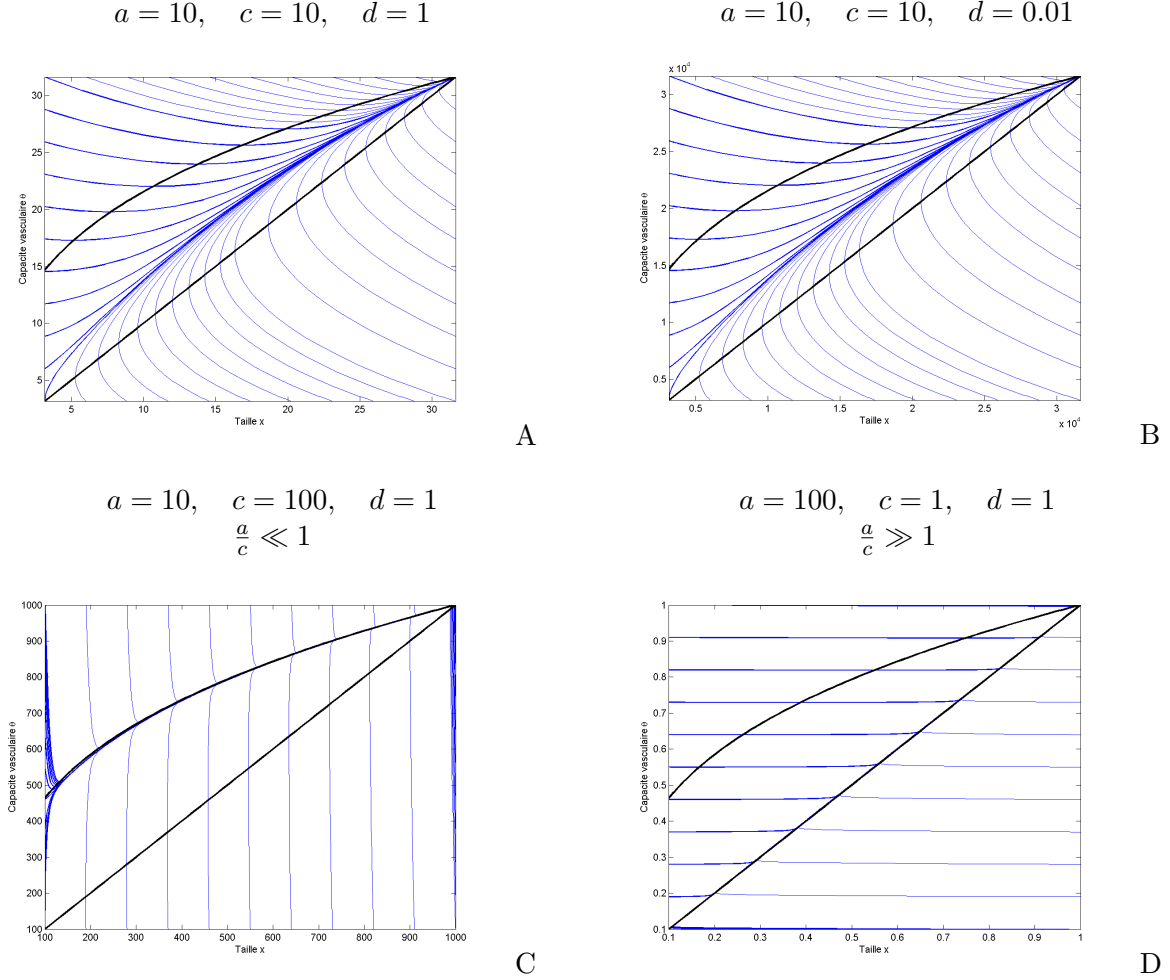
Figure 9: Various phase plans of the system (6) for different values of the parameters. The thick black curves represent the nullclines.

In the system (9), we see that the speeds of the dynamics of x and θ are respectively driven by the parameters a and c. Rescaling the time by $u = at$, we obtain

$$\left\{ \begin{array}{l} \frac{d\overline{x}}{du} = \overline{x} \log\left(\frac{\overline{\theta}}{\overline{x}} \right) \\ \frac{a}{c} \frac{d\overline{\theta}}{du} = [\overline{x} - \overline{\theta}\overline{x}^{2/3}] \end{array} \right. .$$

Hence we have a slow-fast dynamic driven by the ratio $\frac{a}{c}$. Indeed, when $\frac{a}{c}$ is very small, then the dynamic in θ is much faster than the dynamic in x and goes much faster to the equilibrium. The dynamic is then equivalent to the one of the equation

$$\left\{ \begin{array}{l} \frac{d\overline{x}}{du} = \overline{x} \log\left(\frac{\overline{\theta}}{\overline{x}} \right) \\ 0 = [\overline{x} - \overline{\theta}\overline{x}^{2/3}] \end{array} \right.$$

that is, the system evolves along the nullcline $G_2(x, \theta) = 0$. On the opposite case, when $\frac{a}{c} >> 1$, the system will evolve along the nullcline $G_1 = 0$. These two limit behaviors are illustrated in the figures 9.C and 9.D.

3.3   Anti-angiogenic therapy

The interest of the model of Hahnfeldt et al. is to enable integration of an anti-angiogenic (AA) treatment so as to be able to simulate *in silico* various AA drugs as well as various schedules for a given drug. The therapy is integrated in the model through a death term in the equation for θ in the system (6) which becomes

$$\dot{\theta}(t) = cx(t) - dx(t)^{2/3}\theta(t) - \underbrace{eg(t)\theta(t)}_{Treatment}$$

with $g(t)$ a function describing the effective concentration of the drug and e an efficacity parameter. The function $g(t)$ is given by a one-compartmental pharmacokinetic model (see section 1.4 for more details on pharmacokinetics) : $\dot{g}(t) = -clr\, g(t) + u(t)$, with clr the elimination rate of the drug and $u(t)$ the entrance debit of the drug. Considering that the drug is injected by bolus (very fast injection of the whole dose of the drug) with the same dose D at each administration, we take $u(t) = \sum_{i=1}^{N} D\delta_{t=t_i}$ where N is the total number of administrations and δ is the Dirac measure. We then get

$$g(t) = D\sum_{i=1}^{N} e^{-clr(t-t_i)}\mathbf{1}_{t \geq t_i}.$$

It is now possible to simulate the effect of various treatments and to compare with experimental data, which is done by the authors for three AA drugs : endostatin and angiostatin which are endogenous inhibitors and TNP-470 (exogenous inhibitor). These three molecules inhibit the proliferation of endothelial cells. The authors estimate the values of the parameters e and clr for each drug by fitting the model to the data, keeping the estimated values for the growth without treatment for the other parameters. The values are given in the table 3. In the figure

	TNP-470	Endostatin	Angiostatin
e $(day^{-1}conc^{-1})$	1.3	0.66	0.15
clr (day^{-1})	10.1	1.7	0.38

Table 3: Estimated values of the treatments parameters from [HPFH99]

10 we compare the three treatments and we observe that angiostatin and endostatin are able to contain the tumoral growth but not TNP-470. The fitting of the parameters gives informations on proper characteristics for each drug : for example TNP-470 seems to exhibit a high clearance. The authors then use the model to make predictions for different temporal administration protocols for endostatin and angiostatin which reveal to be in excellent agreement with their data.

Although this model has been confronted only to mice data and not human ones, and that its ability to reproduce the data has been verified only in [HPFH99], these results are very
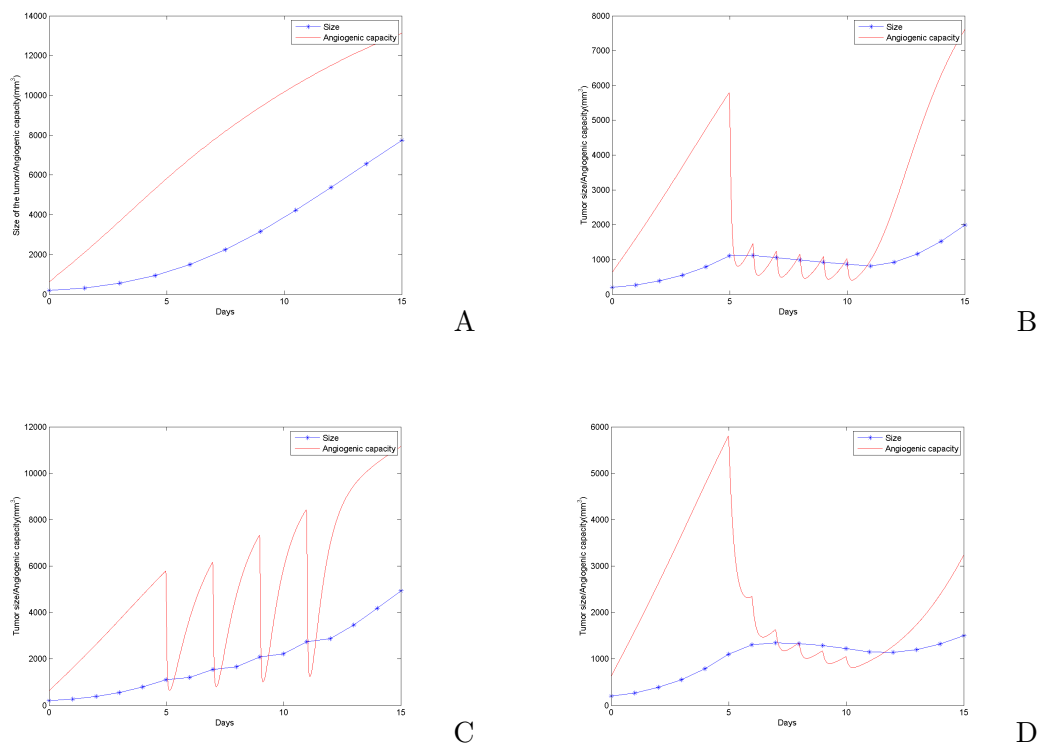
Figure 10: The different treatments from Hahnfeldt et al., with $x_0 = 200mm^3$. The therapy is administrated from days 5 to 10 (11 for TNP-470). A : without treatment. B : Endostatin, 20 mg/day. C : TNP-470, 30 mg/2 days. D : Angiostatin, 20 mg/day.

interesting and motivate the use of this model as a basis for describing tumoral growth in the perspective of the study of AA therapies.

4 Modeling of the therapy. PK - PD

This section is devoted to the modeling of the therapy and will present the basic concepts of pharmacokinetics and pharmacodynamics.

4.1 Short introduction to the principles of pharmacokinetics (PK)

The pharmacokinetics can be defined as "what the body does to the drug", compared to the pharmacodynamics dealing with "what the drug does to the body". It is the science of the elimination and distribution kinetics of drugs in the organism. Some history of the pharmacokinetics can be found in [Wag81] where we learn that the term **pharmacokinetics** first appeared in the literature in 1953 in the text "Der blütspiegel-Kinetic der Konzentrationsabläufe in der Frieslaufflüssigkeit" [Dos53], but some insights of the subject appeared years before, with the

Michaelis-Menten [MM13] equation in 1913 for describing the enzyme kinetics, which is now used for drugs effect under the name of "Emax model". It says that the effect $E([c])$ depends on the concentration $[c]$ *via* the following law :

$$E = \frac{E_{max}[c]}{c_{1/2} + [c]},$$
(10)

with E_{max} and $c_{1/2}$ two constants describing respectively the maximum effect of the drug and the concentration needed to have half of the maximum effect. The birth of what is called now the one-compartmental model dates from 1924 and is due to Widmark and Tandberg [WT24]. We cite now J. Wagner in [Wag81] : "*The word [pharmakocinetics] means the application of kinetics to* pharmakon, *the greek word for drugs and poison.* Kinetics *is that branch of knowledge which involves the change of one or more variables as a function of time. The purpose of pharmacokinetics is to study the time course of drug and metabolite concentrations or amounts in biological fluids, tissues and excreta, and also of pharmacological response, and to construct suitable models to interpret such data. In pharmacokinetics, the data are analyzed using a mathematical representation of the part or the whole of an organism*".

Most of the PK models are constructed by schematically dividing the organism between **compartments** supposed to represent for example the blood system (central compartment), the kidney (elimination compartment), the targeted organ (effect compartment), the absorption mechanism, but they don't necessarily have a biological sense and can be just fictive if the resulting models fits better the data. Each compartment has a virtual distribution volume and various exchange rates between the compartments are defined (see figure 11).
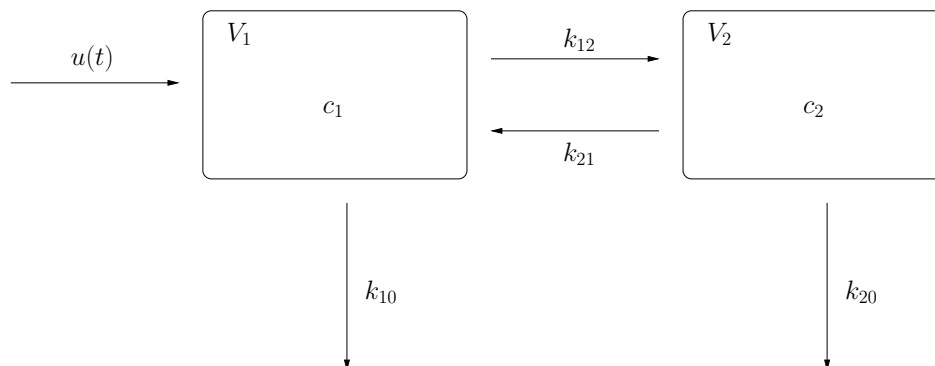
Figure 11: Schematic representation of a 2 compartmental PK model.

Population pharmacokinetics.   This discursive model is then translated into differential equations (most often linear ones), the **structural model** which depends on parameters. These parameters can vary between the patients and it is then of great importance to study statistically the distribution of the parameters in the population, the inter-individual variability. This is done by the branch of population pharmacokinetics which develops both parametric and nonparametric approaches. In the parametric approach, a statistical model is set *a priori*, like for instance the gaussian one, which depends on parameters (mean and covariance matrix in the gaussian

case). The objective is then to choose the parametric statistical model which permits the best fitting of the data and to estimate its parameters. Most of the common statistical methods used in practice are implemented in the open source software MONOLIX[9]. In the nonparametric approach, no structure is imposed on the shape of the distribution of the parameters and the goal is to directly estimate this distribution function. The mathematical difference between both is that the first one mostly reduces to finite-dimensional optimization whereas the second one has to optimize in infinite dimension. Bayesian estimation techniques permit then to use the global information of the parameters distribution in the population in order to infer the parameters of a given patient from just a few data (dosing of the concentration of the drug in the blood at a small number of times).

These statistical tools can help to identify physiological covariates (like the weight for instance) which impact on the circulating concentration of the drug, and thus to better determine the dosage which has to be used for a given patient.

We refer to [Ver10] for further details in pharmacology, in particular about the mechanisms of action of the chemotherapies, and about PKs.

4.2   Some PK models used in the sequel

In this thesis we only use linear PK models. We will now describe these models. The first one is the one used for endostatin, angiostatin and TNP-470 in [HPFH99] and was already described in the section 1.3.1. It is a simple one-comportmental model which leads to an exponential elimination of the drug.

For the Bevacizumab, we based ourselves on the publication [LBE$^+$08] which shows that the PK can be described by a two-compartmental model as the one of figure 11, in which c_1 and c_2 stand for the concentrations in the first and second compartments whose fictive volumes are V_1 and V_2. The term $u(t)$ stands for the entrance flow of drug, assumed to be injected intravenously, the exchange rates between the compartments are denoted by k_{12}, k_{21} and the elimination rate from the central compartment by k_{10}. To translate this discursive picture into equations, we use the principle of conservation of matter to write, on the quantities of matter $q_1 = c_1 V_1$ and $q_2 = c_2 V_2$:

$$\begin{cases} \frac{dq_1(t)}{dt} = -(k_{10} + k_{12})q_1(t) + k_{21}q_2(t) + u(t) \\ \frac{dq_2(t)}{dt} = -(k_{20} + k_{21})q_2(t) + k_{12}q_1(t) \end{cases}$$

which can be rewritten on the concentrations as

$$\begin{cases} \frac{dc_1(t)}{dt} = -(k_{10} + k_{12})c_1(t) + k_{21}\frac{V_2}{V_1}c_2(t) + \frac{u(t)}{V_1} \\ \frac{dc_2(t)}{dt} = -(k_{20} + k_{21})c_2(t) + k_{12}\frac{V_1}{V_2}c_1(t). \end{cases}$$

We then use $c_2(t)$ as being the effective concentration on the vasculature.

The parameters values can be found in the table 4 as well as PK models and parameters of a few cytotoxic drugs.

---

[9]http://software.monolix.org/sdoms/software/
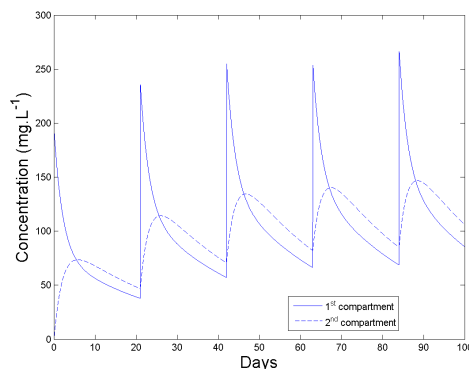
Figure 12: Time-concentration profile for the Bevacizumab according to a two-compartmental PK model. Values of the parameters are given in the table 4. We used a dose of 7,5 mg/kg (with a patient of 70 kg), injected by a 90-min intravenous injection, every three weeks (one of the protocols used in practice described in [LBE$^+$08]).

Drug	PK model	Parameters	Reference
Bevacizumab	2 comp.	V_1=2.66= V_2, k_{10}=0.0779, k_{20}=0, k_{12}=0.223, k_{21}=0.215	Lu et al., 2008 [LBE$^+$08]
Etoposide	2 comp.	V_1=25, V_2=15, k_{10}=1,6, k_{20}=0,8, k_{12}=0,4, k_{21}=0	Barbolosi et al., 2003 [BFCI03]
Temozolomide	2 comp.	V_1=1, V_2=14, k_{10} = 0, k_{20} = 9,36, k_{12}=57,6, k_{21}=0	Panetta et al., 2003 [PKG$^+$03]
Docetaxel	3 comp.	$V_1 = V_2 = V_3$=7,4, k_{10}=123,8, k_{20} = k_{30} = 0, k_{12}=25,44, k_{13}=30,24, k_{21}36,24, k_{23} = k_{32}=0, k_{31}=2,016	Meille et al., 2008 [MIB$^+$08]

Table 4: PK models and parameters for various drugs. Units : volumes in liters, elimination rates in day^{-1}.

4.3   Pharmacodynamics. Interface model

In practice, the effect of the drug is not necessarily proportional to its concentration *in situ*. The aim of pharmacodynamics is to study the relation between the effect and the concentration. We already presented the so-called "E_{max} model" (see equation (10)). In the context of hematotoxicity (= toxicity on white blood cells) induced by the chemotherapies, C. Meille, A. Iliadis, D. Barbolosi, N. Frances and G. Freyer developed in [MIB$^+$08] an interface model which connects the concentrations given by PK models to hematotoxicity of the drugs. It is designed to define an exposure variable $y(t)$ more precise and more flexible than just the AUC (Area Under the Curve) or the time spent by the drug above a threshold concentration. If $c(t)$ is the

concentration output of the PK model, the equation on $y(t)$ is given by

$$\dot{y}(t) = -\alpha e^{-\beta y(t)} y(t) + (c(t) - \gamma)^+$$

and depends on three positive parameters α, β and γ. When $\alpha = 0$ we retrieve the area under the curve over a given threshold γ. With $\beta = 0$ we get a traditional effect-compartment model.

5 Metastatic evolution

Despite the large number of models available for the tumoral growth, no consequent modeling effort has been performed for the metastatic process. As far as we know, other models besides the approach that we use in this thesis which follows directly the work of Iwata, Kawasaki and Shigesada in [IKN00] and has then been studied further mathematically by Barbolosi, Benabdallah, Hubert, Verga [BBHV09] and by Devys, Goudon and Laffitte in [DGL09], are rather few. In [SLK76], Saidel, Liotta and Kleinerman introduce a deterministic phenomenological model with a few parameters for the dynamics of the metastatic process. They use it to yield a better understanding of mouse data obtained in their laboratory and published in [LKS74]. The model takes into account the different stages of the metastatic process, namely tumor vascularization, vessel wall penetration, circulatory transport, target organ arrest and metastases formation by assigning to each stage a compartment for which a differential equation is derived. The model is able to fit the data and the authors then use it to investigate the effects of tumor external massage (reported as provoking an increase of cells release in the circulation) and tumor removal. They also investigate theoretically the effect of inhibition of the vascularization, precessing the development of anti-angiogenic drugs. The same authors also introduced another model in [LSK76], with stochastic basis. However, in both models, we remark that the authors take into account the emission of metastasis by the primary tumor but not by the metastases themselves.

We will now describe our approach (based on [IKN00, BBHV09, DGL09]) for the modeling of the metastatic evolution and how do we integrate the two-dimensional tumoral growth of the previous section in this context. The figure 13 shows a schematic description of the model in the 1D case. The resulting model is the following partial differential equation with boundary and initial conditions

$$\begin{cases} \partial_t \rho(t, X) + \operatorname{div}(\rho(t, X)G(X)) = 0 & \forall (t, X) \in]0, T[\times \Omega \\ -G \cdot \nu(\sigma)\rho(t, \sigma) = N(\sigma) \left\{ \int_\Omega \beta(X)\rho(t, X)dX + \beta(X_p(t)) \right\} & \forall (t, \sigma) \in]0, T[\times \partial\Omega \\ \rho(0, X) = \rho^0(X) & \forall X \in \Omega. \end{cases} \quad (11)$$

where $T > 0$ is an arbitrary final time. It is a linear two-dimensional transport equation with the particularity of having a nonlocal boundary condition. This type of equations, arising quite often in mathematical biology, is sometimes called "renewal equations". We refer to [MD86] for more details on the modeling philosophy in structured population dynamics and also to [Per07].

5.1 Conservation law

The main idea of [IKN00] is to consider the metastases as a population structured in size, modeled by a distribution function ρ. Here since we introduce the vascular capacity as a variable
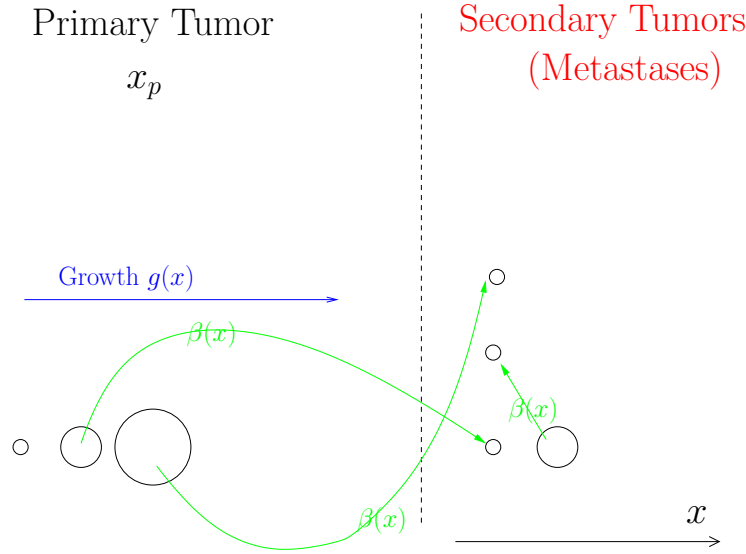
Figure 13: Schematic representation of the metastatic model in 1D.Notations : g(x)=growth rate. $\beta(x)$ = emission rate.

describing the state of a growing tumor, the population will be structured both in size x (= Volume, expressed either in number of cells or in mm^3 using the conversion 1 $mm^3 = 10^6$ cells) and vascular capacity θ (same unit as x). We consider the metastases as particles evolving according to the law of the previous section's model, that is, the trajectory $X(t) = (x(t), \theta(t))$ of each metastasis solves the following differential equation :

$$\frac{dX}{dt} = G(X), \quad G(X) = G(x,\theta) = \begin{pmatrix} ax\ln\left(\frac{\theta}{x}\right) \\ cx - dx^{2/3}\theta \end{pmatrix} = \begin{pmatrix} G_1(x,\theta) \\ G_2(x,\theta) \end{pmatrix}. \tag{12}$$

We assume that each metastasis has size bigger than x_min = the size of one cell and less than $b = \left(\frac{c}{d}\right)^{3/2}$ as it is the maximal reachable size (see proposition 1.8). We also assume that $x_{min} \leq \theta \leq b$. Thus, the metastases evolve in the following trait space

$$\Omega =]x_{min}, b[\times]x_{min}, b[$$

which is proved to be stable under the flow of (12) in the proposition 1.4. The evolution of the population of metastases is now ruled by a **density** $\rho(t, x, \theta)$, or $\rho(t, X)$ with $X = (x, \theta)$ which, for all t is a function in $L^1(\Omega)$ and has unit Number of metastases/Size^2 (notice that the vascular capacity θ has the unit of a size). This means that, if ω is a measurable subset of Ω

$$\text{Number of metastases in } \omega \text{ at time } t = \int_\omega \rho(t, X)dX.$$

Remark 1.11 (Density)**.** *To precise the notion of density, the number of metastases at time t can be viewed as a measure $\mu(t)$ on Ω, through : Number of metastases in ω at time $t = \mu(t)(\omega)$. We are thus implicitly assuming that this measure is absolutely continuous regarding to the Lebesgue measure which thanks to the Radon-Nykodim theorem implies that there exists a $L^1(\Omega)$*

function $\rho(t)$ such that $\mu(t) = \rho(t)\lambda$, where λ stands for the Lebesgue measure in $\mathbb{R}^2$. This assumption does not seem biologically obvious but a lot of what follows could be done considering ρ as a measure.

To describe the time evolution of the population, we use the transport theorem allowing to pass from the Lagrangian description of the evolution of the system (which follows each particle according to (12)) to the Eulerian one describing the evolution of the density ρ.

Theorem 1.12 (Transport theorem)**.** *Let $X(t;y)$ be the flow of the equation (12) and ω a measurable subset of Ω. Denote by $\omega_t = X(t;\omega)$. For all $\rho \in \mathcal{C}^1(\mathbb{R} \times \Omega)$,*

$$\frac{d}{dt}\int_{\omega_t} \rho dX = \int_{\omega_t} (\partial_t\rho + \mathrm{div}(\rho G))\, dX.$$

Proof. The proof is based on the change of variables formula and the fact that if we denote $J(t,y) = \det(D_yX(t;y))$, we have

$$\partial_t |J(t,y)| = \mathrm{div}(G)|J| \tag{13}$$

(see the proof below). Thus we can compute

$$
\begin{aligned}
\frac{d}{dt}\int_{\omega_t} \rho(t,X)dX &= \frac{d}{dt}\int_\omega \rho(t,X(t,y))J(t,y)dy \\
&= \int_\omega \partial_t\rho(t,X(t,y)) + G(X(t,y))\cdot\nabla\rho(t,X(t,Y))J(t,y) + \rho(t,X(t,y))\partial_t J(t,y)dy \\
&= \int_{\omega_t} (\partial_t\rho(t,X) + \mathrm{div}(\rho G))\, dX
\end{aligned}
$$

which proves the result. To prove the identity (13), we use that $D_yX(t;y)$ solves the following problem

$$
\begin{cases}
\frac{\partial}{\partial t}D_yX(t;y) = DG(X(t;y))D_yX(t;y) \\
X(0;y) = Id
\end{cases}
$$

to compute, using the fact that the determinant is an alternating multilinear form and denoting X_1, X_2 the components of X

$$
\begin{aligned}
\partial_t J &= \partial_t \det(\nabla_y X_1, \nabla_y X_2) = \det(\nabla G_1 \cdot D_yX, \nabla_y X_2) + \det(\nabla_y X_1, \nabla G_2 \cdot D_yX) \\
&= \det(\partial_{y_1}G_1\nabla_y X_1 + \partial_{y_2}G_1\nabla_y X_2, \nabla_y X_2) + \det(\nabla_y X_1, \partial_{y_1}G_2\nabla_y X_1 + \partial_{y_2}G_2\nabla_y X_2) \\
&= \mathrm{div}(G)J
\end{aligned}
$$

Then, since $X(t;\cdot)$ is a $\mathcal{C}^1$-diffeomorphism for all t, it has a sign and thus $|J|$ is differentiable and we have $\partial_t|J(t,y)| = \mathrm{sgn}(J(t,y))\mathrm{div}(G(X(t;y)))J(t,y) = \mathrm{div}(G(X(t;y)))|J(t,y)|$. $\qquad\square$

This theorem allows us, thanks to the following **conservation law** : for all $\omega \subset \Omega$

$$\frac{d}{dt}\int_{\omega_t} \rho\, dX = 0,$$

to obtain the transport equation on the density

$$\partial_t\rho + \mathrm{div}(\rho G) = 0. \tag{14}$$

5.2   Boundary condition. Renewal equation

So far, we have modeled the growth process of the metastases and now we integrate the emission process of new metastasis, which has two sources : emission by the primary tumor and emission by the metastasis themselves. The rate of new metastases arriving in the system is given by, using the Stokes theorem

$$\frac{d}{dt}\int_{\Omega}\rho(t,X)dX = -\int_{\Omega}\operatorname{div}(\rho(t,X)G(X))dX = -\int_{\partial\Omega}\rho(t,\sigma)G(\sigma)\cdot\nu(\sigma)d\sigma$$

where we denoted by ν the external unit normal vector to the boundary $\partial\Omega$ which exists almost everywhere since Ω is a square. Notice that the last term is non-negative since $G(\sigma)\cdot\nu(\sigma)\leq 0$, $\forall t>0$, $a.e.\,\sigma\in\partial\Omega$ from expressions (12), expressing the fact that there are no metastase leaving the system. We also assumed that ρ is regular enough to have a trace on the boundary. We denote by $\mathbf{b}(\sigma,x,\theta)$ the birth rate of new metastasis with size and angiogenic capacity $\sigma\in\partial\Omega$ by metastasis of size x and angiogenic capacity θ per unit time, and by $f(t,\sigma)$ the term corresponding to metastases produced by the primary tumor. Expressing the equality between the number of metastasis arriving in Ω per unit time and the total rate of new metastasis created by both the primary tumor and metastasis themselves, we should have for all $t>0$

$$-\int_{\partial\Omega}\rho(t,\sigma)G(\sigma)\cdot\nu d\sigma = \int_{\partial\Omega}\int_{\Omega}\mathbf{b}(\sigma,X)\rho(t,X)dX + f(t,\sigma)d\sigma. \qquad (15)$$

We assume that the emission rates of the primary and secondary tumors are equal and thus take $f(t,\sigma) = \mathbf{b}(\sigma,X_p(t))$ where $X_p(t)$ represents the primary tumor and solves the ODE system (12) endowed with initial conditions. An important feature of the model is to assume that **the vasculature of the neo-metastasis is independent from the one which emitted it**. The assumption is that the newly created metastases settle in a new environment which has no link with the one of the metastasis which emitted it. There is no apparent reason for a cell which detach from a tumor to carry with it some vasculature of this tumor. The place where the neo-metastasis settles is independent from the place it comes from. Though, there is no experimental data which support this hypothesis, up to our knowledge. Mathematically, this means that there exists a function $N:\partial\Omega\to\mathbb{R}$ and a function $\beta:\Omega\to\mathbb{R}$ such that

$$\mathbf{b}(\sigma,X) = N(\sigma)\beta(x,\theta).$$

The function β is the emission rate of new metastasis per tumour per unit time and N is their distribution at birth.
We also assume that newly created metastases have size $x=1$ cell, in view of the following remarks

1. The passing vascular holes by which a metastasis pass to escape from the tumor have diameter of order 100 nanometers. It is hard to imagine that more than one cell (whose typical size is the micrometer) could pass through such a small hole.

2. If the cells detach from the tumor, it means that the cadherin (transmembrane proteins responsible for cell-cell adhesion) rate falls. Thus it seems unlikely that the cells lose cadherins from one side and keep sufficient to form a cluster on the other side.

3. Even in the assumption of the detachment of a cluster of cells, it would be composed of at most a dozen of cells since 1 and the hypothesis of size 1 cell for the neo-metastasis would stay in a convenient approximation. We also assume that there is no metastasis of maximal size b nor maximal or minimal angiogenic capacity because they should come from metastasis outside of Ω since G points inward all along $\partial\Omega$.

This implies that the support of N is included in $\{\sigma \in \partial\Omega; \ \sigma = (x_{min}, \theta), \ x_{min} \leq \theta \leq b\}$. Although we have no reference to provide about the shape of the angiogenic birth distribution of the metastases, we assume it to be uniformly centered around a mean value θ_0, thus we take

$$N(x_{min}, \theta) = \frac{1}{2\Delta\theta}\mathbf{1}_{\theta\in[\theta_0-\Delta\theta,\theta_0+\Delta\theta]},$$

with $\Delta\theta$ a dispersion parameter of the new metastasis around θ_0. However, any other expression could be considered for N (for example a gaussian distribution) provided it has integral 1 without affecting the analysis of part II. Using that equation (15) should be verified for each subset of the boundary, we obtain the boundary condition of (11), namely

$$-G \cdot \nu(\sigma)\rho(t,\sigma) = N(\sigma)\left\{\int_\Omega \beta(X)\rho(t,X)dX + \beta\left(X_p(t)\right)\right\}$$

which, coupled with the transport equation (14) and an arbitrary initial condition gives the problem (11).

Following the modeling of [IKN00] for the colonization rate β we take

$$\beta(x,\theta) = mx^\alpha.$$

This colonization rate only accounts for the detaching cells which effectively give rise to a metastase, i.e. which were able to escape the tumor and to survive all the adverse events along the metastatic process. The parameter m is the colonization coefficient and α the so-called fractal dimension of blood vessels infiltrating the tumor. The parameter α expresses the geometrical distribution of the vessels in the tumor. For example, if the vasculature is superficial then α is assigned to $2/3$ thus making x^α proportional to the area of the surface of the tumor (assumed to be spheroidal). Else if the tumor is homogeneously vascularized, then α is supposed to be close to 1. The parameter m can be interpreted as an intrinsic metastatic aggressiveness of the cancer. These two parameters are of fundamental importance as they are expected to capture the metastatic behavior of a given patient.

Remark 1.13.

- *We have assumed that both metastases and primary tumor grow with the same velocity G. This is arguable, for example by the fact that metastases could have the tendency to be more aggressive and grow faster since their cells have underwent more mutations than the initial cell of the primary tumor. Moreover the velocity growth of a metastase can differ depending on its location (lung, brain, skeleton...). Changing the velocity for the primary tumor can be easily done by modifying the source term $f(t,\sigma)$ and we could consider different growth velocities by compartmenting the metastatic population.*

- *We have chosen to take β independent of θ meaning that the emission rate of a tumor depends only on its size and not on its vasculature. We are aware that this is not biologically true since the vasculature plays a fundamental role in escaping the tumor area for detaching cells. Though, we made this assumption in order to keep the model as simple as possible and do the following remarks :*

  a) *with this approach, angiogenesis does impact on metastatisation but indirectly, via accelerating the growth. Thus, in the perspective of anti-angiogenic treatment, the treatment would also reduce the number of emitted metastases.*

  b) *Choosing an expression of β involving θ would not affect the following mathematical analysis.*

  c) *Taking β dependent on θ would certainly require the addition of a parameter to the model, which we want to avoid as most as possible.*

  d) *We performed simulations with a θ-dependent β and they didn't conclude to a better flexibility of the model.*

- *Unlike the previous point, the assumption that $\mathbf{b}(\sigma, X) = N(\sigma)\beta(X)$ is crucial in the mathematical analysis that we perform in the following part. Up to now, we don't know if the theory could be adapted to a general $\mathbf{b}(\sigma, X)$.*

5.3   Integration of a treatment in the metastatic model

In order to take into account for an anti-cancer therapy and more particularly for anti-angiogenic (AA) treatments, we modify the growth function $G(X)$ in adding a killing term on the vasculature as done by Hahnfeldt et al. in [HPFH99]. This deals with the AA drug and we also put a killing term on the tumoral cells to model the action of a cytotoxic drug. The evolution of each tumor is then described by the differential system

$$\begin{cases} \frac{dx}{dt} = G_1(t,x,\theta) = ax\ln\left(\frac{\theta}{x}\right) - h\gamma_C(t)(x - x_{min})^+ \\ \frac{d\theta}{dt} = G_2(t,x,\theta) = cx - d\theta x^{\frac{2}{3}} - e\gamma_A(t)(\theta - \theta_{min})^+, \end{cases} \tag{16}$$

where h and e are efficacy parameters of the cytotoxic and AA drugs respectively, $\gamma_C(t)$ and $\gamma_A(t)$ are functions describing the time evolution of the effective concentration of the drugs on their respective targets (see the section 1.4 for details on their expressions). The parameters x_{min} and θ_{min} are minimal values for the drug to be active (we consider that if the tumor is too small, then the drug is not effective) and $y^+ = \frac{1}{2}(|y| + y)$ or a regularization of this function if needed to avoid regularity issues (for example $y \mapsto y(1/2 + 1/2\tanh(y/K))$ with K being a parameter controlling the slope in zero). In practice, we think about $x_{min} = \theta_{min} = 1$ which is the minimal biologically relevant value in terms of number of cells (or $x_{min} = \theta_{min} =$ the minimal size of a tumor = the size of one cell). From a mathematical point of view, this ensures that the solutions of (16) stay in Ω for all time. We will still denote $G(t, X)$ the vector field $(G_1(t, X), G_2(t, X))$ in the following, indicating through the time dependence that the growth dynamic is perturbed by the action of a therapy. The equation on the evolution of the density of metastases then becomes

$$\begin{cases} \partial_t\rho(t,X) + \operatorname{div}(\rho(t,X)G(t,X)) = 0 & \forall(t,X) \in]0,T[\times\Omega \\ -G \cdot \nu(t,\sigma)\rho(t,\sigma) = N(\sigma)\left\{\int_\Omega \beta(X)\rho(t,X)dX + \beta(X_p(t))\right\} & \forall(t,\sigma) \in]0,T[\times\partial\Omega \\ \rho(0,X) = \rho^0(X) & \forall X \in \Omega \end{cases} \tag{17}$$

and the action of the treatment is taken into account in the velocity field of this transport equation, which still points inward all along the boundary using the assumption that the therapy is ineffective for tumors with size $x = 1$ or vascular capacity $\theta = 1$. Notice that in particular, the treatment does not appear as a killing term in this equation. In view of the mathematical analysis, the difference between the equation (17) and (11) is the fact that the latter is an **autonomous** equation, whose analysis is performed in the chapter 4 while the former is a **non-autonomous** one (mathematical and numerical analysis in the chapter 5).

Chapter 2

An example of a mechanistic model for vascular tumoral growth

In this chapter, we describe some work in collaboration with Floriane Lignet, Benjamin Ribba, F. Billy, Thierry Colin and Olivier Saut initiated during the CEMRACS (Centre d'Eté Mathématique de Recherche Avancée en Calcul Scientifique) at the summer of 2009, as part of the Angio project. The objectives of the project were to couple a multiscale mecanistic spatial model of vascular tumor growth previously developed in [RCS10, RSC$^+$06, BRS$^+$09] with a molecular model of intracellular pathways intervening in angiogenesis established by Floriane Lignet during her Master 2's practice, and to use then the model to investigate the problem of combination of a chemotherapy and an anti-angiogenic drug.

We will first very briefly review mechanistic modeling in the section 2.1, then present the model that we take from Billy et al. [BRS$^+$09] as well as the improvements that we did in the section 2.2, shortly describe the simulation techniques used to numerically solve the model in the section 2.3 and then present interesting simulation results regarding to the combination of chemotherapy and anti-angiogenic drugs in the section 2.4.

1 A very short review of mechanistic modeling

We begin with a very short description of the extensive literature on mechanistic models of tumoral growth. A history of the mathematical modeling of solid tumor growth is presented by Araujo and McElwain in [AM04], where it is stated that the first models of cancer growth appeared in the 1930's, but were really impulsed by the seminal work of Greenspan in the 1970's (see for example [Gre72]). Two problems that drive the development of mathematical approaches are :

1. Explain the empirically observed slowdown of the tumoral growth. Indeed, the growth typically starts with an exponential phase which then goes to a linear one.

2. Understand the passing from non-growing, stable, benign tumor (adenoma, or carcinoma *in situ*) to an invasive, growing, malignant tumor.

Models of multicellular spheroids were developed, splitting the malignant cells between two (or more) types : proliferative and non-proliferative cells. The development of a necrotic core in the tumor was then advanced as an explanation for the problem 1 (for recent work on necrosis, see for example [FGG11]). Mechanistic modeling of cancer became a very active field in the 1990s, with more publication in this decade than in the previous years combined according to [AM04]. The models started to integrate cell migration within the tumor and more complex structures where modeled such as "tumor cords" (accumulation of cancerous cells around a blood vessel implying change from spherical to cylindrical symmetry) [BG00, BFGS08] to go beyond spheroid models which are valid as experimental *in vitro* models but fail for *in vivo* situations where vascular growth has to be more deeply described. A novel approach appeared, describing the neoplastic tissue as a continuum medium composed of various phases, with analogy to multiphasic fluids. The velocity of each phase is then retrieved by mechanical considerations, for example deriving from a pressure gradient (Darcy's law).

Another approach consists in using reaction-diffusion equations to describe tumoral invasion of healthy tissue as a propagating front. A good example of such a model is provided by Gatenby and Gawlinski in [GG96] where the model investigates a novel biological hypothesis, namely that invasion is mediated by a bigger acidity of the tumoral tissue. The authors then perform experiments to confirm their hypothesis and propose the use of a critical parameter of the model as a prognostic tool for aggressiveness of a given patient's cancer. On the value of this parameter depends the type of the tumor, from benign to malignant, thus providing an answer to problem 2, driven by the mathematical approach. It is worth noting that this model is relatively simple, with only few parameters which the authors could find either in the literature or obtain through fitting to data.

In [Fri04], Friedman proposes a unification of various models of cancer growth and their mathematical challenges. The models assume spherical symmetry and consist eventually in free boundary problems where evolution of the tumor is reduced to evolution of the boundaries between the phases and the boundary of the tumor itself. These boundaries result principally from level-sets of the nutrient concentration (most often reduced to oxygen only) which diffuses from the external environment and is consumed by the cells. The principal mathematical problem beyond establishing the well-posedness of the model is to investigate the stability of an equilibrium point which represents a dormant state of the tumor. The dependency of this stability

on critical parameters of the system offers an answer to problem 2 : if the equilibrium is stable then the tumor will not grow beyond this size whereas if there is no nontrivial stable equilibrium point the tumor will show unlimited growth.

The integration of the cell-cycle dynamic is also taken into account, through age-structured models (see for example [BBCRP08]).

While all these models are often concerned only with avascular tumor growth, recent models take into account the angiogenesis process, offering new insights to the problem 1 (see [MWO04] for a review). In [OAMB09], Owen, Alarcon, Maini and Byrne develop a complex model of angiogenesis which takes into account for the normalisation process of the vasculature described by [Jai01]. The model is hybrid since it integrates continuous variables as well as discrete stochastic rules for the evolution of the cells (cellular automaton). They perform simulations giving rise to various situations depending on the balance between angiogenesis and vessel pruning.

A particular feature of cancer modeling explaining the large interest of the mathematical modeling community for this topic is the fact that the cancer is a perfect example of a biologic complex system, requiring systemic analysis and thus a multiscale approach, with various interactions between the involved levels (molecular, cellular, tissular, ...). In this context, the work of H. Byrne and coworkers has to be mentioned (see for example [BvLO⁺08]). Other mechanistic models of tumoral growth can be found in [BCG⁺10, RSC⁺06, RCS10, BRS⁺09, HGM⁺09]. See also [LFJ⁺10] for a recent impressive review of continuous models as well as discrete and hybrid ones, focusing on the morphology (spatial shape) of tumor development. Although it represents an important part of mechanistic models, we have not mentioned the cellular automaton approach since we did not study this part of cancer modeling. Let us only mention [EAC⁺09] for an interesting application of such a model on the cancer stem cell hypothesis.

2   Model

The model originally designed by B. Ribba, T. Colin and S. Schnell in [RCS10] included three scales : genetic, cellular and tissular and was used for application to analysis of irradiation therapies, with the aim to rationalize the comprehension of avascular tumor growth and to help designing more efficient radiotherapy protocols. In [RSC⁺06], the genetic level is dropped. The model is designed to investigate *in silico* the clinical failure of metalloproteinases[10] inhibitors, through identifying critical parameters in the efficacy of cytostatic inhibitors of metalloproteinases. In the PhD thesis of Frederique Billy [Bil09] (see also [BRS⁺09]), the model is enriched to take into account for angiogenesis and vascular growth in order to investigate anti-angiogenic treatments (endostatin in this case). The model is able to reproduce a so-called rebound effect after anti-angiogenic therapy which shows the complexity of determining the best dose and time administration protocol. We will use this model as a basis : most of the feature that we use are taken from it. Our aim is twofold :

1. Integrate an intra-cellular scale in the model for the VEGF pathways (F. Lignet master's thesis work).

---

[10]Metalloproteinases are enzymes produced by cancer cells which degrade the basal membrane and the extra-cellular matrix allowing cancer invasion

2. Investigate the combination of anti-angiogenic (AA) therapy and chemotherapy (CT), in particular the balance between the decrease of delivery of the drug due to vessel disruption and the "normalization effect" (also called "vascular pruning") of the vasculature after AA therapy.

We present now the modeling as well as some interesting simulation results.

Two scales are involved here : molecular (intra-cellular pathways activated by the VEGF) and tissular (spatio-temporal dynamic of tumoral and endothelial cells densities). The main improvement of the model and novelty of our work compared to the one of [BRS$^+$09], besides the coupling with the molecular model, is to introduce a **quality of the vasculature**, in order to take into account for the normalization process described in [Jai01]. A schematic description of the model can be find in the figure 1, a summary of the macroscopic model equations in the table 1 and of the macroscopic parameters in the table 2. The following is organized as follows : we first describe the mechanistic model of tumor growth in 2.2.1, then the model for angiogenesis in 2.2.2 and the integration of treatments in 2.2.3. The main novelties in the modeling with respect to Billy et al. [BRS$^+$09] are the paragraphs on the molecular model and the quality of the vasculature in the angiogenesis section.
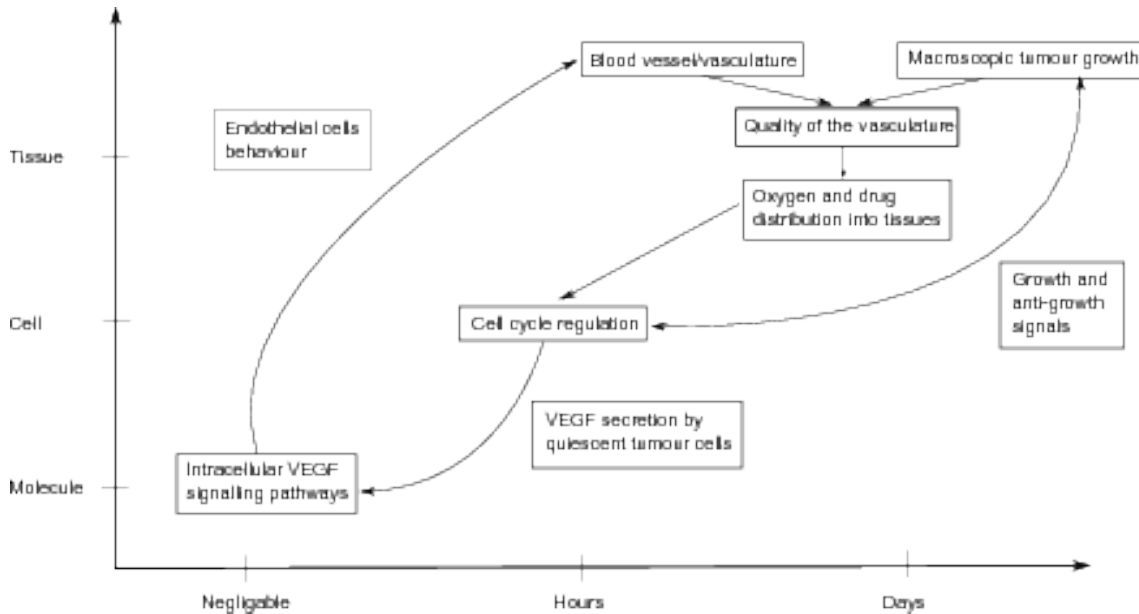
Figure 1: Schematic description of the model

The variables involved are **densities** (volumic fractions) of cells, and **concentrations** of chemical entities. For most of them, the dynamic will be modeled by partial differential equations written in the plan $\mathbb{R}^2$ and thus will most often not be endowed with boundary conditions.

2.1 Model of tumor growth

The tissue is considered as a **multiphasic fluid**, each phase corresponding to a phase of the cellular cycle. The densities of proliferating cells (phase G1 or G2) are structured in age a to

take into account for the progression during the cell cycle. The different variables involved and their corresponding equations are :

- The density $P_1 = P_1(t, a, x, y)$ of **cells in phase** $G1$. The cells are advected with a velocity $\mathbf{v_{P_1}}$ in space and evolve in age inside $G1$ phase with constant speed 1. Writing the conservation of the mass we obtain the equation :

$$\partial_t P_1 + \partial_a P_1 + \mathrm{div}(\mathbf{v_{P_1}} P_1) = 0 \tag{1}$$

- The density $P_2 = P_2(t, a, x, y)$ grouping **cells in phases** $S, G2$ **et** M. The cells are advected with a velocity $\mathbf{v_{P_2}}$ in space and evolve in age in phase $G2$ with constant speed 1. The equation is :

$$\partial_t P_2 + \partial_a P_2 + \mathrm{div}(\mathbf{v_{P_2}} P_2) = 0 \tag{2}$$

- The density $Q = Q(t, x, y)$ of **cells in the quiescent phase** $G0$, not structured in age since cells in this phase are blocked in the cycle. The cells are advected with a velocity $\mathbf{v_Q}$ in space. The entrance and exit of the phase $G0$ depend on two external conditions : overcrowding (local excess of cells) and hypoxia (lack of oxygen), which are modeled by two functions : f representing low-hypoxia and overcrowd, and g representing high-hypoxia. The expressions of these two functions are :

$$f(x, y, t) = \begin{cases} 1 & \text{if } \int_0^{a_{max,P_1}} P_1(t, a, x, y)da + 2\int_0^{a_{max,P_2}} P_2(t, a, x, y)da + Q(t, x, y) \leq \tau_0 \\ & \text{and } [O_2](t, x, y) \geq \tau_{1,h} \\ 0 & \text{else} \end{cases},$$

where a_{max,P_1} and a_{max,P_2} are the durations of phase G1 and phases S,G2 and M respectively, $[O_2]$ is the local concentration of oxygen and $\tau_{1,h}$ is the threshold of low hypoxia. The function g is given by

$$g(x, y, t) = \begin{cases} 1 & \text{si } [O_2] \geq \tau_{2,h} \\ 0 & \text{else} \end{cases}$$

with $\tau_{2,h} \leq \tau_{1,h}$ is the threshold of high-hypoxia. The density Q receives the cells from the end of the phase $G1$ if external conditions quite bad (overcrowd and moderate hypoxia, ie $f \geq 1$). These cells all go to the beginning of phase $SG2M$ when external conditions improve, regarding to the criteria represented by function f (the $[\partial_t f]^+$ term in the equation), and go to apoptosis if the hypoxia becomes too high (the $[\partial_t g]^-$ term in the equation).

The equation is [11] :

$$\partial_t Q + \text{div}(\mathbf{v_Q} Q) = g(1-f)P_1(a = a_{max,P_1}) - [\partial_t f]^+ Q(t^-) + [\partial_t g]^- Q(t^-) \qquad (3)$$

- The density $A = A(t, x, y)$ of **cells in the apoptotic phase**, neither age-structured. The cells are advected with a velocity $\mathbf{v_A}$ in space. When hypoxia is high, the cells in the end of phase $G1$ go directly to apoptosis, at the exact moment when this high-hypoxia occurs. The equation is :

$$\partial_t A + \text{div}(\mathbf{v_A} A) = (1-g)P_1(a = a_{max,P_1}) - [\partial_t g]^- Q(t^-) \qquad (4)$$

- The **boundary condition in age** for P_1 reflects mitosis and for P_2 the passing through the check point at the end of P_1 : if external conditions are satisfactory cells at then end of phase P_1 go to phase P_2. It also models reentering in the cycle of quiescent cells at the moment where conditions go to unfavorable to favorable. These boundary conditions are given by :

$$\begin{cases} P1(a = 0) = 2P2(a = a_{max,P2}) \\ P2(a = 0) = fP1(a = a_{max,P1}) + [\partial_t f]^+ Q(t^-) \end{cases} \qquad (5)$$

- Equation of the **spatial velocity v**. In order to complete the system, we need to describe the velocity fields that we have in equations (1), (2), (3) and (4). The velocity here is the velocity resulting from the fact that cells push each other. To derive the equation, we follow the approach of [AP02] and formulate four hypothesis:

  1. The velocities are the same in each phase :

  $$\mathbf{v}_\phi = \mathbf{v} \quad \forall \phi, \ \phi = P_1, \ P_2, \ Q, \ A$$

  2. Darcy's Law, which is the fact that the velocity is derived from a potential which we assimilate to a pressure p. We have :

  $$\mathbf{v} = -k\nabla p, \qquad (6)$$

  with $k = k(x, y)$ a permeability coefficient.

---

[11]This equation might seem a bit astonishing due to the terms $[\partial_t f]^+$ and $[\partial_t g]^-$ which are not regular functions but rather measures as they are the derivatives of piecewise constant functions. To understand better what does the equation means and that it models what we want, forget the spatial dependence and consider just a case for which $f(t) = \mathbf{1}_{t \geq t^*}$, meaning that the external conditions go from the unfavorable to the favorable situation at time t^*. Then $[\partial_t f]^+ = \delta_{t=t^*}$, the Dirac mass at time t^*. Consider then the Cauchy problem

$$\begin{cases} \partial_t Q = -\delta_{t=t^*} Q(t^-) \\ Q(0) = 0 \end{cases}$$

in the sense of distributions, with $Q(t^-) = \lim_{\substack{s \to t \\ s < t}} Q(s)$, which exists since Q is a BV function. Then $Q(t) = Q_0 \mathbf{1}_{t \leq t^*}$ solves the Cauchy problem, which is adequate since we want that all the quiescent cells reenter the cell cycle at the moment where the conditions go from unfavorable to favorable.

3. Saturation of the medium. We take into account some healthy tissues H that includes all the non-cancerous tissues. So, the space not filled by cancer cells is filled by H : there is **saturation** of each infinitesimal control volume. The healthy tissue is advected at the same velocity $\mathbf{v}$ and the equation is then :

$$\partial_t H + \text{div}(\mathbf{v}H) = 0 \tag{7}$$

4. The volume occupied by the endothelial cells is negligible.

Using the last two hypothesis, we get

$$\int_0^{a_{max,P_1}} P_1 da + \int_0^{a_{max,P_2}} P_2 da + Q + A + H = N_{max} \tag{8}$$

with N_{max} being a constant, the maximal number of cells per volume unit. Eventually, we sum the equations (1) (2) (3) (4) and (7), then by integrating in age and using (8), we get :

$$\text{div}(\mathbf{v}) = P_2(a = a_{max,P_2}).$$

And with the second hypothesis, the equation on the pressure :

$$-\text{div}(k\nabla p) = P_2(a = a_{max,P_2}) \tag{9}$$

Remark 2.1. *Assumption 4 is arguable. If we don't take it into account, the calculus are changed. Setting $N = \int_0^{a_{max,P_1}} P_1 da + \int_0^{a_{max,P_2}} P_2 da + Q + A + H$, $Source(E) = \tau E(1 - \frac{E}{N_{max}}) - aE$ and $\mathbf{v}_E = \chi(1 - \frac{E}{N_{max}})(1 - \frac{\sum n_\phi}{N_{max}})$ (see below the equations on the endothelial cells), we get*

$$\mathbf{v} \cdot \nabla N + N\text{div}(\mathbf{v}) = -\text{div}(\mathbf{v}_E E) + Source(E) + P_2(a = a_{max,P_2}),$$

and the equation on the pressure becomes :

$$-\text{div}(k\nabla p)N - k\nabla p \cdot \nabla N = -\text{div}(\mathbf{v}_E E) + Source(E) + P_2(a = a_{max,P_2}).$$

2.2   Model of angiogenesis

Molecular model

This part of the model is the result of the master 2's work of Floriane Lignet and is reproduced here for sake of completeness. A summary of the model equations is in the table 3 and the parameters values can be found in table 4. The molecular model describes the mechanism activated by binding of VEGF to its receptor, the VEGFR-2, at the surface of endothelial cells. This binding leads to the phosphorylation of tyrosine residues on the intracellular part of the receptor. This can activate cytoplasmic proteins, and triggers signaling pathways. The PLCy1/PKC/MAPK pathway stimulates the cell proliferation, the p38/MAPKAPK/Hsp27 pathway activates the cell migration and the PI3K/Akt pathway improves the resistance to apoptotic signals, enhances the vessels permeability and stimulates the cell growth.

The dynamic of the molecular system in translated by a system of ordinary differential equations, with the following hypothesis :
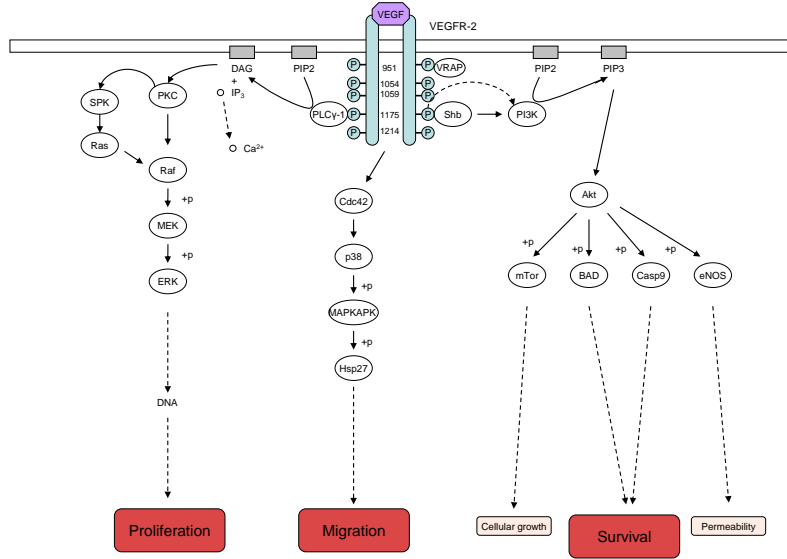
Figure 2: Schematic representation of the molecular model

- the molecular concentration are continuous,

- reactions happen in a homogenous medium, in a volume large enough

- reactions are deterministic.

We associate to each molecule a differential equation that describes the dynamic of its concentration over the time :

$$\frac{dc_i}{dt} = \sum v_{prod,c_i} - \sum v_{cons,c_i}$$

with v_{prod,c_i} and v_{cons,c_i} the speed of reaction producing and consuming the molecule c_i, the sum being taken over all reactions where c_i is involved. For each reaction, we define its speed according to the reaction type, and consider it either as a production or consumption speed for each molecule involved.

- For reversible reactions, like complexes formation $A + B \leftrightarrow AB$ the velocity is given by :

$$v = k_1[A][B] - k_{-1}[AB]$$

- For irreversible reaction, like formation of new products $A \rightarrow B$ the velocity is described by a sigmoidal equation :

$$v = \frac{V_{max}[A]}{K + [A]},$$

with V_{max} the maximal speed of the reaction, and K the amount of molecule A needed to have half of the maximal speed.

Theoretical outputs are associated to this model that represent the effect of the stimulation by VEGF of several cell mechanisms. We define outputs for proliferation (p_r), migration (χ) and resistance to apoptotic signals (a) as functions of the VEGF concentration $[V]$ which is the input of the molecular model. They are all taken as sigmoidal functions of the concentration of the end molecule in the pathway :

$$p_r\left([V]\right) = Sigmo(ERK), \quad \chi\left([V]\right) = Sigmo(Hsp27), \quad a\left([V]\right) = Sigmo(BAD + Casp9).$$

The values of these outputs are taken at the equilibrium, considering that the molecular dynamics are faster than the tissular ones. An example of explicit expression for the sigmoidal function can be :

$$Sigmo(z) = \frac{k_0 + k_1}{2} - \frac{k_0 - k_1}{2} \tanh\left(\frac{z - N_{50}}{K_{50}}\right)$$

with k_0 and k_1 the values in $-\infty$ and $+\infty$ respectively, N_{50} the threshold value and K_{50} controlling the slope of the curve at this threshold.

Endothelial cells dynamics

To reproduce the angiogenic process, we use the model of F. Billy et al. [BRS$^+$09] and divide the endothelial population into two different kinds of cells. The first one, called **unstable endothelial cells** which density is denoted by E has the following properties :

- Due to VEGF stimulation, it **proliferates** with a rate $p_r([V])$ that depends on the concentration of VEGF in a way given by the molecular model. Moreover, this proliferation is limited by the environmental conditions with a logistic law with parameter N_E as carrying capacity.

- The unstable endothelial cells are sensitive to **apoptotic signals** with a rate $a_E([V])$ computed from the molecular model.

- They undergo a **chemotaxis process** resulting in migration up along the gradient of VEGF. The migration coefficient $\chi([V])$ is also given by the molecular model. This coefficient is limited in a logistic way (carrying capacity N_{max}) when the number of endothelial cells is two high, thus expressing the affinity of endothelial cells one to each other.

- They **maturate** to become **stable endothelial cells**, when the total number of endothelial cells is bigger than a given threshold τ_E, with a rate μ. This models the formation of efficient vessels when the number is large enough.

The equation resulting from all these assumptions is :

$$\partial_t E + \underbrace{\operatorname{div}(\chi([V])E(1 - \frac{E}{N_{max}})\nabla[V])}_{chemotaxis} = \underbrace{p_r([V])E(1 - \frac{E + Es}{N_E})}_{proliferation} - \underbrace{a([V])E}_{apoptosis} - \underbrace{\mu([V])\mathbf{1}_{(E+Es \geq \tau_E)}E}_{maturation}$$
(10)

Then we have the **stable endothelial cells**, denoted by Es which are created by maturation of the unstable ones. They are able to supply oxygen to the tumor, and are more resistant

to apoptotic signals (meaning $a_{Es} \geq a$). The equation describing the time evolution of their density is the following EDO :

$$\frac{d}{dt}Es = \underbrace{\mu \mathbf{1}_{(E+Es \geq \tau_E)}E}_{maturation} - \underbrace{a_{Es}Es}_{apoptosis} \tag{11}$$

Quality of the vasculature

Here we introduce one of the main novelty comparing to [BRS$^+$09] : the introduction of a so-called quality of the vasculature. To describe the fact that the neovasculature is not well organized, we modulate the permeability of stable endothelial cells by the total density of the unstable endothelial cells inside the tumor, assumed to be a global criteria to describe the quality (efficiency) of the vasculature. We note

$$R(t) = \frac{\int E(t,x,y)dxdy}{Vol(Tumor)} \tag{12}$$

the total density of unstable endothelial cells inside the tumor, where

$$Vol(Tumor) = \int_{\mathbb{R}^2} \mathbf{1}_{P_1+P_2+Q+A>0}$$

and we apply a sigmoid law to define a quality coefficient

$$\Pi = 1 - \frac{R^{\gamma_n}}{R^{\gamma_n} + (R_{0.5})^{\gamma_n}} \tag{13}$$

which we will refer as the "quality of the vasculature" and is close to 1 if there is little unstable blood vessels (good vasculature) and close to zero if the number of unstable vessels is large (bad vasculature). This coefficient is of fundamental importance in our model since it will permit to take into account the normalization effect of the anti-angiogenic drugs on the vasculature. It will appear in the boundary conditions of the diffusion equations on the oxygen, AA and CT drugs, modulating the amount of the delivered entity by the vascular support composed of stable endothelial cells.

Remark 2.2. *The definition* (12)*, that we use for R is arguable. We could also choose R as being the proportion of unstable endothelial cells in the vasculature and set $R = \frac{\int E(t,x,y)dxdy}{\int (E(t,x,y)+Es(t,x,y))}$. This was our first choice but we dropped it for the following reason : with R defined this way, in an angiogenesis scenario, E starts to grow and Es is close to zero thus leading to a bad quality, so this is what is expected. But when the situation is stabilized, $Es \gg E$ and this would lead to a good quality (R close to 0). But we are trying to model a situation where angiogenesis leads to a situation with poor quality of the vasculature. With our choice of R given by* (12)*, since angiogenesis is always occurring to supply vascular support to the newly formed cancerous tissue, there is always unstable endothelial cells if the tumor is growing and thus angiogenesis leads to a bad-quality vasculature. Our definition makes Π being a global quantity of the vasculature.*

Chemical entities. Coupling of the tumor growth and angiogenesis models

The chemical entities interfering in the model are : the VEGF concentration and the oxygen concentration.

- The **VEGF concentration** $[V]$. The VEGF is produced by the tumoral cells in quiescent phase (phase Q) if there is hypoxia, with a rate $\alpha_{[V]}$. It is consumed by unstable endothelial cells with a constant rate $\delta_{[V]}$, and is degraded by the organism with a constant rate $\xi_{[V]}$. It undergoes a diffusion process in space, with a diffusion coefficient $K_{[V]}(x,y)$ which is higher in the healthy region than in the tumoral region.We assume that the diffusion process happens at a lower time scale and take the equation at its equilibrium state :

$$-\mathrm{div}(K_{[V]}\nabla[V]) = \alpha_{[V]}Q1_{[0_2]\leq\tau_{1,h}} - \delta_{[V]}E[V] - \xi_{[V]}[V]. \tag{14}$$

- The **oxygen concentration** $[O_2]$. Its dynamic is modeled the same way as VEGF. It diffuses with a rate $K_{[O_2]}(x,y) = K_{[V]}(x,y)$, is consumed by the cells in phase ϕ with a rate $\alpha_{[O_2],\phi}$ and is produced by the **stable vessels**, composed of stable EC (note that only the stable vessels are able to deliver oxygen). We assume the diffusion dynamic is faster than the ones of the cellular movements and growth in age, so we take the equation at equilibrium :

$$\begin{cases} -\mathrm{div}(K_{[O_2]}\nabla[O_2]) = -\sum_\phi \alpha_{[O_2],\phi}\phi \\ [O_2] = \Pi C_{max} \end{cases} \qquad \text{where } Es \geq \tau_v \tag{15}$$

where τ_v is a threshold representing the necessary amount of stable endothelial cells to have a blood vessel, and C_{max} the oxygen concentration in blood. The oxygen supply by the vessels is taken into account in the boundary condition of this equation. Notice the presence of the quality coefficient Π in the boundary condition expressing the modulation of oxygen delivered by the stable vessels regarding to the quality of the vasculature.

For both the equation on the oxygen and the VEGF, we use the same diffusion coefficient that we model as being medium-dependent : the diffusion is slower in tumoral tissue than in healthy tissue.

$$K_{[V]} = K_{[O2]} = K = Sigmo(CellNumber)$$

where $Sigmo$ is a sigmoïdal function (hyperbolic tangent for example), and

$$CellNumber(x,y) = \int_{\mathbb{R}^2} P_1 + P_2 + Q + A dxdy$$

is the total amount of tumoral cells located on (x,y).

2.3   Treatments

We will investigate the effect of anti-angiogenic drugs on the tumor growth and on the formation and persistence of the tumor vasculature. The drugs diffuse from the vasculature and

spread in the tissue in a similar way than oxygen or VEGF. The diffusing amount depends on the vessel permeability Π, which depends on the density of unstable cells. We denote the concentration of the antiangiogenic drug by $[AA]$ and the equation we use is :

$$
\begin{cases}
-\underbrace{\text{div}(K\nabla[AA])}_{Diffusion} = - \underbrace{[V]\dfrac{Emax_{AA}[AA]}{AA_{50}+[AA]}}_{Annihilation\,when\,contact\,with\,VEGF} \\
[AA] = \underbrace{\Pi Conc_{[AA]}(t)Es}_{Source} \qquad\qquad \text{where } Es \geq \tau_v
\end{cases}
\tag{16}
$$

where $Conc_{[AA]}(t)$ is the concentration of the drug coming from its pharmacokinetic and is delivered to the tumour by the stable vessels Es (boundary condition of the equation). By now, we just consider an monoclonal anti-body that inhibit the free VEGF, with a sigmoidal law.

As the VEGF is inhibited by the drug, its dynamic become :

$$
-\text{div}(K_{[V]}\nabla[V]) = \alpha_{[V]}Q1_{[0_2]\leq\tau_{1,h}} - \delta_{[V]}E[V] - \xi_{[V]}[V] - \underbrace{[V]\dfrac{Emax_{AA}[AA]}{AA_{50}+[AA]}}_{Effect\,of\,the\,drug}
\tag{17}
$$

where $[AA]$ is the anti-angiogenic concentration, $Emax_{AA}$ is the maximal effect of the drug and AA_{50} is the amount of drug required to produce half of the maximal effect.

As we aim to investigate the coupling between anti-angiogenic drugs and chimiotherapies, we also integrate a cytotoxic drug, which we denote by $[C]$. Its concentration is also **dependent on the quality of the vasculature** Π. The equation is similar to the one on the anti-angiogenic drug, without the annihilation term due to contact with VEGF but with an elimination term of parameter ξ_C.

$$
\begin{cases}
-\underbrace{\text{div}(K\nabla[C])}_{Diffusion} = -\xi_C[C] \\
[C] = \underbrace{\Pi Conc_{[C]}(t)Es}_{Source} \qquad \text{where } Es \geq \tau_v
\end{cases}
\tag{18}
$$

Its effect is integrated by killing a fraction of the mitotic cells in the last stage of the phase $SG2M$, the effect being modulated by an Emax law with $E_{max,C}$ and C_5. The equation on P_2 becomes

$$
\partial_t P_2 + \partial_a P_2 + \text{div}(\mathbf{v}P_2) = -P_2\delta_{a=a_{max}}\dfrac{E_{max,C}[C]}{C_{50}+[C]}.
\tag{19}
$$

Entity	Model equation	Equation number
Density of proliferative tumour cells	$\frac{\partial P_1}{\partial t} + \frac{\partial P_1}{\partial a} + \text{div} \cdot (\mathbf{v} P_1) = 0$	(1)
	$P_1(t, a = 0, x, y) = 2 P_2(t, a = a_{max,P_2}, x, y)$	(5)
	$\frac{\partial P_2}{\partial t} + \frac{\partial P_2}{\partial a} + \text{div} \cdot (\mathbf{v} P_2) = -P_2 \delta_{a=a_{max,P_2}} \frac{E_{max,C} [C]}{C_{50} + [C]}$	(19)
	$P_2(t, a = 0, x, y) = f P_1(t, a = a_{max,P_1}, x, y) + [\partial_t f]^+ Q(t^-)$	(5)
Density of quiescent tumour cells	$\frac{\partial Q}{\partial t} + \text{div} \cdot (\mathbf{v} Q) = g(1-f) P_1(a = a_{max,P_1}) - \left[\frac{\partial f}{\partial t}\right]^+ Q(t^-) + \left[\frac{\partial g}{\partial t}\right]^- Q(t^-)$	(3)
Density of apoptotic tumour cells	$\frac{\partial A}{\partial t} + \text{div} \cdot (\mathbf{v} A) = (1-g) P_1(a = a_{max,P_1}) - \left[\frac{\partial g}{\partial t}\right]^- Q(t^-)$	(4)
Density of healthy cells	$\frac{\partial H}{\partial t} + \text{div} \cdot (\mathbf{v} H) = 0$	(7)
Velocity and pressure	$\mathbf{v} = -k\nabla p, \; -\text{div}(k\nabla p) = P_2(a = a_{max,P2})$	(6) and (9)
Density of immature EC	$\frac{\partial E}{\partial t} + \text{div} \cdot (\chi([V]) E (1 - \frac{E}{N_E}) \nabla [V]) = p_r([V]) E (1 - \frac{E+E_s}{N_{max}}) - a([V]) n_E - \mu([V]) \mathbf{1}_{E+E_s - \tau_E} E$	(10)
Density of mature EC	$\frac{\partial E_s}{\partial t} = \mu \mathbf{1}_{E+E_s - \tau_E} E - a_{E_s} E_s$	(11)
Quality of the vasculature	$R = \frac{\int \frac{E(t,x,y)dxdy}{Vol(Tumor)}}{\quad} \qquad \mathbf{\Pi} = 1 - \frac{R^{\gamma n}}{R^{\gamma n} + R_{0.5}^{\gamma n}}$	(12) and (13)
Concentration of Oxygen	$-\text{div}(K_{[O_2]} \nabla [O_2]) = -\sum_\phi \alpha_{[O_2], \phi} \phi \quad \text{and} \quad [O_2] = \mathbf{\Pi} C_{max} \text{ where } Es \geq \tau_v$	(15)
Concentration of VEGF	$-\text{div} \cdot (K_{[V]} \nabla [V]) = \alpha_{[V]} Q_{[O_2] \leq \tau_{1,h}} - \delta_{[V]} n_E [V] - \xi_{[V]} [V] - [V] \frac{Emax_{AA}[AA]}{AA_{50} + [AA]}$	(17)
Concentration of chemotherapy	$-\text{div} \cdot (K \nabla [C]) = -\xi_{[C]} [C] \quad \text{and} \quad [C] = \mathbf{\Pi} P_{[C]}(t) \text{ where } Es \geq \tau_v$	(18)
Concentration of AA drug	$-\text{div} \cdot (K \nabla [AA]) = -[V] \frac{Emax_{AA}[AA]}{AA_{50} + [AA]} \quad \text{and} \quad [AA] = \mathbf{\Pi} P_{[AA]}(t) \text{ where } Es \geq \tau_v$	(16)

Table 1: Summary of the macroscopic model equations

Parameter	Description	Value	Unit
τ_0	Threshold of overcrowd	$5 \cdot 10^4$	cell
$\tau_{1,h}$	Threshold of moderate hypoxia	$4 \cdot 10^{-7}$	M
$\tau_{2,h}$	Threshold of severe hypoxia	$4 \cdot 10^{-9}$	M
N_{max}	Total density of tumour and/or healthy cells	10^5	cell/mm2
$a_{max,P1}$	Maximum duration of phase P1	5	time
$a_{max,P2}$	Maximum duration of phase P2	8	time
$\alpha_{[V]}$	Secretion rate of VEGF by quiescent cells	10^{-8}	M/cell
$\delta_{[V]}$	consumption rate of VEGF by immature EC	0	M/cell
$\xi_{[V]}$	Degradation rate of VEGF	0	M^{-1}
N_E	Maximum number of endothelial cells	10^5	cell
μ	Rate of maturation for EC	0.5	cell/time
τ_E	Minimum quantity of immature EC leading to maturation	$5 \cdot 10^2$	cell
a_{Es}	Apoptosis rate of unstable endothelial cells	0	cell/time
γ_n	Sigmoidal coefficient for the computation of vasculature quality	0.5	cell/mm2
$R_{0.5}$	density of EC leading to the half of the maximal vasculature quality	$8 \cdot 10^{-3}$	cell/mm2
$\alpha_{[O_2],P_1}$	Oxygen consumption of the P_1 tumour cells	10^{-4}	M/cell
$\alpha_{[O_2],P_2}$	Oxygen consumption of the P_2 tumour cells	10^{-4}	M/cell
$\alpha_{[O_2],Q}$	Oxygen consumption of the quiescent tumour cells	$0.25 \cdot 10^{-4}$	M/cell
τ_V	Number of mature EC needed to form a functional blood vessel	10^4	cell
$\xi_{[C]}$	Degradation rate of chemotherapy	$1.25 \cdot 10^{-4}$	M/time
$Emax_{AA}$	Maximal effect of the AA drug on VEGF	1	none
AA_{50}	Amount of AA drug producing half of the maximal effect	0.5	M
$E_{max,C}$	Maximal effect of the chemotherapy on $P-2$ cells	0.75	none
C_{50}	Amount of chemotherapy producing half of the maximal effect	0.2	M

Table 2: Summary of the model parameters

3 Simulation techniques

To simulate the model, we mainly inspired from and used a previously existing numerical code, developed by B. Ribba, F. Billy, T. Colin and O. Saut. Since we cannot simulate in the whole plan, we restrict ourselves to a (large) square that we uniformly discretize.

3.1 Initial conditions

To initiate the model, we place in the grid a circular tumour composed mainly by P_1 and P_2 proliferative cells and a small part of quiescent cells. Then we randomly place EC in the tumour area, mainly stable EC and a small fraction of unstable EC. Depending on the density of cells over the domain, we compute the diffusion coefficient for VEGF, oxygen, cytotoxic and AA drugs. We compute the diffusion of VEGF secreted by the EC. From the distribution of VEGF, we calculate the values of angiogenesis parameters with the molecular model. Then, we evaluate the quality of the vasculature depending on the distribution of unstable EC. This permits us to simulate the delivery of oxygen by the vasculature. Once all the variables of the system are initialized,we can simulate the cell cycle.

3.2 Cellular loop

The simulation is based on a recursive loop with a time step which corresponds to the passage of tumour cells from one age to the next. Computations of the advection equations are performed using a splitting technique, meaning that to solve an equation of the type

$$\partial_t \phi + \partial_a \phi + \text{div}(\mathbf{v}_\phi \phi) = S, \tag{20}$$

we solve first the equation $\partial_t \phi + \partial_a \phi = S$, then the equation $\partial_t \phi + \text{div}(\mathbf{v}_\phi \phi) = 0$. More precisely, if we write the equation (20) as $\partial_t \phi = A\phi + B\phi + S$, with $A\phi = \partial_a \phi$ and $B\phi = \text{div}(\mathbf{v}\phi)$, we discretize it in time in the following way

$$\begin{cases} \psi^{n+1} = \phi^n + A_h \phi^n dt + S^n dt \\ \phi^{n+1} = \psi^{n+1} + B_h \psi^{n+1} dt \end{cases}$$

with A_h and B_h and S^n being suitable discrete versions of A, B and S.

At each step, we first compute the passage of the cells in age, depending on the environmental conditions (oxygen and local density of cells) of the previous step. We can extract the variation in mass due to proliferation $P_2(a = a_{max,P_2})$. We retrieve the pressure by solving the elliptic equation (9) with zero-boundary condition, using a finite-volume scheme. The velocity is computed using Darcy's Law presented in eq. (6). We compute then the transport part, again by splitting between a pure transport part and an amplification one due to the non-zero divergence of the velocity. The pure transport part is solved using an explicit upwind-scheme, corresponding to the equation :

$$\frac{\partial \phi}{\partial t} + \mathbf{v} \cdot \nabla \phi = 0, \tag{21}$$

with suitable sub time steps in order to respect stability conditions, namely $||v_x||_\infty dt < dx$ and $||v_y||_\infty dt < dy$, with v_x and v_y being respectively the x and y components of the velocity. Finally, the amplification part is computed through an explicit Euler scheme.

Then we compute the proliferation and the migration of the endothelial cells depending on the local amount of cells, VEGF repartition and the angiogenesis parameters describing proliferation, migration and apoptosis rate taken at the equilibrium and all computed at the previous time step. The computation technique used is similar to the one used to compute the dynamics of tumour cells (splitting and upwind scheme for the transport).

The diffusion equations (pressure, VEGF, Oxygen, drugs) are solved using a finite-volume scheme and with homogeneous Dirichlet boundary conditions. A penalization method is used to deal with the complex boundary conditions appearing in the equation for the oxygen and the drugs, transforming it into a penalized right-hand side.

From the distribution of VEGF, we retrieve the angiogenesis parameters at each location, at the steady state of the molecular model. To save computation time, we calculate *a priori* a database of values of the angiogenesis functions $p_r([V])$, $a([V])$ and $\chi([V])$ for a large and small-discretized range of possible VEGF values. At each time step, angiogenesis parameters are extracted from this base, depending on the local amount of VEGF. But our numerical scheme also allows a simultaneous computation of these parameters for a precise quantity of angiogenic factor.

The equations are solved in the following order : age transport for the cancerous cell densities, pressure, velocity, spatial transport for the cancerous cell densities, amplification, endothelial cells densities, chemotherapy, anti-angiogenic drug, oxygen, VEGF, VEGF parameters. At each new time step t^{n+1}, in an equation on some quantity X involving another quantity Y, we use the value Y^{n+1} if it has been computed before, according to the previous order, and the value Y^n else.

3.3   Values of the parameters

Most of the parameters of the model are not available in the literature and we fixed their values arbitrarily, for the major part, on the basis of reasonable expected values (the values used in the simulations are summarized in the table 2). As a consequence, we don't precise the time unit since it has no relevance. It can be fixed by assigning a unit to the value of the time-length of the cell-cycle phases. For example, if we assume that the total length of the cell cycle is 13h, then we get that 1 time unit = 1 hour, since $a_{max,P_1} + a_{max,P_2} = 13$. We could fix the value of one time unit by considering a particular cancer (breast, lung, liver, etc...).

4   Results

We use now the model to perform various simulations to investigate qualitatively the behavior of vascular tumoral growth. We first look at the untreated case, then the effect of an anti-angiogenic (AA) drug and finally the combination of a cytotoxic and an AA.

4.1 Vascular tumoral growth

The figures 3 and 4 present two-dimensional simulations of the tumoral growth in a vascular context, that is with the ability of the tumor to induce neo-angiogenesis in the surrounding endothelium. First, the tumor grows and formation of a quiescent core due to hypoxia and overcrowd appears in the center. The proliferative phase is mostly located at the periphery (see fig. 3). The total growth of the tumor is slowed down until angiogenesis occurs. This angiogenesis is due to emission of VEGF by the quiescent cells which induces proliferation and migration of first the unstable endothelial cells which then mature into stable endothelial cells able to deliver oxygen (see fig. 4). Thanks to this, quiescent cells can reenter the cell cycle and proliferation induces an accelerated growth of the tumor.

Proliferative cells P_2 Quiescent cells Q

Total cancerous cells
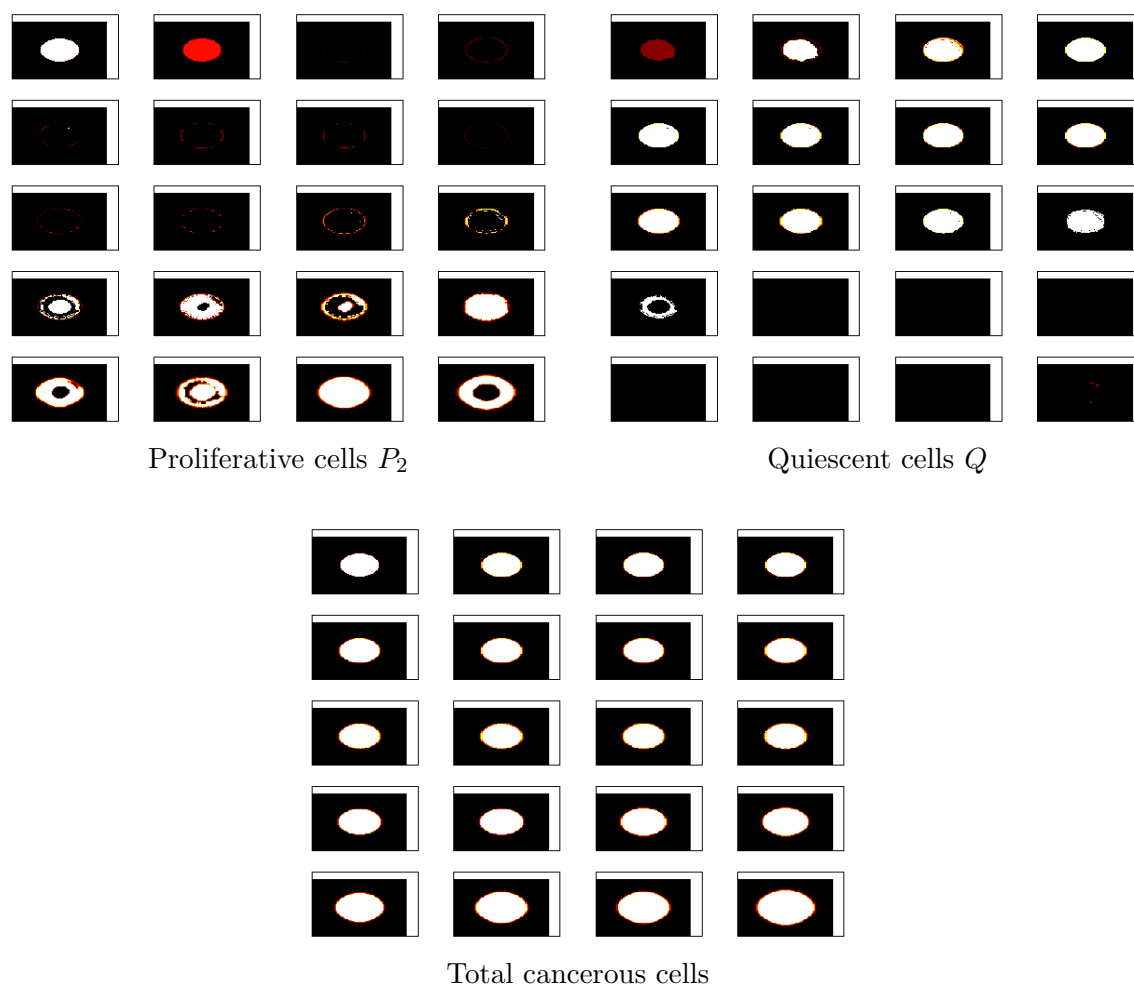
Figure 3: Two-dimensional growth of the tumor. On each figure, the starting time is up left and time evolves from left to right and downward.

Unstable endothelial cells   Stable endothelial cells

Oxygen
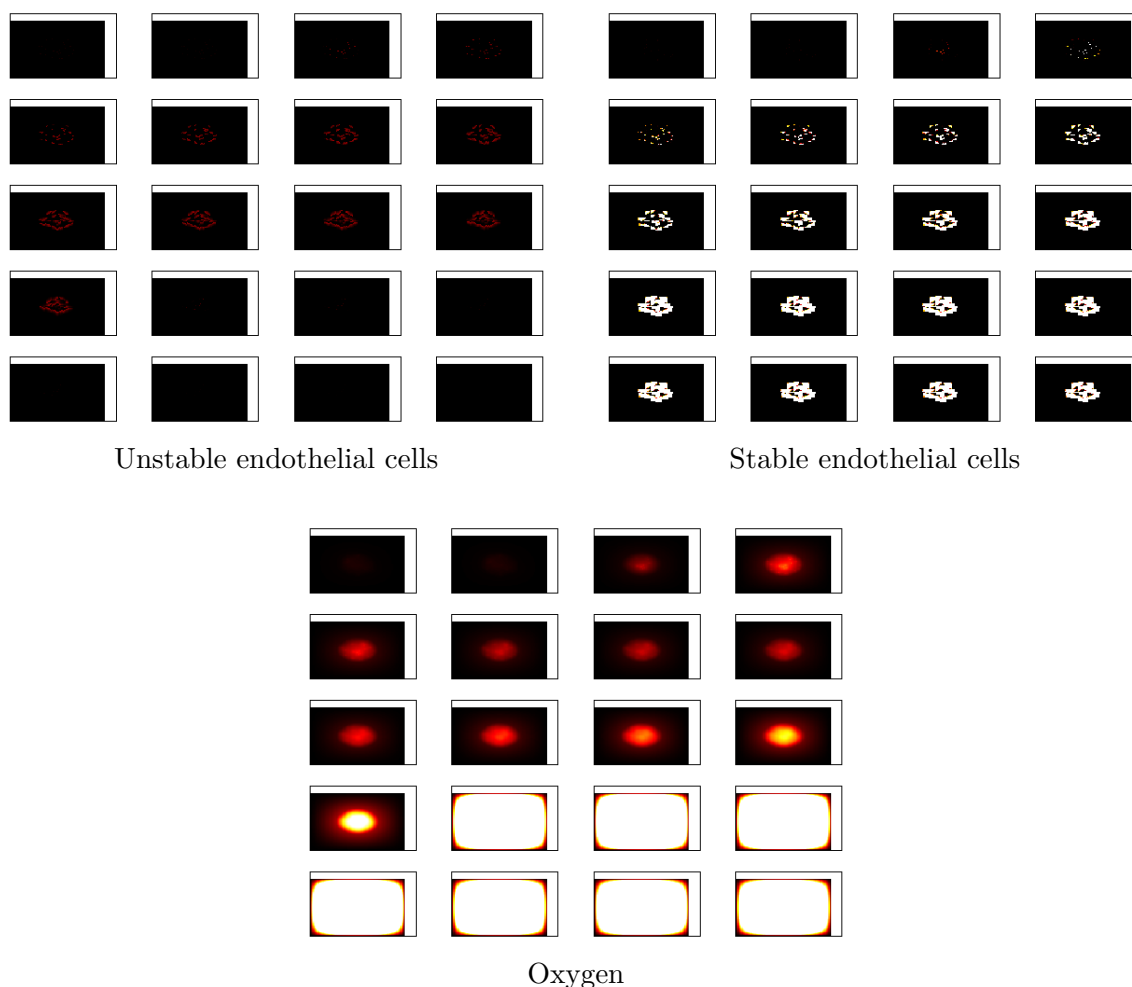
Figure 4: Angiogenesis

4.2   Anti-angiogenic treatment

Two antagonist effects are expected from the application of an AA treatment in our modeling. First, by inhibiting the VEGF we expect angiogenesis to be stopped and the tumor to be suffocated, being deprived from access to the nutrients (oxygen here). On the opposite, by stopping the proliferation of unstable endothelial cells and inhibiting their VEGF-induced mechanisms of resistance to apoptosis, we expect an amelioration of the quality of the vasculature, as it is proportional to the amount of unstable endothelial cells in our model . This should lead to a better supply of the oxygen and thus a paradoxical effect of the AA to improve tumor growth instead of deteriorating it. Though, this effect should not last long, being compensated by the long-term loss of vasculature. To investigate these two effects, we simulated two types of administration the AA drug : a long one, designed to check that the AA effect is able to induce tumor regression (see figure 5) and a short one (see figure 6) aimed at observing the effect of the so-called normalisation of the vasculature [Jai01].

Remark 2.3. *In the simulations of this model, we don't integrate the pharmacokinetics of the drugs, as we first wanted to investigate qualitatively and theoretically the effects. Thus we take the concentrations of the drugs in the blood as being constant in time.*

In the figure 5 a long lasting AA treatment is applied from times 60 to 120. After a positive effect on the tumor growth due to the normalisation of the vasculature (fig. 5.D), the loss of vasculature expressed by the diminution of stable endothelial cells in the figure 5.C induces high hypoxia in the tumoral cells, leading to apoptosis.

The figure 6 describes the effect of a short AA treatment (time 60 to 65) on tumoral growth and the quality of the vasculature. We observe the normalization effect during the application of the treatment (fig. 6.B), leading to a transient faster growth of the tumor (fig. 6.A). But after this phase, tumor growth is finally slower than without treatment due to the loss of vasculature induced by the AA treatment, even for a short time.

4.3 Combination of a chemotherapy and an anti-angiogenic treatment

We want now to theoretically simulate the combination of an AA drug and a chemotherapy (CT) and address the problem of the best combination of the two drugs. Indeed, the balance of two phenomena makes the combination non-trivial. On one hand, by reducing the vasculature, the AA reduces the supply of the CT drug to the tumor. On the other hand, by improving the quality of the vasculature in cleaning it from the inefficients unstable endothelial cells, one may expect a better delivery of the CT on a short term after the AA. Though, this better delivery of the CT comes with a better delivery of oxygen... First we simulate the effect of a CT alone, delivered between times 60 and 65 on a total simulation time of 100 (figure 7).

We observe that the tumor growth is slowed down during the treatment and then starts back with the same velocity as without treatment. Then, we investigate in the figure 8 the combination of an AA drug applied first from times 60 to 65, as in the figure 6 and of a CT from times 69 to 74, since we identified a delay of 9 between the beginning of the AA and the beginning of the CT as being optimal (see below). We observe a synergistic effect : the combination treatment is better than both the AA and the CT alone. The tumor is reduced significantly during the CT treatment and on a larger time-scale, its growth rate is also reduced.

To investigate the question of the optimal combination of an AA and a CT, we fix the application of the AA during times 60 and 65 and vary the starting time of the CT. We then observe various indicators to determine whether the combination is beneficial or harmful and, in the first situation, to determine heuristically the optimal delay D between the AA and the CT. The results are shown in the figure 9, where are plotted the situation of a CT alone given at time 60+D and the combination of an AA during t=60 and t=65 and a CT during t=60+D and t=65+D (same duration of the AA and CT treatments, though realistic protocols don't do so).

In the figure 9.A, we plotted the tumor size at the end of simulation as a function of the delay. The effect of the combination is always beneficial with this indicator and the best delay seems to be 8 or 9. Though, this indicator might be biased from the fact that the larger the delay, the shorter the time between the end of the CT and the end of the simulation.
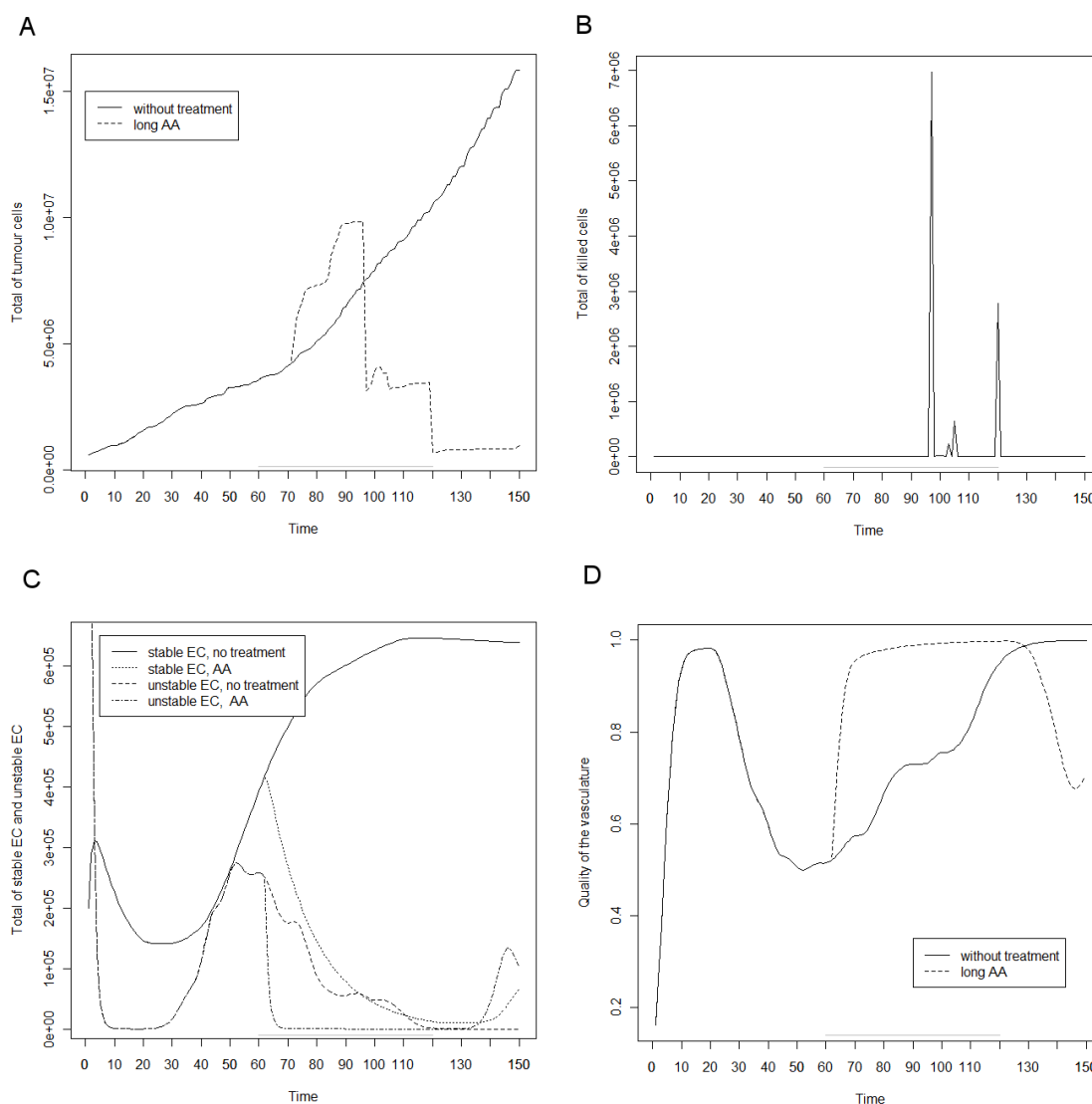
Figure 5: Effect of a long anti-angiogenic treatment on tumour behavior. The AA is applied from time 60 to 120 (times indicated by the horizontal line). A total number of tumour cells, B total number of cells killed at each time, C quantities of stable endothelial cells, divided by 10, in continuous lines, and unstable endothelial cells in dashed lines, D quality of the vasculature.

The figure 9.B shows another indicator, called Time Efficacy Index (TEI). It is defined as the time needed for the tumor growth curve to reach the size at t=90 of an untreated tumor. We subtract then 90 to this time. We observe that it is almost always negative, meaning that the tumor growth is faster than when the CT is applied alone and thus a harmful effect of the combination occurs. This is due to the acceleration of the growth provoked by the amelioration of the quality of the vasculature following the administration of the AA. Though, for 4 delays (namely 6, 7, 8 and 9) the combination is beneficial and the TEI is improved.
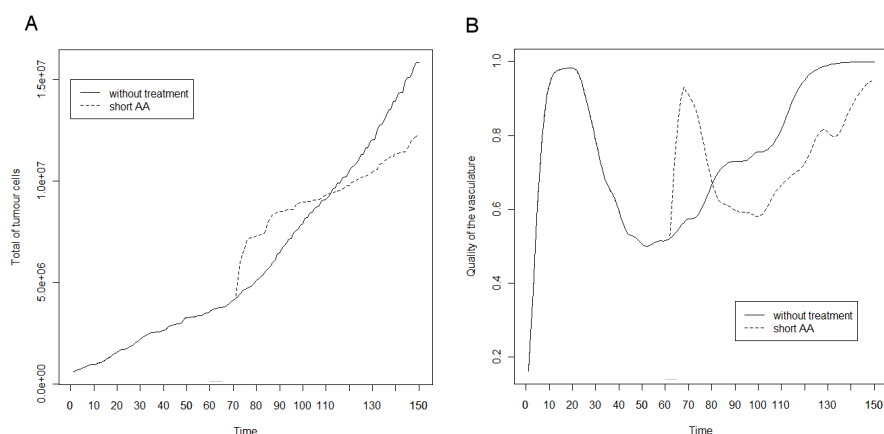
Figure 6: Effect of a short anti-angiogenic treatment on tumour behavior. The AA is applied from time 60 to 65 (times indicated by the horizontal line). A tumoral growth and B quality of the vasculature.
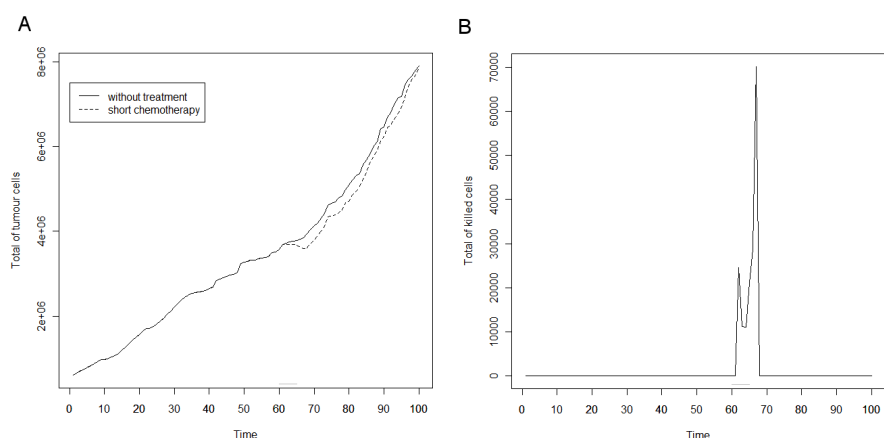
Figure 7: Effect of a short chemotherapy on tumour behaviour. The treatment is applied between times 60 and 65 (horizontal line): A tumoral growth, and B number of killed cells.

Another interesting quantity is the total amount of CT delivered, that is $\int_0^T \int_{\mathbb{R}^2} [C](t,x,y)dxdydt$ (fig. 9.C). As expected, in the situation of a CT alone, it goes better and better due to angiogenesis. In the context of the combination however, it is first improved thanks to the normalisation of the vasculature, but then decreases and is lower than in the CT alone situation, because of the negative effect of the AA on the vasculature. The best delay for this indicator is 6.

The figure 9.D presents another indicator : the relative variation of tumor size during the chemotherapy, that is between the start time and the end time of the CT. In the administration of a CT alone, this indicator stays close to 0, since the CT stops the growth in our simulation, consistently with figure 7. When the AA is administrated alone, we retrieve the acceleration
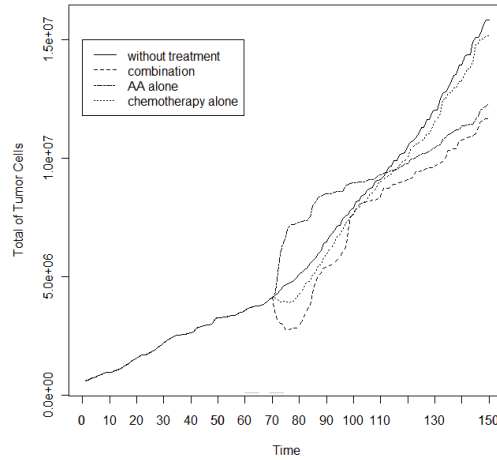
Figure 8: Effect of the combination of an AA drug and a chemotherapy. Tumour behaviour without treatment (continuous line), with AA drug alone (small dashes), with CT alone (alternate dashes) and with a combination of the two treatments (large dashes), the times of application of AA and CT are indicated with the grey lines (respectively 60-65 and 69-74).

effect inducing a sharp increase in the tumor burden. Interestingly, almost for the same delays the effect of the combination is maximized, inducing a reduction in the tumor mass up to 25.84% for the best delay 9 (which we use for the simulation of the figure 8). Notice that this best delay is not the same as the best delay regarding to the amount of CT delivered. Quite surprisingly, for the delay 11, the effect is deleterious, exhibiting an increase of 29.53%. How can this be explained?

It is due to the following synergistic effect between the AA and the CT, that we did not expect : the CT kills the cells in the last age of the proliferative phase, which is a problem since a large part of the tumor is composed of quiescent cells thus unreachable for the CT. When the AA is administrated, the normalisation effect and thus the better supply of oxygen induces that quiescent cells go back to the proliferative phase, massively from the modeling. But why such a difference between delays 9 and 11? Because, since proliferative cells are killed by the CT only in the last age, we have to wait the time of the P_2 phase (8 in our case) for the new arrived quiescent cells to reach the last age and to be killed. This is why the delay 9 is the best. If the CT waits too long then all these former quiescent cells have passed the end of the P_2 phase, have divided and provoked a sharp increase of the tumor burden.

5   Conclusion

This model is the example of a mechanistic one, integrating multiple phenomenas happening at various time scales. We defined a theoretical notion of quality of the vasculature allowing to take into account for the normalization action of the AA drugs, which seems to play an important
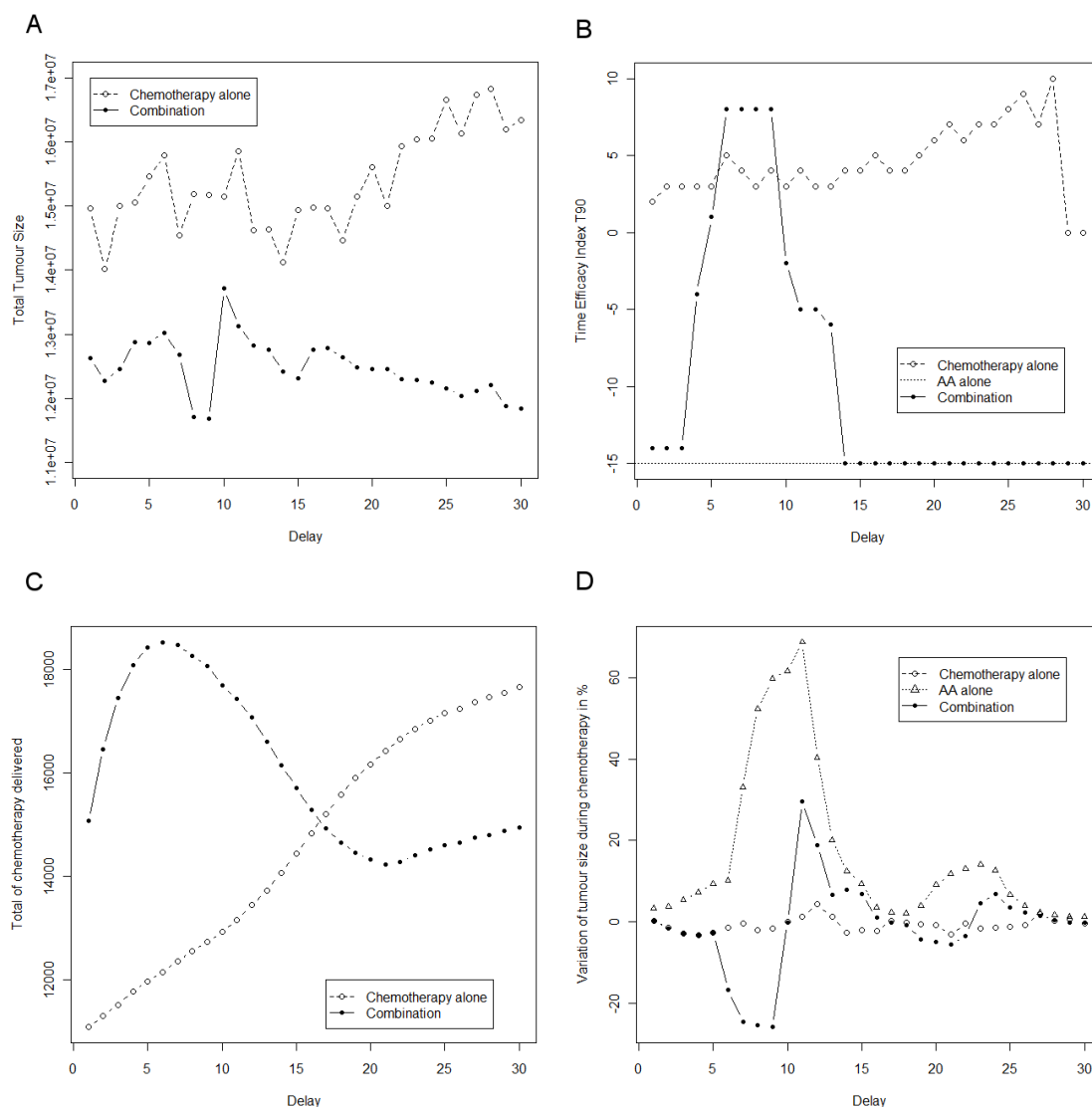
Figure 9: Outputs describing treatments effects, when the chemotherapy is applied alone (empty dots), in combination with an AA treatment (full dots) or for the AA alone (dashed line), depending on the delay of application of the chemotherapy after the beginning of the cure at time 60 : A size of the tumour at the end of the simulation ; B Time Efficacy Index : time needed by the tumour to reach the size of an untreated tumour at t=90, the green line represent the TEI for the AA alone ; C total amount of chemotherapy delivered to the tumour ; D effect of the chemotherapy, during its application.

role for the administration of the therapies. The coupling with an intracellular model allows to test different situations where one or several molecular pathways are altered, like in the case of the mutation of the RAS gene, though we didn't investigate this aspect of the model.

The model has been used as a theoretical tool to simulate different scenarii for AA therapy,

as well as for the combination of an AA and a CT therapy. In particular, we identified a theoretical optimal value for the delay between the starting times of the AA and CT therapies. This value seems to be highly dependent on the parameters values, especially on the total length of the phases S, G2 and M of the cell cycle; it also depends on the assumption we made that the CT kills cells only during the M phase (end of the P_2 phase). The results are based on the quality of vasculature Π whose value depends also strongly on the parameters used for its definition and which have no real biological meaning. In the context of practical application, they would have to be estimated through confrontation with datas. These results emphasize the fundamental importance of the **scheduling** in the administration of the drugs, especially in CT-AA combined therapies. They suggest the existence of an optimal **therapeutic window** in the delay between administration of the AA and of the CT.

As a first step, we only considered a single administration of each drug and did not investigate the global scheduling. This is an important question for which it is necessary to take into account more deeply the pharmacokinetics/pharmacodynamics of the drugs. Also, in the context of the normalization hypothesis, we investigated the combination in the sense of the influence of the AA on the delivery and effectiveness of the CT, implicitly choosing to give the AA before the CT. We notice that, in this modeling framework, the beneficial effect of vascular pruning can only be obtained administrating the drugs in this order.

The major issue of this model is its parametrization. Indeed, there is often not enough biological data to give values for the large number of parameters and even if it would be the case, for clinical application it seems hardly possible to run all the biological tests for each patient. Moreover, a lot of simplification hypothesis have been done, for instance relatively to mechanics of the tumoral tissue (by assuming Darcy's law for instance, or neglecting mechanical interactions between the endothelium and the neoplastic tissue). Hence, this model has to be thought as a theoretical tool, useful to give qualitative intuitions and to rationalize a complex underlying biology.

6   Appendix. Equations and parameters of the molecular model

reaction	rate equation
$VEGF + VEGFR \leftrightarrow VEGF.VEGFR$	$k1 * VEGF * VEGFR - km1 * VEGF.VEGFR$
$VEGF.VEGFR \leftrightarrow VEGFR.P$	$k2 * VEGF.VEGFR - km2 * VEGFR.P$
$VEGFR.P \rightarrow Cdc42$	$k3 * VEGFR.P$
$VEGFR.P + PLCy1 \leftrightarrow VEGFR.PLCy1$	$k4 * VEGFR.P * PLC - km4 * VEGFR.PLC$
$VEGFR.PLCy1 \leftrightarrow VEGFR.PLCy1.P$	$k5 * VEGFR.PLC - km5 * VEGFR.PLC.P$
$VEGFR.PLCy1.P \leftrightarrow VEGFR.P + PLCy1.P$	$k6 * VEGFR.PLC.P - km6 * VEGFR.P * PLC.P$
$PLCy1.P + PIP2 \rightarrow DAG + IP3$	$k7 * PLC.P * PIP2$
$DAG \rightarrow PKC$	$k8 * DAG$
$PKC \rightarrow SPK$	$k9 * PKC$
$PKC \rightarrow RAF$	$k10 * PKC$
$SPK \rightarrow RasGTP$	$k11 * SPK$
$RasGTP + Raf \rightarrow Raf.P$	$k12 * RASGTP * \frac{RAF}{(K12+RAF)}$
$Raf.P \rightarrow Raf$	$k13 * \frac{RAF.P}{(K13+RAF.P)}$
$Raf.P + MEK \rightarrow MEK.P$	$k14 * RAF.P * \frac{MEK}{K14*(1+\frac{MEK.P}{K16})+MEK}$
$MEK.P + PP2A \rightarrow MEK$	$k15 * MEK.P * \frac{PP2A}{K15*(1+\frac{MEK.PP}{K17}+\frac{AKT.PI.P}{K30}+\frac{AKT.PI.PP}{K32})+MEK.P}$
$MEK.P + Raf.P \rightarrow MEK.PP$	$k16 * RAF.P * \frac{MEK.P}{K16*(1+\frac{MEK}{K14})+MEK.P}$
$MEK.PP + PP2A \rightarrow MEK.P$	$k17 * MEK.PP * \frac{PP2A}{K17*(1+\frac{MEK.P}{K15}+\frac{AKT.PI.P}{K30}+\frac{AKT.PI.PP}{K32})+MEK.PP}$
$MEK.PP + ERK \rightarrow ERK.P$	$k18 * MEK.PP * \frac{ERK}{K18*(1+\frac{ERK.P}{K20})+ERK}$
$ERK.P + MKP3 \rightarrow ERK$	$k19 * ERK.P * \frac{MKP3}{K19*(1+\frac{ERK.PP}{K21})+ERK.P}$
$MEK.PP + ERK.P \rightarrow ERK.PP$	$k20 * MEK.PP * \frac{ERK.P}{k20(1+\frac{ERK}{K18})+ERK.P}$
$ERK.PP + MKP3 \rightarrow ERK.P$	$k21 * \frac{ERK.PP}{K21*(1+\frac{ERK.P}{K19})+ERK.PP}$
$VEGFR.P + PI3K \leftrightarrow VEGFR.PI3K$	$k22 * VEGFR.P * PI3K - km22 * VEGF.PI3K$
$VEGFR.PI3K \leftrightarrow VEGFR.PI3K.P$	$k23 * VEGFR.PI3K - km23 * VEGF.PI3K.P$
$VEGFR.PI3K.P \leftrightarrow VEGFR.P + PI3K.P$	$k24 * VEGFR.PI3K.P - km24 * VEGFR.P * PI3K.P$
$PI3K.P \rightarrow PI3K$	$k25 * \frac{PI3K.P}{K25+PI3K.P}$
$PI3K.P + PIP2 \rightarrow PIP3$	$k26 * PIP2 * \frac{PI3K.P}{K26+PIP2}$
$PIP3 \rightarrow PIP2$	$k27 * \frac{PIP3}{K27+PIP3}$
$PIP3 + Akt \leftrightarrow PIP3.AKT$	$k28 * PIP3 * AKT - km28 * AKT.PIP3$
$Akt.PIP3(+PDK) \rightarrow Akt.PI.P$	$k29 * \frac{AKT.PIP3}{K29*(1+\frac{AKT.PI.P}{K31})+AKT.PIP3)}$
$Akt.PI.P + PP2A \rightarrow Akt.PIP3$	$k30 * AKT.PI.P * \frac{PP2A}{K30(1+\frac{MEK.P}{K15}+\frac{MEK.PP}{K18}+\frac{AKT.PI.PP}{K32})+AKT.PI.P}$
$Akt.PI.P(+PDK) \rightarrow Akt.PI.PP$	$k31 * \frac{AKT.PI.P}{K31*(1+\frac{AKT.PIP3}{K29})+AKT.PI.P}$
$Akt.PI.PP + PP2A \rightarrow Akt.PI.P$	$k32 * AKT.PI.PP * \frac{PP2A}{K32(1+\frac{MEK.P}{K15}+\frac{MEK.PP}{K18}+\frac{AKT.PI.P}{K30})+AKT.PI.PP}$
$Akt.PI.PP + mTOR \leftrightarrow Akt.PI.PP.mTOR$	$k33 * AKT.PI.PP * MTOR - km33 * AKT.PI.PP.MTOR$
$Akt.PI.PP + BAD \leftrightarrow Akt.PI.PP.BAD$	$k34 * AKT.PI.PP * BAD - km34 * AKT.PI.PP.BAD$
$Akt.PI.PP + Casp9 \leftrightarrow Akt.PI.PP.Casp9$	$k35 * AKT.PI.PP * CASP - km35 * AKT.PI.PP.CASP$
$Akt.PI.PP + eNOS \leftrightarrow Akt.PI.PP.eNOS$	$k36 * AKT.PI.PP * ENOS - km36 * AKT.PI.PP.ENOS$
$Akt.PI.PP.mTOR \leftrightarrow Akt.PI.PP.mTOR.P$	$k37 * AKT.PI.PP.MTOR - km37 * AKT.PI.PP.MTOR.P$
$Akt.PI.PP.BAD \leftrightarrow Akt.PI.PP.BAD.P$	$k38 * AKT.PI.PP.BAD - km38 * AKT.PI.PP.BAD.P$
$Akt.PI.PP.Casp9 \leftrightarrow Akt.PI.PP.Casp.P$	$k39 * AKT.PI.PP.CASP - km39 * AKT.PI.PP.CASP.P$
$Akt.PI.PP.BAD \leftrightarrow Akt.PI.PP.BAD.P$	$k40 * AKT.PI.PP.ENOS - km40 * AKT.PI.PP.ENOS.P$
$Akt.PI.PP.mTOR.P \leftrightarrow Akt.PI.PP + mTOR.P$	$k41 * AKT.PI.PP.MTOR.P - km41 * AKT.PI.PP * MTOR.P$
$Akt.PI.PP.BAD.P \leftrightarrow Akt.PI.PP + BAD.P$	$k42 * AKT.PI.PP.BAD.P - km42 * AKT.PI.PP * BAD.P$
$Akt.PI.PP.Casp9.P \leftrightarrow Akt.PI.PP + Casp9.P$	$k43 * AKT.PI.PP.CASP.P - km43 * AKT.PI.PP * CASP.P$
$Akt.PI.PP.eNOS.P \leftrightarrow Akt.PI.PP + eNOS.P$	$k44 * AKT.PI.PP.ENOS.P - km44 * AKT.PI.PP * ENOS.P$
$cdc42 + p38 \leftrightarrow cdc42.p38$	$k45 * CDC42 * P38 - km45 * CDC42.P38$
$cdc42.p38 \rightarrow p38.P$	$k46 * CDC42.P38$
$p38.P + MAPKAPK \leftrightarrow p38.P.MAPKAPK$	$k47 * P38.P * MAPKAPK - km47 * P38.P.MAPKAPK$
$p38.P.MAPKAPK \rightarrow MAPKAPK.P$	$k48 * P38.P.MAPKAPK$
$MAPKAPK.P + Hsp27 \leftrightarrow MAPKAPK.P.Hsp27$	$k49 * HSP27 * MAPKAPK.P - km49 * MAPKAPK.P.HSP27$
$MAPKAPK.P.Hsp27 \rightarrow Hsp.P$	$k50 * MAPKAPK.P.HSP27$
$PLCy1.P \rightarrow PLCy1$	$k51 * \frac{PLC.P}{K51+PLC.P}$
$ERK.PP \longrightarrow \text{proliferation}(p)$	$\frac{k52*ERK_P P^g}{km52^g+ERK_P P^g}$
$BAD.P + CASP.PB25 \longrightarrow \text{resistance to apoptosis}(a)$	$k53 * \frac{km53^g}{km53^g+(BAD_P+CASP_P)^g}$
$HSP27.P + ENOS.P \longrightarrow \text{migration}(\chi)$	$k54 * \frac{(HSP27_P+ENOS_P)^g}{km54^g+(HSP27_P+ENOS_P)^g}$

Table 3: Table of the molecular model equations

parameter	value	reference	parameter	value	reference
k1	0.01	est	km1	1	est
k2	0.1	est	km2	1	est
k3	1	est			
k4	0.1	est	km4	1	est
k5	1	est	km5	0.1	est
k6	10	est	km6	0.1	est
k7	1	est	K7	100	
k8	0.1	est			
k9	0.1	est			
k10	0.1	est			
k11	0.01	est			
k12	1.53	[HKN$^+$03]	K12	11.7	[HKN$^+$03]
k13	0.25	[Kho00]	K13	8	[Kho00]
k14	3.5	[HKN$^+$03]	K14	317	[HKN$^+$03]
k15	0.06	[HKN$^+$03]	K15	2200	[HKN$^+$03]
k16	2.9	[HKN$^+$03]	K16	317	[HKN$^+$03]
k17	0.06	[HKN$^+$03]	K17	60	[HKN$^+$03]
k18	9.5	[HKN$^+$03]	K18	146000	[HKN$^+$03]
k19	0.3	[HKN$^+$03]	K19	160	[HKN$^+$03]
k20	16	[HKN$^+$03]	K20	146000	[HKN$^+$03]
k21	0.27	[HKN$^+$03]	K21	60	[HKN$^+$03]
k22	0.001	est	km22	4	est
k23	9.85	est	km23	0.1	est
k24	45.8	est	km24	0.05	est
k25	2620	[HKN$^+$03]	K25	3680	[HKN$^+$03]
k26	16.9	[HKN$^+$03]	K26	39.1	[HKN$^+$03]
k27	170	[HKN$^+$03]	K27	9.02	[HKN$^+$03]
k28	507	[HKN$^+$03]	km28	234	[HKN$^+$03]
k29	20000	[HKN$^+$03]	K29	80000	[HKN$^+$03]
k30	0.11	[HKN$^+$03]	K30	4.35	[HKN$^+$03]
k31	20000	[HKN$^+$03]	K31	80000	[HKN$^+$03]
k32	0.21	[HKN$^+$03]	K32	12	[HKN$^+$03]
k33	1	est	km33	0.5	est
k34	1	est	km34	0.5	est
k35	1	est	km35	0.5	est
k36	1	est	km36	0.5	est
k37	1	est	km37	0.5	est
k38	1	est	km38	0.5	est
k39	1	est	km39	0.5	est
k40	1	est	km40	0.5	est
k41	1	est	km41	0.5	est
k42	1	est	km42	0.5	est
k43	1	est	km43	0.5	est
k44	1	est	km44	0.5	est
k45	1	est	km45	0.4	est
k46	1	est			
k47	1	est	km47	0.5	est
k48	1	est			
k49	1	est	km49	0.5	est
k50	1	est			
k51	10	est	K51	10	est
k52	1	est	km52	25	est
k53	1	est	km53	1.8	est
k54	1	est	km54	20	est

Table 4: Values of the parameters of the molecular model.

Part II

Analyse mathématique et numérique

This part is devoted to mathematical analysis of the model for metastatic evolution introduced in section 1.5. Turning first our interest to the autonomous case (i.e. without therapy), functional analysis of a particular Sobolev space is required to rigorously establish the properties of the operator corresponding to the evolution equation. This is performed in the chapter 3, allowing chapter 4 to establish well-posedness of the model, regularity of the solutions and their asymptotic behavior. Introduction and numerical analysis of a Lagrangian scheme in the chapter 5 proves existence to the non-autonomous case. An error estimate is also provided. Eventually the effect of concentrating into a Dirac mass the boundary distribution of the metastases is investigating in chapter 6.

Part of the chapter 4 (without the numerical illustrations) gave rise to the publication [Ben11a] and chapters 5 and 6 have been accepted for publication (respectively [Ben11b] and [Ben11c]).

All along this part, the main idea used to prove the results is to straighten the trajectories of the growth rate, i.e. the method of characteristics.

Chapter 3

Study of the space $W^p_{\mathrm{div}}(\Omega)$

Let Ω be an open set in $\mathbb{R}^d$, $G \in \mathcal{C}^1(\overline{\Omega})^d$ a regular vector field. For $1 \le p \le \infty$, we define the space

$$W^p_{\mathrm{div}}(\Omega) := \{V \in L^p(\Omega) \mid \exists g \in L^p(\Omega) \text{ s. t. } \int_\Omega VG \cdot \nabla\phi = -\int_\Omega g\phi, \ \forall\phi \in \mathcal{C}^1_c(\Omega)\}$$

The function g of this definition is denoted $\mathrm{div}(GV)$. We endow this space with the norm

$$||V||_{W^p_{\mathrm{div}}} = ||V||_{L^p} + ||\mathrm{div}(GV)||_{L^p}.$$

Functional analysis of this space is required for the theoretical analysis of our model's evolution equation.

Remark 3.1. *Since* $\mathrm{div}(G) \in L^\infty$, *for* $V \in W^p_{\mathrm{div}}(\Omega)$, *we can define*

$$G \cdot \nabla V := \mathrm{div}(GV) - V\mathrm{div}(G) \in L^p(\Omega)$$

and the space $W^p_{\mathrm{div}}(\Omega)$ *is also the space of* L^p *functions such that there exists a function* $g \in L^p(\Omega)$ *verifying*

$$\int_\Omega V\mathrm{div}(G\phi) = -\int_\Omega g\phi, \quad \forall\phi \in \mathcal{C}^1_c(\Omega).$$

This space already appeared for the study of the boundary problem for the transport equation in [Bar70, Ces84, Ces85]. We turn our interest on two problems :

1. Density of regular functions up to the boundary $C^1(\overline{\Omega})$ in $W^p_{\mathrm{div}}(\Omega)$

2. Traces and integration by part formula

and describe the approach we use to deal with these issues in the case of our model, with a particular focus on the second one which is our main need in the study of the space $W^p_{\mathrm{div}}(\Omega)$, consisting in straightening the integral curves of the field G and proving a conjugation theorem between $W^{1,1}(]0, +\infty[\,; L^1(\partial\Omega))(\Omega)$ and $W^{1,1}(]0, +\infty[; L^1(\partial\Omega))$. We prove a similar result for $W^\infty_{\mathrm{div}}(\Omega)$. We also describe two classical approaches : by regularization and by duality techniques.

Lemma 3.2. $(W_{\mathrm{div}}^p(\Omega)\,,\,||\cdot||_{W_{\mathrm{div}}^p})$ *is a Banach space.*

Proof. Let V_n be a Cauchy sequence in $W_{\mathrm{div}}^p(\Omega)$. By completeness of $L^p(\Omega)$, there exists $V, W \in L^p(\Omega)$ such that $V_n \xrightarrow{L^p} V$, and $\mathrm{div}(GV_n) \xrightarrow{L^p} W$. Then, for every $\phi \in \mathcal{C}_c^1(\Omega)$

$$
\begin{array}{ccc}
\int \mathrm{div}(GV_n)\phi & \longrightarrow & \int W\phi \\
\| & & \| \\
-\int V_n G \cdot \nabla\phi & \longrightarrow & -\int V G \cdot \nabla\phi
\end{array}
$$

Thus $W \in W_{\mathrm{div}}(\Omega)$ and $W = \mathrm{div}(GV)$. $\qquad\qquad\square$

1 Conjugation approach

For this section, we place ourselves in the framework of our model, with

$$
\Omega =]1,b[\times]1,b[, \quad G(X) = G(x,\theta) = \begin{pmatrix} ax\ln\left(\frac{\theta}{x}\right) \\ cx - dx^{2/3}\theta \end{pmatrix} = \begin{pmatrix} G_1(x,\theta) \\ G_2(x,\theta) \end{pmatrix}. \tag{1}
$$

We will prove a so-called conjugation theorem between $W_{\mathrm{div}}^p(\Omega)$ and $W^{1,1}(]0,+\infty[;L^1(\partial\Omega))$ for $p = 1, \infty$ consisting in straightening the characteristics (integral curves of G), as illustrated in the figure 1.
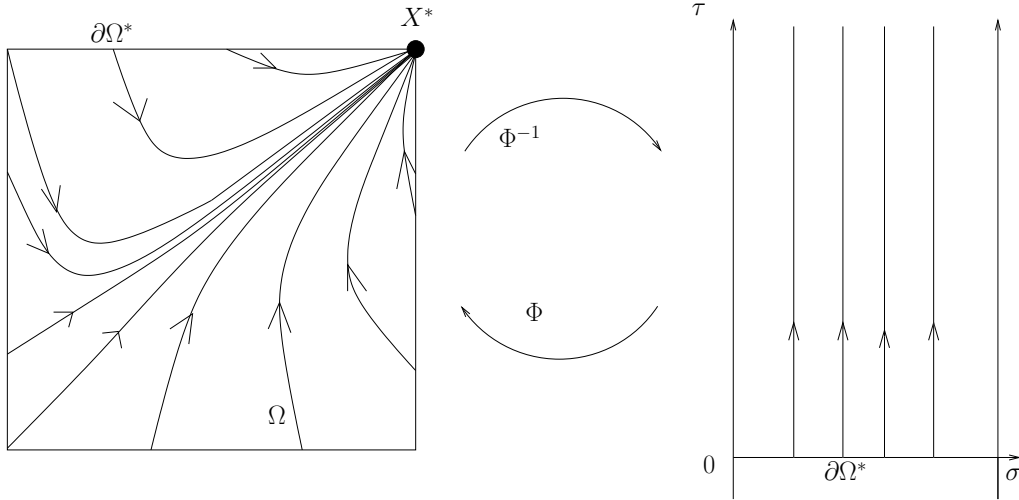
Figure 1: Φ is a locally bilipschitz homeomorphism.

1.1 Change of variables

We will now turn our interest to the flow defined by the solutions of the system of ODE

$$
\begin{cases} \frac{d}{dt}X(t) = G(X(t)) \\ X(0) = \sigma \end{cases} \tag{2}
$$

as it will play a fundamental role in the sequel. We define the application

$$\Phi : \begin{array}{ccc} [0,\infty[\times\partial\Omega & \to & \overline{\Omega} \\ (\tau,\sigma) & \mapsto & \Phi_\tau(\sigma) \end{array}$$

as being the solution of the system (2) at time τ with the initial condition $\sigma \in \partial\Omega$. We will show that

$$\Phi : [0,\infty[\times\partial\Omega^* \to \overline{\Omega}^*$$

is an homeomorphism locally bilipschitz, $\partial\Omega^* = \partial\Omega\backslash\{(b,b)\}$ and $\overline{\Omega}^* = \overline{\Omega}\backslash\{(b,b)\}$. We also define $X^* = (b,b)$. In order to have a candidate for the inverse of Φ, we define for $(x,\theta) \in \overline{\Omega}$

$$\tau(x,\theta) = \inf\{\tau \geq 0|\ \Phi_{-\tau}(\mathrm{x},\theta) \in \partial\Omega^*\}, \quad \sigma(\mathrm{x},\theta) = \Phi_{-\tau(\mathrm{x},\theta)}(\mathrm{x},\theta). \tag{3}$$

Lemma 3.3. *For all $(x,\theta) \in \overline{\Omega}$ there exists $0 \leq \tau < \infty$ such that $\Phi_{-\tau}(x,\theta) \in \partial\Omega$.*

Proof. Let $X = (x,\theta) \in \overline{\Omega}$. We will argue by contradiction. Suppose that for all $\tau \geq 0$, $\Phi_{-\tau}(X) \in \overline{\Omega}$ which is compact. The Poincaré-Bendixson theorem (see section 1.3.2 of chapter 1) then implies that the only possibilities for the asymptotic behavior of the trajectory are either convergence to the only critical point of $-G : (b,b)$ or convergence to a closed orbit (limit cycle or homoclinic orbit starting and ending in (b,b)). The second point is prohibited as it is established that G has no closed orbit in $\overline{\Omega}$ (proposition 1.8 of chapter 1) and thus neither has $-G$. The first possibility leads also to a contradiction for the same argument since it would imply the existence of a homoclinic orbit from the convergence in positive time of $\Phi_\tau(X)$ to (b,b). $\qquad\square$

The time $\tau(x,\theta)$ is the time spent in Ω and $\sigma(x,\theta)$ is the entrance point of the characteristic passing through the point (x,θ). From the Lipschitz regularity of Ω we can't expect Φ to be globally $\mathcal{C}^1$, this is why we introduce the following open sets :

$$\Omega_i = \{\Phi_\tau(\sigma);\ \sigma \in \partial\Omega_i,\ \tau \in]0,\infty[\}, \quad i = 1,2,3,4$$

where

$$\partial\Omega_1 =](1,1),(1,b)[,\ \partial\Omega_2 =](1,b),(b,b)[,\ \partial\Omega_3 =](b,b),(b,1)[,\ \partial\Omega_4 =](b,1),(1,1)[.$$

The restriction of Φ to $]0,\infty[\times\partial\Omega_i$ is a diffeomorphism, as established in the following proposition and illustrated in the figure 1.

Proposition 3.4 (Properties of the flow)**.**
(i) The application Φ is a diffeomorphism $]0,\infty[\times\partial\Omega_i \to \Omega_i$ and for every $\tau \geq 0$ and almost every $\sigma \in \partial\Omega$

$$J_\Phi(\tau,\sigma) = G \cdot \nu(\sigma)e^{\int_0^\tau \mathrm{div}(G(\Phi_s(\sigma)))ds} \tag{4}$$

where $J_\Phi(\tau,\sigma) = \det(D\Phi)$ is the Jacobian determinant of Φ.
(ii) Globally, Φ is an homeomorphism $[0,\infty[\times\partial\Omega^* \to \overline{\Omega}^*$ locally bilipschitz with inverse $(x,\theta) \mapsto (\tau(x,\theta),\sigma(x,\theta))$.

Remark 3.5. *The regularity proven here on Φ validates the use of Φ as a change of variables (see [Dro01b] for locally Lipschitz changes of variables).*

Proof.

• Φ *is one-to-one and onto* $[0, \infty[\times \partial\Omega^* \to \overline{\Omega}^*$. Let $X = (x, \theta) \in \Omega$. We have $\Phi(\tau(X), \sigma(X)) = X$ because $\Phi_{-\tau(X)}(X) = \sigma(X)$ implies $X = \Phi_{\tau(X)}(\sigma(X))$ (indeed $\Phi_{-\tau}$ is the inverse of Φ_τ when τ is fixed from the semigroup property of the flow coming from the Cauchy-Lipschitz theorem). For the injectivity, if there exists (τ, σ), $(\tau', \sigma') \in [0, \infty[\times \partial\Omega^*$ such that $\Phi_\tau(\sigma) = \Phi_{\tau'}(\sigma')$, with for instance $\tau < \tau'$, then $\Phi_{\tau'-\tau}(\sigma) = \sigma'$ which is impossible since, following remark 1.6 after the lemma 1.5 in the chapter 1, we have $\Phi_{\tau'-\tau}(\sigma) \in \Omega$. Hence $(\tau, \sigma) \mapsto \Phi_\tau(\sigma)$ is one-to-one and from

$$\Phi_{\tau(\Phi_\tau(\sigma))}(\sigma(\Phi_\tau(\sigma))) = \Phi_{\tau(\Phi_\tau(\sigma))}(\Phi_{-\tau(\Phi_\tau(\sigma))}(\Phi_\tau(\sigma))) = \Phi_\tau(\sigma),$$

we get $(\tau(\Phi_\tau(\sigma)), \sigma(\Phi_\tau(\sigma))) = (\tau, \sigma)$. Thus Φ is one-to-one and onto and $\Phi^{-1}(x, \theta) = (\tau(x, \theta), \sigma(x, \theta))$.

• Φ *is a diffeomorphism on* $]0, \infty[\times \partial\Omega_i$. Using the general theorem of dependency on the initial conditions for ODEs, Φ is $\mathcal{C}^1(]0, \infty[\times \partial\Omega_i)$ and if we call $\sigma(s)$ a parametrization of $\partial\Omega_i$, we have $\frac{\partial\Phi}{\partial s}(\tau, \sigma(s)) = D_y\Phi_\tau(\sigma(s)) \circ \sigma'(s)$, and the following characterization of $\frac{\partial\Phi}{\partial s}(\tau, \sigma(s))$ stands : for each s, it is the solution of the differential equation

$$\begin{cases} \frac{dZ}{d\tau} = DG(\Phi) \circ Z \\ Z(0) = \sigma'(s) \end{cases}$$

Using this characterization, we can derive the formula (4) for the Jacobian $J_\Phi(\tau, \sigma)$. We have $J_\Phi(\tau, \sigma) = \frac{\partial\Phi}{\partial s} \wedge \frac{\partial\Phi}{\partial \tau} = \frac{\partial\Phi}{\partial s} \wedge G(\Phi)$, and differentiating in τ we get

$$\frac{\partial}{\partial\tau} J_\Phi(t, \sigma) = DG \circ \frac{\partial\Phi}{\partial s} \wedge G(\Phi) + \frac{\partial\Phi}{\partial s} \wedge DG \circ G(\Phi)$$
$$= \text{trace}(DG) J_\Phi(t, \sigma) = \text{div}(G) J_\Phi(t, \sigma).$$

Hence, for all $\sigma(s)$, using that $J_\Phi(0, \sigma(s)) = \sigma'(s) \wedge G(\sigma(s)) = |\sigma'(s)| G \cdot \overrightarrow{\nu}(\sigma(s)) \neq 0$ on $]0, \infty[\times \partial\Omega_i$, we obtain the formula

$$J_\Phi(t, \sigma(s)) = |\sigma'(s)| G \cdot \overrightarrow{\nu}(\sigma(s)) \exp\left(\int_0^t \text{div}(G(\Phi(\tau, \sigma(s)))) d\tau\right) \neq 0. \tag{5}$$

We get (4) by choosing a parametrization with velocity equal to one. In the sequel, we fix this parametrization. We can then apply the global inversion theorem to conclude that Φ is a $\mathcal{C}^1$-diffeomorphism $]0, \infty[\times \partial\Omega_i \to \Omega_i$.

• *Globally.* From the given properties of the vector field G, we can extend the flow to a neighborhood V of $\overline{\Omega}$, and we have that it is $\mathcal{C}^1([0, \infty[\times V)$ (see [Dem96], XI p.305). Hence Φ, which is the restriction of this application to $[0, \infty[\times \partial\Omega^*$ with $\partial\Omega^*$ being Lipschitz, is locally Lipschitz. Remark here that it is not globally Lipschitz since $\frac{\partial}{\partial\sigma}\Phi_\tau(\sigma)$ can blow up when τ goes to infinity, due to the singularity at X^*.

To show that Φ^{-1} is also locally Lipschitz on $\overline{\Omega}^*$ we consider some compact set $K \subset \overline{\Omega}^*$ and show that Φ^{-1} is Lipschitz on K. We define $K_i = \overline{\Omega_i} \cap K$, and $\widetilde{K_i} := \Phi^{-1}(K_i) \subset [0, \infty[\times \overline{\partial\Omega_i}$. Now since Φ is the restriction of a globally $\mathcal{C}^1$ application, we have $\Phi \in \mathcal{C}^1(\widetilde{K_i})$, meaning that its differential $D\Phi$ is continuous up to the boundary of $\widetilde{K_i}$. Moreover using the formula (5), we see that the value of $D\Phi$ on $\partial\widetilde{K_i}$ is invertible since we avoid the singularity at X^*. Hence, using the continuity of the inverse application we obtain that $D\Phi^{-1} = (D\Phi)^{-1}$ is continuous on K_i. Thus $\Phi^{-1} \in \mathcal{C}^1(K_i)$ and so it is Lipschitz on each K_i. It remains to see that Φ^{-1} is globally continuous in order to conclude. This is based on the following lemma, which we do not demonstrate here.

Lemma 3.6. *The mapping* $\begin{array}{ccc} \Omega & \to &]0,\infty[\\ X & \mapsto & \tau(X) \end{array}$ *is continuous.*

With this lemma, we also get the continuity of $\sigma(X) = \Phi_{-\tau(X)}(X)$. Finally Φ^{-1} is globally continuous on $\overline{\Omega}^*$ and Lipschitz on each K_i, so it is Lipschitz on K. $\qquad\qquad\square$

1.2   Conjugation of $W_{\mathrm{div}}^p(\Omega)$ and $W^{1,p}(]0,+\infty[\,;\,L^p(\partial\Omega))$

For a function $V \in L^1(\Omega)$, belonging to $W_{\mathrm{div}}^1(\Omega)$ means that it is weakly differentiable along the characteristics. The next theorem of this section makes this more precise. We recall first the definition of Banach-valued Sobolev spaces (see [Dro01a] for more details about this question).

Definition 3.7 (Banach-valued Sobolev spaces)**.** *Let I be a real interval, X a Banach space and A a measurable space. We define*

$$W^{1,1}(I\,;\,X) := \left\{ u \in L^1(I\,;\,X);\ \exists v \in L^1(I\,;\,X)\ s.t.\ \forall \phi \in \mathcal{C}_c^1(I),\ \int_I u(t)\phi'(t)dt = -\int_I v(t)\phi(t)dt \right\}$$

$$W_\tau^{1,\infty}(I\times A) := \left\{ u \in L^\infty(I\times A);\ \exists v \in L^\infty(I\times A)\ s.t. \forall \phi \in \mathcal{C}_c^1(I),\ \int_I u(t)\phi'(t)dt = -\int_I v(t)\phi(t)dt \right\}$$

Remark 3.8. *We distinguish the definition for $p = 1$ and $p = \infty$ to avoid troubles caused by the fact that in general $L^\infty(I\times A) \neq L^\infty(I\,;\,L^\infty(A))$ (see [Dro01a], p. 28).*

Theorem 3.9 (Conjugation of $W_{\mathrm{div}}^1(\Omega)$ and $W^{1,1}(]0,+\infty[\,;\,L^1(\partial\Omega)))$**.** *The spaces $W_{\mathrm{div}}^1(\Omega)$ and $W^{1,1}(]0,+\infty[\,;\,L^1(\partial\Omega))$ are conjugated via Φ in the following sense :*

$$V \in W_{\mathrm{div}}^1(\Omega) \Leftrightarrow (V \circ \Phi)|J_\Phi| \in W^{1,1}(]0,+\infty[\,;\,L^1(\partial\Omega)).$$

For functions in $W_{\mathrm{div}}^\infty(\Omega)$, we have

$$V \in W_{\mathrm{div}}^\infty(\Omega) \Leftrightarrow (V \circ \Phi) \in W_\tau^{1,\infty}(]0,+\infty[\times\partial\Omega).$$

Moreover, for $p = 1,\infty$ and $V \in W_{\mathrm{div}}^p(\Omega)$ we have almost everywhere

$$\partial_\tau (V \circ \Phi |J_\Phi|^{1/p}) = \begin{cases} (\mathrm{div}(GV) \circ \Phi)|J_\Phi| & if\ p = 1 \\ (G\cdot\nabla V) \circ \Phi & if\ p = \infty \end{cases}$$

where we use the notation $1/\infty = 0$. The applications

$$\begin{array}{ccc} W_{\mathrm{div}}^1(\Omega) & \to & W^{1,1}((0,+\infty);L^1(\partial\Omega)) \\ V & \mapsto & V \circ \Phi|J_\Phi| \end{array} \quad and \quad \begin{array}{ccc} W_{\mathrm{div}}^\infty(\Omega) & \to & W_\tau^{1,\infty}(]0,+\infty[\times\partial\Omega) \\ V & \mapsto & V \circ \Phi \end{array}$$

are isometries.

Remark 3.10.

  • *In particular, we deduce from the theorem applied to the function $V = 1$ that $|J_\Phi| \in W^{1,1}(]0,+\infty[\,;\,L^1(\partial\Omega))$ and we recognize the well-known formula*

$$\partial_\tau |J_\Phi|(\tau,\sigma) = \mathrm{div}(G(\Phi_\tau(\sigma)))|J_\Phi|(\tau,\sigma), \quad a.e.\ (\tau,\sigma) \in]0,+\infty[\times\partial\Omega.$$

- *Since by proposition 3.4, we have* $|J_\Phi|^{-1} \in W^{1,\infty}_{loc}([0,\infty[\times\partial\Omega^*)$ *we deduce that for* $V \in W^1_{\mathrm{div}}(\Omega)$

$$V(\Phi_\tau(\sigma)) = V(\Phi_\tau(\sigma))|J_\Phi| \times |J_\Phi|^{-1} \in W^{1,1}_{loc}([0,\infty[\,;\,L^1_{loc}(\partial\Omega^*))$$

with

$$\partial_\tau V(\Phi_\tau(\sigma)) = G \cdot \nabla V(\Phi_\tau(\sigma))$$

Proof. We first show the theorem on $W^1_{\mathrm{div}}(\Omega)$ and then for $W^\infty_{\mathrm{div}}(\Omega)$

- We prove now $(V \in W^1_{\mathrm{div}}(\Omega)) \Rightarrow (\widetilde{V} := (V \circ \Phi)|J_\Phi| \in W^{1,1}(]0,+\infty[\,;\,L^1(\partial\Omega)))$. Let $V \in W_{\mathrm{div}}(\Omega)$ and remark that $\widetilde{V} \in L^1(]0,\infty[\times\partial\Omega)$ since $|J_\Phi|$ is the Jacobian of the change of variable between Ω and $]0,\infty[\times\partial\Omega^*$. Then, using the definition of $W^{1,1}(]0,+\infty[\,;\,L^1(\partial\Omega))$ we have to prove that there exists a function $g \in L^1(]0,\infty[\times\partial\Omega)$ such that for every function $\widetilde{\psi} \in \mathcal{C}^\infty_c(]0,\infty[)$

$$\int_0^\infty \widetilde{V}(\tau,\sigma)\widetilde{\psi}'(\tau)d\tau = -\int_0^\infty g(\tau,\sigma)\widetilde{\psi}(\tau)d\tau, \quad a.e.\ \sigma \in \partial\Omega.$$

As we aim to use the change of variable Φ which lives in $]0,\infty[\times\partial\Omega$, we will rather prove that for every function $\zeta \in Lip(\partial\Omega)$ (the Lipschitz functions on $\partial\Omega$)

$$\int_{\partial\Omega} \left\{ \int_0^\infty \widetilde{V}(\tau,\sigma)\widetilde{\psi}'(\tau)d\tau \right\} \zeta(\sigma)d\sigma = \tag{6}$$
$$\int_{\partial\Omega} \left\{ -\int_0^\infty \mathrm{div}(GV)(\Phi_\tau(\sigma))|J_\Phi|\widetilde{\psi}(\tau)d\tau \right\} \zeta(\sigma)d\sigma$$

which is sufficient to prove the result. Let now fix $\widetilde{\psi} \in \mathcal{C}^\infty_c(]0,\infty[)$ and define the function

$$\psi(x,\theta) := \widetilde{\psi}(\tau(x,\theta))$$

with $\tau(x,\theta)$ the time spent in Ω defined in the section 3.1.1. Then ψ has compact support in Ω and is Lipschitz as the composition of a regular function and a locally Lipschitz function (see prop. 3.4 for the locally Lipschitz regularity of the function $(x,\theta) \mapsto \tau(x,\theta)$), thus differentiable almost everywhere and the reverse formula $\widetilde{\psi}(\tau) = \psi(\Phi_\tau(\sigma))$ (for any $\sigma \in \partial\Omega$ since the function ψ depends only on the time spent in Ω) yields

$$\widetilde{\psi}'(\tau) = G(\Phi_\tau(\sigma)) \cdot \nabla\psi(\Phi_\tau(\sigma)), \quad a.e.\ \tau \in]0,\infty[,\ \forall\sigma \in \partial\Omega$$

since $\tau \mapsto \Phi_\tau(\sigma)$ is $\mathcal{C}^1$. Hence $\widetilde{\psi}'(\tau(x,\theta)) = G(\Phi_{\tau(x,\theta)}(\sigma(x,\theta))) \cdot \nabla\psi(\Phi_{\tau(x,\theta)}(\sigma(x,\theta))) = G(x,\theta) \cdot \nabla\psi(x,\theta)$ and doing now the change of variables in the left hand side of (6) yields

$$\int_{\partial\Omega} \left\{ \int_0^\infty \widetilde{V}(\tau,\sigma)\widetilde{\psi}'(\tau)d\tau \right\} \zeta(\sigma)d\sigma = \int_\Omega V(x,\theta)\zeta(\sigma(x,\theta))G(x,\theta) \cdot \nabla\psi(x,\theta)dxd\theta \tag{7}$$

Still denoting $\zeta(x,\theta)$ the function $\zeta(\sigma(x,\theta))$, we remark that this function only depends on the entrance point $\sigma(x,\theta)$ and thus we have

$$(G \cdot \nabla\zeta)(\Phi_\tau(\sigma)) = \partial_\tau(\zeta(\Phi_\tau(\sigma))) = \partial_\tau(\zeta(\sigma)) = 0, \quad \forall\tau \geq 0,\ a.e\ \sigma$$

To pursue the calculation, we need to regularize the Lipschitz functions ζ and ψ in order to use them in the distributional definition of $\mathrm{div}(GV)$. We use the following lemma, whose proof can be found in [Tar07], p.60.

Lemma 3.11. *Let* $f \in W^{1,\infty}(\Omega)$ *with* Ω *a Lipschitz domain. Then there exists a sequence* $f_n \in \mathcal{C}^\infty(\overline{\Omega})$ *such that*

$$f_n \xrightarrow{W^{1,p}} f \ \forall 1 \le p < \infty, \ f_n \to f \ L^\infty \ weak - *, \ \nabla f_n \to \nabla f \ L^\infty \ weak - *.$$

Now let $\psi_n \to \psi$ and $\zeta_m \to \zeta$ as in the lemma. From the demonstration of the lemma which is done by convolution with a mollifier, since ψ has compact support, so does ψ_n for n large enough. Now remark that for each n and m

$$G \cdot \nabla(\psi_n \zeta_m) = \zeta_m G \cdot \nabla \psi_n + \psi_n G \cdot \nabla \zeta_m.$$

The test function $\psi_n \zeta_m$ is now valid in the distributional definition of $\mathrm{div}(GV)$ and we have

$$\int_\Omega V\zeta_m G \cdot \nabla \psi_n dx d\theta = \int_\Omega V G \cdot \nabla(\psi_n \zeta_m) dx d\theta - \int_\Omega V\psi_n G \cdot \nabla \zeta_m$$
$$= -\int_\Omega \mathrm{div}(GV)\psi_n \zeta_m dx d\theta - \int_\Omega V\psi_n G \cdot \nabla \zeta_m dx d\theta$$

Letting first n going to infinity, then m and remembering that $G \cdot \nabla \zeta = 0$ yields

$$\int_\Omega V\zeta G \cdot \nabla \psi dx d\theta = -\int_\Omega \mathrm{div}(GV)\psi\zeta dx d\theta.$$

Now doing back the change of variables Φ^{-1} gives the identity (6).

• We show now the reverse implication. Let $\widetilde{V} \in W^{1,1}(]0,+\infty[; L^1(\partial\Omega))$ and $\psi \in \mathcal{C}_c^\infty(\Omega)$. Define $V(x,\theta) := (\widetilde{V} \circ \Phi^{-1})|J_{\Phi^{-1}}|$ and $\widetilde{\psi}(\tau,\sigma) := \psi(\Phi_\tau(\sigma))$. Hence $\widetilde{\psi}$ is $\mathcal{C}_c^1$ in the variable τ and we have $\partial_\tau \widetilde{\psi} = (G \cdot \nabla \psi) \circ \Phi$. Now

$$\int_\Omega V G \cdot \nabla \psi dx d\theta = \int_{\partial\Omega} \int_0^\infty \widetilde{V}(\tau,\sigma)\partial_\tau \widetilde{\psi}(\tau,\sigma) d\tau d\sigma = -\int_{\partial\Omega}\int_0^\infty \partial_\tau \widetilde{V} \widetilde{\psi} d\tau d\sigma$$
$$= -\int_\Omega \partial_\tau \widetilde{V} \circ \Phi^{-1} \psi dx d\theta$$

Hence we have proved that $V \in W_{\mathrm{div}}(\Omega)$ and that $\mathrm{div}(GV) = \partial_\tau \widetilde{V} \circ \Phi^{-1}$.

• We prove now the part of the theorem on $W_{\mathrm{div}}^\infty(\Omega)$. Let $U \in W_{\mathrm{div}}^\infty(\Omega) \subset W_{\mathrm{div}}^1(\Omega)$. Then $U \circ \Phi \in L^\infty(]0,\infty[\times\partial\Omega)$. Moreover, applying the second point of the remark following the theorem, we have

$$\partial_\tau U(\Phi_\tau(\sigma)) = G \cdot \nabla U(\Phi_\tau(\sigma)) \in L^\infty(]0,\infty[\times\partial\Omega).$$

Using that for $\widetilde{U} \in W^{1,\infty}((0,+\infty); L^\infty(\partial\Omega))$ we have locally $G \cdot \nabla U := \partial_\tau \widetilde{U} \circ \Phi^{-1} \in L^\infty(\Omega)$ with $U = \widetilde{U} \circ \Phi^{-1}$ gives the reverse implication. $\qquad\square$

1.3   Generalization. Limits of the method

Our method is able to manage situations where $G \cdot \nu$ vanishes but not changes sign. It should adapt to the case of an open set Ω and a field G such that an analogous to proposition 3.4 holds, that is when all the trajectories remain in Ω for all time and hit the boundary. In general situations, this may be not the case since : 1) trajectories can never hit the boundary and 2)

trajectories can enter and leave Ω. Then we don't have anymore $\Omega \simeq]0, \infty[\times \partial\Omega$. To deal with these issues, we should introduce, as done in Bardos [Bar70]

$$\partial\Omega^- := \{\sigma \in \partial\Omega;\ G \cdot \nu < 0\}, \quad \partial\Omega^+ := \{\sigma \in \partial\Omega;\ G \cdot \nu > 0\}, \quad \partial\Omega^0 := \{\sigma \in \partial\Omega;\ G \cdot \nu = 0\}.$$

Using then the entrance time defined in (3) and the convention $\inf(\emptyset) = +\infty$ we could define the set

$$\Omega^- = \{X \in \overline{\Omega};\ \tau(X) < \infty \text{ and } \sigma(X) \in \partial\Omega^-\}$$

and could try to apply our approach to this set. The first problem arising is that $\Phi^{-1}(\Omega^-)$ is not anymore a rectangle. Introducing the total time spent in Ω by

$$T(\sigma) = \inf\{\tau > 0;\ \Phi_\tau(\sigma) \notin \Omega\}.$$

We have

$$\Phi^{-1}(\Omega^-) = \{(\tau, \sigma) \in [0, \infty[\times \partial\Omega^-;\ 0 \leq \tau \leq T(\sigma)\}$$

and everything depends on the shape of this set. If $T(\sigma) \geq \underline{T}$, $\forall\, \sigma \in \partial\Omega^-$, then $[0, \underline{T}] \times \partial\Omega^- \subset \Phi^{-1}(\Omega^-)$ and a similar proposition as proposition 3.4 could be established for Ω^- locally near the boundary, which would then be sufficient to have a trace theorem. The same approach can be done for the set Ω^+ of trajectories which go out of Ω by $\partial\Omega^+$. The set of trajectories remaining in Ω for ever will never hit the boundary and are thus not to be considered and as proved in Bardos [Bar70] using the Sard theorem, the set of trajectories hitting $\partial\Omega^0$ has measure zero in Ω.

The main difficulty arises thus when the life time $T(\sigma)$ is not bounded from below which appears if $G \cdot \nu$ changes sign on $\partial\Omega$ (see section 3.3.2 for more details on this case).

2 Density of $\mathcal{C}^1(\overline{\Omega})$ of $W^p_{\mathrm{div}}(\Omega)$

Two classical approaches can be used to address this problem : by duality or by direct regularization. In this section, we will describe what gives our approach concerning the problem and then we will describe how to treat the problem by the two approaches aforementioned. The proofs are mainly inspired from Brezis [Bre83] or Adams [AF03] in the case of classical Sobolev spaces for the regularization approach and from Girault-Raviart [GR79] and Boyer-Fabrie [BF06] for the duality one. We will not deal with the density of $\mathcal{C}^1(\Omega)$ in $W^p_{\mathrm{div}}(\Omega)$, that is of regular functions but not up to the boundary (Meyers Serrin theorem in the case of classical Sobolev spaces, see [AF03]).

2.1 Conjugation approach

In the case of (1), for $p = 1$ the conjugation theorem should allow to transport the density result known for $W^{1,1}(]0, +\infty[;\ L^1(\partial\Omega))$ into $W^p_{\mathrm{div}}(\Omega)$. However it doesn't achieve this aim for the following reasons : the regularity of the change of variable depends on the regularity of the boundary of Ω (Lipschitz in the case of a square) and thus we can't expect density of $\mathcal{C}^1$ functions. Yet, we could be satisfied with the density of Lipschitz functions. This is neither achieved because the singularity of the field in the upper corner implies that Φ is only locally bilipschitz. The only theorem which is straightforward from the theorem 3.9 is the following.

Theorem 3.12. *Let Ω and G be given by* (1), *and $p = 1$. The set $Lip_{loc}(\overline{\Omega}^*)$ is dense in $W^p_{\mathrm{div}}(\Omega)$, where $Lip_{loc}(\overline{\Omega}^*)$ is the set of locally Lipschitz functions of $\overline{\Omega}^* = \overline{\Omega} \setminus (b, b)$.*

2.2   Regularization approach

A classical technique to prove the result (as in Brezis [Bre83] or Adams [AF03] for instance) is to argue by regularization. Let

$$\rho \in \mathcal{C}^\infty_c(\mathbb{R}^d), \rho \geq 0, \ \int_{\mathbb{R}^d} \rho(x)dx = 1, \ \mathrm{supp}\rho \subset B(0,1), \ \rho_\varepsilon(x) = \frac{1}{\varepsilon^d}\rho(\frac{x}{\varepsilon}) \in \mathcal{C}^\infty_c(\mathbb{R}^d)$$

be a mollifier (notice that $\mathrm{supp}\rho_\varepsilon \subset B(0,\varepsilon)$). The problem is that the derivation along G doesn't behave so well with convolution than in the case of standard Sobolev spaces since we have

$$G \cdot \nabla(v * \rho_\varepsilon) \neq (G \cdot \nabla v) * \rho_\varepsilon.$$

Moreover, the convolution written don't have a sense since the involved functions are defined on $\mathbb{R}^d$. To deal with these issue we will use a commutation lemma (see also [DL89] or [Per07], p.157) as well as adapted definitions of the convolution. We follow the standard way which begins by proving the density on each compact subset of Ω, without assuming any regularity on the boundary of the domain.

Proposition 3.13. *Let Ω be an open set in $\mathbb{R}^d$ and $v \in W^p_{\mathrm{div}}(\Omega)$. There exists a sequence $v_n \in \mathcal{C}^1_c(\Omega)$ such that for all open set $\omega \subset\subset \Omega$[12] :*

$$v_n \to v, \quad in \quad W^p_{\mathrm{div}}(\omega).$$

Proof. Let $v \in W^p_{\mathrm{div}}(\Omega)$, $\omega \subset\subset$, $\alpha \in \mathcal{C}^1_c(\Omega)$ a truncature function such that $\alpha = 1$ on ω and $u = \alpha v$. We define the convolution on Ω of u and ρ_ε by, for ε small enough (such that $\mathrm{supp}(\alpha) + B(0,\varepsilon) \subset \Omega$)

$$u_\varepsilon(x) = u *_\Omega \rho_\varepsilon(x) := \int_\Omega u(y)\rho_\varepsilon(x-y)dy = \int_{B(x,\varepsilon)} u(y)\rho_\varepsilon(x-y), \quad \forall x \in \omega.$$

Remark that This convolution shares the same property of the usual one and in particular we have

$$u *_\Omega \rho_\varepsilon \xrightarrow{L^p(\omega)} u = v, \quad in \ L^p(\omega)$$

$$(G \cdot \nabla u) *_\Omega \rho_\varepsilon \xrightarrow{L^p(\omega)} G \cdot \nabla u = G \cdot \nabla v, \quad in \ L^p(\omega).$$

As noticed above we don't have $G \cdot \nabla(v * \rho_\varepsilon) = (G \cdot \nabla v) * \rho_\varepsilon$ but the following commutation lemma allows to conclude.

Lemma 3.14. *Let $G \in \mathcal{C}^1(\overline{\Omega})$ and $u \in W^p_{\mathrm{div}}(\Omega)$. Then*

$$R_\varepsilon = G \cdot \nabla(u *_\Omega \rho_\varepsilon) - (G \cdot \nabla u) *_\Omega \rho_\varepsilon \xrightarrow{L^p(\omega)} 0.$$

---

[12]This notation means : there exists a compact set K such that $\omega \subset K \subset \Omega$

Remark 3.15. *This lemma is also true under weaker assumptions on the regularity of G, for example $G \in W^{1,1}(\Omega)^d$ and is in the heart of the theory of renormalized solutions for the transport equation (see [DL89] and [Per07], p. 157)*

Proof. Let $x \in \omega$. One one hand we have

$$G \cdot \nabla(u *_\Omega \rho_\varepsilon) = G(x) \cdot \nabla \int_\Omega u(y)\rho_\varepsilon(x-y)dy = \int_\Omega u(y)\frac{G(x)}{\varepsilon^{d+1}} \cdot \nabla\rho\left(\frac{x-y}{\varepsilon}\right)dy$$

whereas on the other hand, noticing that for $x \in \omega$, $y \mapsto \rho_\varepsilon(x-y) \in \mathcal{C}_c^1(\Omega)$ and using the distribution definition of $G \cdot \nabla u$ we have

$$(G \cdot \nabla u) *_\Omega \rho_\varepsilon(x) = \int_\Omega G \cdot \nabla u(y)\rho_\varepsilon(x-y)dy = -\int_\Omega u(y)\mathrm{div}_y\left[G(y)\frac{1}{\varepsilon^d}\rho\left(\frac{x-y}{\varepsilon}\right)\right]dy$$

$$= \int_\Omega u(y)\frac{G(y)}{\varepsilon^{d+1}} \cdot \nabla\rho\left(\frac{x-y}{\varepsilon}\right)dy - \int_\Omega u(y)\mathrm{div}(G(y))\rho_\varepsilon(x-y)dy.$$

Hence we have

$$R_\varepsilon(x) = R_\varepsilon^1(x) + R_\varepsilon^2(x) = \int_\Omega u(y)\frac{G(x) - G(y)}{\varepsilon^{d+1}} \cdot \nabla\rho\left(\frac{x-y}{\varepsilon}\right)dy + (u\,\mathrm{div}(G)) *_\Omega \rho_\varepsilon(x)$$

The term R_ε^2 tends to $u(x)\mathrm{div}(G(x))$ in $L^p(\Omega)$. For the first term, we do the change of variables $z = \frac{x-y}{\varepsilon}$ to get

$$R_1^\varepsilon(x) = -\int_{|z| \leq 1} u(x-\varepsilon z)\frac{G(x) - G(x-\varepsilon z)}{\varepsilon} \cdot \nabla\rho(z)\,dz.$$

Now, since

$$u(x-\varepsilon z) \xrightarrow[\varepsilon\to 0]{L^p(\omega \times B(0,1))} u(x)$$

$$\frac{G(x) - G(x-\varepsilon z)}{\varepsilon} \cdot \nabla\rho(z) \xrightarrow[\varepsilon\to 0]{L^\infty(\omega \times B(0,1))} DG(x) \cdot z$$

we obtain, since ω is bounded that

$$R_1^\varepsilon(x) \xrightarrow{L^p(\omega)} -u(x)\int_{|z| \leq 1} DG(x) \cdot z \cdot \nabla\rho(z)dz = -u(x)\mathrm{div}(G(x))$$

where the last identity is obtained after integration by part. This yields the result. □

□

We want now to prove the density of regular functions **up to the boundary**. This can be done only under regularity hypothesis on the open set Ω that we need to precise. Brezis' approach for classical Sobolev spaces consists in defining an extension operator : $W^{1,p}(\Omega) \to W^{1,p}(\mathbb{R}^d)$ and then regularize. This seems more delicate to do in our case in particular if the tangential part of the field G vanishes on the boundary. However, the approach of Adams [AF03] does extend word for word to our case, with a regularity condition for Ω given by the segment condition.

Definition 3.16 (Segment condition, Adams [AF03] p.68)**.** *We say that a domain Ω satisfies the segment condition if every $x \in \partial\Omega$ has a neighborhood U_x and a nonzero vector y_x such that if $z \in \overline{\Omega} \cap U_x$, then $z + ty_x \in \Omega$ for $0 < t < 1$.*

Theorem 3.17. *Let Ω be an open set satisfying the segment condition. Then the set $\mathcal{C}^1(\overline{\Omega}) := \{\phi_{|\Omega};\ \phi \in \mathcal{C}^1(\mathbb{R}^d)\}$ is dense in $W_{\mathrm{div}}^p(\Omega)$ for $1 \leq p < \infty$.*

Proof. The proof of Adams [AF03] p.68-70 works identical in our case, using the proposition 3.13. We don't give details here, but rather the main arguments. Let $u \in W_{\mathrm{div}}^p(\Omega)$. First use a truncation function to be reduced to the case with boundary support. Then introduce a partition of unity $\{\psi_j\}$ associated with a finite covering extracted from the covering of the support of u by the open sets U_x given by the segment condition, plus an "interior" open set. Then, approximate $u_j = \psi_j u$ by a function $u_{j,t}(x) = u_j(x + ty)$ with y given by the segment condition. This last function gets out of Ω and can be approximated thanks to the proposition 3.13. The only thing that remains to be checked is that $u_{j,t} \xrightarrow{W_{\mathrm{div}}^p(\Omega)} u_j$ as $t \to 0$ which works the same in our case than in the classical Sobolev one. $\qquad\square$

2.3   Duality approach

Definition 3.18. *Let $W_{\mathrm{div},0}^p(\Omega)$ be the completion for the norm of $W_{\mathrm{div}}^p(\Omega)$ of regular functions with bounded support in Ω*

$$W_{\mathrm{div},0}^p(\Omega) = \overline{\mathcal{C}_c^1(\Omega)}^{\,\|\|_{W_{\mathrm{div}}^p}}.$$

We will need the following proposition.

Proposition 3.19. *Let Ω be an open set satisfying the segment condition and $u \in L^p(\Omega)$ such that there exists $v \in L^p(\Omega)$ such that*

$$\int_\Omega u \operatorname{div}(G\phi) + \int_\Omega v\phi = 0, \quad \forall \phi \in \mathcal{C}^1(\overline{\Omega}). \tag{8}$$

Then $u \in W_{\mathrm{div},0}^p(\Omega)$.

Proof. First notice that $u \in W_{\mathrm{div}}^p(\Omega)$ and $v = G \cdot \nabla u$, by taking $\phi \in \mathcal{C}_c^1(\Omega)$ in (8). The argument of the proof is to remark that $\overline{u}$, defined as the extension by zero outside Ω is in $W_{\mathrm{div}}^p(\Omega_1)$ where Ω_1 is such that $\Omega \subset\subset \Omega_1$ and $G \in \mathcal{C}^1(\Omega_1)$. This implies that $u \in W_{\mathrm{div},0}^p(\Omega)$, using the same proof as Adams, p. 159, that we don't detail here and which works the same way as the proof of theorem 3.17, only using a function $u_{j,t}(x) = u_j(x - ty)$ in order to push the support of u_j strictly inside Ω and then using the following lemma (same proof as Brezis, p. 171) to conclude.

Lemma 3.20. *Let $u \in W_{\mathrm{div}}^p(\Omega)$ with $\operatorname{supp} u \subset\subset \Omega$. Then $u \in W_{\mathrm{div},0}^p(\Omega)$.*

$\qquad\square$

This proposition allows us to prove the theorem, by a density argument. The idea of the proof is inspired of Girault-Raviart [GR79] and Boyer-Fabrie [BF06], p. 127.

Theorem 3.21. *Let $1 \leq p < \infty$ and Ω satisfying the segment property. The space $\mathcal{C}^1(\overline{\Omega})$ is dense in $W_{\mathrm{div}}^p(\Omega)$.*

Proof. Let L be an element of the dual of $W_{\mathrm{div}}^p(\Omega)$ vanishing on $\mathcal{C}^1(\overline{\Omega})$. We will show that L is zero which will imply the result by a corollary of the Hahn-Banach theorem. We need the following lemma for the representation of linear forms on W_{div}^p, whose proof can be done in the same way than the proposition VIII.13 of Brezis [Bre83], p. 135.

Lemma 3.22. *Let L be a continuous linear form on W_{div}^p. There exist $f \in L^{p'}$ and $g \in L^{p'}$ (with $p' = \frac{p}{p-1}$ such that*

$$L(u) = \int_\Omega fu + \int_\Omega g\,\mathrm{div}(Gu), \quad \forall u \in W_{\mathrm{div}}^p.$$

Thus we have $f, g \in L^{p'}$ such that

$$L(u) = \int_\Omega fu + \int_\Omega g\,\mathrm{div}(Gu) = 0, \quad \forall u \in \mathcal{C}^1(\overline{\Omega}).$$

This implies that $g \in W_{\mathrm{div}}^{p'}$ and that $f = G \cdot \nabla g$. Moreover, the proposition 3.19 implies that $g \in W_{\mathrm{div},0}^p$ and thus that there exists a sequence $g_n \in \mathcal{C}_c^1(\Omega)$ such that $g_n \xrightarrow{\|\cdot\|_{W_{\mathrm{div}}^{p'}}} 0$. Hence we have, by definition of $u \in W_{\mathrm{div}}^p$

$$\int_\Omega g_n\mathrm{div}(Gu) + \int_\Omega G \cdot \nabla g_n u = 0, \quad \forall u \in W_{\mathrm{div}}^p$$

and passing to the limit we obtain

$$\int_\Omega g\,\mathrm{div}(Gu) + \int_\Omega G \cdot \nabla g u = 0, \quad \forall u \in W_{\mathrm{div}}^p$$

which concludes. $\qquad\square$

3   Traces

We address now the second problem which was our main objective in the study of $W_{\mathrm{div}}^p(\Omega)$ for our model, since it is necessary to define the domain of the operator as well as for proving its dissipativity. We seek now to define a trace for a function in $W_{\mathrm{div}}^p(\Omega)$, which is in principle defined almost everywhere in Ω and thus not defined on the $d-1$-dimensional boundary of Ω. Let us first briefly recall what is the approach used to prove trace results in the case of $W^{1,1}(\Omega)$ (which extends to the case $W^{1,p}(\Omega)$ but we explain here with $p = 1$ for keeping simplicity). In [Bre83], p.196 it is done first for the case of $\mathbb{R}_+^d = \{x \in \mathbb{R}^d;\ x_d > 0\}$ by writing, first for a regular function

$$\phi(\sigma, 0) = -\int_0^\infty \partial_\tau \phi(\sigma, s)ds$$

thus

$$\int_{\mathbb{R}^{d-1}} |\phi(\sigma,0)|d\sigma \leq \int_{\mathbb{R}_+^d} |\partial_\tau \phi(\sigma, s)|dsd\sigma$$

which gives the continuity of the trace operator $\gamma : \mathcal{C}^1(\overline{\Omega}) \subset W^{1,1}(\mathbb{R}^d_+) \to L^1(\mathbb{R})$. Then use the density of $\mathcal{C}^1(\overline{\Omega})$ to extend this operator. For a regular open set (see [AF03, Tar07]) we use a partition of unity and the change of maps as new coordinates to be reduced to the case of $\mathbb{R}^d_+$.

3.1 Conjugation approach for our model

In the case of assumptions (1) and $p = 1$ or ∞, thanks to the theorem 3.9, we can transport the theory of vector-valued Sobolev spaces (for which we refer to [Dro01b]) to $W^p_{\mathrm{div}}(\Omega)$. We first recall the following proposition.

Proposition 3.23 (Properties of $W^{1,1}([0,\infty[; L^1(\partial\Omega^*)))$). *The following stands*

1. $W^{1,1}([0,\infty[; L^1(\partial\Omega^*)) \hookrightarrow C([0,\infty); L^1(\partial\Omega^*))$

2. *Integration by part formula : for all function $u \in W^{1,1}([0,\infty[; L^1(\partial\Omega^*))$ and all $v \in W^{1,\infty}([0,\infty[; L^\infty(\partial\Omega^*))$, for almost every $\sigma \in \partial\Omega$*

$$\int_0^\infty u(\tau,\sigma)\partial_\tau v(\tau,\sigma)d\tau + \int_0^\infty \partial_\tau u(\tau,\sigma)v(\tau,\sigma)dt = -u(0,\sigma)v(0,\sigma).$$

As a direct corollary using theorem 3.9, we get

Proposition 3.24 (Trace and integration by part). *Let $p = 1$ or ∞ and $V \in W^p_{\mathrm{div}}(\Omega)$. We call* **trace** *of V the following function*

$$\gamma(V)(\sigma) = (V \circ \Phi)(0,\sigma), \quad \forall \sigma \in \partial\Omega$$

We have $\gamma(V)G \cdot \nu \in L^p(\partial\Omega)$ and there exists $C > 0$ such that

$$||\gamma(V)G \cdot \nu||_{L^p(\partial\Omega)} \leq C||V||_{W^p_{\mathrm{div}}(\Omega)}, \quad \forall V \in W^p_{\mathrm{div}}(\Omega)$$

Moreover, if $V \in W^p_{\mathrm{div}}(\Omega)$ and $U \in W^\infty_{\mathrm{div}}(\Omega)$. Then

$$\int\int_\Omega U\mathrm{div}(GV) + \int\int_\Omega VG \cdot \nabla U = -\int_{\partial\Omega} \gamma(V)\gamma(U)G \cdot \nu$$

Remark 3.25. *Notice that within our framework of the conjugation theorem, we didn't need to prove the density of $\mathcal{C}^1(\overline{\Omega})$ in $W^p_{\mathrm{div}}(\Omega)$ in order to construct the traces and have the integration by part formula.*

3.2 Extensions to more general situations

If $G \cdot \nu$ doesn't vanish on $\partial\Omega$.

Assume that Ω is regular and that $G \cdot \nu$ doesn't vanish on $\partial\Omega$ (see figure 2), then there should be no obstacle to use the classical approach : reduce the problem to the case of $\mathbb{R}^d_+$ and then straighten the trajectories of the field by using the change of variables $x = \Phi_\tau(\sigma)$ which should be at least Lipschitz in that case.
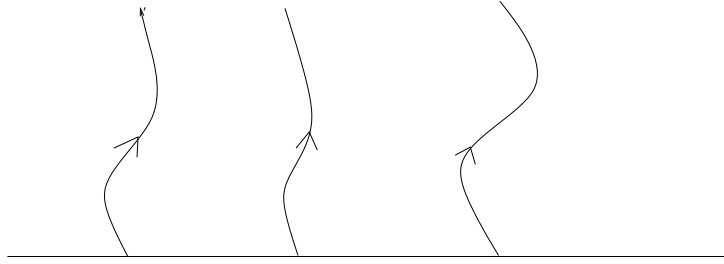
Figure 2: Non-vanishing field on the boundary

If $G \cdot \nu$ vanishes

Then two things : by following the characteristics we can't expect defining a trace where the field vanishes. To the best, we can hope to have a trace living in $L^p(\partial\Omega; |G \cdot \nu| d\sigma)$, for example by using a change of variables and a theorem similar to the theorem 3.9. First, away from points where $G \cdot \nu$ vanishes we can do as previously and define a trace in $L^1_{loc}(\partial\Omega^*)$ where $\partial\Omega^* := \partial\Omega \setminus \{\text{points where } G \cdot \nu \text{ vanishes}\}$. But the method fails in points where $G \cdot \nu$ vanishes because Φ is not anymore bilipschitz, see the Figure 3 and the formula (4).
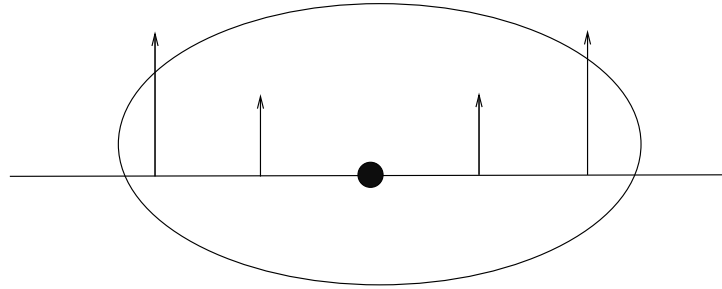
Figure 3: The normal component of the field vanishes.

Actually we have to be even more careful. What has to be taken into account if the **life time** in Ω, defined by
$$T(\sigma) = \inf \left\{ \tau > 0; \ \Phi_\tau(\sigma) \notin \Omega \right\}.$$

If the lifetime is uniformly bounded from below

If $T(\sigma) \geq \underline{T} > 0$ for almost every $\sigma \in \partial\Omega$, then a similar conjugation theorem as theorem 3.9 should work to define a trace on
$$\partial\Omega^- := \{\sigma \in \partial\Omega; \ G \cdot \nu(\sigma) < 0\} \text{ and } \partial\Omega^+ := \{\sigma \in \partial\Omega; \ G \cdot \nu(\sigma) > 0\}.$$

Indeed, for $\partial\Omega^-$ for example, we have $\Phi^{-1}(\Omega) \supset]0, \underline{T}[\times \partial\Omega^-$ and thus for $V \in W^1_{\text{div}}(\Omega)$ we would have $\widetilde{V} \in W^{1,1}(]0, \underline{T}[\times \partial\Omega^-)$ which would give a trace $\gamma^- V \in L^1(\partial\Omega^-; G \cdot \nu)$. The same would work for $\partial\Omega^+$ by considering $-G$ instead of G.

If the lifetime is not uniformly bounded from below

We are in the situation where $G \cdot \nu$ changes sign on $\partial\Omega$, see Figure 4.
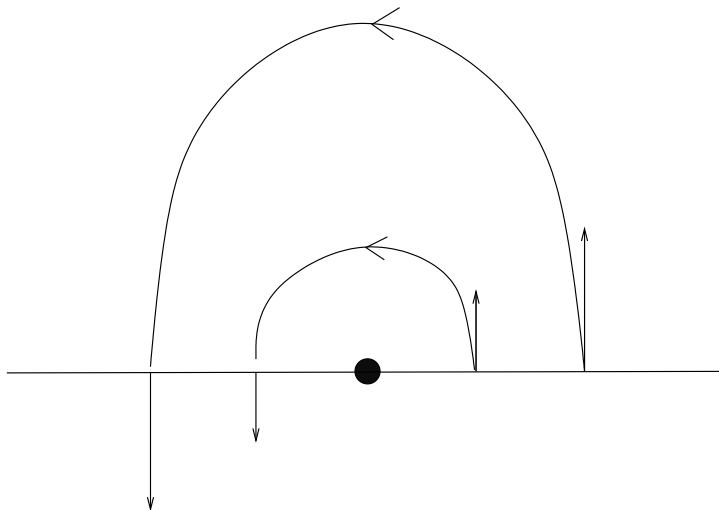
Figure 4: $G \cdot \nu$ changes sign

Things complicate : the trace $L_{loc}^{1}(\partial\Omega^{-}) \cap L_{loc}^{1}(\partial\Omega^{+})$ is not in $L^{1}(\partial\Omega; G \cdot \nu)$. Bardos gives the following counter example in [Bar70], p.206 (see Figure 5) :

$$\Omega =]-1,1[\times]0,1[,\ G(x_1, x_2) = (-1, x_1),\ u(x_1, x_2) = (x_2 + \frac{x_1^2}{2})^{-\alpha}$$
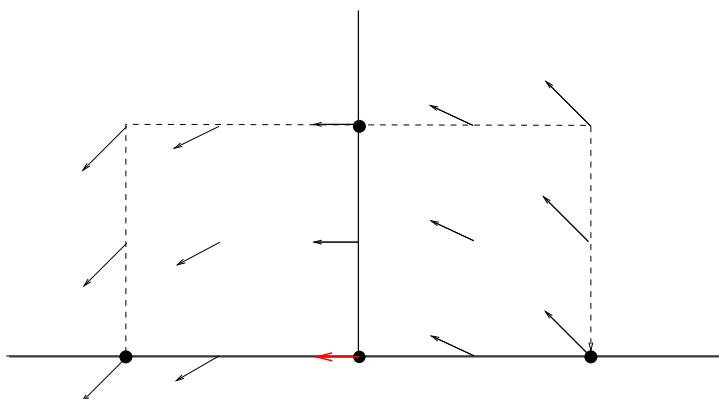
Figure 5: Counter example from Bardos.

Then

$$\int_{-1}^{1} dx_1 \int_{0}^{1} \frac{dx_2}{(x_2 + \frac{x_1^2}{2})^\alpha} = \frac{1}{-\alpha + 1} \int_{-1}^{1} \left[\frac{1}{(1 + \frac{x_1^2}{2})^{\alpha-1}} - 2^{\alpha-1} \frac{1}{x_1^{2(\alpha-1)}} \right] dx_1$$

thus, $u \in L^1(\Omega) \Leftrightarrow 2(\alpha - 1) < 1 \Leftrightarrow \alpha < 3/2$ and to integrate in x_2 we supposed $\alpha \neq 1$. Thus we take

$$1 < \alpha < 3/2$$

On the other hand

$$G \cdot \nabla u = -x_1(x_2 + \frac{x_1^2}{2})^{-\alpha-1} + x_1(x_2 + \frac{x_1^2}{2})^{-\alpha-1} = 0$$

thus u is constant along the trajectories and $u \in W^1_{\text{div}}(\Omega)$. But $u_{|x_2=0} = \frac{2^\alpha}{x_1^{2\alpha}}$ is in $L^1(]-1, 1[)$ only if $\alpha < \frac{1}{2}$. Thus, $u \notin L^1(\partial\Omega)$ if $1 < \alpha < 3/2$. And even more : by noticing that $|G \cdot \nu| = |x_1|$, we have $u|x_2 = 0 \in L^1(\partial\Omega; G \cdot \nu) \Leftrightarrow \alpha < 1$. Thus

$$u_{|\partial\Omega} \notin L^1(\partial\Omega^+; G \cdot \nu), \ u_{|\partial\Omega} \notin L^1(\partial\Omega^-; G \cdot \nu).$$

The appropriate trace space is

$$L^1(\partial\Omega; T_1(\sigma)G \cdot \nu d\sigma)$$

where $T_1(\sigma) = min(1, T(\sigma))$. The demonstration can be found in [Ces84, Ces85]. In the context of low regularity of the field, Boyer [Boy05] also proves the result.

Remark 3.26. *In the case of our model (assumptions* (1)*), we have $T(\sigma) = +\infty$ for all $\sigma \in \partial\Omega$ and thus $L^1(\partial\Omega; T_1(\sigma)G \cdot \nu d\sigma) = L^1(\partial\Omega; G \cdot \nu d\sigma)$, consistently with the proposition 3.24.*

3.3 Duality approach. Normal trace in $H^{-1/2}(\Omega)$.

The duality approach furnishes an alternative way to define a trace, *via* the integration by part formula. For simplicity, we explain the method in the case $p = 2$, that we take from Boyer-Fabrie [BF06], p. 128. We denote by γ_0 the trace operator on $H^1(\Omega)$ and recall that the image of $H^1(\Omega)$ by this operator is the space $H^{1/2}(\partial\Omega)$ on which the norm can be defined by

$$||\phi||_{H^{1/2}} = \inf\{||\overline{\phi}||_{H^1}; \ \gamma_0\overline{\phi} = \phi\}.$$

We denote by $H^{-1/2}(\partial\Omega)$ the dual space of $H^{1/2}(\partial\Omega)$. The proposition is the following

Proposition 3.27. *Let Ω be a Lipschitz open set. The application γ_ν which associates to $u \in \mathcal{C}^1(\overline{\Omega})$ the trace $uG \cdot \nu_{|\partial\Omega}$ extends to a continuous linear application from $W^2_{\text{div}}(\Omega)$ into $H^{-1/2}(\partial\Omega)$ and we have*

$$\int_\Omega \text{div}(Gv)w + \int_\Omega v \, G \cdot \nabla w = < \gamma_\nu v, \gamma_0 w >_{H^{-1/2}(\partial\Omega), H^{1/2}(\partial\Omega)}, \quad \forall v \in W^2_{\text{div}}(\Omega), \ \forall w \in H^1(\Omega).$$

$$(9)$$

Proof. There exists a continuous operator $R : H^{1/2}(\partial\Omega) \to H^1(\partial\Omega)$ such that $\gamma_0 R\phi = \phi$, $\forall\, \phi \in H^{1/2}(\partial\Omega)$. For $v \in W_{\mathrm{div}}^2(\Omega)$ we define

$$L_v : \quad \begin{array}{ccc} H^{1/2}(\partial\Omega) & \longrightarrow & \mathbb{R} \\ \phi & \longmapsto & \int_\Omega \mathrm{div}(vG)R\phi + \int_\Omega vG \cdot \nabla R\phi \end{array} \; .$$

Now

$$|L_v(\phi)| \le ||R\phi||_{L^2}||\mathrm{div}(Gv)||_{L^2} + ||G||_{L^\infty}||\nabla R\phi||_{L^2}||v||_{L^2}$$
$$\le C||v||_{W_{\mathrm{div}}^2}||\phi||_{H^{1/2}(\partial\Omega)}$$

which shows that for each v, L_v is continuous and that $v \mapsto L_v$ is also continuous. We denote L_v by $\gamma_\nu v$ and to prove (9) we argue by density : for $u \in \mathcal{C}^1(\overline{\Omega})$, the classical integration by part formula valid in $H^1(\Omega)$ tells us that, for $w \in H^1(\Omega)$

$$\int_\Omega \mathrm{div}(Gu)w + \int_\Omega u\, G \cdot \nabla w = \int_{\partial\Omega} u\gamma_0 w G \cdot \nu = \int_\Omega \mathrm{div}(uG)R\gamma_0 w + \int_\Omega uG \cdot \nabla R\gamma_0 w$$
$$= <\gamma_\nu u, \gamma_0 w>_{H^{-1/2}(\partial\Omega)} \; .$$

this identity being true for every $u \in \mathcal{C}^1(\overline{\Omega})$, the density of this space in $W_{\mathrm{div}}^2(\Omega)$ established in the theorem 3.21 allows to conclude that it is true for all $u \in W_{\mathrm{div}}^2(\Omega)$ and ends the proof. $\qquad\square$

Remark 3.28.
• *This proof uses the density of $\mathcal{C}^1(\overline{\Omega})$ in $W_{\mathrm{div}}^2(\Omega)$, which was not the case of the conjugation approach.*
• *The normal trace constructed lives in $H^{-1/2}(\partial\Omega) \supset L^2(\partial\Omega)$ whereas it is known that the trace is more regular, for example in $L^2(\partial\Omega)$ under some conditions on G (namely, that the life time in Ω is bounded from below).*
• *The above proposition should extend to the case $1 \le p < \infty$.*

4   Calculus with functions in $W_{\mathrm{div}}^p(\Omega)$

4.1   A few notions on absolute continuity

We give now a few notions about absolute continuity which will be useful in the following subsection. Absolute continuity is a necessary and sufficient condition for an almost everywhere differentiable function in the classical sense to have its derivative coinciding with its derivative in the distribution sense (the indicator function of $\mathbb{R}^+$ gives a counter example). It also characterizes the function with derivative in L^1 which are integral of this derivative and permits to avoid the devil's staircase type pathologies (this function is continuous on $[0,1]$, almost everywhere derivable with null derivative and takes values 0 in 0 and to 1 in 1).

Definition 3.29 (Absolute continuity)**.** *Let I be a real interval, X a Banach space and $f : I \to X$. The three following definitions are equivalent and if f satisfies one of them one says that f is **absolutely continuous**.*
    (1) $\exists\, g \in L^1(I\,;\,X)$ such that

$$f(x) - f(y) = \int_y^x g(t)dt \quad \forall x, y \in I$$

(2) $\forall\,\varepsilon > 0,\ \exists\,\delta > 0$ *such that for all sequence* $(a_n, b_n) \in I^2$,

$$\sum |b_n - a_n| < \delta \Rightarrow \sum \|f(b_n) - f(a_n)\| < \varepsilon$$

(3) For a real-valued function f *: if* A *is a borelian set with* $\lambda(A) = 0$, *then* $\lambda(f(A)) = 0$, *where* λ *stands for the Lebesgue measure.*

The useful proposition for our purpose is the following :

Proposition 3.30. *Let* $f : I \to X$ *be an absolutely continuous function such that* $f \in L^1(I\,;X)$, *then*

$$f \in W^{1,1}(I\,;X)$$

Remark 3.31. *The result of this proposition could almost seem trivial since from the first definition above,* f *has a classical derivative almost everywhere, which is in* L^1. *What is important here is that the a.e. derivative and the distribution one are equal (which is not a priori obvious, think again to the Heaviside function).*

Proof. Let f satisfying the hypotheses.
- First we have $f \in L^1(I\,;X)$
- From the above definition of absolute continuity, since almost every point of an L^1 function are Lebesgue points, f is differentiable almost everywhere , with $f' = g \in L^1(I\,;X)$. It remains to check that the distributional derivative of f coincides with g. Let thus $I = (a,b)$, $\phi \in \mathcal{C}_c^\infty(I)$, $[a_0, b_0]$ the support of ϕ and x_0 such that $a < x_0 < a_0$. We have, using the Fubini theorem at the second line :

$$\int_a^b f(x)\phi'(x)\,dx = \int_{x_0}^b f(x)\phi'(x)\,dx = \int_{x_0}^b f(x_0)\phi'(x)\,dx + \int_{x_0}^b \Big(\int_{x_0}^x g(t)\,dt\Big)\phi'(x)\,dx$$

$$= \int_{x_0}^b g(t)\int_t^b \phi'(x)\,dx\,dt$$

$$= -\int_{x_0}^b g(t)\phi(t)\,dt = -\int_a^b g(t)\phi(t)\,dt$$

and hence the result. $\qquad\square$

4.2 Composition of a $W_{\text{div}}^1(\Omega)$ function with a Lipschitz function

We place ourselves in the context of our model (assumptions (1)) and show now a chain rule result for the composition of a Lipschitz function H with a function $V \in W_{\text{div}}^1(\Omega)$ by using our conjugation approach.

Proposition 3.32.
(i) Let $V \in W_{\text{div}}^1(\Omega)$ *and* $U \in W_{\text{div}}^\infty(\Omega)$. *Then* $UV \in W_{\text{div}}^1(\Omega)$ *and*

$$\text{div}(GVU) = V\,(G \cdot \nabla U) + U\,\text{div}(GV)$$

(ii) Let $H : \mathbb{R} \to \mathbb{R}$ *a Lipschitz function and* $V \in W_{\text{div}}^1(\Omega)$. *Then*

$$H(V) \in W_{\text{div}}(\Omega)$$

and, almost everywhere

$$\mathrm{div}(GH(V)) = H'(V)G \cdot \nabla V + H(V)\mathrm{div}(V)$$

Remark 3.33. *In particular for $V \in W_{\mathrm{div}}^1(\Omega)$, $|V| \in W_{\mathrm{div}}^1(\Omega)$ and, almost everywhere*

$$G \cdot \nabla |V| = \mathrm{sgn(V)} G \cdot \nabla V$$

with $\mathrm{sgn(V)} = \mathbb{1}_{\mathrm{V}>0} - \mathbb{1}_{\mathrm{V}<0}$.

Proof. Using the conjugation theorem 3.9, (i) is a consequence of the theorem on the product of a function in $W^{1,1}(]0,+\infty[\,;\,L^1(\partial\Omega))$ and a function in $W_\tau^{1,\infty}(]0,+\infty[\times\partial\Omega)$ (see [DD07], p.66 adapting the proof to the case of Banach-valued Sobolev spaces).
(ii) Let H and V satisfying the hypothesis. First remark that H being Lipschitz and Ω bounded, the function $H(V)$ is in $L^1(\Omega)$. Now define $\overline{V}(\tau,\sigma) = V(\Phi_\tau(\sigma))$. We will show that $H(\overline{V})|J_\Phi| \in W^{1,1}(]0,+\infty[\,;\,L^1(\partial\Omega))$, in order to apply theorem 3.9. Following remark 3.10, the function $\overline{V}$ is in $W_{loc}^{1,1}([0,\infty[\,;\,L_{loc}^1(\partial\Omega^*))$. Thus it is absolutely continuous in τ and bounded and H being Lipschitz yields $H(\overline{V})$ absolutely continuous (from the second point of the definition 3.29). Hence $H(\overline{V}) \in W_{loc}^{1,1}([0,\infty[\,;\,L_{loc}^1(\partial\Omega^*))$. We conclude the proof by using that

$$\begin{aligned}
\partial_\tau(H(\overline{V})|J_\Phi|) &= \partial_\tau(H(\overline{V}))|J_\Phi| + \mathrm{div}(G)H(\overline{V})|J_\Phi| \\
&= H'(\overline{V})\partial_\tau\widetilde{V}|J_\Phi| + \mathrm{div}(G)H(\overline{V})|J_\Phi| \in L^1(]0,\infty[\times\partial\Omega)
\end{aligned}$$

which requires the following proposition (see also [SV69]) to have $\partial_\tau(H(\overline{V})) = H'(\overline{V})\partial_\tau\overline{V}$.

Proposition 3.34. *Let H be a Lipschitz function and $u \in W^{1,1}([0,T]\,;\,L^1(\partial\Omega))$. Then $H \circ u \in W^{1,1}([0,T]\,;\,L^1(\partial\Omega))$, and*

$$\partial_\tau(H \circ u)(\tau,\sigma) = H'(u(\tau,\sigma))\partial_\tau u(\tau,\sigma), \quad a.e.\ \tau \in [0,T],\ \sigma \in \partial\Omega.$$

Proof. Using absolute continuity, we have that $H(u) \in W^{1,1}([0,T]\,;\,L^1(\partial\Omega))$. From the definition of Banach-valued Sobolev spaces, we have that for almost every $\sigma \in \partial\Omega$, $u(\cdot,\sigma) \in W^{1,1}([0,T])$. We require now the following lemma.

Lemma 3.35. *Let u be an absolutely continuous real function defined on an interval I and A a borelian set. Then*

$$\lambda(u(A)) = 0 \Leftrightarrow u' = 0,\ a.e.\ in\ A$$

Remark 3.36. *A corollary of this result is that if $u \in W^{1,1}$, then $u' = 0$ on its level sets.*

Proof.
$\Rightarrow$ Let $B = \{x \in A; |u'(x)| > 0\}$ and $B_n = \{x \in B : |u(y) - u(x)| \geq \frac{|x-y|}{n}$ for $|x-y| < \frac{1}{n}\}$. $B = \cup_n B_n$. Let $E = I \cap B_n$ with I an interval with length less than $1/n$. Since $\lambda(u(A)) = 0$, for all ϵ there exists a sequence of intervals (I_k) covering $u(A)$ and such that $\sum_k \lambda(I_k) \leq \epsilon$. Let $E_k = u^{-1}(I_k) \cap E$, $\cup E_k$ covers E. Hence

$$\lambda(E) \leq \sum_k \lambda(E_k) \leq \sum_k \sup_{x,y\in E_k}|x-y| \leq \sum_k n\sup_{x,y\in E_k}|u(x)-u(y)|.$$

But $\sup_{x,y \in E_k}|u(x) - u(y)| \leq \lambda(I_k)$, since $u(E_k) \subset I_k$. Thus

$$\lambda(E) \leq n\epsilon.$$

As n is fixed and ϵ arbitrary, we deduce that $\lambda(E) = 0$, thus $\lambda(B_n) = 0$ and $\lambda(B) = 0$.

$\Leftarrow$: Let A such that $u' = 0$, *a.e.* in A. We define $A_k = \{x \in A; 0 < |u'(x)| \leq k\}$. We have $\lambda(u(A)) \leq \sum_k \lambda(u(A_k))$. As the measure of A_k is the infimum of the sums of lengths of intervals covering A_k, and since on each interval there exists α, β such that $u(\alpha, \beta) = \int_\alpha^\beta u'(x)dx \leq$, by covering A_k by an union of intervals, we deduce that $\lambda(u(A_k)) \leq \int_{\cup_i u_i(\alpha_i, \beta_i)} u'(x)dx$. As u' is in L^1, by continuity of the integral with respect to the measure, we obtain that for all ϵ, $\int_{\cup_i (\alpha_i, \beta_i)} u'(x)dx = \int_{A_k} u'(x)dx + \epsilon \leq k\lambda(A_k) + \epsilon$. We deduce $\lambda(u(A_k)) \leq k\lambda(A_k)$. By hypothesis, $\lambda(A_k) = 0$ for all k, hence the result. $\qquad\square$

Let $Z = \{z \in \mathbb{R};\ \text{H is not derivable}\}$ and $S = u^{-1}(Z) \subset [0, T] \times \partial\Omega$.

• In $[0, T] \times \partial\Omega \setminus S$, for almost every $\sigma \in \partial\Omega$, $\tau \mapsto u(\tau, \sigma)$ is derivable almost everywhere and the usual chain rule can be applied giving the required formula.

• In S, since from the definition of Banach-valued Sobolev spaces, we have that for almost every σ, $u(\cdot, \sigma) \in W^{1,1}([0, T])$. Denoting $S_\tau = \{\tau \in [0, T]; \exists \sigma \in \partial\Omega\, s.t.\, (\tau, \sigma) \in S\}$, $u(S_\tau, \sigma) \subset u(S) = Z$ and $\lambda(u(S_\tau, \sigma)) = 0$. Hence from the lemma 3.35, $\partial_\tau u(\tau, \sigma) = 0$ for almost every $(\tau, \sigma) \in S$. On the other hand we can apply the same argument to $H \circ u$ since $\lambda(H(u(S))) = \lambda(H(Z)) = 0$ from H being absolutely continuous and $\lambda(Z) = 0$. We obtain thus $0 = \partial_\tau(H \circ u) = H'(u)\partial_\tau u$ almost everywhere in S which ends the proof. $\qquad\square$

$\qquad\qquad\qquad\qquad\qquad\qquad\qquad\qquad\qquad\qquad\qquad\qquad\qquad\qquad\qquad\square$

Remark 3.37. *The proof of the theorem should extend to the case of a locally Lipschitz function H such that $H(V) \in L^1(\Omega)$ and $H'(V) \in L^\infty(\Omega)$.*

Chapter 4

Autonomous case. Model without treatment

In this chapter we will focus on the mathematical study of the model established in the modeling part for the evolution of the metastatic population represented by its density ρ, in the case without treatment which corresponds to an autonomous growth rate.

The problem is the following partial differential equation endowed with a nonlocal boundary condition :

$$\begin{cases} \partial_t \rho(t,X) + \mathrm{div}(\rho(t,X)G(X)) = 0 & \text{in } Q \\ -G \cdot \nu(\sigma)\rho(t,\sigma) = N(\sigma)\int_\Omega \beta(X)\rho(t,X)dX + f(t,\sigma) & \text{in } \Sigma \\ \rho(0,X) = \rho^0(X) & \text{in } \Omega. \end{cases} \tag{1}$$

with the following definitions

$$G(X) = G(x,\theta) = \begin{pmatrix} ax\ln\left(\frac{\theta}{x}\right) \\ cx - dx^{2/3}\theta \end{pmatrix}, \quad b = \left(\frac{c}{d}\right)^{\frac{3}{2}}, \quad \Omega =]1,b[\times]1,b[, \quad \overline{\Omega}^* = \overline{\Omega} \setminus (b,b)$$

$$Q =]0,+\infty[\times\Omega, \ \Sigma =]0,+\infty[\times\partial\Omega \ \partial\Omega^* = \partial\Omega \setminus (b,b)$$

and the following hypotheses on the data

$$\beta \in L^\infty(\Omega), \ \beta \geq 0 \ a.e., \ f \in L^1(]0,+\infty[\times\partial\Omega)$$

$$N \in Lip(\partial\Omega) \text{ with compact support in } \partial\Omega^*, \ N \geq 0, \ \int_\partial \Omega N = 1. \tag{2}$$

This type of problem is often called *renewal equations* and can be classified as part of the so-called structured population equations arising in mathematical biology which have the following general expression

$$\begin{cases} \partial_t\rho + \mathrm{div}(F(t,X,\rho)) = -\mu(t,X,\rho) & Q \\ -G \cdot \nu\rho(t,\sigma) = B(t,\sigma,\rho) & \sigma \in \partial\Omega \ s.t. \ G \cdot \nu(\sigma) < 0 \\ \rho(0,X) = \rho^0(X) & \Omega \end{cases}. \tag{3}$$

The introduction of such equations in the linear case is due to Sharpe and Lotka in 1911 [SL11] and McKendrick in 1926 [McK26]. Three major approaches can be distinguished in attacking theoretically this type of problems :

1. By transforming the problem into an *integral equation* (see the book of M. Ianelli [Ian95])

2. By typical partial differential equations tools inherited from the kinetic theory like *entropy methods* (see the book of B. Perthame [Per07] and [MMP05])

3. By using *semigroup* techniques (see the book of G. Webb [Web85] and also Diekmann and Metz [MD86]).

Although these equations have been widely studied both in the linear and nonlinear cases (see [PT08] for a survey in the nonlinear case), a complete general theory has not been achieved yet, even in the linear case. Indeed, most of the models have the so called structuring variable X being one-dimensional and often representing the age, thus evolving with $F(t,a,\rho) = \rho$. A difficulty on the regularity of solutions is introduced when the velocity is non-constant and vanishes (see [BBHV09, DGL09]). Dealing with situations in dimensions higher than one is not a common thing.

In our case, the model is a linear equation, with

$$F(t,X,\rho) = G(X)\rho$$

structured in two variables : $X = (x, \theta)$ with x the size of metastasis and θ the so-called "vascular capacity". The velocity field G vanishes on the boundary of the domain, which is a square. Moreover, we have an additional source term in the boundary condition of the equation. As far as we now, the mathematical analysis for multi-dimensional models is done only in situations where one of the structured variables is the age and thus with the first component of G being constant (see for instance [TZ88, AC03, Dou07]). In the context of the follicular control during the ovarian process, a nonlinear model structured in dimension two with both components of the velocity field G being non-constant is introduced in [EMSC05] but no mathematical analysis is performed due to the complexity of the model.

In the present chapter, we address the problem of the mathematical analysis of our model, namely : existence, uniqueness, regularity and asymptotic behavior of the solutions. Following the method used in [BK89] and [BBHV09], we use a semigroup approach to deal with existence and regularity of the solutions. The main difficulties we have to deal with in this two dimensional problem come from the singularity of the velocity field, as well as the presence of a time-dependent source term in the boundary condition. During the study, we take a particular attention on the problems of regularity of the solutions and approximation of weak solutions by regular ones, which led us to study the space

$$W_{\mathrm{div}}(\Omega) = \left\{ V \in L^1(\Omega); \ \mathrm{div}(GV) \in L^1(\Omega) \right\}$$

in the previous chapter (chapter 3). The chapter is organized as follows : in the section 4.1 we present the definition of weak solutions, introduce the semigroup formulation of the problem and establish equivalence between weak and mild solutions. The section 4.2 is devoted to the study of the properties of the underlying operator and in the section 4.3 we apply our study to the evolution equation from our model.

1   Formalization of the problem

We start by precising the notion of solution that we use for functions in $\mathcal{C}([0, +\infty[; L^1(\Omega))$.

Definition 4.1 (Weak solution)**.** *Let $\rho^0 \in L^1(\Omega)$ and $f \in L^1(]0, \infty[\times\partial\Omega)$. We call weak solution of the problem* (1) *any function $\rho \in \mathcal{C}([0, \infty[; L^1(\Omega))$ which verifies : for every $T > 0$ and every function $\phi \in \mathcal{C}_c^1([0, T] \times \overline{\Omega}^*)$*

$$\int_0^T \int_\Omega \rho[\partial_t \phi + G \cdot \nabla \phi] dt dx d\theta + \int_\Omega \rho^0(x, \theta)\phi(0, x, \theta) dx d\theta \tag{4}$$

$$- \int_\Omega \rho(T, x, \theta)\phi(T, x, \theta) dx d\theta - \int_0^T \int_{\partial\Omega} N(\sigma) \left(\int_\Omega \beta(x, \theta)\rho(t, x, \theta) dx d\theta \right) \phi(t, \sigma) d\sigma dt = 0$$

Analyzing the equation (1) indicates that the solution is the sum of two terms : an homogeneous one associated to the initial condition, which solves the equation without the source term f (which we will refer to as the homogeneous equation)

$$\begin{cases} \partial_t \rho + \mathrm{div}(G\rho) = 0 & \forall\, (t, x, \theta) \in Q \\ -G \cdot \nu \rho(t, \sigma) = N(\sigma) \int_\Omega \beta \rho(t) dx d\theta & \forall\, (t, \sigma) \in \Sigma \\ \rho(0, x, \theta) = \rho^0(x, \theta) & \forall\, (x, \theta) \in \Omega \end{cases} \tag{5}$$

and a non-homogeneous term associated to the contribution of the source term $f(t, \sigma)$ and solution to the equation (which will be refered as the non-homogeneous equation)

$$\begin{cases} \partial_t \rho + \text{div}(G\rho) = 0 & \forall (t, x, \theta) \in Q \\ -G \cdot \nu \rho(t, \sigma) = N(\sigma) \int_\Omega \beta \rho(t) dx d\theta + f(t, \sigma) & \forall (t, \sigma) \in \Sigma \\ \rho(0, x, \theta) = 0 & \forall (x, \theta) \in \Omega \end{cases} \tag{6}$$

For existence and uniqueness of solutions, we will deal with the homogeneous problem using the semigroup theory and with the non-homogeneous one via a fixed point argument.

We reformulate (5) as a Cauchy problem

$$\begin{cases} \partial_t \rho(t) = A\rho(t) \\ \rho(0) = \rho^0 \end{cases} . \tag{7}$$

To do so, we use the space :

$$W_{\text{div}}(\Omega) = \{V \in L^1(\Omega) | \text{ div}(GV) \in L^1(\Omega)\},$$

whose study has been performed in the chapter 3 and the following operator

$$A \;\; : \;\; \begin{aligned} D(A) \subset L^1(\Omega) & \rightarrow & L^1(\Omega) \\ V & \mapsto & -\text{div}(GV) \end{aligned} \;\; ,$$

where

$$D(A) = \{V \in W_{\text{div}}(\Omega); \; -G.\nu \cdot \gamma(V)(\sigma) = N(\sigma) \int_\Omega \beta(x, \theta) V(x, \theta) dx d\theta, \; \forall \sigma \in \partial\Omega\}. \tag{8}$$

where $\gamma(V)$ is the trace application well defined for functions in $W_{\text{div}}(\Omega)$ from proposition 3.24.

There are three definitions of solutions : the classical (or regular) solutions, the mild solutions and the distributional solutions (definition 4.1 with the source term $f = 0$), the second and third ones being two *a priori* different types of weak solutions. We give the definition of classical and mild solutions from [EN00] II.6, p.145 and will prove in the section 4.3 that they are the same ones (proposition 4.20).

Definition 4.2 (Classical solution)**.** *A function $\rho : [0, +\infty[\rightarrow L^1(\Omega)$ is called a classical solution of* (7) *if*

  (i) $\rho \in \mathcal{C}^1([0, +\infty[; L^1(\Omega))$

 (ii) $\rho(t) \in D(A)$ for all $t \geq 0$

(iii) ρ solves (7)

Remark 4.3. • *The boundary condition is integrated in the fact that $\rho(t) \in D(A)$*
• *Hypothesis (i) and (ii) allow equation* (7) *to have a sense.*

We define now the mild solutions ([EN00], II.6, p.146).

Definition 4.4 (Mild solution). *A continuous function $\rho : [0, +\infty[\to L^1(\Omega)$ is called a mild solution of (7) if*

   (i) $\int_0^t \rho(s)ds \in D(A)$, *for all $t \geq 0$*

   (ii) $\rho(t) = A \int_0^t \rho(s)ds + \rho^0$

Remark 4.5. • *Notice that we only impose to the function $\rho(t)$ to be continuous and not anymore differentiable as in the previous definition*
• *If $\rho^0 \notin D(A)$, we don't have $\rho(t) \in D(A)$ and thus even the boundary condition is solved in a weak sense.*

Definition 4.6 (Mild solution). *A function $\rho \in \mathcal{C}([0, +\infty[; L^1(\Omega))$ is a called a mild solution of the equation (7) if $\int_0^t \rho(s)ds \in D(A)$ for all $t \geq 0$ and*

$$\rho(t) = A \int_0^t \rho(s)ds + \rho^0.$$

2   Properties of the operator

We will now establish some properties of the operator $(A, D(A))$. The first one is its closedness.

Lemma 4.7. *The operator $(A, D(A))$ is closed.*

Proof. Let $V_n \in D(A)$ be a sequence of functions converging in L^1 to a function V, and assume that $AV_n \xrightarrow{L^1} W$. Then, for every $\phi \in \mathcal{C}_c^1(\Omega)$

$$\begin{array}{ccc}
\int AV_n\phi & \to & \int W\phi \\
\| & & \| \\
\int V_n G \cdot \nabla\phi & \to & \int V G \cdot \nabla\phi,
\end{array}$$

Thus $W \in W_{\mathrm{div}}(\Omega)$ and $W = AV$. It remains to check that V satisfies the boundary condition. This comes from the continuity of the trace application (prop. 3.24) and the fact that now $V_n \xrightarrow{W_{\mathrm{div}}(\Omega)} V$. $\square$

2.1   Density of $D(A)$ in $L^1(\Omega)$

Proposition 4.8. *The space $D(A)$ is dense in $L^1(\Omega)$*

Proof. The proof follows the one done in [BK89] in dimension 1, although some technical difficulties appear in dimension 2. Since $\mathcal{C}_c^1(\Omega)$ is dense in $L^1(\Omega)$, it is sufficient to approximate any function $f \in \mathcal{C}_c^1(\Omega)$ by functions of $D(A)$, for the L^1 norm. Thus let $f \in \mathcal{C}_c^1(\Omega)$ be a fixed function. The proof is divided in two steps :
• *First step* Assume that there exists a sequence $h_n : \overline{\Omega} \to \mathbb{R}$ such that :

$$\begin{aligned}
&(i) -G \cdot \nu(\sigma)h_n(\sigma) = N(\sigma),\ \forall \sigma \in \partial\Omega \\
&(ii)\ h_n \xrightarrow[n\to\infty]{L^1} 0 \\
&(iii)\ h_n \in W^{1,\infty}(\Omega)
\end{aligned} \qquad (9)$$

We will prove the existence of such functions in the second step. Then let

$$f_n = f + a_n h_n$$

with $a_n \in \mathbb{R}$ chosen to have the boundary condition required to have $f_n \in D(A)$. More precisely, in order to have $f_n \in D(A)$, a_n should verify :

$$-G \cdot \nu(\sigma) f_n(\sigma) = a_n N(\sigma) = N(\sigma) \int_\Omega \beta f_n dx d\theta$$
$$= N(\sigma) \left\{ \int_\Omega \beta f dx d\theta + a_n \int_\Omega \beta h_n dx d\theta \right\}$$

So it suffices to take

$$a_n = \frac{\int_\Omega \beta f dx d\theta}{1 - \int_\Omega \beta h_n dx d\theta}.$$

Then we remark that, since $||h_n||_{L^1(\Omega)} \to 0$ and β is in L^∞, for n sufficiently large, $|\int \beta h_n| \le 1/2$, so $|1 - \int_\Omega \beta h_n dx d\theta| \ge 1 - |\int_\Omega \beta h_n dx d\theta| \ge 1/2$ and $|a_n| \le 2||\beta||_{L^\infty} ||f||_{L^1}$. The sequence a_n being now proved to be bounded, we have $f_n \xrightarrow{L^1} f$. Furthermore, since $h_n \in W^{1,\infty}(\Omega) \subset W^{1,1}(\Omega) \subset W_{\mathrm{div}}(\Omega)$, we have $f_n \in D(A)$ which concludes the proof.

• *Second step* It remains to find a sequence h_n verifying (9). Let $\Gamma \subset\subset \partial\Omega^* = \partial\Omega\backslash(b,b)$ be the support of $N(\sigma)$ and for each $n \in \mathbb{N}$ let V_n be an open neighborhood of Γ such that

$$\mathrm{mes}(V_n) \to 0, \quad (b,b) \notin \overline{V_n}$$

where mes stands for the two-dimensional Lebesgue measure. There exists a function $\phi_n \in \mathcal{C}_c^1(\mathbb{R}^2)$ such that

$$\phi_n(x,\theta) = \begin{cases} 1 & \text{if } (x,\theta) \in \Gamma \\ 0 & \text{if } (x,\theta) \in V_n^c \end{cases} \quad 0 \le \phi_n \le 1$$

Then, we extend the function $H(\sigma) = \frac{N(\sigma)}{-G\cdot\nu(\sigma)}$: $\partial\Omega^* \to \mathbb{R}$ to a function $\overline{H} : \overline{V_n} \cap \overline{\Omega} \to \mathbb{R}$ by following the characteristics :

$$\overline{H}(x,\theta) = H(\sigma(x,\theta)) \quad \forall (x,\theta) \in \overline{V_n} \cap \overline{\Omega}$$

where we recall that $\sigma(x,\theta)$ is the entrance point in $\overline{\Omega}$ of the characteristic passing by (x,θ), defined in the section 3.1.1. We showed that the function $\sigma : \overline{\Omega}^* \to \partial\Omega^*$ is locally Lipschitz (prop. 3.4). Since $(b,b) \notin \overline{V_n}$, the function σ is Lipschitz on $\overline{V_n} \cap \overline{\Omega}$. Now H is Lipschitz on $\partial\Omega$ (meaning that the composition of H and a parametrization of $\partial\Omega$ is Lipschitz), so in the end the function $\overline{H}$ is Lipschitz. Eventually, the function

$$h_n(x,\theta) = \begin{cases} (\overline{H}\phi_n)(x,\theta) & \text{if } (x,\theta) \in \overline{V_n} \cap \overline{\Omega} \\ 0 & \text{if } (x,\theta)\overline{\Omega}\backslash\overline{V_n} \end{cases}$$

has the required properties. Indeed, $h_n \in W^{1,\infty}(\Omega)$ since h_n is Lipschitz. Moreover, the facts that $\mathrm{supp}(h_n) \subset V_n \cap \Omega$ and $||h_n||_{L^\infty(\Omega)} \le ||H||_{L^\infty(\partial\Omega)} < \infty$ (since N has compact support in $\partial\Omega^*$) imply that $h_n \xrightarrow{L^1} 0$. $\qquad\square$

We are now interested in characterizing the adjoint of the operator $(A, D(A))$. We will see that the first eigenvector of $(A^*, D(A^*))$ plays an important role in the structure of the equation in the asymptotic behavior (see theorem 4.23). First we recall the definition of the adjoint of A (see [Bre83], chap.2 p. 27).

Definition 4.9 (Adjoint of A)**.** *The domain of A^* is defined by*

$$D(A^*) = \{U \in L^\infty(\Omega); \ \exists c > 0 \ s.t. \ |_{L^\infty} < U, AV >_{L^1}| \leq c||V||, \ \forall V \in D(A)\}$$

and for $U \in D(A^*)$, A^*U is the unique element in $L^\infty(\Omega)$ such that

$$_{L^\infty} < U, AV >_{L^1} =_{L^\infty} < A^*U, V >_{L^1}, \ \forall V \in D(A).$$

Proposition 4.10 (Domain and expression of A^*)**.**

$$D(A^*) = \{U \in L^\infty; \ G \cdot \nabla U \in L^\infty\} = W^\infty_{\text{div}}(\Omega) \tag{10}$$

$$A^*U = G \cdot \nabla U + \beta \int_{\partial\Omega} U(\sigma)N(\sigma)d\sigma.$$

Proof. • The inclusion $W^\infty_{\text{div}}(\Omega) \subset D(A^*)$ follows from the proposition 3.24. The second inclusion $D(A^*) \subset W^\infty_{\text{div}}(\Omega)$ requires a little much of work. For a function $U \in D(A^*)$, we will show that $\phi \mapsto < U, \text{div}(G\phi) >$ can be extended in a continuous linear form on L^1, which will allow us to conclude using the Riesz theorem that $U \in W^\infty_{\text{div}}$. To do this, it is sufficient to show that there exists a constant $c \geq 0$ such that

$$| < U, A\phi >_{\mathcal{D}',\mathcal{D}} | \leq c||\phi||_{L^1} \quad \forall \phi \in \mathcal{D}(\Omega), \tag{11}$$

where $\mathcal{D}(\Omega) = \mathcal{C}_c^\infty(\Omega)$. This is almost done by the definition of the domain $D(A^*)$ except the fact that $\mathcal{D}(\Omega)$ is not a subset of $D(A)$. We are driven to use the following trick. Define the space :

$$\mathcal{D}_0(\Omega) = \{\phi \in \mathcal{D}(\Omega); \ \int_\Omega \beta\phi = 0\}$$

which is a subspace of $D(A)$. We will project a given function in $\mathcal{D}(\Omega)$ on $\mathcal{D}_0(\Omega)$. Let $\phi_1 \in \mathcal{D}(\Omega)$ be a fixed function such that $\int_\Omega \beta\phi_1 = 1$. Then

$$\phi = \underbrace{\phi - \left(\int \beta\phi\right)\phi_1}_{\in \mathcal{D}_0(\Omega) \subset D(A)} + \underbrace{\left(\int \beta\phi\right)\phi_1}_{\in \mathbb{R}\phi_1}.$$

So eventually, denoting as c_1 the constant given by the belonging of U to $D(A^*)$

$$| < U, A\phi >_{\mathcal{D}',\mathcal{D}} | = | < U, A(\phi - \left(\int \beta\phi\right)\phi_1) > + < U, \left(\int \beta\phi\right)A\phi_1 > |$$

$$\leq (c_1 + c_1||\beta||_{L^\infty}||\phi_1||_{L^1} + ||\beta||_{L^\infty}||U||_{L^\infty}||A\phi_1||_{L^1})||\phi||_{L^1}$$

which shows (11) and thus yields the result. $\qquad\square$

2.2   Spectral properties and dissipativity

In order to have a candidate for a stable asymptotic distribution of the solutions of our equation, we are interested in the stationary eigenvalue problem :

$$\begin{cases} \quad (\lambda, V, \Psi) \in \mathbb{R}_+^* \times D(A) \times D(A^*) \\ \quad\quad AV = \lambda V, \quad A^*\Psi = \lambda\Psi \\ \int_\Omega V\Psi dx d\theta = 1, \ \Psi \geq 0, \ \int_{\partial\Omega} N\Psi d\sigma = 1 \end{cases} \tag{12}$$

Proposition 4.11 (Existence of solutions to the eigenproblem)**.** *Under the assumption*

$$\int_0^\infty \int_{\partial\Omega} \beta(\Phi_\tau(\sigma)) N(\sigma) d\tau d\sigma > 1, \tag{13}$$

there exists a unique solution (λ_0, V, Ψ) *to the eigenproblem* (12)*. Moreover, we have the following **spectral equation** on* λ_0 *:*

$$\boxed{\int_0^{+\infty} \int_{\partial\Omega} \beta(\Phi_\tau(\sigma)) N(\sigma) e^{-\lambda_0 \tau} d\tau d\sigma = 1} \tag{14}$$

The direct eienvector is given by

$$V(\Phi_\tau(\sigma)) = C_{\lambda_0} N(\sigma) e^{-\lambda_0 \tau} |J_\Phi|^{-1}, \quad \forall \tau > 0, \ a.e \ \sigma \in \partial\Omega \tag{15}$$

where C_{λ_0} *is a positive constant and* $|J_\Phi|$ *is the jacobian of* Φ *from section* 3.1.1*. The adjoint eigenvector* Ψ *is given by :*

$$\Psi(\Phi_\tau(\sigma)) = e^{\lambda_0 \tau} \int_\tau^\infty \beta(\Phi_s(\sigma)) e^{-\lambda_0 s} ds \quad \forall \tau > 0, \ a.e \ \sigma \in \partial\Omega. \tag{16}$$

Hence we have

$$\frac{\inf \beta}{\lambda_0} \leq \Psi(x, \theta) \leq \frac{\sup \beta}{\lambda_0} \quad \forall (x, \theta) \in \Omega$$

Remark 4.12. *In the model we use in practice, where* $\beta(x, \theta) = mx^\alpha$ *the condition* (13) *is fulfilled since* $\int_0^\infty \int_{\partial\Omega} \beta(\Phi_\tau(\sigma)) N(\sigma) d\tau d\sigma = \infty$*, and the inequalities on* Ψ *write*

$$\frac{m}{\lambda_0} \leq \Psi(x, \theta) \leq \frac{mb^\alpha}{\lambda_0} \quad \forall (x, \theta) \in \Omega.$$

Proof. • *Direct eigenproblem.*
⋄ We use the following change of variable, which consists in transforming a function of $W_{\mathrm{div}}(\Omega)$ into a function of $W^{1,1}(]0, +\infty[\,; L^1(\partial\Omega))$:

$$\widetilde{V}(\tau, \sigma) = -V(\Phi_\tau(\sigma)) |J_\Phi|, \quad \forall \tau \in [0, +\infty[, \ \sigma \in \partial\Omega$$

where we recall that $|J_\Phi| = -G \cdot \nu(\sigma) e^{\int_0^\tau \mathrm{div}(G(\Phi_s(\sigma))) ds}$ is the jacobian of the application Φ : $(\tau, \sigma) \mapsto \Phi_\tau(\sigma)$ (see section 3.1.1).
Rewriting the problem on $\widetilde{V}$ and denoting $\widetilde{\beta}(\tau, \sigma) = \beta(\Phi_\tau(\sigma))$, we get

$$\begin{cases} \quad \partial_\tau \widetilde{V} + \lambda \widetilde{V} = 0 \\ \widetilde{V}(0, \sigma) = N(\sigma) \int \widetilde{\beta}\widetilde{V} d\tau d\sigma' \end{cases} \tag{17}$$

Direct computations show that Problem 17 has a solution if

$$1 = \int_0^\infty \int_{\partial\Omega} N(\sigma)\widetilde{\beta}(\tau,\sigma)e^{-\lambda\tau}d\sigma d\tau \tag{18}$$

and conversely, if λ_0 is a solution of the equation (18), we get solutions to the problem (17) given by

$$\widetilde{V}(\tau,\sigma) = C_{\lambda_0}N(\sigma)e^{-\lambda_0\tau} \tag{19}$$

and we can then fix the constant $C_{\lambda_0} > 0$ in order to have the normalization condition $1 = \int_\Omega V\Psi dxd\theta$ with Ψ the dual eigenvector defined below.

$\diamond$ We now prove that there exists a unique solution to equation (18) under the hypothesis (13). Indeed, let us define the function $F : \mathbb{R} \to \overline{\mathbb{R}}$ by

$$F(\lambda) = \int_0^\infty \left(\int_{\partial\Omega} N(\sigma)\widetilde{\beta}(\tau,\sigma) \right) e^{-\lambda\tau}d\sigma d\tau \tag{20}$$

It is the Laplace transform of the function $\tau \mapsto \int_{\partial\Omega} N(\sigma)\widetilde{\beta}(\tau,\sigma)d\sigma$. The condition (13) means that $F(0) > 1$ and F being strictly decreasing on $\mathbb{R}$ and continuous on $]0,+\infty[$, the equation (18) has a unique solution in $\mathbb{R}$, $\lambda_0 \in]0,+\infty[$.

$\diamond$ From (19), we obtain that $\widetilde{V} \in W^{1,1}(]0,+\infty[\,;L^1(\partial\Omega))$. Using the theorem 3.9 we deduce that $V \in W_{\mathrm{div}}(\Omega)$.

Remark 4.13. *Here the theorem 3.9 takes its interest since it is not completely obvious that the composition of $\widetilde{V}$ by Φ^{-1} would give a function in $W_{\mathrm{div}}(\Omega)$, due to the fact that the change of variable Φ (and Φ^{-1}) is not globally Lipschitz.*

• *Adjoint eigenproblem.*
$\diamond$ Expression of Ψ. Using the expression of the adjoint operator $(A^*, D(A^*))$ from the proposition 4.10, the adjoint spectral problem reads, along the characteristics : find $\Psi \in W_{\mathrm{div}}^\infty(\Omega)$ such that

$$\partial_\tau \Psi(\Phi_\tau(\sigma)) = \lambda_0 \Psi(\Phi_\tau(\sigma)) - \beta(\Phi_\tau(\sigma)) \int_{\partial\Omega} \Psi(\sigma')N(\sigma')d\sigma' \tag{21}$$

from which we get, for each function $\Psi(\sigma)$ defined on the boundary, a solution to the equation given by

$$\Psi(\Phi_\tau(\sigma)) = \Psi(\sigma)e^{\lambda_0\tau} - \int_{\partial\Omega} \Psi(\sigma')N(\sigma')d\sigma' \int_0^\tau \beta(\Phi_s(\sigma))e^{\lambda_0(\tau-s)} \tag{22}$$

$\diamond$ Non-negative solution. To get a non-negative solution we are driven to the following condition

$$\Psi(\sigma) \geq \int_{\partial\Omega} \Psi(\sigma')N(\sigma')d\sigma' \int_0^\infty \beta(\Phi_s(\sigma))e^{-\lambda_0 s}ds, \quad a.e\ \sigma \in \partial\Omega$$

Now, if the inequality is strict, multiplying by $N(\sigma)$ and integrating on $\partial\Omega$ gives

$$1 > \int_{\partial\Omega} \int_0^\infty \beta(\Phi_s(\sigma))e^{-\lambda_0 s}dsd\sigma$$

which belies the spectral equation (18). We are thus driven to choose

$$\Psi(\sigma) = \int_{\partial\Omega} \Psi(\sigma')N(\sigma')d\sigma' \int_0^\infty \beta(\Phi_s(\sigma))e^{-\lambda_0 s}ds, \quad \forall \sigma \in \partial\Omega \tag{23}$$

Defining $g(\sigma) = \int_0^\infty \beta(\Phi_s(\sigma))e^{-\lambda_0 s}ds$, this means that $\Psi(\sigma)$ is in the vector space generated by $g(\sigma)$. Then it remains to have the suitable normalization constant. Remembering the spectral equation (18) verified by λ_0 shows that the function $\Psi(\sigma) = g(\sigma)$ is appropriate. We finally get (16) from (22), which gives $\Psi \in L^\infty$ and $||\Psi||_{L^\infty} \le \frac{||\beta||_{L^\infty}}{\lambda_0}$.

$\diamond$ Regularity of Ψ. Using the equation (21) verified by Ψ we get $\partial_\tau \Psi(\Phi_\tau(\sigma)) \in L^\infty$ and so using the conjugation theorem of $W_{\mathrm{div}}^\infty(\Omega)$ and $W_\tau^{1,\infty}(]0,\infty[\times\partial\Omega)$ (theorem 3.9, where this last space is the Sobolev space with only the derivative with respect to the first variable is in $L^\infty(]0,\infty[\times\partial\Omega)$), we have $\Psi \in W_{\mathrm{div}}^\infty(\Omega)$. $\qquad\square$

Remark 4.14. *The previous proof takes advantage of the particular structure that the birth rate* $\mathbf{b}(\sigma, X)$ *is written as the product of a distribution function for neo-metastases at birth* $N(\sigma)$ *and a function* $\beta(X)$. *This corresponds to the biological hypothesis of independence between the vascular capacity of the progeny and the vascular capacity of the seeding tumor. In the case of a coupling between these, or in another model having an arbitrary birth rate* $\mathbf{b}(\sigma, X)$, *the previous proof cannot adapt. Maybe use of the Krein-Rutman theorem should then be considered, as done in [Dou07].*

We end this paragraph with the proof of the maximality of the operator $(A, D(A))$ which permits to control the norm of the resolvent of A and, combined to the property of dissipativity which is proven below, permits to prove that the spectrum of $(A, D(A))$ is included in a left half plane. These properties are the basis of the proof of the Hille-Yosida theorem which basically consists in approximating the unbounded operator $(A, D(A))$ by the resolvents $(\lambda I - A)$ which are bounded, and thus permits to build a semigroup whose generator is $(A, D(A))$. See the reference [EN00], paragraph II.3 for details.

Proposition 4.15 (Maximality of A)**.** *For* $Re(\lambda) > \lambda_0$, *we have* $Im(\lambda I - A) = L^1(\Omega)$. *In other words, for every* $\lambda \in \mathbb{C}$ *such that* $Re(\lambda) > \lambda_0$ *and for each* $f \in L^1(\Omega)$, *the equation*

$$\lambda V + \mathrm{div}(GV) = f \tag{24}$$

has a solution $V \in D(A)$.

Remark 4.16. *The following proof gives also the uniqueness of the solution but this is not strictly required at this point for our purpose. Anyway, the dissipativity of the operator that we prove hereafter implies also the uniqueness.*

Proof. $\bullet$ Using the same technique as in the proof of the existence of a direct eigenvector just before (proposition 4.11), we write the equation along the characteristics and obtain the following equation on $\widetilde{V}(\tau, \sigma) = V(\Phi_\tau(\sigma))|J_\Phi|$:

$$\begin{cases} \lambda\widetilde{V} + \partial_\tau\widetilde{V} = \widetilde{f}, & \forall \tau \in]0, +\infty[, \ a.e \ \sigma \in \partial\Omega \\ \widetilde{V}(0, \sigma) = N(\sigma)\int_\Omega \widetilde{\beta}\widetilde{V}d\tau d\sigma', & a.e \ \sigma \in \partial\Omega \end{cases} \tag{25}$$

where $\widetilde{f}(\tau, \sigma) = f(\Phi_\tau(\sigma))$ and $\widetilde{\beta}(\tau, \sigma) = \beta(\Phi_\tau(\sigma))$. For a regular function $\widetilde{V} \in W^{1,1}(]0, +\infty[; L^1(\partial\Omega))$ the solution is given by

$$\widetilde{V}(\tau, \sigma) = \widetilde{V}(0, \sigma)e^{-\lambda\tau} + \int_0^\tau e^{-\lambda(\tau-s)}\widetilde{f}(s, \sigma)ds, \quad a.e \ \sigma \in \partial\Omega \tag{26}$$

and the boundary condition gives

$$\widetilde{V}(0,\sigma) = N(\sigma)\left\{\int_0^\infty \int_{\partial\Omega} \widetilde{\beta}(\tau,\sigma')\widetilde{V}(\tau,\sigma')e^{-\lambda\tau}d\sigma'd\tau + \int_0^\infty \int_{\partial\Omega} \widetilde{\beta}(\tau,\sigma')\int_0^\tau e^{-\lambda(\tau-s)}\widetilde{f}(s,\sigma')dsd\sigma'd\tau\right\}.$$
(27)

So we have a solution to (25) if we have a function $\widetilde{V}(0,\sigma)$ verifying (27) which implies that there exists a constant $C_\lambda \in \mathbb{R}$ such that :

$$\widetilde{V}(0,\sigma) = C_\lambda N(\sigma)$$

Re-injecting in (27) we have

$$C_\lambda N(\sigma) = N(\sigma)\left\{C_\lambda F(\lambda) + \int_0^\infty \int_{\partial\Omega} \widetilde{\beta}(\tau,\sigma')\int_0^\tau e^{-\lambda(\tau-s)}\widetilde{f}(s,\sigma')dsd\sigma'd\tau\right\}$$

with the function $F(\lambda)$ being defined in (20). Dividing by $N(\sigma)$ in some σ for which $N(\sigma) \neq 0$, we have

$$C_\lambda = C_\lambda F(\lambda) + \underbrace{\int_0^\infty \int_{\partial\Omega} \widetilde{\beta}(\tau,\sigma')\int_0^\tau e^{-\lambda(\tau-s)}\widetilde{f}(s,\sigma')dsd\sigma'd\tau}_{:=B_\lambda=constant}$$

Using now the main argument, given in the proof of proposition 4.11, which is that

$$F(\lambda) \neq 1 \quad \forall\, Re(\lambda) > \lambda_0$$

we can choose

$$C_\lambda = \frac{B_\lambda}{1 - F(\lambda)}$$

to get a function $\widetilde{V}(0,\sigma) = C_\lambda N(\sigma)$ which, through formula (26), yields a solution of (25).
• Now we want to use our usual theorem of conjugation (theorem 3.9) to see that the function

$$V = \widetilde{V}(\Phi^{-1})|J_{\Phi^{-1}}|$$
(28)

is a solution of the equation (24) which belongs to $D(A)$. To this purpose, we have to check that

$$\widetilde{V} \in W^{1,1}(]0,+\infty[\,;\,L^1(\partial\Omega))$$

$\diamond$ $\widetilde{V} \in L^1((0,+\infty) \times \partial\Omega)$: we can write the expression of $\widetilde{V}$

$$\widetilde{V}(\tau,\sigma) = C_\lambda N(\sigma)e^{-\lambda\tau} + \int_0^\tau e^{-\lambda(\tau-s)}\widetilde{f}(s,\sigma)ds = D(\tau,\sigma) + E(\tau,\sigma)$$

When integrating, using that $\int N = 1$ we have

$$||\widetilde{V}||_{L^1} \leq \frac{C_\lambda}{\lambda} + \int_0^\infty e^{-\lambda\tau}\left\{\int_0^\tau e^{\lambda s}\int_{\partial\Omega}|\widetilde{f}(s,\sigma)|d\sigma ds\right\}d\tau$$

then, integrating by part the second term we obtain

$$||\widetilde{V}||_{L^1} \leq \frac{C_\lambda}{\lambda} + \frac{||f||_{L^1}}{\lambda} < \infty$$

$\diamond$ Then, the first term D is in $W^{1,1}(]0,+\infty[\,;\,L^1(\partial\Omega))$ as it is the product of a function in $W^{1,\infty}(\partial\Omega)$ with a function in $\mathcal{C}^1([0,+\infty[)$ with derivative in $L^1(0,+\infty)$. The second term $E(\tau,\sigma)$ is also in $W^{1,1}(]0,+\infty[\,;\,L^1(\partial\Omega))$ as it can be written as the product of $e^{-\lambda\tau}$ and $\int_0^\tau g(s,\sigma)ds$ with $g \in L^1(]0,+\infty[\times\partial\Omega)$.
Finally, using the theorem 3.9, the function V given by (28) is in $D(A)$ and is a solution of (24). $\qquad\square$

2.3 Dissipativity of $(A, D(A))$

The last property that we need to establish for our operator $(A, D(A))$ in order to apply the Lumer-Philips theorem is its dissipativity. We first recall the definition.

Definition 4.17. *An operator $(A, D(A))$, with $D(A) \subset X$, X being a Banach space, is said to be dissipative if for every $x \in D(A)$ and every $j(x) \in J(x) := \{x' \in X'; \ ||x||_X^2 = ||x'||_{X'}^2 =_{X'} < x, x' >_X\}$, we have*

$$_{X'} < Ax, j(x) >_X \leq 0$$

We prove now that the operator $(A - \omega I, D(A))$ possesses this property for ω large enough.

Proposition 4.18. *The operator $(A - \omega I, D(A))$ is dissipative for every $\omega \geq ||\beta||_{L^\infty(\Omega)}$*

Proof. Let $V \in D(A)$ and define $j(V) = \frac{V}{|V|} \mathbf{1}_{V \neq 0} ||V||_{L^1} \in J(V)$. We have

$$_{L^1} < AV, j(V) >_{L^\infty} = - \int_\Omega \text{div}(GV) j(V) \tag{29}$$

Now let us notice that using the proposition 3.32 from our study of W_{div} with the function $H = |\cdot|$ we have

$$|V| \in W_{\text{div}}(\Omega) \text{ and } \text{div}(G|V|) = \text{sgn}(V)\text{div}(GV),$$

with $\text{sgn}(V) = \frac{V}{|V|} \mathbf{1}_{V \neq 0}$. Furthermore the formula of integration by part (proposition 3.24) legitimates the following calculation

$$- \int_\Omega \text{div}(GV)j(V) = -||V||_{L^1} \int_\Omega \text{div}(GV)\text{sgn}(V) = -||V||_{L^1} \int_\Omega \text{div}(G|V|)$$

$$= -||V||_{L^1} \int_{\partial\Omega} \gamma(|V|) G \cdot \nu$$

We then remark that since the very definition of the trace of a function of $W_{\text{div}}(\Omega)$ (definition 3.24), we have

$$\gamma(|V|) = |\gamma(V)|$$

Now using the boundary condition

$$-\gamma(V) G \cdot \nu(\sigma) = N(\sigma) \int_\Omega \beta V,$$

and reminding that $G \cdot \nu(\sigma) \leq 0$ and $||N||_{L^1(\partial\Omega)} = 1$, we get

$$_{L^1} < AV, j(V) >_{L^\infty} = ||V||_{L^1} \int_{\partial\Omega} |\gamma(V) G \cdot \nu| = ||V||_{L^1} \int_{\partial\Omega} N(\sigma) |\int_\Omega \beta V|$$

$$\leq ||V||_{L^1}^2 ||\beta||_{L^\infty}$$

So

$$_{L^1} < AV - \omega V, j(V) >_{L^\infty} \leq ||V||_{L^1(\Omega)}^2 (||\beta||_{L^\infty(\Omega)} - \omega) \leq 0,$$

for $\omega \geq ||\beta||_{L^\infty}$. This concludes the demonstration of the proposition. $\square$

Corollary 4.19. *Under the assumptions* (2) *the operator* $(A, D(A))$ *generates a semigroup on* $L^1(\Omega)$ *denoted by* e^{tA} *and we have*

$$|||e^{tA}||| \leq e^{t||\beta||_{L^\infty}}$$

Proof. Let us denote $\widetilde{A} = A - \omega I$ with some $\omega \geq ||\beta||_{L^\infty(\Omega)}$, in order to move back the spectrum of A to the left. Then the operator $(\widetilde{A}, D(A))$ is closed (lemma 4.7), densely defined (proposition 4.8), dissipative (proposition 4.18), and for $\widetilde{\lambda} > \lambda_0 - \omega$, $Im(\widetilde{\lambda} I - \widetilde{A}) = L^1(\Omega)$ (proposition 4.15). Thus, applying the Lumer-Philips theorem (see [EN00] II.3, p. 83), the operator $(\widetilde{A}, D(A))$ generates a contraction semigroup which we denote by $e^{t\widetilde{A}}$. By rescaling this contraction semigroup we define $e^{tA} := e^{\omega t} e^{t\widetilde{A}}$ to obtain a quasi-contractive semigroup whose generator is $(A, D(A))$. $\square$

3 Existence and asymptotic behavior

First, we establish equivalence between mild and weak solutions of the homogeneous problem.

Proposition 4.20. *Let* $\rho \in \mathcal{C}([0, \infty[; L^1(\Omega))$, *then*

$$(\rho \text{ is a mild solution of } (5)) \Leftrightarrow (\rho \text{ is a weak solution of } (5))$$

Proof. • *First implication* $\Rightarrow$: It comes from the fact that mild solutions are limit of classical ones. Indeed, it will be proved in the section 4.2 that A is the generator of a semigroup e^{tA}. Thus, by density of the domain, there is a sequence $\rho_n^0 \in D(A)$ such that $\rho_n^0 \xrightarrow{L^1} \rho^0$. Then there exists $M > 0$ and $\omega > 0$ such that for all $T > 0$

$$||\rho_n - \rho||_{\mathcal{C}([0,T];L^1(\Omega))} = ||e^{tA}(\rho_n^0 - \rho^0)||_{\mathcal{C}([0,T];L^1(\Omega))} \leq Me^{\omega T}||\rho_n^0 - \rho^0||_{L^1(\Omega)}.$$

Classical solutions are weak solutions and passing to the limit in the identity (4) gives the result.
• *Second implication* $\Leftarrow$: Let $\rho \in \mathcal{C}([0, \infty[; L^1(\Omega))$ be a weak solution in the sense of definition 4.1 with $f = 0$. Define the function $R(t) = \int_0^t \rho(s)ds$. We verify now that $R(t) \in W_{\text{div}}(\Omega)$ by using the definition. Fix $t \geq 0$ and a function $\phi \in \mathcal{C}_c^1(\Omega)$. Using the function $\phi(t, x, \theta) \equiv \phi(x, \theta)$ in (4), we have

$$\int_\Omega \int_0^t \rho(s)ds(G \cdot \nabla\phi)dxd\theta = -\int_\Omega \rho^0(x, \theta)\phi(x, \theta)dxd\theta + \int_\Omega \rho(t, x, \theta)\phi(x, \theta)dxd\theta$$

Therefore $R(t) \in W_{\text{div}}(\Omega)$ and $\rho(t) = A \int_0^t \rho(s)ds + \rho^0$.

We now prove the boundary condition part in order to have $R(t) \in D(A)$. Let $\phi(\sigma)$ be a continuous function on $\partial\Omega$, with compact support in $\partial\Omega^*$. We can extend it to a function of $\mathcal{C}_c(\overline{\Omega}^*)$, still denoted by ϕ. Now, using the density of $\mathcal{C}_c^1(\overline{\Omega}^*)$ in $\mathcal{C}_c(\overline{\Omega}^*)$, choose a family $\phi_\varepsilon \in \mathcal{C}_c^1(\overline{\Omega}^*)$ such that $\phi_\varepsilon \xrightarrow{L^\infty} \phi$. For each ε, using the test function $\phi_\varepsilon(t, x, \theta) \equiv \phi_\varepsilon(x, \theta)$ in (4), we have for every $t \geq 0$

$$\int_\Omega R(t)G \cdot \nabla\phi_\varepsilon + \int_\Omega \rho^0(x, \theta)\phi_\varepsilon(x, \theta)dxd\theta - \int_\Omega \rho(t, x, \theta)\phi_\varepsilon(x, \theta)dxd\theta =$$
$$\int_{\partial\Omega} N(\sigma)\phi_\varepsilon(\sigma)d\sigma \int_\Omega \beta(x, \theta)R(t)dxd\theta$$

As $R(t) \in W_{\text{div}}(\Omega)$, and $-\text{div}(GR) = \rho - \rho^0$ by passing to the limit in ε, we obtain

$$\int_{\partial\Omega} \gamma(R(t))G \cdot \nu\phi = \int_{\partial\Omega} N\phi \int_{\Omega} \beta R, \quad \forall t \geq 0.$$

This identity being true for any function $\phi \in \mathcal{C}_c(\partial\Omega^*)$, we have the required boundary condition on $R(t)$. This ends the proof. $\qquad\square$

3.1   Well-posedness of the equation

Existence for the non-homogeneous problem

Proposition 4.21.
(i) Let $f \in L^1(]0,\infty[; L^1(\partial\Omega))$ and assume (2). There exists a unique solution of the non-homogeneous problem (6), denoted by $\mathcal{T}f$ and we have

$$\mathcal{T}f \in \mathcal{C}([0,\infty[; L^1(\Omega)).$$

(ii) If $f \in \mathcal{C}^1([0,\infty[; L^1(\partial\Omega))$ and $f(0) = 0$ then

$$\mathcal{T}f \in \mathcal{C}^1([0,\infty[; L^1(\Omega)) \cap \mathcal{C}([0,\infty[; W_{\text{div}}(\Omega)).$$

Moreover, we have the positivity property

$$(f \geq 0) \Rightarrow (\mathcal{T}f \geq 0).$$

Proof. The proof is based on a fixed point argument. It is divided in three steps : first we prove the point (ii) using the Banach fixed point theorem following the method of [Per07], then thanks to an estimate in $\mathcal{C}([0,\infty[, L^1(\Omega))$ we construct weak solutions as limits of regular solutions, and finally we prove uniqueness.
• *Step 1.* ⋄ As usual now, we first simplify the problem using the conjugation theorem (theorem 3.9). We use the change of variable $\tilde{\rho} = \rho(\Phi_\tau(\sigma))|J_\Phi|$ and still denoting ρ for $\tilde{\rho}$ and β for $\tilde{\beta} = \beta(\Phi_\tau(\sigma))$, we consider the following non-homogeneous problem with nonzero initial condition

$$\begin{cases} \partial_t \rho + \partial_\tau \rho = 0 \\ \rho(t,\sigma) = N(\sigma) \int \beta w + f(t,\sigma) \\ \rho(0) = \rho^0 \end{cases} \tag{30}$$

Let $\rho^0 \in D(A)$ and $f \in \mathcal{C}^1([0,\infty[; L^1(\partial\Omega))$ with $f(0) = 0$. For $T > 0$ we define the space

$$X_T = \{w \in \mathcal{C}^1([0,T]; L^1(]0,\infty[\times\partial\Omega); \ w(0,\cdot) = \rho^0\}.$$

It is a complete metric space. To $w \in X_T$ we associate the solution ρ of the equation (30), namely

$$\rho(t,\tau,\sigma) = \underbrace{\left\{ N(\sigma) \int_0^\infty \int_{\partial\Omega} \beta w(t-\tau,\tau',\sigma')d\tau' d\sigma' + f(t-\tau,\sigma) \right\}}_{:=H(t-\tau,\sigma)} \mathbf{1}_{t>\tau} + \rho^0(\tau-t,\sigma)\mathbf{1}_{t<\tau}$$

and define the linear operator $\mathcal{T}_{\rho^0,f}$ by $\mathcal{T}_{\rho^0,f}w := \rho$. Note here that $w \geq 0$ implies $\rho \geq 0$ if $\rho^0 \geq 0$ and $f \geq 0$, and that $H \in \mathcal{C}^1([0,T]; L^1(\partial\Omega))$.

$\diamond$ Regularity of ρ. We now show that $\rho \in X_T$ and that $\rho \in \mathcal{C}([0,T]; W^{1,1}(]0,+\infty[\,; L^1(\partial\Omega)))$. Indeed we have

$$\rho(t,\tau,\sigma)\mathbf{1}_{t>\tau} = H(t-\tau,\sigma)\mathbf{1}_{t>\tau}, \quad \rho(t,\tau,\sigma)\mathbf{1}_{t<\tau} = \rho^0(\tau-t,\sigma)\mathbf{1}_{t<\tau}. \tag{31}$$

From these expressions we get that $\rho \in \mathcal{C}([0,T]; L^1(]0,\infty[\times\partial\Omega))$ since the two functions H and ρ^0 are in L^1.

Moreover, $H(0,\sigma) = N(\sigma)\int\beta\rho^0 = \rho^0(0)$ from the compatibility conditions contained in the facts that $w \in X_T$, $f(0) = 0$ and $\rho^0 \in D(A)$. This allows to conclude that $\rho(t,\cdot) \in \mathcal{C}([0,\infty[; L^1(\partial\Omega))$. Furthermore, from the expressions (31), we see that for each t, $\rho(t,\cdot) \in W^{1,1}((0,t), L^1(\partial\Omega)) \cap W^{1,1}((t,\infty), L^1(\partial\Omega))$ since $\rho^0 \in D(A)$ and $H \in \mathcal{C}^1([0,T]; L^1(\partial\Omega))$. Combining this with the continuity in τ gives $\rho(t,\cdot) \in W^{1,1}(]0,+\infty[\,; L^1(\partial\Omega))$. Finally from the expression of $\partial_\tau\rho$ obtained differentiating in τ the expressions (31) we get

$$\rho \in \mathcal{C}([0,T], W^{1,1}(]0,+\infty[\,; L^1(\partial\Omega))).$$

It remains to show that $\rho \in \mathcal{C}^1([0,T]; L^1(]0,\infty[\times\partial\Omega))$. For the sake of simplicity we forget the dependency on σ since everything can be done the same way replacing $L^1(\cdot)$ by $L^1(\cdot; L^1(\partial\Omega))$ in the following. We define for almost every t and τ

$$\partial_t\rho(t,\tau) := \partial_t H(t-\tau)\mathbf{1}_{t>\tau} - \partial_t\rho^0(\tau-t)\mathbf{1}_{t<\tau}$$

and compute

$$\begin{aligned}
\frac{1}{h}||\rho(t+h) - \rho(t) - h\partial_t\rho(t)||_{L^1([0,\infty[)} =& \frac{1}{h}||H(t+h-\cdot) - H(t-\cdot) - h\partial_t H(t-\cdot)||_{L^1([0,t[)} \\
&+ \underbrace{\frac{1}{h}||H(t+h-\cdot) - \rho^0(\cdot-t) - h\partial_t\rho^0(\tau-t)||_{L^1(]t,t+h[)}}_{A} \\
&+ \frac{1}{h}||\rho^0(\cdot-t-h) - \rho^0(\cdot-t) - h\partial_t\rho^0(\cdot-t)||_{L^1([t+h,\infty[)}
\end{aligned}$$

The first and the last terms go to zero when h tends to zero since H is in $\mathcal{C}^1([0,T]; L^1(]0,\infty[))$ and ρ^0 is in $D(A)$. To deal with the last term A, we write

$$A \leq \frac{1}{h}\int_t^{t+h}|H(t+h-\tau) - \rho^0(\tau-t)|d\tau + \int_t^{t+h}\partial_t\rho^0(\tau-t)d\tau$$

The first term goes to zero because of the compatibility condition $H(0) = \rho^0(0)$ and also the last one because $\partial_t\rho^0 \in L^1$. We can then conclude $\rho \in \mathcal{C}^1([0,T]; L^1(]0,\infty[))$.

$\diamond$ The previous considerations show that the operator $\mathcal{T}_{\rho^0,f}$ has values in X_T. Now, if w_1 and w_2 are in X_T we have

$$\mathcal{T}_{\rho^0,f}w_1 - \mathcal{T}_{\rho^0,f}w_2 = N\int_0^\infty\int_{\partial\Omega}\beta(w_1-w_2)d\tau d\sigma\mathbf{1}_{t>\tau}$$

and

$$\partial_t\mathcal{T}_{\rho^0,f}w_1 - \partial_t\mathcal{T}_{\rho^0,f}w_2 = N\int_0^\infty\int_{\partial\Omega}\beta(\partial_t w_1 - \partial_t w_2)d\tau d\sigma\mathbf{1}_{t>\tau}$$

Thus
$$||\mathcal{T}_{\rho^0,f}w_1 - \mathcal{T}_{\rho^0,f}w_2||_{X_T} \leq T||\beta||_{L^\infty}||w_1 - w_2||_{X_T}$$

Now we choose $T < 1/||\beta||_{L^\infty}$, hence the operator $\mathcal{T}_{\rho^0,f}$ is a contraction and the Banach fixed point theorem gives existence of a fixed point for $\mathcal{T}_{\rho^0,f}$ which is then a solution on $[0,T]$ of the equation (30). Remark that this fixed point is non-negative if the source term f is, since it is obtained as the limit of the iterates of the operator applied to any non-negative function w. Now since T does not depend on ρ^0 we can iterate the process and obtain a solution on $[T, 2T]$, $[2T, 3T]$, etc... to finally get a solution on $[0, \infty[$. Transporting the regularity facts back to Ω by using the conjugation theorem 3.9 ends the point (ii).

• *Step 2.* Denote by $\mathcal{T}f$ the fixed point of the operator $\mathcal{T}_{0,f}$, defined up to now only when f is regular and satisfies the compatibility condition $f(0) = 0$, one has

Lemma 4.22. *Let $f \in \mathcal{C}^1([0, \infty[; L^1(\partial\Omega))$ with $f(0) = 0$ and $\mathcal{T}f$ be the solution of the equation (30) with a zero initial condition. Then for all $T > 0$*

$$||\mathcal{T}f||_{\mathcal{C}([0,T];L^1(\Omega))} \leq e^{T||\beta||_\infty} \int_0^T |f(s)|e^{-||\beta||_\infty s}ds$$

Proof. The solution $\mathcal{T}f = \rho$ being regular, the function $|\rho|$ also verifies the equation and integrating on Ω yields

$$\frac{d}{dt}\int_\Omega |\rho|(t)d\tau d\sigma = |\int_\Omega \beta\rho(t)dxd\theta + \int_{\partial\Omega} f(t,\sigma)d\sigma| \leq ||\beta||_\infty \int_\Omega |\rho|(t)dxd\theta + \int_{\partial\Omega} |f(t,\sigma)|d\sigma$$

and a Gronwall lemma gives the result. □

Now let $f \in L^1(]0, \infty[; L^1(\partial\Omega))$ and choose a sequence $f_n \in \mathcal{C}^1([0, \infty[, L^1(\partial\Omega))$ with $f_n(0) = 0$ such that $f_n \xrightarrow{L^1} f$. The previous lemma shows that the sequence $(\mathcal{T}f_n)_{n\in\mathbb{N}}$ is a Cauchy sequence in $\mathcal{C}([0,T]; L^1(\Omega))$ for all $T > 0$. So it converges to a function denoted by $\mathcal{T}f$ which is in $\mathcal{C}([0,T]; L^1(\Omega))$. Since we can do this for each $T > 0$, we thus construct a function $\mathcal{T}f$ in $\mathcal{C}([0, \infty[; L^1(\Omega))$. Using the definition of weak solutions (definition 4.1), we can pass to the limit in the expression (4) written on $\mathcal{T}f_n$ to see that the function $\mathcal{T}f$ is a weak solution of the non-homogeneous problem with zero initial data. The non-negativity of $\mathcal{T}f$ for a positive data f is ensured because we can choose the sequence f_n to be non-negative and extract a subsequence such that $\mathcal{T}f_n$ converges almost everywhere.

• *Step 3.* It remains to show the uniqueness of the solution. If ρ_1 and ρ_2 are two solutions of the non-homogeneous equation (30), then $\rho_1 - \rho_2$ is a weak solution of the homogeneous equation (5) with zero initial condition. From the proposition 4.20 the weak solutions in the sense of the distributions are the same than the mild solutions and thus $\rho_1 - \rho_2$ is a mild solution of the homogeneous equation and hence is zero by uniqueness of the mild solutions since A generates a semigroup (proposition 4.19). □

Existence for the global problem

Theorem 4.23 (Existence, uniqueness and regularity)**.**
(i) Let $\rho^0 \in L^1(\Omega)$ and $f \in L^1(]0, \infty[\times\partial\Omega)$, and assume (2). There exists a unique weak solution of the equation (1), given by

$$\rho = e^{tA}\rho^0 + \mathcal{T}f$$

with $\mathcal{T}f$ being a weak solution of the non-homogeneous equation (6) *and e^{tA} the semigroup generated by A.*

(ii) If $\rho^0 \in D(A)$ and $f \in \mathcal{C}^1([0, \infty[; L^1(\partial\Omega))$ and verifies $f(0) = 0$, then we have

$$\rho \in \mathcal{C}^1([0, \infty[; L^1(\Omega)) \cap \mathcal{C}([0, \infty[; W_{\mathrm{div}}(\Omega)).$$

3.2   Properties of the solutions and asymptotic behavior

In the next proposition, we prove some useful properties of the solutions, which naturally appear in the L^1_Ψ norm defined by

$$||V||_{L^1_\Psi} = \int_\Omega |V|\Psi dx d\theta, \tag{32}$$

with Ψ the dual eigenvector from proposition 4.11. We should notice that when $\beta \in L^\infty(\Omega)$ and $\beta \geq \delta > 0$, by the inequalities from proposition 4.11, the L^1_Ψ norm is equivalent to the L^1 norm. Hence the solutions have finite L^1_Ψ norm. The main idea in the proof of the following proposition is to use various entropies in the space L^1_Ψ, and is based on ideas from [Per07] and [MMP05]

Proposition 4.24. *Let $\rho^0 \in L^1(\Omega)$ and ρ the solution of the equation* (1). *The following properties hold :*

(i)

$$\int_\Omega |\rho(t)|\Psi \leq e^{\lambda_0 t} \left\{ \int_\Omega |\rho^0|\Psi + \int_0^t \int_{\partial\Omega} \Psi(\sigma)e^{-\lambda_0 s}|f|(s,\sigma)d\sigma ds \right\}, \quad \forall t \geq 0 \tag{33}$$

(ii) (Evolution of the mean-value in L^1_Ψ)

$$\int_\Omega \rho(t)\Psi = e^{\lambda_0 t} \left\{ \int_\Omega \rho^0 \Psi + \int_0^t \int_{\partial\Omega} \Psi(\sigma)e^{-\lambda_0 s}f(s,\sigma)d\sigma ds \right\}, \quad \forall t \geq 0$$

(iii) (Comparison principle) If $f \geq 0$

$$\rho_1^0 \leq \rho_2^0 \quad \Rightarrow \quad \rho_1(t) \leq \rho_2(t) \quad \forall t \geq 0$$

Remark 4.25. *The property (iii) implies the **positivity** of the semigroup e^{tA}.*

Proof. Each time we aim to prove something on weak solutions, we will start proving it for classical solutions and then use the density of $D(A)$ to conclude. So, let do the calculations with a strong solution ρ associated to an initial condition ρ^0 in $D(A)$ and a function $f \in \mathcal{C}^1(]0, \infty[; L^1(\partial\Omega))$ with $f(0) = 0$, for which the calculations can be justified. We first recall that the dual eigenvector Ψ which belongs to $W_{\mathrm{div}}^\infty(\Omega)$ verifies the following equation :

$$G \cdot \nabla\Psi - \lambda_0 \Psi = -\beta \tag{34}$$

since by the construction of Ψ and the spectral equation $\int_{\partial\Omega} \Psi(\sigma)N(\sigma)d\sigma = 1$. Defining

$$\widetilde{\rho}(t, x, \theta) = e^{-\lambda_0 t}\rho(t, x, \theta)$$

we have the following equation on $\widetilde{\rho}$:

$$\partial_t\widetilde{\rho} + \operatorname{div}(G\widetilde{\rho}) + \lambda_0\widetilde{\rho} = 0, \tag{35}$$

with the same initial condition as for ρ and a suitable boundary condition. Using that $\widetilde{\rho} \in W_{\operatorname{div}}(\Omega)$ and $\Psi \in W_{\operatorname{div}}^{\infty}(\Omega)$ and the proposition on the product of functions (proposition 3.32), we have the following equation on $\widetilde{\rho}\Psi$:

$$\partial_t(\widetilde{\rho}\Psi) + \operatorname{div}(G\widetilde{\rho}\Psi) = -\beta\widetilde{\rho}. \tag{36}$$

Property (i). Let us first state the following lemma.

Lemma 4.26. *Assume that $\rho^0 \in L^1(\Omega)$, $f \in L^1(]0, \infty[\times\partial\Omega)$ and let ρ be the associated weak solution of the equation* (1). *Then the function $|\rho|$ solves the same equation, with the initial condition $|\rho^0|$ and the boundary condition*

$$-G \cdot \nu(\sigma)|\rho(t,\sigma)| = \left| N(\sigma) \int_\Omega \beta\rho \, dx d\theta + f(t,\sigma) \right|$$

Proof. For a regular solution of the equation ρ associated to a regular initial condition $\rho^0 \in D(A)$ and a regular data f, we can use the proposition 3.32 with the function $H(\cdot) = |\cdot|$ to have that $|\rho(t)| \in W_{\operatorname{div}}(\Omega)$ and

$$\operatorname{div}(G|\rho|) = \operatorname{sgn}(\rho)G \cdot \nabla\rho + |\rho|\operatorname{div}(G)$$

Since ρ is regular in time, by multiplying the equation by $\operatorname{sgn}(\rho)$ we get the result. For a solution $\rho \in \mathcal{C}([0,\infty[; L^1(\Omega))$ we obtain the result by density of the strong solutions. $\square$

Thanks to this lemma, in the same way that the equation (36), we have the following equation for $|\widetilde{\rho}|$:

$$\partial_t(|\widetilde{\rho}|\Psi) + \operatorname{div}(G|\widetilde{\rho}|\Psi) = -\beta|\widetilde{\rho}|$$

From this we get that

$$
\begin{aligned}
\frac{d}{dt}\int_\Omega |\widetilde{\rho}|\Psi \, dx d\theta &= -\int_{\partial\Omega} \gamma(|\widetilde{\rho}|)\Psi G \cdot \nu \, d\sigma - \int_\Omega \beta(x,\theta)|\widetilde{\rho}(t,x,\theta)| \, dx d\theta \\
&= \int_{\partial\Omega} \Psi(\sigma)\left| N(\sigma)\int_\Omega \beta(x,\theta)\widetilde{\rho}(t,x,\theta) \, dx d\theta + e^{-\lambda_0 t}f(t,\sigma) \right| - \int_\Omega \beta(x,\theta)|\widetilde{\rho}|(t,x,\theta) \, dx d\theta \\
&\leq \int_{\partial\Omega} |f(t,\sigma)|e^{-\lambda_0 t}\Psi(\sigma)
\end{aligned}
$$

from which we deduce the first property after integrating in time. To deal with weak solutions we again use the density of regular solutions.

Property (ii). For the evolution of the mean value, we integrate the identity (36) to obtain

$$\frac{d}{dt}\int_\Omega \widetilde{\rho}\Psi \, dx d\theta - \int_{\partial\Omega} N(\sigma)\Psi(\sigma) \, d\sigma \int_\Omega \beta\widetilde{\rho} \, dx d\theta - \int_{\partial\Omega} e^{-\lambda_0 t}f(t,\sigma)\Psi(\sigma) \, d\sigma = -\int_\Omega \beta\widetilde{\rho} \, dx d\theta$$

Now remember that by construction $\int_{\partial\Omega} N(\sigma)\Psi(\sigma) \, d\sigma = 1$ to get

$$\frac{d}{dt}\int_\Omega \widetilde{\rho}\Psi \, dx d\theta = e^{-\lambda_0 t}\int_{\partial\Omega} f(t,\sigma)\Psi(\sigma) \, d\sigma$$

and thus the conclusion for a regular solution. To conclude for a weak solution, use again a density argument.

(*iii*) Writing the solution of the global problem as $\rho = e^{tA}\rho^0 + \mathcal{T}f$, we only have to prove the positivity for the homogeneous part since the positivity of the non-homogeneous one has been established in the proposition 4.21. It can be proved in the same way as the contraction principle (first property) but using the negative part function instead of the absolute value. We take a non-negative initial condition $\rho^0 \geq 0$ and will show that the associated solution of the homogeneous equation $\rho(t) = e^{tA}\rho^0$ is non-negative for all time. Let denote by $(x)^- = \max(-\mathrm{x}, 0)$ and use this function in the equation. Indeed it is a Lipschitz function which is valid for the use of the proposition 3.32, and proceeding exactly as in the lemma 4.26, we get that $(\widetilde{\rho})^-$ satisfies equation (36) :

$$\partial_t((\widetilde{\rho})^- \Psi) + \operatorname{div}(G(\widetilde{\rho})^- \Psi) = -\beta(\widetilde{\rho})^-$$

Then, integrating in space gives

$$\frac{d}{dt} \int_\Omega (\widetilde{\rho})^- \Psi dx d\theta = \left(\int_\Omega \beta\widetilde{\rho} dx d\theta \right)^- - \int_\Omega \beta(\widetilde{\rho})^- dx d\theta \leq 0,$$

by using the Jensen inequality. Hence we have, using the positivity of Ψ

$$0 \leq \int_\Omega (\widetilde{\rho})^- \Psi dx d\theta \leq \int_\Omega (\rho^0)^- \Psi dx d\theta = 0$$

So $(\rho)^- = 0$ which means that $\rho \geq 0$. The density of $D(A)$ again gives the result for weak solutions. $\qquad\square$

Proposition 4.27 (Asymptotic behavior)**.** *Assume that*

$$\int_0^\infty \int_{\partial\Omega} \beta(\Phi_\tau(\sigma))N(\sigma)d\tau d\sigma > 1,$$

and that there exists $\mu > 0$ such that $\beta - \mu\Psi \geq 0$. Let $\rho^0 \in L^1(\Omega)$, $f \in L^1(]0,\infty[\times\partial\Omega)$, ρ the associated solution to the global problem and $(\lambda_0, V, \Psi) \in \mathbb{R}_+^* \times D(A) \times D(A^*)$ be solutions to the direct and adjoint eigenproblems. We have :

$$\boxed{||\rho(t)e^{-\lambda_0 t} - m(t)V||_{L^1_\Psi} \leq e^{-\mu t} \left\{ ||\rho^0 - m_0 V||_{L^1_\Psi} + 2 \int_0^t e^{-(\lambda_0 - \mu)s} \int_{\partial\Omega} |f|(s,\sigma)\Psi(\sigma)ds \right\}},$$

where $||f||_{L^1_\Psi} = \int_\Omega |f|\Psi$, and $m(t) = e^{-\lambda_0 t}\int_\Omega \rho(t)\Psi = \int_\Omega \rho^0\Psi + \int_0^t e^{-\lambda_0 s}\int_{\partial\Omega} f(s,\sigma)\Psi(\sigma)d\sigma ds.$

Remark 4.28. *Notice that choosing $\mu < \lambda_0$ gives the convergence of the integral*

$$\int_0^\infty e^{-(\lambda_0 - \mu)s} \int_{\partial\Omega} |f|(s,\sigma)\Psi(\sigma)ds$$

and thus the exponential convergence to zero of the right hand side of the inequality.

Remark 4.29. *The hypothesis of the theorem are fulfilled in the case of biological applications where $\beta(x,\theta) = mx^\alpha$, because we have then $\beta \geq m > 0$ and $\Psi \in L^\infty(\Omega)$.*

Proof. Again we start with a regular solution $\rho(t, x, \theta)$. We then follow the calculation done in [Per07] III.7 pp.66-67, adapting the method to take into account the contribution of the source term. Define the function

$$h(t, x, \theta) = \rho(t, x, \theta)e^{-\lambda_0 t} - m(t)V(x, \theta)$$

which satisfies $\int_\Omega h(t)\Psi = 0$ for all non-negative t, by the property of evolution of the mean value and since $\int_\Omega V\Psi = 1$. As the direct eigenvector V solves the equation (35), h solves the equation

$$\partial_t h + \mathrm{div}(hG) + \lambda_0 h = -e^{-\lambda_0 t}FV$$

where $F(t) := \int_{\partial\Omega} f(t, \sigma)\Psi(\sigma)$. Multiplying the equation by the function $\mathrm{sgn}(h)$ gives the following equation on $|h|$

$$\partial_t |h| + \mathrm{div}(|h|G) + \lambda_0 |h| = -e^{-\lambda_0 t}FV\mathrm{sgn}(h)$$

Multiplying this equation by Ψ, the equation on Ψ by $|h|$ and then summing the both gives

$$\partial_t(|h|\Psi) + \mathrm{div}(G|h|\Psi) = -\beta|h| - e^{-\lambda_0 t}FV\Psi\mathrm{sgn}(h)$$

Now integrating in (x, θ) yields :

$$\frac{d}{dt}\int_\Omega |h|\Psi dx d\theta = \int_{\partial\Omega} \Psi(\sigma)\left| N(\sigma)\int_\Omega \beta h dx d\theta + e^{-\lambda_0 t}f(t, \sigma)\right| d\sigma - \int_\Omega \beta|h| dx d\theta$$

$$- e^{-\lambda_0 t}F\int_\Omega V\Psi\mathrm{sgn}(h)dx d\theta$$

$$\leq \underbrace{\left|\int_\Omega \beta h dx d\theta\right| - \int_\Omega \beta|h| dx d\theta}_{A} + 2e^{-\lambda_0 t}\overline{F}(t)$$

where $\overline{F}(t) := \int_{\partial\Omega} |f(t, \sigma)|\Psi(\sigma)$, using the positivity of the eigenvectors V and Ψ and the facts that $\int_\Omega V\Psi = 1$ and $\int_{\partial\Omega} N\Psi = 1$. We compute

$$A \leq \left|\int_\Omega \beta h dx d\theta - \mu\int_\Omega \Psi h dx d\theta\right| - \int_\Omega \beta|h| dx d\theta \leq \int_\Omega (\beta - \mu\Psi)|h| dx d\theta - \int_\Omega \beta|h| dx d\theta$$

$$\leq -\mu\int_\Omega \Psi|h| dx d\theta$$

where we used that $\beta - \mu\Psi \geq 0$.
A Gronwall lemma finally gives

$$\int_\Omega |h(t)|\Psi \leq e^{-\mu t}\left\{\int_\Omega |h(0)|\Psi + 2\int_0^t e^{-(\lambda_0-\mu)s}F(s)ds\right\}$$

which is the required result. For an initial data in $L^1(\Omega)$, remark that it is possible to pass to the limit in the previous expression and thus to use the density of regular solutions. $\square$

4   Numerical illustrations of the asymptotic behavior

For investigation of the asymptotic behavior, since the eigenelements after change of variables are decoupled in the product of a function along the boundary and a function depending on the time τ along the characteristic (see formula (37) below), we consider the simulation of the system along only one characteristic, taking $N(\sigma) = \delta_{\sigma=\sigma_0}$, the Dirac mass centered on the point $\sigma_0 = (1, \theta_0)$ (see the chapter 6 for further considerations on this point). We recall the expressions of the direct and dual eigenvectors V and Ψ, from proposition 4.11.

$$\overline{V}(\tau) = V(\Phi_\tau(\sigma_0)) = C_{\lambda_0} e^{-\lambda_0 \tau} |J_\Phi|^{-1}, \quad \forall \tau > 0 \tag{37}$$

$$\overline{\Psi}(\tau) = \Psi(\Phi_\tau(\sigma_0)) = e^{\lambda_0 \tau} \int_\tau^\infty \beta(\Phi_s(\sigma)) e^{-\lambda_0 s} ds, \quad \forall \tau > 0.$$

with the malthus exponent λ_0 solving the following spectral equation

$$\int_0^{+\infty} \beta(\Phi_\tau(\sigma_0)) e^{-\lambda_0 \tau} d\tau = 1. \tag{38}$$

4.1   Asymptotic behavior for realistic parameters

We first look at the asymptotic behavior of the model with the fitted growth parameters from [HPFH99] and some reasonable values of m and α as well as initial conditions. The parameters values are given by :

$$\begin{array}{c} a = 0.192, \quad c = 5.85, \quad d = 0.00873, \\ m = 10^{-3}, \quad \alpha = \frac{2}{3}, \quad x_0 = x_{0,p} = 10^{-6}, \quad \theta_0 = \theta_{0,p} = 10^{-5}. \end{array} \tag{39}$$

We estimate then the value of λ_0 by numerically computing the asymptotic slope of the total number of metastases and check its relevance by computing also the value of the spectral equation (38). This is illustrated in the figure 1.

$$\lambda_0 = 0.05$$

$$\int_0^{+\infty} \beta(\Phi_\tau(\sigma_0)) e^{-\lambda_0 \tau} d\tau = 1.00067$$
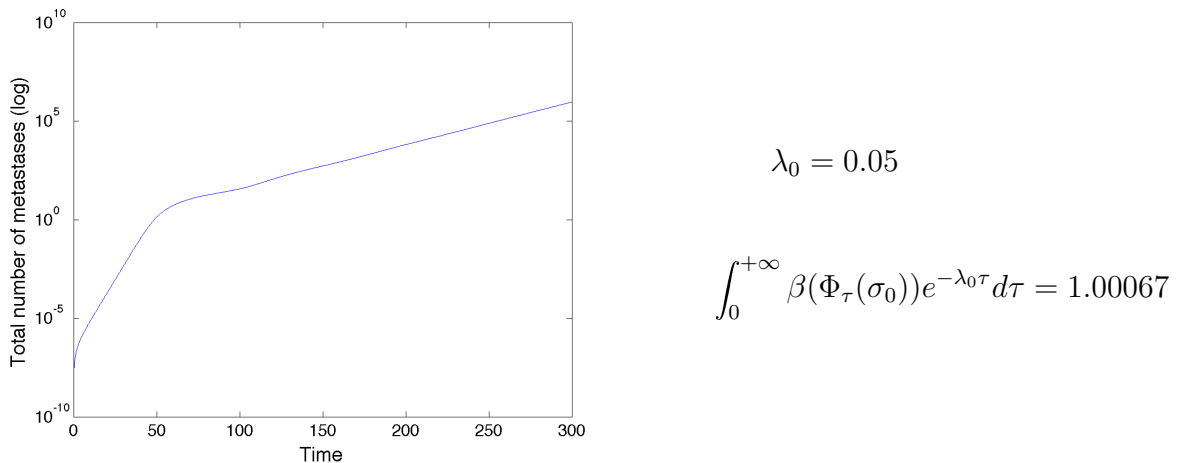
Figure 1: Number of metastases for large times in log-scale and computation of the value of λ_0 as well as $\int_0^{+\infty} \beta(\Phi_\tau(\sigma_0)) e^{-\lambda_0 \tau} d\tau$.

We then look at the eigenelements and compare our computed solution at the final time with $e^{\lambda_0 T}\overline{V}(\tau)$ as well as the shape of the dual eigenvector which for technical reasons we don't compute on the whole interval, since its computation for each τ requires the computation of an integral until infinity. This is illustrated in the Figure 2.
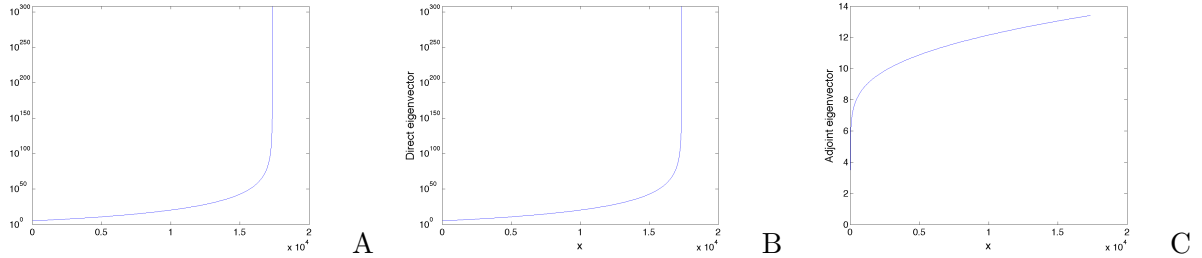
Figure 2: Eigenelements. The figures represent the x-projection of functions defined on the curve $\{\Phi_\tau(\sigma_0),\ 0 \leq \tau < \infty\}$ A. Asymptotic distribution $\rho(T,X)$ B. $e^{\lambda_0 T}V(X)$. B. Dual eigenvector

4.2 Influence of the parameters on the Malhus value λ_0

In order to investigate further the asymptotic behavior of the system, we consider numerically more convenient parameters and initial conditions, which we will refer to as "base parameters" and are given by

$$a = 1, \quad c = 1, \quad d = 0.22$$
$$m = 1.5, \quad \alpha = 1 \tag{40}$$
$$x_0 = x_{0,p} = 1, \quad \theta_0 = \theta_{0,p} = 5$$

and first investigate the effect of varying parameters around this position on the malthus parameter λ_0 that we numerically compute. We also numerically compute an approximation of $\int_0^{+\infty} \beta\left(\Phi_\tau(\sigma_0)\right) e^{-\lambda_0 \tau} d\tau$ which should be equal to 1 according to the theory (proposition 4.11). Some results are given in the table 1.

Parameter	Base	$m = 1$	$\alpha = 0.1$	$a = 10$	$d = 0.01$	$c = 10$
λ_0	2.52289	1.90673	1.58651	5.13798	2.61644	3.06971
$\int_0^{+\infty} \beta\left(\Phi_\tau(\sigma_0)\right) e^{-\lambda_0 \tau} d\tau$	1.00708	1.00184	1.01002	0.950986	1.00765	1.01014

Table 1: Value of the malthus exponent λ_0 for different values of the parameters. The base parameters are used, changing only one value each time.

4.3 Shape of the direct eigenvector

When looking at the Figure 2 we remark that the direct eigenvector seems not to belong to L^∞ and a legitimate question arises : what governs the shape of the eigenvector?

From its expression (37), remembering the formula $|J_\Phi|(\tau, \sigma_0) = G_1(1, \theta_0)e^{\int_0^\tau \text{div}(G(\Phi_s(\sigma_0)))ds}$

(see proposition 3.4 of chapter 3), we have

$$\overline{V}(\tau) = e^{h(\tau)}, \; h(\tau) = -\lambda_0 \tau - \int_0^\tau \operatorname{div}(G(\Phi_s(\sigma_0)))ds.$$

We can compute that

$$\operatorname{div}(G(\Phi_s(\sigma_0))) \xrightarrow[s\to+\infty]{} \operatorname{div}(G)\left(\left(\frac{c}{d}\right)^{3/2}, \left(\frac{c}{d}\right)^{3/2}\right) = c - a - \frac{2}{3}\left(\frac{c}{d}\right)^{3/2}$$

and derive that asymptotically

$$h(\tau) \sim \left(a + \frac{2}{3}\left(\frac{c}{d}\right)^{3/2} - c - \lambda_0\right)\tau. \tag{41}$$

From this we can predict that, since basic considerations show that λ_0 is increasing with respect to m, for large values of m, then V should be in L^∞ (and even going to zero at X^*). Indeed, with the growth parameters given by (39), for large values of m this is the case, as shown in the Figure 3.A (the same parameters with $m = 10^{-3}$ exhibit an unbounded direct eignevector, see Figure 2). Interestingly and in connection with the fact that increasing α does not always increase λ_0 (see Figure 5 of chapter 7), especially for large values of m, we observe in Figure 3.B that for $\alpha = 1$, with the same value of m, then the eigenvector does not belong to L^∞ anymore. This indicates that in the expression (41), the balance between the growth parameters and λ_0 is in favor of the first ones. Indeed the respective values of λ_0 for $\alpha = 0.6$ and $\alpha = 1$ are 10.7805 and 2.67727. This behavior is the opposite than the one depicted in the paper of Iwata et al. [IKN00] in the one-dimensional case, where the size is expressed in number of cells and thus is bigger than 1. Expressing the size in mm^3 as we did and considering a large value of m exhibits thus a different behavior. However, in the following results below of the table 2 we have the same qualitative behavior as in Iwata et al., namely a bounded eigenvector for $\alpha = 1$ and unbounded for $\alpha = 0.1$.
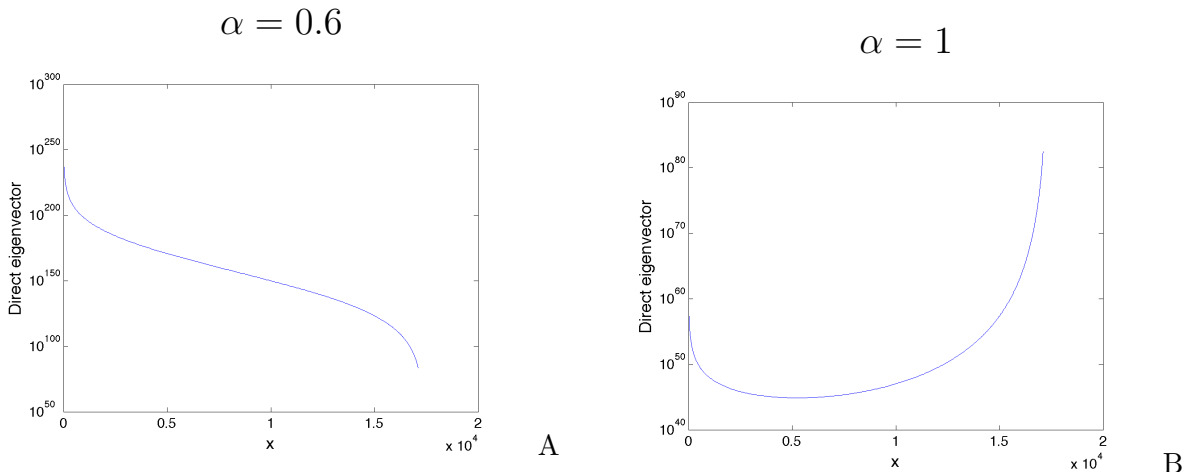
Figure 3: Two different shapes of the direct eigenvector (multiplied here by $e^{\lambda_0 T}$) depending on the value of α, with $m = 10^5$.

To investigate further this fact, we start from the base parameters given by (40), for which the eigenvector is bounded and we vary each parameter one by one, guided by formula (41), to obtain a non-bounded eigenvector. We were able to obtain such a fact for each parameter except for d for which we stopped investigate because we were reaching too small numerical values (until $d = 10^{-12}$) without obtaining an unbounded eigenvector, whereas formula (41) predicts that small values of d should do so. However, the overall behavior suggested that smaller values could produce such a fact. For the other parameters, everything happens as predicted by (41) namely we can pass from a bounded eigenvector to an unbounded one by : increasing a, increasing c, decreasing m or decreasing α. The results are reported in the table 2.

Parameter	a	d	c	m	α
$V \in L^\infty$	1	0.22	1	1.5	1
$V \notin L^\infty$	10	$*$	10	0.5	0.1

Table 2: Investigation of the boundedness of the direct eigenvector with respect to the parameter values (see text for the specifity of d).

Chapter 5

Non autonomous case. Theoretical and numerical analysis

In this chapter, we present some mathematical and numerical analysis of the model established in the chapter 1, section 1.5 in the non-autonomous case that is, when both cytotoxic and AA treatments are present and with a general growth field G (i.e. the growth law of the tumours) satisfying the hypothesis that there exists a positive constant δ such that $-G(t,\sigma) \cdot \nu(\sigma) \geq \delta > 0$ for all $t > 0$ and almost every $\sigma \in \partial\Omega$ where ν is the normal to the boundary $\partial\Omega$ of the domain Ω where metastases live, meaning that G points inward the domain. We first simplify the problem by straightening the characteristics of the equation, in the same way as we did in the study of $W^p_{\text{div}}(\Omega)$ (see chapter 3). We perform some theoretical analysis first at the continuous level (uniqueness and a priori estimates). Then we introduce an approximation scheme which follows the characteristics of the equation (lagrangian scheme). The introduction of such schemes in the area of size-structured population equations can be found in [ALM99] for one-dimensional models. Here, we go further in the lagrangian approach by doing the change of variables straightening the characteristics and discretizing the simple resulting equation, in the case of a general class of two-dimensional non-autonomous models. We prove existence of the weak solution to the continuous problem through the convergence of this scheme *via* discrete a priori L^∞ bounds and establish an error estimate in the case of more regular data, that we illustrate numerically.

We recall that the problem we consider is given by

$$\begin{cases} \partial_t \rho(t, X) + \text{div}(\rho(t, X) G(t, X)) = 0 & \forall (t, X) \in]0, T[\times \Omega \\ -G \cdot \nu(t, \sigma) \rho(t, \sigma) = N(\sigma) \int_\Omega \beta(X) \rho(t, X) dX + f(t, \sigma) & \forall (t, \sigma) \in]0, T[\times \partial \Omega \\ \rho(0, X) = \rho^0(X) & \forall X \in \Omega. \end{cases} \quad (1)$$

where, in the case of the model from section 1.5 of chapter 1, $G(t, x, \theta) = (G_1(t, x, \theta), G_2(t, x, \theta))$ is given by

$$\begin{cases} G_1(t, x, \theta) = ax \ln\left(\frac{\theta}{x}\right) - h\gamma_C(t)(x - x_{min})^+ \\ G_2(t, x, \theta) = cx - d\theta x^{\frac{2}{3}} - e\gamma_A(t)(\theta - \theta_{min})^+ \end{cases} \quad (2)$$

1 Analysis at the continuous level

In the autonomous case, that is when G depends only on X and there is no treatment, the analysis of the equation (1) has been performed in the chapter 4. It was proven existence, uniqueness, regularity and asymptotic behavior of solutions. We present now some analysis on the equation (1) with a more general growth field G than the one from our model given by (2).

Let $\Omega =]1, b[^2$ and $G : \mathbb{R} \times \overline{\Omega} \to \mathbb{R}^2$ be a $\mathcal{C}^1$ vector field. We make the following assumption on G :

$$\exists \delta > 0, \; -G(t, \sigma) \cdot \nu(\sigma) \geq \delta > 0 \quad \forall \, 0 \leq t \leq T, \; a.e. \, \sigma \in \partial \Omega, \quad (3)$$

which means that G points inward all along the boundary for all times and that the metastases can't go out of Ω (and thus are never removed from the system). We do the following assumptions on the data :

$$\rho^0 \in L^\infty(\Omega), \; \beta \in L^\infty(\Omega), \; N \in L^\infty(\partial\Omega), \; N \geq 0, \; \int_{\partial\Omega} N(\sigma) d\sigma = 1, \; f \in L^\infty(]0, T[\times \partial\Omega). \quad (4)$$

Remark 5.1.
• *In the case of G being given by (2) if there is no treatment (that is, if $e = h = 0$, or $t \leq t_1$) then we don't have $-G(t, \sigma) \cdot \nu(\sigma) \geq \delta > 0$ all along the boundary since G vanishes at the point (b, b). But since the problem was solved in this case (see chapter 4) we consider that the time 0 is the starting time of the treatment and that either e or h is positive, which makes the assumption (3) true. Notice that this assumption implies that the treatment is ineffective on metastases with minimal size or angiogenic capacity, which is true in our case (see the expressions (2)).*
• *The following analysis at the continuous level extends to the case where Ω has a boundary which is piecewise $\mathcal{C}^1$ except in a finite number of points.*

Definition 5.2 (Weak solution). *We say that $\rho \in L^\infty(]0, T[\times \Omega)$ is a weak solution of the problem (1) if for all test function ϕ in $\mathcal{C}^1([0, T] \times \overline{\Omega})$ with $\phi(T, \cdot) = 0$*

$$\int_0^T \int_\Omega \rho(t, X) \left[\partial_t \phi(t, X) + G(t, X) \cdot \nabla \phi(t, X) \right] dX dt + \int_\Omega \rho^0(X) \phi(0, X) dX$$
$$+ \int_0^T \int_{\partial\Omega} \left\{ N(\sigma) B(t, \rho) + f(t, \sigma) \right\} \phi(t, \sigma) = 0 \quad (5)$$

where we denoted $B(t, \rho) := \int_\Omega \beta(X) \rho(t, X) dX$.

Remark 5.3. *By approximating a Lipschitz function by $\mathcal{C}^1$ ones, it is possible to prove that the definition of weak solutions would be equivalent with test functions in $W^{1,\infty}([0, T] \times \overline{\Omega})$ vanishing at time T.*

1.1   Change of variables

Our approach is based on the method of characteristics and consists in straightening the characteristics to simplify the problem through a change of variables. Let $\Phi(t; \tau, \sigma)$ be the solution of the differential equation

$$\begin{cases} \frac{d}{dt}\Phi(t; \tau, \sigma) = G(t, \Phi(t; \tau, \sigma)) \\ \Phi(\tau; \tau, \sigma) = \sigma \end{cases}.$$

For each time $t > 0$, we define the entrance time $\tau^t(X)$ and entrance point $\sigma^t(X)$ for a point $X \in \Omega$:

$$\tau^t(X) := \inf\{0 \le \tau \le t;\ \Phi(\tau; t, X) \in \Omega\},\ \sigma^t(X) := \Phi(\tau^t(X); t, X).$$

We consider the sets

$$\Omega_1^t = \{X \in \Omega;\ \tau^t(X) > 0\},\ \Omega_2^t = \{X \in \Omega;\ \tau^t(X) = 0\}$$

and

$$Q_1 := \{(t, X) \in [0, T] \times \overline{\Omega};\ X \in \overline{\Omega_1^t}\},\ Q_2 := \{(t, X) \in [0, T] \times \overline{\Omega};\ X \in \overline{\Omega_2^t}\}.$$

We also define $\widetilde{Q_1} := \{(t, \tau, \sigma);\ 0 \le \tau \le t \le T,\ \sigma \in \partial\Omega\} = \Phi^{-1}(Q_1)$ and notice that

$$\Sigma_1 := [0, T] \times \partial\Omega = \{(t, X);\ \tau^t(X) = 0\},\ \text{and } \Sigma_2 = \{(t, \Phi(t; 0, \sigma));\ 0 \le t \le T,\ \sigma \in \partial\Omega\} = \{(t, X);\ \tau^t(X) = 0\}.$$

See figure 1 for an illustration. We can now introduce the changes of variables that we will constantly use in the sequel. The proof of the following proposition is very similar to the one of proposition 3.4 and is postponed to the section 5.4.

Proposition 5.4 (Change of variables). *The maps*

$$\Phi_1 : \begin{array}{ccc} \widetilde{Q_1} & \to & Q_1 \\ (t, \tau, \sigma) & \mapsto & (t, \Phi(t; \tau, \sigma)) \end{array} \quad \text{and } \Phi_2 : \begin{array}{ccc} [0, T] \times \overline{\Omega} & \to & Q_2 \\ (t, Y) & \mapsto & (t, \Phi(t; 0, Y)) \end{array}$$

are bilipschitz. The inverse of Φ_1 is $(t, X) \mapsto (t, \tau^t(X), \sigma^t(X))$ and the inverse of Φ_2 is $(t, X) \mapsto (t, Y(X))$ with $Y(X) = \Phi(0; t, X)$. Denoting $J_1(t; \tau, \sigma) = |\det(D\Phi_1)|$ and $J_2(t; Y) = |\det(D\Phi_2)|$, where $D\Phi_i$ stands for the differential of Φ_i, we have :

$$J_1(t; \tau, \sigma) = |G(\tau, \sigma) \cdot \nu(\sigma)| e^{\int_\tau^t \operatorname{div} G(u, \Phi(u; \tau, \sigma)) du} \text{ and } J_2(t; Y) = e^{\int_0^t \operatorname{div} G(u, \Phi(u; 0, Y)) du} \quad (6)$$

We refer to the appendix of this chapter for the proof of this result and to the figure 1 for an illustration.

Using these changes of variables we can write for a function $f \in L^1(]0, T[\times \Omega)$

$$\int_0^T \int_\Omega f(X) dX = \int_0^T \int_0^t \int_{\partial\Omega} f(\Phi_1(t; \tau, \sigma)) J_1(t; \tau, \sigma) d\sigma d\tau + \int_0^T \int_\Omega f(\Phi_2(t; 0, Y)) J_2(t; Y) dY.$$

We want to decompose the equation (1) into two subequations : one for the contribution of the boundary term and one for the contribution of the initial condition. Defining

$$\widetilde{\rho}_1(t, \tau, \sigma) := \rho(t, \Phi(t; \tau, \sigma)) J_1(t; \tau, \sigma) \text{ and } \widetilde{\rho}_2(t, Y) := \rho(t, \Phi(t; 0, Y)) J_2(t; Y) \quad (7)$$
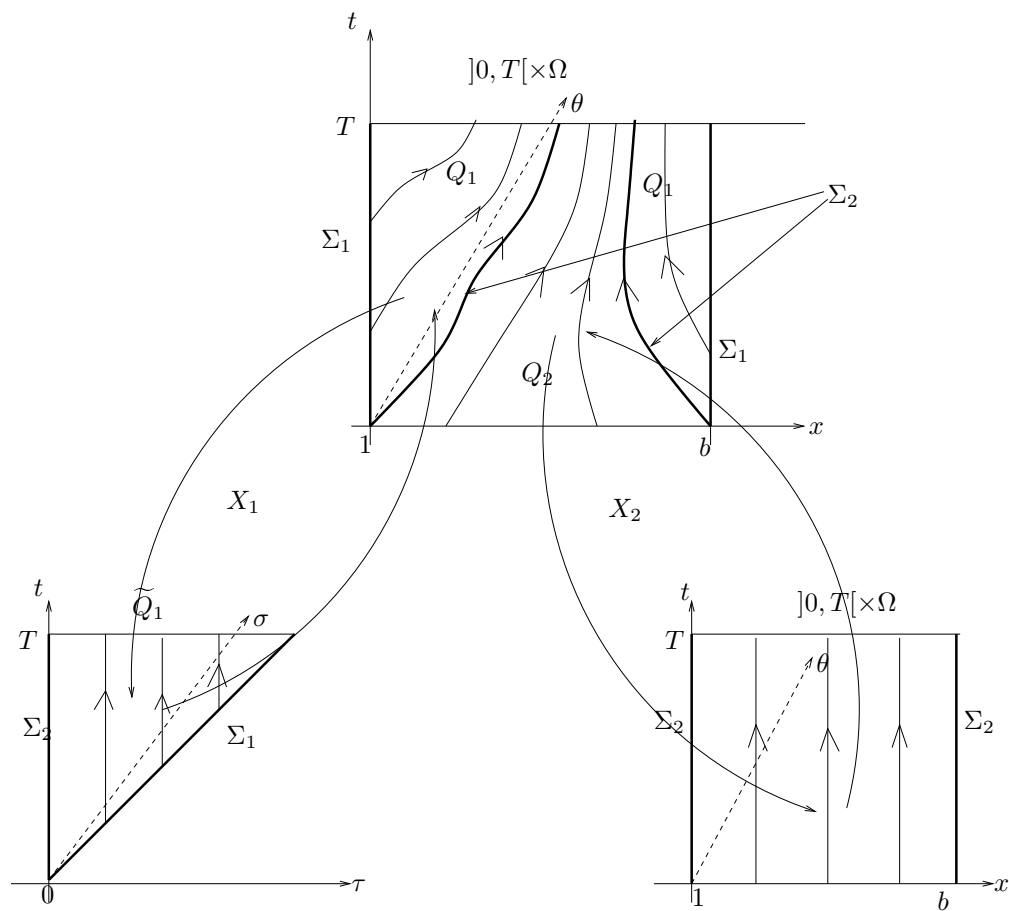
Figure 1: The two changes of variables Φ_1 and Φ_2 (represented only on the plane $\theta = 1$).

we have, when the solution is regular : $\partial_t \widetilde{\rho}_1 = (\partial_t \rho + \operatorname{div}(\rho G)) J_1 = 0$ and the same for $\widetilde{\rho}_2$. It is thus natural to introduce the following equations

$$
\begin{cases}
\partial_t \widetilde{\rho}_1(t, \tau, \sigma) = 0 & 0 < \tau \le t < T, \ \sigma \in \partial\Omega \\
\widetilde{\rho}_1(\tau, \tau, \sigma) = N(\sigma) \widetilde{B}(\tau, \widetilde{\rho}_1, \widetilde{\rho}_2) + f(\tau, \sigma) & 0 < \tau < T, \ \sigma \in \partial\Omega
\end{cases}
\tag{8}
$$

where we denoted

$$
\widetilde{B}(\tau, \widetilde{\rho}_1, \widetilde{\rho}_2) = \int_0^\tau \int_{\partial\Omega} \beta(\Phi(\tau; s, \sigma)) \widetilde{\rho}_1(\tau, s, \sigma) d\sigma ds + \int_\Omega \beta(\Phi(\tau; 0, Y)) \widetilde{\rho}_2(\tau, Y) dY,
$$

and

$$
\begin{cases}
\partial_t \widetilde{\rho}_2 = 0 & t > 0, \ Y \in \Omega \\
\widetilde{\rho}_2(0; Y) = \rho^0(Y) & Y \in \Omega.
\end{cases}
\tag{9}
$$

We precise the definition of weak solutions to these equations.

Definition 5.5. *We say that a couple $(\widetilde{\rho}_1, \widetilde{\rho}_2) \in L^\infty(\widetilde{Q}_1) \times L^\infty(]0, T[\times\Omega)$ is a weak solution of the equations* (8)-(9) *if for all $\widetilde{\phi}_1 \in \mathcal{C}^1(\overline{Q}_1)$ with $\widetilde{\phi}_1(T, \cdot) = 0$ we have :*

$$
\int_0^T \int_0^t \int_{\partial\Omega} \widetilde{\rho}_1(t, \tau, \sigma) \partial_t \widetilde{\phi}_1(t, \tau, \sigma) d\sigma d\tau dt + \int_0^T \int_{\partial\Omega} \left\{ N(\sigma) \widetilde{B}(t, \widetilde{\rho}_1, \widetilde{\rho}_2) + f(t, \sigma) \right\} \widetilde{\phi}_1(t, t, \sigma) = 0,
\tag{10}
$$

and for all $\widetilde{\phi}_2 \in \mathcal{C}^1([0, T] \times \overline{\Omega})$ with $\widetilde{\phi}_2(T, \cdot) = 0$ we have

$$
\int_0^T \int_\Omega \widetilde{\rho}_2(t, Y) \partial_t \widetilde{\phi}_2(t, Y) dt + \int_\Omega \rho^0(Y) \widetilde{\phi}_2(0, Y) dY = 0.
\tag{11}
$$

Remark 5.6. *If $\widetilde{\rho}_1$ is a regular function which solves* (8), *then the weak formulation is satisfied since we have :*

$$
\int_0^T \int_0^t \int_{\partial\Omega} \widetilde{\rho}_1(t, \tau, \sigma) \partial_t \widetilde{\phi}_1(t, \tau, \sigma) d\sigma d\tau dt = \underbrace{\int_0^T \int_{\partial\Omega} \widetilde{\phi}_1(T, \tau, \sigma) \widetilde{\rho}_1(T, \tau, \sigma) d\tau d\sigma}_{=0}
$$

$$
- \int_0^T \int_0^t \widetilde{\phi}_1(t, \tau, \sigma) \partial_t \widetilde{\rho}_1(t, \tau, \sigma) d\sigma d\tau dt - \int_0^T \int_{\partial\Omega} \widetilde{\phi}_1(t, t, \sigma) \widetilde{\rho}_1(t, t, \sigma) d\sigma dt.
$$

We prove now the following theorem, establishing the equivalence between the problem (1) and the problem (8)-(9).

Theorem 5.7 (Equivalence between problem (1) and problem (8)-(9))**.** *Let $\rho \in L^\infty(]0, T[\times\Omega)$ be a weak solution of the equation* (1). *Then $(\widetilde{\rho}_1, \widetilde{\rho}_2)$ given by* (7) *is a weak solution of* (8)-(9). *Conversely, if $\widetilde{\rho}_1$ and $\widetilde{\rho}_2$ are weak solutions of* (8) *and* (9), *then the function defined by*

$$
\rho(t, X) := \widetilde{\rho}_1(t, \tau^t(X), \sigma^t(X)) J_1^{-1}(t, \tau^t(X), \sigma^t(X)) \mathbf{1}_{X \in \Omega_1^t} + \widetilde{\rho}_2(t, Y(X)) J_2^{-1}(t, Y(X)) \mathbf{1}_{X \in \Omega_2^t}
\tag{12}
$$

is a weak solution of (1).

Proof.

• *Direct implication.* Let ρ be a weak solution of the equation (1). We will prove that $\widetilde{\rho}_2$ defined by (7) solves (9). Let $\widetilde{\phi}_2 \in \mathcal{C}^1([0,T] \times \overline{\Omega})$ with $\widetilde{\phi}_2(T, \cdot) = 0$. We define, for $X \in Q_2$, $\phi_2(t, X) := \widetilde{\phi}_2(t, Y(X)) \in W^{1,\infty}(Q_2)$ and we intend to extend it in a Lipschitz function of $[0,T] \times \overline{\Omega}$ so that we can use it as a test function in the weak formulation for ρ (see remark 5.3). We define, for $(t, \tau, \sigma) \in \widetilde{Q}_1$, $\widetilde{\phi}_1^\varepsilon(t, \tau, \sigma) = \widetilde{\phi}_2(t, \sigma)\zeta_\varepsilon(\tau)$ with $\zeta_\varepsilon(\tau)$ being a truncature function in $\mathcal{C}^1([0, +\infty[)$ such that $0 \le \zeta_\varepsilon \le 1$, $\zeta_\varepsilon(0) = 1$, $\zeta_\varepsilon(\tau) = 0$ for $\tau \ge \varepsilon$. Then $\widetilde{\phi}_1^\varepsilon \in W^{1,\infty}(\widetilde{Q}_1)$ and we set $\phi_1^\varepsilon(t, X) := \widetilde{\phi}_1^\varepsilon(t, \tau^t(X), \sigma^t(X)) \in W^{1,\infty}(Q_1)$ since $\tau^t(X)$ and $\sigma^t(X)$ are Lipschitz from proposition 5.4. We define then

$$\phi^\varepsilon := \left\{ \begin{array}{l} \phi_1^\varepsilon \text{ on } Q_1 \\ \phi_2 \text{ on } Q_2 \end{array} \right. .$$

The function ϕ^ε is Lipschitz on Q_1, Lipschitz on Q_2 and $\phi^\varepsilon \in \mathcal{C}([0,T] \times \overline{\Omega})$ since $Q_1 \cap Q_2 = \{(t, X); \tau^t(X) = 0\}$. Thus $\phi^\varepsilon \in W^{1,\infty}([0,T] \times \overline{\Omega})$ with $\phi^\varepsilon(T, \cdot) = 0$. Using ϕ^ε as a test function in (5), we have

$$\int_{Q_1} \rho[\partial_t \phi_1^\varepsilon + G \cdot \nabla \phi_1^\varepsilon]dXdt + \int_0^T \int_{\partial\Omega} \{N(\sigma)B(t, \rho) + f(t, \sigma)\} \phi_1^\varepsilon(t, \sigma)dtd\sigma$$
$$+ \int_{Q_2} \rho[\partial_t \phi_2 + G \cdot \nabla \phi_2]dXdt + \int_\Omega \rho^0(X)\phi_2(0, X)dX = 0 = I_\varepsilon^1 + I_2.$$

By doing the change of variables Φ_1 in the term I_1^ε and noticing that $\phi_1^\varepsilon(t, \sigma) = \widetilde{\phi}_1^\varepsilon(t, t, \sigma) = \widetilde{\phi}_2(t, \sigma)\zeta_\varepsilon(t)$, we obtain

$$I_1^\varepsilon = \int_0^T \int_0^t \widetilde{\rho}_1(t, \tau, \sigma)\partial_t \widetilde{\phi}_1(t, \sigma)\zeta^\varepsilon(\tau)d\sigma d\tau dt + \int_0^T \int_{\partial\Omega} B(t, \rho)\widetilde{\phi}_2(t, \sigma)\zeta^\varepsilon(t)d\sigma \xrightarrow[\varepsilon \to 0]{} 0.$$

Now doing the change of variables Φ_2 in the second term I_2 and noticing that $\partial_t \widetilde{\phi}_2(t, Y) = \partial_t(\phi_2(t, \Phi(t; 0, Y))) = \partial_t \phi_2(t, \Phi(t; 0, Y)) + G(t, \Phi(t; 0, Y)) \cdot \nabla \phi_2(t, \Phi(t; 0, Y))$ gives the result. The equation on $\widetilde{\rho}_1$ is proved in the same way.

• *Reverse implication.* Let $\widetilde{\rho}_1$ and $\widetilde{\rho}_2$ be solutions of (8) and (9) respectively. Define $\rho(t, X)$ by (12), and consider a test function $\phi \in \mathcal{C}^1([0,T] \times \overline{\Omega})$ with $\phi(T, \cdot) = 0$. Then $\phi_1 := \phi_{|Q_1} \in \mathcal{C}^1(Q_1)$, with $\phi_1(T, \cdot) = 0$, thus $\widetilde{\phi}_1(t, \tau, \sigma) := \phi_1(t, \Phi_1(\tau, \sigma))$ is valid as a test function in the weak formulation of (8). In the same way $\widetilde{\phi}_2(t, Y) := \phi_2(t, \Phi_2(Y))$ with $\phi_2 := \phi_{|Q_2}$ is valid as a test function for (9). Thus we have

$$\int_{\widetilde{Q}_1} \widetilde{\rho}_1(t, \tau, \sigma)\partial_t \widetilde{\phi}_1(t, \tau, \sigma)d\sigma d\tau dt + \int_0^T \int_{\partial\Omega} \widetilde{B}(t, \widetilde{\rho}_1, \widetilde{\rho}_2)\widetilde{\phi}_1(t, t, \sigma)d\sigma dt$$
$$+ \int_0^T \int_\Omega \widetilde{\rho}_2(t, y)\partial_t \widetilde{\phi}_2(t, y)dtdy + \int_\Omega \rho^0(y)\widetilde{\phi}_2(0, y)dy = 0$$

Doing the changes of variables gives the weak formulation of (1). $\square$

This theorem simplifies the structure of the problem (1). In some sense, it formalizes the method of characteristics in the framework of weak solutions for our problem. The characteristics are straightened (see figure 1) and the directional derivative along the field (t, G) is transformed in only a time derivative. Moreover, integrating the jacobians (which contains the transformation of areas) in the definitions of $\widetilde{\rho}_1$ and $\widetilde{\rho}_2$, these functions are constant in time. The continuous analysis and discrete approximation of the problem (1) is thus simplified.

1.2   Uniqueness

We will present two different methods to establish uniqueness of weak solutions to the problem
(1), the second one being known from us by B. Perthame :

1. By *a priori* L^1 and L^∞ estimates obtained directly on weak solutions

2. By proving existence of regular solutions to the adjoint problem

A priori continuous estimates

To obtain *a priori* estimates on the solutions of the equation in order to prove uniqueness, we
need a trace for a solution to the transport equation as well as the fact that $|\rho|$ also solves
the equation. These issues are treated in the papers of Bardos [Bar70] and Beals-Protopopescu
[BP87]. We will use a result well adapted for our aim from Boyer [Boy05].

Theorem 3.1 from [Boy05] . *Let $\rho \in L^\infty(]0,T[\times\Omega)$ be a solution, in the distribution sense,
to the equation :*

$$\partial_t \rho + \mathrm{div}(\rho G) = 0. \tag{13}$$

(i) *The function ρ lies in $\mathcal{C}([0,T];L^p(\Omega))$, for any $1 \le p < \infty$. Furthermore, ρ is continuous
in time with values in $L^\infty(\Omega)$ weak-$*$.*

(ii) *There exists a function $\gamma\rho \in L^\infty(]0,T[\times\partial\Omega; |d\mu_G|)$, with $d\mu_G = (G \cdot \nu)dtd\sigma$, such that for
any $h \in \mathcal{C}^1(\mathbb{R})$, for any test function $\phi \in \mathcal{C}^1([0,T] \times \overline{\Omega})$, and for any $[t_0,t_1] \subset [0,T]$, we
have*

$$\int_{t_0}^{t_1} \int_\Omega h(\rho)(\partial_t \phi + \mathrm{div}(G\phi))dtdX + \int_\Omega h(\rho(t_0))\phi(t_0)dX - \int_\Omega h(\rho(t_1))\phi(t_1)dX$$

$$- \int_{t_0}^{t_1} \int_{\partial\Omega} h(\gamma\rho)\phi G \cdot \nu dtd\sigma - \int_{t_0}^{t_1} \int_\Omega h'(\rho)\rho\,\mathrm{div}(G)\phi dtdX = 0 \tag{14}$$

Remark 5.8.
  • *By approximating the function $s \mapsto |s|$ by $\mathcal{C}^1$ functions, it is possible to show that the
formula (14) stands with $h(s) = |s|$.*
  • *The second point of the proposition implies in particular that $h(\rho)$ has a trace which is
$h(\gamma\rho)$.*
  • *In [Boy05], this proposition is proved in the case of a much less regular field G but with
the technical assumption that $\mathrm{div}(G) = 0$, which is not the case here. Though, the proof can be
extended to our case.*

Thanks to this result, we can prove the following proposition.

Proposition 5.9 (Continuous *a priori* estimates)**.** *Let $\rho \in L^\infty(]0,T[\times\Omega)$ be a weak solution of
the equation (1). The following estimates hold*

$$||\rho(t,\cdot)||_{L^1(\Omega)} \le e^{t||\beta||_{L^\infty}}||\rho^0||_{L^1(\Omega)} + \int_0^t e^{(t-s)||\beta||_{L^\infty}} \int_{\partial\Omega} |f(s,\sigma)|d\sigma ds \tag{15}$$

and

$$||\rho||_{L^\infty(]0,T[\times\Omega)} \leq C_\infty \tag{16}$$

with

$$C_\infty = \left(||N||_{L^\infty}||\beta||_{L^\infty}||\rho||_{L^\infty(L^1)} + ||f||_{L^\infty} \right) ||G||_{L^\infty} e^{T||\operatorname{div} G||_{L^\infty}} + ||\rho^0||_{L^\infty} e^{T||\operatorname{div} G||_{L^\infty}}$$

Proof.

• *Estimate in L^1.* Let ρ be a weak solution of the equation (1). Then in particular it solves (13) in the sense of distributions. Thus the proposition 5.1.2.0 applies and gives a trace $\gamma\rho \in L^\infty(]0,T[\times\partial\Omega; |d_{\mu G}|)$. Now, by using (14) with $h(s) = s$ and the definition of weak solutions to the equation (1) we have that for all $\phi \in \mathcal{C}_c^1([0,T[\times\overline{\Omega})$

$$\int_0^T \int_{\partial\Omega} \gamma\rho(t,\sigma)\phi(t,\sigma)G(t,\sigma) \cdot \nu d\sigma dt = \int_0^T \int_{\partial\Omega} \left\{ N(\sigma) \int_\Omega \beta(X)\rho(t,X)dX + f(t,\sigma) \right\} \phi(t,\sigma)d\sigma dt$$

which gives

$$-\gamma\rho(t,\sigma)G(t,\sigma) \cdot \nu = N(\sigma) \int_\Omega \beta(X)\rho(t,X)dX + f(t,\sigma), \quad a.e. \tag{17}$$

In view of the remark 5.8, we know that $|\rho|$ is also a weak solution to the equation (1), with initial data $|\rho^0|$ and boundary data $|N(\sigma)B(t,\rho) + f(t,\sigma)|$. By integrating this equation on Ω and using the divergence formula, we obtain in the distribution sense :

$$\frac{d}{dt} \int_\Omega |\rho(t,X)|dX = -\int_{\partial\Omega} G(t,\sigma) \cdot \nu|\gamma\rho(t,\sigma)|d\sigma = \int_{\partial\Omega} |N(\sigma)B(t,\rho) + f(t,\sigma)| \, d\sigma$$

and thus

$$\frac{d}{dt} \int_\Omega |\rho(t,X)|dX \leq ||\beta||_\infty \int_\Omega |\rho(t,X)|dX + |f(t,\sigma)|.$$

A Gronwall lemma concludes.

• *Estimate in L^∞.* Using the proposition 5.7, we have $\tilde{\rho}_1$ and $\tilde{\rho}_2$ solving (8) and (9). By doing the changes of variables, using the definitions of $\tilde{\rho}_1$ and $\tilde{\rho}_2$ and the formulas (6), we see that

$$||\rho(t,\cdot)||_{L^1(\Omega)} = ||\tilde{\rho}_1(t,\cdot)||_{L^1(]0,t[\times\partial\Omega)} + ||\tilde{\rho}_2(t,\cdot)||_{L^1(\Omega)}, \quad \forall t > 0$$

$$||\rho||_{L^\infty(]0,T[\times\Omega)} \leq ||\tilde{\rho}_1||_{L^\infty(\widetilde{Q}_1)} ||G||_{L^\infty(\partial\Omega)} e^{T||\operatorname{div} G||_\infty} + ||\tilde{\rho}_2||_{L^\infty(]0,T[\times\Omega)} e^{T||\operatorname{div} G||_\infty}$$

But solving explicitely the equation (8), we have

$$\begin{aligned}
|\tilde{\rho}_1(t,\tau,\sigma)| = |\tilde{\rho}_1(\tau,\tau,\sigma)| &= \left| N(\sigma)\widetilde{B}(t,\tilde{\rho}_1,\tilde{\rho}_2) + f(t,\sigma) \right| \\
&\leq ||N||_\infty ||\beta||_\infty (||\tilde{\rho}_1(\tau,\cdot)||_{L^1} + ||\tilde{\rho}_2(\tau,\cdot)||_{L^1}) + ||f||_{L^\infty} \\
&\leq ||N||_\infty ||\beta||_\infty ||\rho(\tau,\cdot)||_{L^1} + ||f||_{L^\infty}
\end{aligned}$$

On the other hand, for $\tilde{\rho}_2$ we have $||\tilde{\rho}_2||_{L^\infty(]0,T[\times\Omega)} = ||\tilde{\rho}_2(0)||_{L^\infty(\Omega)} = ||\rho^0||_{L^\infty(\Omega)}$. □

Remark 5.10. *The expression* (17) *shows that in the case of a zero boundary data f, the trace $\gamma\rho$ has some extra regularity, namely it is $\mathcal{C}([0,T]; L^1(\partial\Omega))$.*

Corollary 5.11 (Uniqueness)**.** *If ρ and ρ' are two weak solutions of the problem* (1)*, then $\rho = \rho'$ almost everywhere.*

Formal adjoint problem

We place ourselves in a slightly more general framework with

$$N \in \mathcal{M}(\partial\Omega), \ f \in L^{\infty}(]0,T[;\mathcal{M}(\partial\Omega)).$$

where the space measures we use will be denoted by $\mathcal{M}$ and design the dual spaces of bounded continuous functions on the underlying set. We will denote by $<,>$ the corresponding duality products. We want to prove uniqueness of weak solutions $\rho \in L^{\infty}(]0,T[;\mathcal{M}(\Omega))$ for the following equation, which is the weak formulation of solution to problem (1) for measure data N and f : for all $\psi \in \mathcal{C}^1([0,T] \times \overline{\Omega})$ with $\psi(T,\cdot) = 0$

$$\int_0^T < \rho, \partial_t \psi + G(t,x,\theta) \cdot \nabla\psi + \beta < N, \psi_{|\partial\Omega}(t,\cdot) > dx d\theta > + < \rho^0, \psi(0,\cdot) > + \quad (18)$$

$$< f(t,\cdot), \psi_{|\partial\Omega}(t,\cdot) > dt = 0.$$

Since the equation is linear, we have to prove that if ρ satisfies the problem with zero initial and boundary data, that is : for all $\psi \in \mathcal{C}^1([0,T] \times \overline{\Omega})$ with $\psi(T,\cdot) = 0$

$$\int_0^T < \rho, \partial_t \psi + G \cdot \nabla\psi + \beta < N, \psi_{|\partial\Omega}(t,\cdot) >> dt = 0, \quad (19)$$

then $\rho = 0$. It will result from the existence of regular solutions to the adjoint problem, proven in the following proposition.

Proposition 5.12. *Let $S \in \mathcal{C}_c^1(]0,T[\times\Omega)$. We assume that $\beta \in \mathcal{C}^1(\overline{\Omega})$. Then there exists $\psi \in \mathcal{C}^1([0,T] \times \overline{\Omega})$ with $\psi(T,\cdot) = 0$ such that*

$$\begin{cases} \partial_t \psi + G(t,x,\theta) \cdot \nabla\psi + \beta(x,\theta) < N, \psi_{|\partial\Omega}(t,\cdot) >= S, & t > 0, \ (x,\theta) \in \Omega \\ \psi(T,x,\theta) = 0 \end{cases} \quad (20)$$

Proof. Using the method of characteristics to solve explicitly the problem if we assume that there exists a solution, we obtain

$$\psi(t,\Phi(t;T,y)) = - \int_T^t \beta(\Phi(s;T,y)) < N, \psi_{|\partial\Omega}(s,\cdot) > ds + \int_T^t S(s,\Phi(s;T,y)) ds.$$

If we set $\widetilde{\psi}(t,y) = \psi(t,\Phi(t;T,y))$, $\widetilde{\beta}(y) = \beta(\Phi(s;T,y))$ and $\widetilde{S}(t,y) = S(t,\Phi(t;T,y))$, we can rewrite it

$$\widetilde{\psi}(t,y) = \int_T^t \widetilde{S}(s,y) - \widetilde{\beta}(s,y) < N, \psi_{|\partial\Omega}(s,\cdot) > ds. \quad (21)$$

We have the following regularities : $\widetilde{\beta}, \widetilde{S} \in \mathcal{C}^1([0,T] \times \overline{\Omega})$ since the change of variables we use here is a diffeomorphism. We need the following compatibility condition on $\psi(t,\sigma)$ for $\sigma \in \partial\Omega$, using that $\sigma = \Phi(t;T,y) \Leftrightarrow y = \Phi(T;t,\sigma)$ and defining $y(t,\sigma) = \Phi(T;t,\sigma)$, $f(t,\sigma) := \widetilde{\psi}(t,\Phi(T;t,\sigma))$:

$$f(t,\sigma) = - \int_T^t \widetilde{\beta}(s,y(t,\sigma)) < N, f(s,\cdot) > ds + \int_T^t \widetilde{S}(s,y(t,\sigma)) ds. \quad (22)$$

Concerning regularity, notice that $y(t,\sigma) \in \mathcal{C}^1([0,T];\mathcal{C}(\partial\Omega))$ since $\partial_t(\Phi(T;t,\sigma)) = -D_y\Phi(T;t,\sigma)\circ G(t,\sigma)$.

Lemma 5.13. *Let $S \in \mathcal{C}_c^1(]0,T[\times\Omega)$ and $\beta \in \mathcal{C}^1(\overline{\Omega})$. Then there exists a solution $\overline{f} \in \mathcal{C}^1([0,T]; \mathcal{C}(\partial\Omega))$ to the integral equation* (25) *and there exists two constants $A(S,T)$ and $B(S,T)$ such that*

$$||\overline{f}||_{L^\infty(]0,T[\times\partial\Omega)} \leq T||S||_{L^\infty(]0,T[\times\Omega)} e^{T||N||_{\mathcal{M}(\partial\Omega)}||\beta||_{L^\infty(\Omega)}}. \tag{23}$$

Proof. Let $T_1 \in [0,T[$ and define the following operator :

$$\mathcal{T} : \begin{array}{ccc} \mathcal{C}([T_1,T] \times \partial\Omega) & \rightarrow & \mathcal{C}([T_1,T] \times \partial\Omega) \\ f & \mapsto & -\int_T^t \widetilde{\beta}(s,y(t,\sigma)) <N,f(s,\cdot)> ds + \int_T^t \widetilde{S}(s,y(t,\sigma))ds \end{array}$$

Then $\mathcal{T}$ is well defined in the claimed spaces and is a contraction if $(T-T_1)||\beta||_\infty||N||_{\mathcal{M}} < 1$. We use then the Banach fixed point theorem and a bootstrap argument. The announced regularity comes from formula (25). Indeed, we can compute

$$\partial_t f(t,\sigma) = \widetilde{S}(t,y(t,\sigma)) + \int_T^t \partial_y \widetilde{S}(s,y(t,\sigma))\partial_t y(t,\sigma)ds$$
$$- \widetilde{\beta}(t,y(t,\sigma)) <N,f(t,\cdot)> - \int_T^t \partial_y \widetilde{\beta}(s,y(t,\sigma))\partial_t y(t,\sigma) <N,f(s,\cdot)> ds.$$

For the σ derivative, we have

$$\partial_\sigma f(t,\sigma) = -\int_T^t \partial_y \widetilde{\beta}(s,y(t,\sigma))\partial_\sigma y(t,\sigma) <N,f(s,\cdot)> ds + \int_T^t \partial_y \widetilde{S}(s,y(t,\sigma))\partial_\sigma y(t,\sigma)ds.$$

$\diamond$ To establish (23), we use (25) to obtain, setting $\overline{f}(t) = f(T-t)$:

$$||\overline{f}(t)||_{L^\infty(\partial\Omega)} \leq ||\beta||_{L^\infty}||N||_{\mathcal{M}} \int_0^t ||\overline{f}(s)||_{L^\infty(\partial\Omega)}ds + T||S||_{L^\infty}$$

from which we get (23), using a Gronwall lemma.

$\square$

Thanks to this lemma, the formula (21) gives the function $\widetilde{\psi}$ and we also see that we have $\widetilde{\psi}(T,\cdot) = 0$ and $\widetilde{\psi} \in \mathcal{C}^1([0,T] \times \Omega)$. Now, using the inverse change of variables $\psi(t,X) = \widetilde{\psi}(t,\Phi(T;t,X))$, we get the regularity on ψ since for each $t > 0$, $X \mapsto \Phi(T;t,X)$ is a diffeomorphism. $\square$

Corollary 5.14. *The weak solution of the equation* (18) *is unique.*

Proof. Let $\rho \in L^\infty(]0,T[; \mathcal{M}(\Omega))$ solving (19) and $S \in \mathcal{C}_c^1(]0,T[\times\Omega)$. Suppose first that $\beta \in \mathcal{C}^1(\overline{\Omega})$. The previous proposition ensures that

$$\int_0^T <\rho,S> dt = 0.$$

The function S being arbitrary this implies $\rho = 0$.
For $\beta \in \mathcal{C}_b(\Omega)$ by regularization there exists a sequence $\beta_n \in \mathcal{C}^1(\overline{\Omega})$ converging to β in $\mathcal{C}_b(\Omega)$.

Let then $S \in \mathcal{C}_c^1(]0, T[\times \Omega)$. The resolution of the problem (20) with data β_n gives a function ψ_n that we put in the definition of weak solutions (18) (with data β). We get

$$\int_0^T < \rho(t, \cdot), S > dt + \int_0^T < \rho(t, \cdot), (\beta - \beta_n) >< N, \psi_{|\partial\Omega}(t, \cdot) > dt$$

Using the L^∞ estimate (23) for n large enough we have $|\psi_n(t, \sigma)| \le C$ for all $(t, \sigma) \in]0, T[\times \partial\Omega$, with C a constant independent of n. We conclude by passing to the limit in n. $\qquad\square$

Remark 5.15. *For a data $\beta \in L^\infty(\Omega)$ (in the case $N \in L^1(\partial\Omega)$ and $\rho \in L^\infty(]0, T[; L^1(\Omega)))$ the previous proof applies : by regularization we approach β by a sequence $\beta_n \in \mathcal{C}^1(\overline{\Omega})$ which converges to β for the weak-$*$ topology of $L^\infty(\Omega)$. Hence the uniqueness result also stands.*

2   Approximated solutions and application to the existence

As can be seen in the figure 2, for the parameters taken from the literature, the area where the solution is positive (characteristics coming from a part of the left edge of the square, represented in red) is very small compared to the area of the domain. A finite differences or finite volume
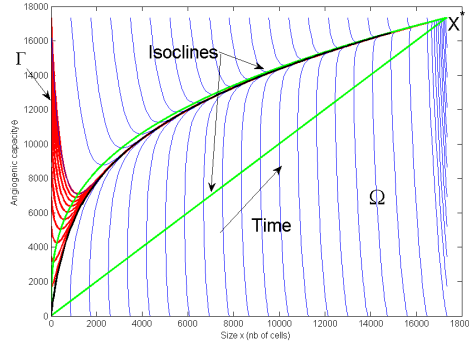
Figure 2: Phase plan of the velocity field given by (2) without treatment, i.e. with $e = h = 0$ with the parameters from [HPFH99] : $a = 0.192$, $c = 5.85$, $d = 8.73 \times 10^{-3}$. B. $a = 0.192$, $c = 0.1$, $d = 1.4923 \times 10^{-4}$

scheme written on a cartesian mesh of the square would not exploit this feature of the model and would loose a lot of time calculating the solution in areas where it is zero. Therefore, we rather use a lagrangian scheme based on discretizing the characteristics of the equation which in our framework consists in discretizing the equations (8)-(9), in view of proposition 5.7.

In this section, we build a weak solution to the equation (1). We will achieve the existence by convergence of an approximation scheme to the problem (8)-(9) where the difficulty is restricted to approximation of the boundary condition. Then we establish an error estimate in the case of more regular data and numerically illustrate the result. In order to avoid heavy notations, we forget about the tilda when referring to the problem (8)-(9).

2.1 Construction of approximated solutions of the problem (8)-(9)

Let $0 = t_0 < ... < t_k < .. < t_{K+1} = T$ be a uniform subdivision of $[0, T]$ with $t_{k+1} - t_k = \delta t$. For the equation (9), let the uniform subdivisions $1 = x_1 < ... < x_l < ... < x_{L+1} = b$ and $1 = \theta_1 < ... < \theta_m < ... < \theta_{L+1} = b$, with $x_{l+1} - x_l = \theta_{m+1} - \theta_m = \delta x$. The scheme for the equation (9) is then given by :

$$\begin{cases} \rho_2^0(l, m) = \frac{1}{(\delta x)^2} \int_{x_l}^{x_{l+1}} \int_{\theta_m}^{\theta_{m+1}} \rho^0(x, \theta) dx d\theta & 1 \le l, m \le L \\ \rho_2^{k+1}(l, m) = \rho_2^k(l, m) & 0 \le k \le K, \ 1 \le l, m \le L \end{cases} . \tag{24}$$

That is, $\rho_2^k(l, m) = \rho_2^0(l, m)$ for all k, l, m.

For the discretization of the equation (8), for each k let $0 = \tau_0 < ... < \tau_i < ... < \tau_k = t_k$ with $\tau_{i+1} - \tau_i = \delta t$. Let $\sigma : [0, 4b] \to \partial\Omega$ be defined by $\sigma(s) = \begin{cases} (1, 1+s) & s \in [0, b] \\ (1+s-b, b) & s \in [b, 2b] \\ (b, 3b-s) & s \in [2b, 3b] \\ (4b-s, b) & s \in [3b, 4b] \end{cases}$

be a parametrization of $\partial\Omega$ with $|\sigma'(s)| = 1$ a.e., so that for $g \in L^1(\partial\Omega)$ we have $\int_{\partial\Omega} g(\sigma) d\sigma = \int_0^{4b} g(\sigma(s)) ds$. Let $0 = s_1 < ... < s_j < ... < s_{M+1} = 4b$ be an uniform subdivision with $s_{j+1} - s_j = \delta\sigma$. The scheme is given by

$$\begin{cases} \rho_1^0(0, j) = N_j B^0((\rho_2^0)_{l,m}) + f_j^0 & 1 \le j \le M \\ \rho_1^{k+1}(i, j) = \rho_1^k(i, j) & 0 \le k \le K, \ 0 \le i \le k, \ 1 \le j \le M \\ \rho_1^{k+1}(k+1, j) = N_j B^{k+1}(\rho_1^{k+1}, \rho_2^{k+1}) + f_j^{k+1} & 0 \le k \le K, \ 1 \le j \le M \end{cases} \tag{25}$$

with

$$B^k(\rho_1^k, \rho_2^k) = \sum_{i=1}^{k-1} \sum_{j=1}^{M} \beta_{i,j}^1 \rho_1^k(i, j) \delta t \delta\sigma + \sum_{l,m=1}^{L} \beta_{l,m}^2 \rho_2^k(l, m) (\delta x)^2$$

meant to approximate

$$\int_0^{t_k} \int_{\partial\Omega} \beta(\Phi(t_k; \tau, \sigma)) \rho_1(t_k, \tau, \sigma) d\tau d\sigma + \int_\Omega \beta(\Phi(t_k; 0, Y)) \rho_2(t_k, Y) dY$$

and

$$\beta_{i,j}^1 := \frac{1}{\delta t \delta\sigma} \int_{\tau_i}^{\tau_{i+1}} \int_{\sigma_j}^{\sigma_{j+1}} \beta(\Phi(t_k; \tau, \sigma)) d\sigma d\tau, \quad \beta_{l,m}^2 := \int_{x_l}^{x_{l+1}} \int_{\theta_m}^{\theta_{m+1}} \beta(\Phi(t_k; 0, (x, \theta))) dx d\theta$$

$$f_j^k := \frac{1}{\delta t \delta\sigma} \int_{t_k}^{t_{k+1}} \int_{\sigma_j}^{\sigma_{j+1}} f(t, \sigma) d\sigma dt, \quad N_j := \frac{1}{\delta\sigma} \int_{\sigma_j}^{\sigma_{j+1}} N(\sigma) d\sigma. \tag{26}$$

Notice that the schemes (24) and (25) are well-posed since the definition of $\rho_1^{k+1}(k+1, j)$ involves values of $\rho_1^{k+1}(i, j)$ only with $0 \le i \le k$. We denote by $h = \delta t + \delta\sigma + \delta x$ and define now piecewise constant functions $\rho_{1,h}$ and $\rho_{2,h}$ on $\widetilde{Q}_1$ and $[0, T[\times\overline{\Omega}$ by, for $0 \le k \le K$, $1 \le i \le k$, $1 \le j \le M$ and $1 \le l, m \le L$

$$\begin{array}{ll} \rho_{1,h}(t, \tau, \sigma(s)) = \rho_1^k(i, j) & \text{for } t \in [t_k, t_{k+1}[, \ \tau \in]\tau_{i-1}, \tau_i], \ s \in [s_j, s_{j+1}[\\ \rho_{1,h}(t, \tau, \sigma(s)) = 0 & \text{for } t \in [t_k, t_{k+1}[, \ \tau \in]t_k, t], \ s \in [s_j, s_{j+1}[\\ \rho_{2,h}(t, x, \theta) = \rho_2^k(l, m) & \text{for } t \in [t_k, t_{k+1}[, \ x \in [x_l, x_{l+1}[, \ \theta \in [\theta_m, \theta_{m+1}[. \end{array} \tag{27}$$

See the figure 3 for an illustration. Notice that we have
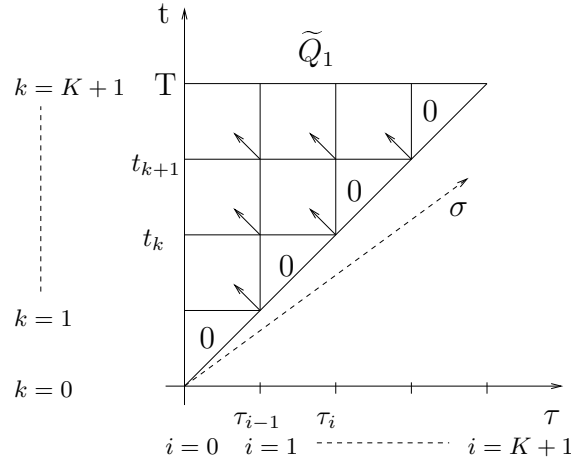
Figure 3: Description of the discretization grid for $\widetilde{Q}_1$, only in the (τ, t) plane. The arrows indicate the index used in assigning values to $\rho_{1,h}$ in each mesh (formula (27)).

$$||\rho_{1,h}(t_k, \cdot)||_{L^1(]0,t_k[\times \partial\Omega)} = \sum_{i=1}^{k} \sum_{j=1}^{M} \left| \rho_1^k(i,j) \right| \delta t \delta\sigma, \ ||\rho_{2,h}(t_k, \cdot)||_{L^1(\Omega)} = \sum_{l,m=1}^{M} \left| \rho_2^k(l,m) \right| (\delta x)^2. \quad (28)$$

Remark 5.16.

    • *We take the same discretization step in x and θ for ρ_2 but it would work the same with two different steps.*

    • *For more regular data, we could take point values instead of* (26).

    • *It will be clear from the following that the scheme would converge the same regardless to the value that we give to $\rho_1^0(0, j)$.*

2.2   Discrete *a priori* estimates

We prove the equivalent of the proposition 5.9 in the discrete case. Notice that there exists a constant C_σ such that $\sum_{j=1}^{M} N_j \delta\sigma \le \int_{\partial\Omega} N(\sigma) d\sigma + C_\sigma \delta\sigma = 1 + C_\sigma \delta\sigma := ||N||_h$ and $\sum_{j=1}^{M} f_j^{k+1} \delta\sigma \le ||f||_{L^\infty(]0,T[;L^1(\partial\Omega))} + C_\sigma \delta\sigma := ||f||_h$.

Proposition 5.17 (Discrete *a priori* estimates)**.** *Let $\left(\rho_1^k(i,j) \right)_{k,i,j}$ and $\left(\rho_2^k(l,m) \right)_{k,l,m}$ be given by* (24) *and* (25) *respectively. Then for all k*

$$||\rho_{2,h}(t_k, \cdot)||_{L^1(\Omega)} = ||\rho^0||_{L^1(\Omega)}, \quad ||\rho_{2,h}||_{L^\infty(]0,T[\times\Omega)} = ||\rho^0||_{L^\infty(\Omega)}$$

$$||\rho_{1,h}(t_k, \cdot)||_{L^1(]0,t_k[\times\partial\Omega)} \le e^{t_k ||\beta||_{L^\infty} ||N||_h} \left\{ ||\rho^0||_{L^1(\Omega)} + \frac{||f||_h}{||\beta||_{L^\infty} ||N||_h} \right\}, \quad (29)$$

$$||\rho_{1,h}||_{L^\infty(\widetilde{Q}_1)} \le ||N||_{L^\infty} ||\beta||_{L^\infty} \max_k \left(||\rho_{1,h}(t_k, \cdot)||_{L^1} + ||\rho^0||_{L^1} \right) + ||f||_{L^\infty}. \quad (30)$$

Moreover, if $\rho^0 \ge 0$ then $\rho_1^k(i,j), \rho_2^k(l,m) \ge 0$ for all k,i,j,l,m.

Proof. The non-negativity of the scheme is straightforward from the definition. The estimate for $\rho_{2,h}$ follows directly from the scheme (25). For the L^1 estimate on $\rho_{1,h}$ we compute, using the scheme (24)

$$
\begin{aligned}
||\rho_{1,h}(t_{k+1},\cdot)||_{L^1(]0,t_{k+1}[\times\partial\Omega)} &= \sum_{i=1}^{k+1}\sum_{j=1}^{M}\left|\rho^{k+1}(i,j)\right|\delta t\delta\sigma \\
&= \sum_{i=1}^{k}\sum_{j=1}^{M}\left|\rho^{k}(i,j)\right|\delta t\delta\sigma + \left|B^{k+1}(\rho_1^{k+1},\rho_2^{k+1})\right|\delta t\sum_{j=1}^{M}N_j\delta\sigma + \delta t\sum_{j=1}^{M}\left|f_j^{k+1}\right|\delta\sigma \\
&\leq ||\rho_{1,h}(t_k)||_{L^1(]0,t_k[\times\partial\Omega)} + \left|B^{k+1}(\rho_1^{k+1},\rho_2^{k+1})\right|\delta t||N||_h + \delta t||f||_h
\end{aligned}
$$

Now from the expression of $B^{k+1}(\rho_1^{k+1},\rho_2^{k+1})$

$$
\left|B^{k+1}(\rho_1^{k+1},\rho_2^{k+1})\right| \leq ||\beta||_{L^\infty}||\rho_{1,h}(t_k,\cdot)||_{L^1} + ||\beta||_{L^\infty}||\rho_{2,h}(t_k,\cdot)||_{L^1}.
$$

Thus we obtain

$$
||\rho_{1,h}(t_{k+1},\cdot)||_{L^1} \leq (1 + ||\beta||_{L^\infty}\delta t||N||_h)\,||\rho_{1,h}(t_k,\cdot)||_{L^1} + ||\beta||_{L^\infty}\delta t||N||_h||\rho_{2,h}(t_k,\cdot)||_{L^1} + \delta t||f||_h
$$

Now using a discrete Gronwall lemma we obtain

$$
||\rho_{1,h}(t_{k+1},\cdot)||_{L^1} \leq e^{||\beta||_{L^\infty}||N||_h t_k}\left\{||\rho_{1,h}(t_0,\cdot)||_{L^1} + \frac{||\beta||_{L^\infty}||N||_h||\rho_{2,h}(t_k,\cdot)||_{L^1} + ||f||_h}{||\beta||_{L^\infty}||N||_h}\right\}
$$

Using $||\rho_{1,h}(t_0,\cdot)||_{L^1} = 0$ and $||\rho_{2,h}(t_k,\cdot)||_{L^1(\Omega)} = ||\rho^0||_{L^1(\Omega)}$ ends the proof of the L^1 estimate. For the L^∞ estimate, we remark that

$$
\begin{aligned}
||\rho_{1,h}||_{L^\infty(\widetilde{Q}_1)} &= \max_k\max_{i,j}|\rho_1^k(i,j)| = \max_k\max_j\left(\left|B^k(\rho_1^k,\rho_2^k)N_j + f_j^k\right|\right) \leq ||N||_{L^\infty}\max_k\left|B^k(\rho_1^k,\rho_2^k)\right| + ||f||_{L^\infty} \\
&\leq ||N||_{L^\infty}||\beta||_{L^\infty}\max_k\left(||\rho_{1,h}(t_k,\cdot)||_{L^1} + ||\rho_{2,h}(t_k,\cdot)||_{L^1}\right) + ||f||_{L^\infty}.
\end{aligned}
$$

$\square$

2.3   Application to existence of solutions to the continuous problem (8)-(9)

Theorem 5.18 (Existence)**.** *Under the assumptions* (4)*, there exists* $\rho_1 \in L^\infty(\widetilde{Q}_1)$ *and* $\rho_2 \in L^\infty(]0,T[\times\Omega)$ *such that* $\rho_{1,h} \underset{h\to0}{\rightharpoonup} \rho_1$ *and* $\rho_{2,h} \underset{h\to0}{\rightharpoonup} \rho_2$ *for the weak-∗ topology of* L^∞*. Furthermore,* (ρ_1,ρ_2) *is the unique weak solution of* (8)-(9)*.*

Proof. Uniqueness of the solution is straightforward for the problem (9) and for the problem (8) it follows from the L^1 estimate on ρ_1 which can be derived following the proof of the proposition 5.9. The proof for the existence is rather classical and consists in passing to the limit in discrete weak formulations of (8) and (9). From the previous proposition, we obtain that the families $\{\rho_{1,h}\}_{\delta t,\delta\sigma}$ and $\{\rho_{2,h}\}_{\delta t,\delta x}$ are bounded in L^∞ and thus there exist $\rho_1 \in L^\infty(\widetilde{Q}_1)$, $\rho_2 \in L^\infty(]0,T[\times\Omega)$ and some subsequences ρ_{1,h_n} and ρ_{2,h_n} such that $\rho_{1,h_n} \underset{h_n\to0}{\rightharpoonup} \rho_1$ and $\rho_{2,h_n} \underset{h_n\to0}{\rightharpoonup} \rho_2$ for the weak-∗ topology of L^∞. We have to prove now that (ρ_1,ρ_2) is a weak solution of

(8)-(9). The uniqueness of solutions to the equation implies then by a standard argument that the whole sequence converges. It remains to prove that (ρ_1, ρ_2) solves (8)-(9).

• *The function ρ_2 is a weak solution of (9).* Let ϕ_2 be a test function for (9). We have

$$\int_0^T \int_\Omega \rho_{2,h_n}(t,Y)\partial_t\phi_2(t,Y)dYdt = \sum_{k=0}^K \sum_{l,m=1}^L \rho_2^k(l,m) \int_{t_k}^{t_{k+1}} \int_{x_l}^{x_{l+1}} \int_{\theta_m}^{\theta_{m+1}} \partial_t\phi_2(t,x,\theta)d\theta dxdt$$

$$= \sum_{k=0}^K \sum_{l,m=1}^L \rho_2^k(l,m)\Phi_2(t_{k+1},l,m)(\delta x)^2 - \sum_{k=0}^K \sum_{l,m=1}^L \rho_2^k(l,m)\Phi_2(t_k,l,m)(\delta x)^2$$

where we denoted $\Phi_2(t_k,l,m) := \frac{1}{(\delta x)^2}\int_{x_l}^{x_{l+1}}\int_{\theta_m}^{\theta_{m+1}}\phi_2(t_k,x,\theta)d\theta dx$. Using the scheme ($\rho_2^k(l,m)$ is constant in k) and $\Phi_2(t_{K+1},l,m) = 0$ since $t_{K+1} = T$, we obtain

$$\int_0^T \int_\Omega \rho_{2,h_n}(t,Y)\partial_t\phi_2(t,Y)dYdt = \sum_{l,m=1}^L \rho_2^K(l,m)\Phi_2(T,l,m)(\delta x)^2 - \sum_{l,m=1}^L \rho_2^0(l,m)\Phi_2(0,l,m)(\delta x)^2$$

$$= - \sum_{l,m=1}^L \rho_2^0(l,m)\Phi_2(0,l,m)(\delta x)^2 = -\int_\Omega \rho_{2,h_n}^0(Y)\phi(0,Y) \xrightarrow[h_n \to 0]{} -\int_\Omega \rho^0(Y)\phi(0,Y)dY$$

since $\rho_{2,h_n}^0 \xrightarrow[h_n \to 0]{L^1} \rho^0$. Observing that the left hand side converges to $\int_0^T \int_\Omega \rho_2 \partial_t\phi_2(t,Y)dYdt$ gives the result.

• *The function ρ_1 is a weak solution of (8).* Let ϕ_1 be a test function for (8). Then the same calculation as above shows, with $\Phi_1(t_k,i,j) := \frac{1}{\delta t \delta\sigma}\int_{\tau_{i-1}}^{\tau_i}\int_{\sigma_j}^{\sigma_{j+1}}\phi_1(t_k,\tau,\sigma)d\sigma d\tau$ and using that $\Phi_1(t_{K+1},i,j) = 0$ as well as $\rho_1^{k+1}(i,j) = \rho_1^k(i,j)$ for $1 \le i \le k$ and $1 \le j \le M$

$$\int_{\widetilde{Q}_1} \rho_{1,h_n}(t,\tau,\sigma)\partial_t\phi_1(t,\tau,\sigma)d\sigma d\tau dt = \sum_{k=1}^K \sum_{i=1}^k \sum_{j=1}^M \rho_1^k(i,j)\Phi_1(t_{k+1},i,j)\delta t\delta\sigma - \sum_{k=1}^K \sum_{i=1}^k \sum_{j=1}^M \rho_1^k(i,j)\Phi_1(t_k,i,j)\delta t\delta\sigma$$

$$= \sum_{i=1}^K \sum_{j=1}^M \rho_1^K(i,j)\Phi_1(t_{K+1},i,j)\delta t\delta\sigma + \sum_{k=1}^{K-1}\sum_{i=1}^k \sum_{j=1}^M \rho_1^k(i,j)\Phi_1(t_{k+1},i,j)\delta t\delta\sigma$$

$$- \sum_{k=1}^{K-1}\sum_{i=1}^{k+1}\sum_{j=1}^M \rho_1^{k+1}(i,j)\Phi_1(t_{k+1},i,j)\delta t\delta\sigma - \sum_{j=1}^M \rho_1^1(1,j)\Phi_1(t_1,1,j)\delta t\delta\sigma$$

$$= - \sum_{k=1}^{K-1}\sum_{j=1}^M \rho_1^{k+1}(k+1,j)\Phi_1(t_{k+1},k+1,j)\delta t\delta\sigma - \sum_{j=1}^M \rho_1^1(1,j)\Phi_1(t_1,1,j)\delta t\delta\sigma$$

$$= - \sum_{k=1}^K \sum_{j=1}^M \left(N_j B^k(\rho_1^k,\rho_2^k) + f_j^k\right)\Phi_1(t_k,k,j)\delta t\delta\sigma$$

Defining the following piecewise constant functions : $B_h(t,\rho_{1,h},\rho_{2,h}) = B^k(\rho_1^k,\rho_2^k)$, $N_h(\sigma(s)) = N_j$, $f_h(t,\sigma(s)) = f_j^k$ and $\Phi_{1,h}(t,\sigma(s)) = \Phi_1(t_k,k,j)$ on $[t_k,t_{k+1}[\times[s_j,s_{j+1}[$, the previous equality reads

$$\int_{\widetilde{Q}_1} \rho_{1,h_n}(t,\tau,\sigma)\partial_t\phi_1(t,\tau,\sigma)d\sigma d\tau dt = \int_{\delta t}^T \int_{\partial\Omega}(B_{h_n}(t,\rho_{1,h_n},\rho_{2,h_n})N_{h_n}(\sigma) + f_{h_n}(t,\sigma))\Phi_{1,h_n}(t,\sigma)d\sigma dt.$$

We need the following lemma in order to conclude.

Lemma 5.19. *We have*

$$B_{h_n}(t, \rho_{1,h_n}, \rho_{2,h_n}) \underset{h_n \to 0}{\rightharpoonup} \widetilde{B}(t, \rho_1, \rho_2) \quad * - L^\infty(]0, T[).$$

Proof. We define the piecewise constant function $\beta_h^1(\tau, \sigma)$ as for N_h and f_h and $\beta_h^2(X) = \beta_{l,m}^2$ for $X \in [x_l, x_{l+1}[\times [\theta_m, \theta_{m+1}[$. Let $t \in [t_k, t_{k+1}[$, then

$$B_h(t, \rho_{1,h}, \rho_{2,h}) = B^k(\rho_1^k, \rho_2^k) = \int_0^t \int_{\partial\Omega} \beta_h^1(\tau, \sigma)\rho_{1,h}(t, \tau, \sigma)d\tau d\sigma - \sum_{j=1}^M \beta_{k,j}^1 \rho_1^k(k, j)\delta t \delta\sigma + \sum_{l,m=1}^L \beta_{l,m}^2 \rho_2^k(l, m)(\delta x)^2$$

since we defined $\rho_h(t, \tau, \sigma) = 0$ for $\tau \in]t_k, t]$. Thus, for $\psi \in L^1(]0, T[)$ we have

$$\int_0^T B_h(t, \rho_{1,h}, \rho_{2,h})\psi(t)dt = \int_0^T \int_0^t \int_{\partial\Omega} \beta_h^1(\tau, \sigma)\rho_{1,h}(t, \tau, \sigma)\psi(t)d\sigma d\tau dt$$

$$- \delta t \sum_{k=0}^K \sum_{j=1}^M \beta_{k,j}^1 \rho_1^k(k, j) \int_{t_k}^{t_{k+1}} \psi(t)dt\delta\sigma$$

$$+ \int_0^T \int_\Omega \beta_h^2(X)\rho_{2,h}(t, X)\psi(t)dXdt$$

and we obtain the result by using $\rho_{1,h_n} \underset{h_n \to 0}{\rightharpoonup} \rho_1 \ * -L^\infty$, $\rho_{2,h_n} \underset{h_n \to 0}{\rightharpoonup} \rho_2 \ * -L^\infty$, $\beta_{h_n} \xrightarrow[h_n \to 0]{L^1} \beta$, $||\beta_{h_n}||_{L^\infty} \leq C$ and noticing that the second term goes to zero in view of the L^∞ bounds on $\rho_{1,h}$ (proposition 5.17) and β. $\qquad \square$

Using the lemma as well as $N_{h_n}, f_{h_n} \underset{h_n \to 0}{\rightharpoonup} N, f \ * -L^\infty$, $||N_{h_n}||_{L^\infty} \leq C$ and $\Phi_{1,h_n} \xrightarrow[h_n \to 0]{\mathcal{C}([0,T] \times \partial\Omega)} \phi(t, t, \sigma)$, the previous calculations give

$$\int_{\widetilde{Q}_1} \rho_{1,h_n}(t, \tau, \sigma)\partial_t \phi_1(t, \tau, \sigma)d\sigma d\tau dt \xrightarrow[h \to 0]{} -\int_0^T \int_{\partial\Omega} \left\{ N(\sigma)\widetilde{B}(t, \rho_1, \rho_2) + f(t, \sigma) \right\} \phi(t, t, \sigma)d\sigma dt.$$

On the other hand the left hand side also goes to $\int_{\widetilde{Q}_1} \widetilde{\rho}_1(t, \tau, \sigma)\partial_t \phi_1(t, \tau, \sigma)d\sigma d\tau dt$. This proves that ρ_1 verifies the definition 5.5 and ends the proof. $\qquad \square$

3 Error estimate

3.1 Error estimate for the problem (8)-(9)

We establish now an error estimate for the approximation of the equations (8)-(9). For this section, we make the following assumptions on the data :

$$\rho^0 \in W^{1,\infty}(\Omega), \ \beta \in W^{1,\infty}(\Omega), \ N \in W^{1,\infty}(\partial\Omega), \ N \geq 0, \ \int_{\partial\Omega} N(\sigma)d\sigma = 1, \ f \in W^{1,\infty}(]0, T[\times \partial\Omega). \tag{31}$$

It can be noticed that in order to perform the weak convergence of the approximated solutions and establish theoretical existence to the continuous problem, we did not need to approximate

the characteristics $\Phi(t; \tau, \sigma)$ of the equation. In view of the error estimate though, we need to use another approximation of $\beta(\Phi(t; \tau, \sigma))$ than (26). We introduce an approximation $\Phi_h(t; \tau, \sigma)$ of the characteristics given by a numerical integrator of the ODE system (2) and define

$$
\begin{aligned}
\beta^1_{i,j} &:= \beta(\Phi_h(t_k; \tau_i, \sigma_j)), \ \beta^2_{l,m} := \beta(\Phi_h(t_k; 0, (x_l, \theta_m))) \\
f^k_j &:= f(t_k, \sigma_j), \ N_j := N(\sigma_j).
\end{aligned}
\tag{32}
$$

For g_1 and g_2 being two continuous functions on $\widetilde{Q}_1$ and $]0, T[\times \Omega$ respectively, we define

$$
\begin{array}{ll}
\mathbb{P}_1 g_1(t, \tau, \sigma(s)) = g_1(t_k, \tau_i, \sigma_j) & \text{for } t \in [t_k, t_{k+1}[, \ \tau \in]\tau_{i-1}, \tau_i], \ s \in [s_j, s_{j+1}[\\
\mathbb{P}_1 g_1(t, \tau, \sigma(s)) = 0 & \text{for } t \in [t_k, t_{k+1}[, \ \tau \in]t_k, t], \ s \in [s_j, s_{j+1}[\\
\mathbb{P}_2 g_2(t, x, \theta) = g_2(t_k, x_l, \theta_m) & \text{for } t \in [t_k, t_{k+1}[, \ x \in]x_l, x_{l+1}], \ \theta \in [\theta_m, \theta_{m+1}[
\end{array}
\ .
$$

Lemma 5.20 (Projection error). *Let $(g_1, g_2) \in W^{1,\infty}(\widetilde{Q}_1) \times W^{1,\infty}(]0, T[\times \Omega)$. Then there exists $C_{\mathbb{P}_1}$ and $C_{\mathbb{P}_2}$ such that*

$$
||g_1(t_k, \cdot) - \mathbb{P}_1 g_1(t_k, \cdot)||_{L^\infty(]0, t_k[)} \leq C_{\mathbb{P}_1} h, \quad ||g_2(t_k, \cdot) - \mathbb{P}_2 g_2(t_k, \cdot)||_{L^\infty(\Omega)} \leq C_{\mathbb{P}_2} h.
\tag{33}
$$

The proof of this lemma is straightforward from the fact that g_1 and g_2 are Lipschitz continuous. We define

$$
e_{1,h} := \rho_{1,h} - \mathbb{P}_1 \widetilde{\rho}_1 \text{ and } e_{2,h} := \rho_{2,h} - \mathbb{P}_2 \widetilde{\rho}_2
\tag{34}
$$

the errors of the schemes, with $(\widetilde{\rho}_1, \widetilde{\rho}_2)$ solving the problem (8)-(9). From the equation (9) we have

$$
\begin{cases}
\widetilde{\rho}_1(t_{k+1}, \tau_i, \sigma_j) = \widetilde{\rho}_1(t_k, \tau_i, \sigma_j) & 0 \leq k \leq K, \ 0 \leq i \leq k, \ 1 \leq j \leq M \\
\widetilde{\rho}_1(\tau_{k+1}, \tau_{k+1}, \sigma_j) = N(\sigma_j) \widetilde{B}(\tau_{k+1}, \widetilde{\rho}_1, \widetilde{\rho}_2) + f(\tau_{k+1}, \sigma_j) & 0 \leq k \leq K, \ 1 \leq j \leq M
\end{cases}
$$

and thus, subtracting this to (24) and denoting $e^k_1(i, j) = e_{1,h}(t_k, \tau_i, \sigma_j)$ we obtain

$$
\begin{cases}
e^{k+1}_1(i, j) = e^k_1(i, j), & 0 \leq k \leq K, \ 0 \leq i \leq k, \ 1 \leq j \leq M \\
e^{k+1}_1(k+1, j) = N_j E^{k+1} + r^{k+1}_j
\end{cases}
\tag{35}
$$

with

$$
\begin{aligned}
E^{k+1} &= \sum_{i=1}^{k} \sum_{j=1}^{M} \beta^1_{i,j} e^{k+1}_1(i, j) \delta t \delta \sigma + \sum_{l,m=1}^{L} \beta^2_{l,m} e^{k+1}_2(l, m) (\delta x)^2 \\
r^{k+1}_j &= N_j \left(B^{k+1} \left((\widetilde{\rho}_1(t_{k+1}, \tau_i, \sigma_j))_{i,j}, (\widetilde{\rho}_2(t_{k+1}, x_l, \theta_m))_{l,m} \right) - \widetilde{B}(t_{k+1}, \widetilde{\rho}_1, \widetilde{\rho}_2) \right).
\end{aligned}
$$

Hence the truncation error of the scheme r^{k+1}_j only comes from the quadrature error of the approximation of the integral in $\widetilde{B}(t_k, \widetilde{\rho}_1, \widetilde{\rho}_2)$.

Lemma 5.21 (Truncation error). *Assume (31), that $(\beta \circ \Phi_1) \widetilde{\rho}_1 \in W^{1,\infty}(\widetilde{Q}_1)$, $(\beta \circ \Phi_2) \widetilde{\rho}_2 \in W^{1,\infty}(]0, T[\times \Omega)$ and that the numerical integrator for the ODE system (2) is of order at least 1. Then there exists C_r such that*

$$
\max_{k,j} |r^k_j| \leq C_r h.
$$

Proof. We have

$$r_j^k = N_j[\sum_{i=1}^{k-1} \sum_{j=1}^{M} \left(\beta_{i,j}^1 - \beta(\Phi_1(t_k; \tau_i, \sigma_j))\right) \widetilde{\rho}_1(t_k, \tau_i, \sigma_j)\delta t \delta \sigma + \sum_{l,m=1}^{L} \left(\beta_{l,m}^2 - \beta(\Phi_2(t_k; x_l, \theta_m))\right) \widetilde{\rho}_2(t_k, x_l, \theta_m) (\delta x)^2$$

$$+ \sum_{i=1}^{k-1} \sum_{j=1}^{M} \beta(\Phi_1(t_k; \tau_i, \sigma_j))\widetilde{\rho}_1(t_k, \tau, \sigma)\delta t \delta \sigma + \sum_{l,m=1}^{L} \beta(\Phi_2(t_k; x_l, \theta_m))\widetilde{\rho}_2(t_k, x_l, \theta_m) (\delta x)^2$$

$$- \int_0^{t_{k-1}} \int_{\partial\Omega} \beta(\Phi_1(t_k; \tau, \sigma))\widetilde{\rho}_1(t_k, \tau, \sigma)d\tau d\sigma - \int_{\Omega} \beta(\Phi_2(t_k, Y))\widetilde{\rho}_2(t_k, Y)dY$$

$$- \int_{t_{k-1}}^{t_k} \int_{\partial\Omega} \beta(\Phi_1(t_k; \tau, \sigma))\widetilde{\rho}_1(t_k, \tau, \sigma)d\tau d\sigma].$$

Thus

$$\left|r_j^k\right| \leq ||N||_{L^\infty}\{||\beta||_{W^{1,\infty}} (||\Phi_{1,h} - \mathbb{P}_1\Phi_1||_{L^\infty}||\mathbb{P}_1\widetilde{\rho}_1||_{L^1} + ||\Phi_{2,h} - \mathbb{P}_2\Phi_2||_{L^\infty}||\mathbb{P}_2\widetilde{\rho}_2||_{L^1})$$

$$+ \sum_{i=1}^{k-1} \sum_{j=1}^{M} \int_{\tau_{i-1}}^{\tau_i} \int_{\sigma_j}^{\sigma_{j+1}} |\mathbb{P}_1\left[(\beta \circ \Phi_1) \widetilde{\rho}_1\right](t_k, \tau, \sigma) - (\beta \circ \Phi_1) \widetilde{\rho}_1(t_k, \tau, \sigma)| \, d\tau d\sigma$$

$$+ \sum_{l,m=1}^{L} \int_{x_l}^{x_{l+1}} \int_{x_m}^{x_{m+1}} |\mathbb{P}_2\left[(\beta \circ \Phi_2) \widetilde{\rho}_2\right](t_k, Y) - (\beta \circ \Phi_2) \widetilde{\rho}_2(t_k, x, \theta)| \, dxd\theta + ||(\beta \circ \Phi_1) \widetilde{\rho}_1||_{L^\infty} h\}.$$

Using the lemma 5.20 and the L^1 a priori estimate of proposition 5.9 gives the result. $\square$

Remark 5.22 (Order of the truncation error). *In order to have a better order for the truncation error we could use a more sophisticated quadrature method like for instance the trapezoid method on Ω for $\widetilde{\rho}_2$ and on $[0, t_{k-1}[\times\partial\Omega$ for $\widetilde{\rho}_1$ (completed by a left rectangle method on $[t_{k-1}, t_k[\times\partial\Omega)$. Adapting the previous proof shows that if the numerical integrator used for the characteristics has order larger than 2, then the truncation error would have order 2 (order of the trapezoid method).*

Proposition 5.23 (Error estimate). *Assume (31) and that $(\widetilde{\rho}_1, \widetilde{\rho}_2) \in W^{1,\infty}(\widetilde{Q}_1) \times W^{1,\infty}(]0, T[\times\Omega)$ is a regular solution of (8)-(9). Let $\rho_{1,h}$ and $\rho_{2,h}$ solve (24) and (25). Then there exists some constants $\widetilde{C}_1$ and $\widetilde{C}_2$ such that*

$$||\rho_{1,h}(t_k, \cdot) - \widetilde{\rho}_1(t_k, \cdot)||_{L^1(]0,t_k[\times\partial\Omega)} \leq \widetilde{C}_1 h, \quad ||\rho_{2,h}(t_k, \cdot) - \widetilde{\rho}_2(t_k, \cdot)||_{L^1(\Omega)} \leq \widetilde{C}_2 h \qquad (36)$$

Proof. In view of the lemma 5.20, it is sufficient to prove the proposition with $\mathbb{P}_s\widetilde{\rho}_s(t_k, \cdot)$ instead of $\widetilde{\rho}_s(t_k, \cdot)$ (with $s = 1, 2$). For the second estimate, we notice that

$$||\rho_{2,h}(t_k, \cdot) - \mathbb{P}_2\widetilde{\rho}_2(t_k, \cdot)||_{L^1(\Omega)} = ||e_{2,h}(t_k, \cdot)||_{L^1(\Omega)} = \sum_{l,m} \left|e_2^k(l, m)\right| (\delta x)^2 = \sum_{l,m} \left|\rho_2^0(l, m) - \rho^0(x_l, \theta_m)\right| (\delta x)^2$$

and the result follows from the definition of $\rho_2^0(l, m)$. For the first one, we have

$$||\rho_{1,h}(t_k, \cdot) - \mathbb{P}_1\widetilde{\rho}_1(t_k, \cdot)||_{L^1(]0,t_k[\times\partial\Omega)} = ||e_{1,h}(t_k, \cdot)||_{L^1(]0,t_k[\times\partial\Omega)} = \sum_{i=1}^{k} \sum_{j=1}^{M} \left|e_1^k(i, j)\right| \delta t \delta \sigma.$$

We can compute, using (35)

$$||e_{1,h}(t_{k+1},\cdot)||_{L^1} \leq \sum_{i=1}^{k}\sum_{j=1}^{M}\left|e_1^{k+1}(i,j)\right|\delta t\delta\sigma + \left|E^{k+1}\right|\delta t\sum_{j=1}^{M}N_j\delta\sigma + \delta t\sum_{j=1}^{M}\left|r_j^{k+1}\right|\delta\sigma$$

$$\leq ||e_{1,h}(t_k,\cdot)||_{L^1} + \delta t||\beta||_\infty||N||_h\left\{||e_{1,h}(t_k,\cdot)||_{L^1} + ||e_{2,h}(t_{k+1},\cdot)||_{L^1}\right\} + C_r h\delta t$$

$$\leq (1 + \delta t||\beta||_\infty||N||_h)||e_{1,h}(t_k,\cdot)||_{L^1} + \widetilde{C}_2||\beta||_\infty||N||_h h\delta t + C_r h\delta t$$

and conclude using a discrete Gronwall lemma. $\qquad\square$

Remark 5.24 (Order of the error)**.**

   • *By looking more carefully at the propagation of errors in the proof, we see that if we set $\rho_2^0(l,m) = \rho^0(l,m)$ (which is valid under (31)), the error on $\widetilde{\rho}_2$ only comes from the projection error.*

   • *If in addition, we follow the remark 5.22 for the approximation of the data, then the error between $\rho_{1,h}$ and $\mathbb{P}_1\widetilde{\rho}_1$ would be of order 2 if we had used a trapezoid method for the integral term in $\widetilde{B}(t_k,\widetilde{\rho}_1,\widetilde{\rho}_2)$.*

3.2   Application to approximation of problem (1)

We explain now how we approximate the solution of (1) from the approximation of the solutions of problems (8)-(9) given by the schemes (24)-(25). We translate formula (12) at the discrete level thanks to $\widetilde{\rho}_{1,h}$, $\widetilde{\rho}_{2,h}$ given by (27) and the solutions $\widetilde{\rho}_1^k(i,j)$, $\widetilde{\rho}_2^k(i,j)$ of the schemes (24) and (25) to define

$$\rho_h(t,X) := \underbrace{\widetilde{\rho}_{1,h}(t,\tau^t(X),\sigma^t(X))J_{1,h}^{-1}(t,\tau^t(X),\sigma^t(X))\mathbf{1}_{X\in\Omega_1^t}}_{:=\rho_{1,h}} + \underbrace{\widetilde{\rho}_{2,h}(t,Y(X))J_{2,h}^{-1}(t,Y(X))\mathbf{1}_{X\in\Omega_2^t}}_{:=\rho_{2,h}}.$$
$$\tag{37}$$

The jacobians of the changes of variables $J_1(t;\tau,\sigma) = |G(\tau,\sigma)\cdot\nu(\sigma)|e^{\int_\tau^t \mathrm{div}\, G(u,\Phi(u;\tau,\sigma))du}$ and $J_2(t;Y) = e^{\int_0^t \mathrm{div}\, G(u,\Phi(u;0,Y))du}$ are approximated respectively by $J_{1,h}$ and $J_{2,h}$, piecewise constant functions constructed similarly as in (27) through $J_1^k(i,j) := e^{\mathcal{T}_1(k,i,j)}$ and $J_2^k(l,m) := e^{\mathcal{T}_2(k,l,m)}$, where $\mathcal{T}_1$ and $\mathcal{T}_2$ are one-dimensional quadrature methods such that $\mathcal{T}_1(k,i,j) \simeq \int_{\tau_i}^{t_k} \mathrm{div}G(\Phi(s;\tau_i,\sigma_j))ds$ and $\mathcal{T}_2(k,l,m) \simeq \int_0^{t_k} \mathrm{div}G(\Phi(s;0,(x_l,\theta_m)))ds$. The errors of these quadrature methods are denoted by r_1, r_2 and are assumed to be of order α_1, α_2 :

$$\overline{r_1} := \max_{k,i,j}|r_1(k,i,j)| \leq C_q(\delta t)^{\alpha_1}, \ \overline{r_2} := \max_{k,l,m}|r_2(k,l,m)| \leq C_q(\delta t)^{\alpha_2}.$$

We have

$$J_1^k(i,j) = J_1(t_k,\tau_i,\sigma_j)e^{-r_1(k,i,j)}, \ J_2^k(l,m) := e^{\mathcal{T}_2(k,l,m)} = J_2(t_k,x_l,\theta_m)e^{-r_2(k,l,m)}. \tag{38}$$

We define the following meshes :

$$V_1(k,i,j) = \{(t,\Phi(t;\tau,\sigma(s))); \ t\in[t_k,t_{k+1}[, \ \tau\in]\tau_{i-1},\tau_i], \ s\in[s_j,s_{j+1}[\}$$
$$V_2(k,l,m) = \{(t,\Phi(t;0,(x_l,\theta_m))); \ t\in[t_k,t_{k+1}[, \ x\in[x_l,x_{l+1}[, \ \theta\in[\theta_m,\theta_{m+1}[\}$$

and, for a function $g\in\mathcal{C}([0,T]\times\overline{\Omega})$

$$\mathbb{P}g(t,X) = g(t_k,\Phi(t_k;\tau_i,\sigma_j))\mathbf{1}_{(t,X)\in V_1(k,i,j)} + g(t_k,\Phi(t_k;0,(x_l,\theta_m)))\mathbf{1}_{(t,X)\in V_2(k,l,m)}. \tag{39}$$

Remark 5.25. *In the same way as the lemma 5.20, there exists a constant $C_\mathbb{P}$ such that for all function $g \in W^{1,\infty}(]0,T[\times\Omega)$*

$$||g - \mathbb{P}g||_{L^1(]0,T[\times\Omega)} \leq C_\mathbb{P}h.$$

Theorem 5.26. *Suppose that $\rho \in W^{1,\infty}(]0,T[\times\Omega)$ solves the problem (1) and let ρ_h be defined by (37). Then there exists a constant C such that*

$$\sup_{t\in[0,T]} ||\rho_h(t,\cdot) - \rho(t,\cdot)||_{L^1(\Omega)} \leq Ch.$$

Proof. In view of the remark 5.25, it is again sufficient to prove the proposition with $\mathbb{P}\rho$ instead of ρ. Let $t \in [t_k, t_{k+1}[$, then $||\rho_h(t,\cdot) - \mathbb{P}\rho(t,\cdot)||_{L^1(\Omega)} = ||\rho_{1,h}(t_k,\cdot) - \mathbb{P}\rho_1(t_k,\cdot)||_{L^1(\Omega_1^{t_k})} + ||\rho_{2,h}(t_k,\cdot) - \mathbb{P}\rho_2(t_k,\cdot)||_{L^1(\Omega_2^{t_k})}$ with $\rho_s(t,X) := \rho(t,X)\mathbf{1}_{X\in\Omega_s^t}$ $(s = 1,2)$. We do the proof only for ρ_1 since it is similar for ρ_2. We also don't write the dependency in σ in order to avoid heavy notations. To obtain the complete proof it suffices to add integrals with respect to σ in the following and σ in all the functions. Doing the change of variables Φ_1 we have, noticing that $\mathbb{P}\rho_1(t_k, \Phi(t_k;\tau)) = \mathbb{P}_1\widetilde{\rho}_1(t_k,\tau)\mathbb{P}_1 J_1^{-1}(t_k,\tau)$

$$||\rho_{1,h}(t_k,\cdot) - \mathbb{P}\rho_1(t_k,\cdot)||_{L^1(\Omega_1^{t_k})} = \int_0^{t_k} \left| \widetilde{\rho}_{1,h}(t_k,\tau)J_{1,h}^{-1}(t_k,\tau) - \mathbb{P}_1\widetilde{\rho}_1(t_k,\tau)\mathbb{P}_1 J_1^{-1}(t_k,\tau) \right| J_1(t_k,\tau)d\tau$$

$$\leq \int_0^{t_k} |\widetilde{\rho}_{1,h}(t_k,\tau)| \left| J_{1,h}^{-1}(t_k,\tau)J_1(t_k,\tau) - 1 \right| d\tau + \int_0^{t_k} |\widetilde{\rho}_{1,h}(t_k,\tau) - \mathbb{P}_1\widetilde{\rho}_1(t_k,\tau)| d\tau +$$

$$+ \int_0^{t_k} |\mathbb{P}_1\widetilde{\rho}_1(t_k,\tau)| \left| 1 - \mathbb{P}_1 J_1^{-1}(t_k,\tau)J_1(t_k,\tau) \right| d\tau.$$

Now we have, using the definition (38)

$$\left| J_{1,h}^{-1}J_1 - 1 \right| = \left| \mathbb{P}J_1^{-1}e^{-r_1}J_1 - 1 \right| \leq \left| e^{\overline{r_1}} \right| \frac{1}{|\mathbb{P}J_1|} |J_1 - \mathbb{P}J_1| + \left| e^{-r_1} - 1 \right|$$

Thus, since $\left|\left| \frac{1}{J_1} \right|\right|_{L^\infty} < \infty$ from formula (6) and the fact that $-G \cdot \nu \geq \delta > 0$, and using $|e^{-r_1} - 1| \leq 2\overline{r_1}$, there exists C_J such that

$$||J_{1,h}^{-1}(t_k,\tau)J_1(t_k,\tau) - 1||_{L^\infty} \leq C_J h, \text{ and } ||1 - \mathbb{P}_1 J_1^{-1}(t_k,\tau)J_1(t_k,\tau)||_{L^\infty} \leq C_J h.$$

The last inequality comes from the lemma 5.20 since $J_1 \in W^{1,\infty}$ from the formula (6). Using then the continuous and discrete *a priori* L^1 estimates and the proposition 5.23 gives the result. $\square$

Remark 5.27. *In the case of less regularity on the solution, we still have $\rho_h \underset{h\to 0}{\rightarrow} \rho$, $* - L^\infty(]0,T[\times\Omega)$. Indeed, we write $\rho_h = \widetilde{\rho}_{1,h}J_{1,h}^{-1} + \widetilde{\rho}_{2,h}J_{2,h}^{-1} = \widetilde{\rho}_{1,h}J_1^{-1} + \widetilde{\rho}_{2,h}J_2^{-1} + \widetilde{\rho}_{1,h}(J_{1,h} - J_1) + \widetilde{\rho}_{2,h}(J_{2,h} - J_2)$. Then we use that for $s = 1,2$ $J_{s,h}^{-1} \underset{h\to 0}{\xrightarrow{L^1}} J_s^{-1}$ as well as $\left|\left| J_{s,h}^{-1} \right|\right|_{L^\infty} \leq Ce^{\overline{r}_s}$ with C a constant. Using the theorem 5.18 for the convergence of $\widetilde{\rho}_{1,h}$ and $\widetilde{\rho}_{2,h}$ gives the result.*

Remark 5.28. *In practical situations we are often only interested in the number of metastases and not in the density ρ itself. Thanks to the formula $\int_\Omega \rho(t,X)dX = \int_0^t \int_{\partial\Omega} \widetilde{\rho}_1(t,\tau,\sigma)d\sigma d\tau + \int_\Omega \rho^0(X)dX$, we don't have to compute the jacobians J_1, J_2 to get the number of metastases. Yet, we still have to compute the characteristics since they are requested in the computation of the boundary condition (see formula (32)).*

3.3   Numerical illustration of the accuracy of the scheme

Analytical solution

The computational cost of a reference solution on a very fine grid is very high. Therefore, since we don't have an analytical expression of the characteristics associated to the vector field G of our model defined by (2), we illustrate the accuracy of our scheme for G given by

$$G_a(x, \theta) = \begin{pmatrix} ax \ln\left(\frac{\theta}{x}\right) \\ a\theta\left(1 - \frac{\theta}{K}\right) \end{pmatrix}$$

with a and K two parameters whose values are fixed to $a = 0.192$, $K = 5000$. This field has a similar phase plan to the one of our model (see Figure 4, considering that we only consider characteristics starting in the left edge of the square) and we can derive an analytical expression for the associated characteristics, given by

$$\theta(t) = \frac{\sigma_\theta K}{(K - \sigma_\theta)e^{-at} + \sigma_\theta} \tag{40}$$

$$x(t) = e^{y(t)}, y(t) = e^{at}\left(\sigma_y + \ln(\theta(t))\left(e^{at} + \frac{K}{\sigma_\theta} - 1\right) + at\left(1 - \frac{K}{\sigma_\theta}\right) - \frac{K}{\sigma_\theta}\ln(\sigma_\theta)\right)$$

with $\sigma = (\sigma_x, \sigma_\theta)$ the starting point of the trajectory at time 0 and $\sigma_y = \ln(\sigma_x)$. See the Figure 4 for a numerical illsutration of the ODE associated to G_a.
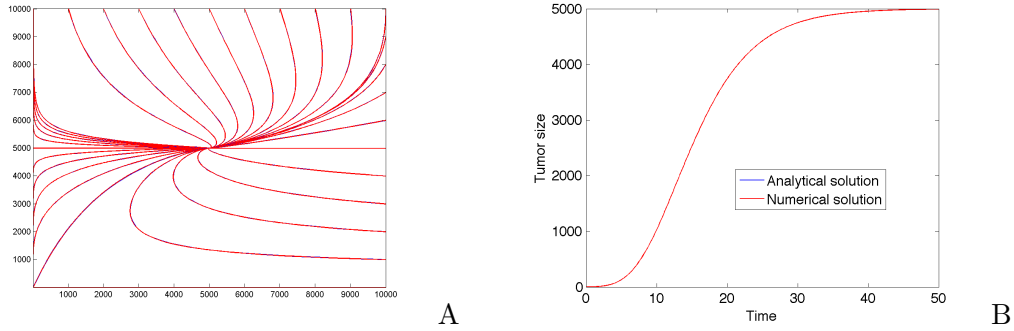
Figure 4: A. Phase plan of the vector field G_a. In blue, exact trajectories computed by formula (40) and in red trajectories numerically computed by a Runge Kutta scheme of order 4 (the curves are mingled). x-axis : size x and y-axis : vascular capacity θ. B. Time evolution of the tumoral size. Initial condition : $x_0 = 1$, $tt_0 = 2000$

The nonlocal term of the boundary condition can be handled by taking β constant equal to 1 and so is taken the source term $f(t)$. We take a null initial condition and thus consider the following problem

$$\begin{cases} \partial_t \rho + \mathrm{div}(\rho G_a) = 0 \\ -G_a \cdot \nu(\sigma)\rho(t, \sigma) = N(\sigma)\left\{\int_\Omega \rho(t, X)dX + 1\right\} \\ \rho(0) = 0 \end{cases} \tag{41}$$

We can compute explicitly the integral of the solution, given by $\int_\Omega \rho(t, X) = e^t - 1$ so that we are able to derive an analytical expression for $\widetilde{\rho}_a(t, \tau, \sigma) = \rho_a(t, \Phi(t; \tau, \sigma)) J_a(t, \tau, \sigma)$, with ρ_a solving (41), Φ_a the change of variable defined explicitly from (40) corresponding to Φ_1 from section 5.1.1 and its associated jacobian $J_a(t, \tau, \sigma) = -G_a \cdot \nu(\sigma) e^{\int_\tau^t \operatorname{div} G(u, \Phi_a(u; \tau, \sigma)) du}$. This expression is given by

$$\widetilde{\rho}_a(t, \tau, \sigma) = N(\sigma) e^\tau \mathbf{1}_{\tau \leq t}$$

so that to get the reference solution $\rho_a(t, \Phi(t; \tau, \sigma)) = \widetilde{\rho}_a J_a^{-1}(t, \tau, \sigma)$ we only need to finely approximate the jacobian, which is numerically tractable since it involves only the approximation of a 1D integral and that we have an exact expression for Φ_a. We use a trapezoid method and a timestep $dt = 5 \cdot 10^{-4}$ to achieve this.

Accuracy of the scheme

From the proof of the error estimates (proposition 5.23 and theorem 5.26) we see that the error on $\widetilde{\rho}$ can be split into : a) an error associated to the discretization of the nonlocal boundary condition, b) an error coming from the numerical integrator used for the characteristics and c) a projection error, whereas the error on ρ has an additional term coming from the approximation of the jacobian (see section 5.3.2). We will not consider the projection error and are aware that taking β constant will cancel the error of the numerical integrator impacting on the boundary condition. However, this error is still present in the approximation of the jacobian and thus in the error on ρ and we are more focused on the error deriving from the approximation of the nonlocal boundary condition. In the figure 5 are presented various illustrations of the convergence of the scheme for the following errors, with $T = 1$:

$$L^1 \text{ error on } \widetilde{\rho} = ||\widetilde{\rho}_h(T, \cdot) - \widetilde{\rho}_a(T, \cdot)||_{L^1(]0, T[\times \partial\Omega)}, \ L^\infty \text{ error on } \rho = ||\rho_h(T, \cdot) - \rho_a(T, \cdot)||_{L^\infty(\Omega)}.$$

Following remark 5.24, we use a trapezoid method (completed by a left rectangle method on $[t_{k-1}, t_k[\times\partial\Omega)$ for the approximation of the integral in the boundary condition and also for the integral intervening in the jacobian. We consider a Runge-Kutta method of order 4 for the discretization of the characteristics. In the figure 5.A, we observe that varying M (number of discretization points of the boundary) with fixed δt does not affect the error. Indeed, this comes from the facts that $N(\sigma)$ is a constant function and that we don't consider the projection error. Considering a nonconstant function for $N(\sigma)$ (like a gaussian one for instance) does produce an impact of M on the error in L^1 norm (data not shown), but since we approximate the solution along each characteristic, the L^∞ error resulting from the discretization of the boundary can only be seen between the exact solution and its projection on the mesh, that we don't consider here. In view of these consideration, we investigate the order of convergence keeping only one characteristic and varying δt.

As shown in the figure 5.B we obtain convergence of order two for both the L^1 error on $\widetilde{\rho}$ and the L^∞ error on ρ, in agreement with remark 5.24. The use of an Euler scheme for the characteristics is also investigated and leads to an order 1 on the L^∞ error on ρ, in concordance with the fact that the numerical integrator is used in the approximation of ρ *via* approximation of the jacobian. Concerning L^1 error on $\widetilde{\rho}$ with Euler we have order 2 (data not shown).
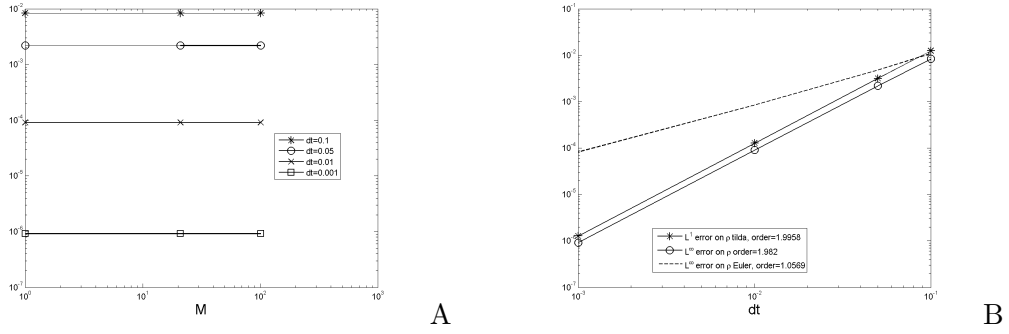
Figure 5: Numerical illustration of the convergence of the scheme. A. L^∞ error on ρ plotted versus M, for different values of δt. B. Various errors plotted versus δt, with $M = 1$.

4   Proof of the proposition 5.4

The result for the second map is classical. For the first one, we have to deal with irregular points of the boundary $\partial\Omega$. We denote by χ the set of such points and set $\chi_t := \{\Phi(t; \tau, \xi);\ \xi \in \chi,\ 0 \leq \tau \leq t\}$. In order to prove the result, it is sufficient to prove that for each fixed t the map

$$\Phi_1^t :\ \begin{array}{ccc}]0, t[\times \partial\Omega \setminus \chi & \to & \Omega_1^t \setminus \chi_t \\ (\tau, \sigma) & \mapsto & \Phi(t; \tau, \sigma) \end{array}$$

is a diffeomorphism, that globally the map $\Phi_1^t : [0, t] \times \partial\Omega \to \overline{\Omega}_1^t$ is bilipschitz and that its inverse is $X \mapsto (\tau^t(X), \sigma^t(X))$. For the first point, since we avoid the irregular points of the boundary by excluding the set χ, we have the C^1 regularity. It remains to prove that $\Phi_1^t(\tau, \sigma)$ is one-to-one and onto, and that its inverse is C^1.

• *The map Φ_1^t is one-to-one and onto.* Let $t > 0$ and $X \in \Omega_1^t$. We have $\Phi_1^t(\tau^t(X), \sigma^t(X)) = \Phi(t; \tau^t(X), \sigma^t(X)) = \Phi(t; \tau^t(X), \Phi(\tau^t(X); t, X)) = \Phi(t; t, X) = X$.
For the injectivity, we remark that if we have $\Phi(t; \tau, \sigma) = \Phi(t; \tau', \sigma')$ with for instance $\tau' < \tau$, then $\sigma = \Phi(\tau; \tau', \sigma')$ which is prohibited by the assumption that $G \cdot \nu(\tau, \sigma) < 0$. Thus Φ_1^t is one-to-one and we have, for $(\tau, \sigma) \in [0, t] \times \partial\Omega :\ \Phi(t; \tau^t(\Phi_1^t(\tau, \sigma)), \sigma(\Phi_1^t(\tau, \sigma))) = \Phi(t; \tau, \sigma)$ which implies $\tau^t(\Phi_1^t(\tau, \sigma)) = \tau$. Thus, we have proven that the inverse of Φ_1^t is $X \mapsto (\tau^t(X), \sigma^t(X))$.

• *The map Φ_1^t is a diffeomorphism.* We will prove the formula (6) for J_1 which will conclude the proof by using the local inversion theorem. We have $J_1(t; \tau, \sigma) = |\partial_\tau \Phi_1^t \wedge \partial_\sigma \Phi_1^t|$, with $\partial_\sigma \Phi_1^t := D_Y \Phi \circ \sigma'$ for σ being a parametrization of $\partial\Omega$ and $D_Y \Phi \in \mathcal{M}_2(\mathbb{R})$ the derivative in Y of $\Phi(t; \tau, Y)$ viewed as the flow on $\overline{\Omega}$. We compute

$$\partial_t(\partial_\tau \Phi_1^t \wedge \partial_\sigma \Phi_1^t) = \partial_\tau \partial_t \Phi_1^t \wedge \partial_\sigma \Phi_1^t + \partial_\tau \Phi_1^t \wedge \partial_t(D_Y \Phi_1^t \circ \sigma') = \partial_\tau(G \circ \Phi_1^t) \wedge \partial_\sigma \Phi_1^t + \partial_\tau \Phi_1^t \wedge DG \circ D_Y \Phi_1^t \circ \sigma'$$
$$= DG \circ \partial_\tau \Phi_1^t \wedge \partial_\sigma \Phi_1^t + \partial_\tau \Phi_1^t \wedge DG \circ \partial_\sigma \Phi_1^t = \mathrm{div}(G)(\partial_\tau \Phi_1^t \wedge \partial_\sigma \Phi_1^t).$$

We compute now directly the value of $J_1(t; t, \sigma)$. We define

$$T(h) = \frac{\Phi_1^t(t; t + h, \sigma) - \Phi_1^t(t; t, \sigma)}{h}$$

and now notice that we can write

$$
\begin{aligned}
\Phi_1^t(t; t, \sigma) &= \Phi_1^t(t; t + h, \Phi_1^t(t + h; t, \sigma)) \\
&= \Phi_1^t(t; t + h, \sigma) + D_Y \Phi_1^t(t; t + h, \sigma)(\Phi_1^t(t + h; t, \sigma) - \Phi_1^t(t; t, \sigma)) + o(h) \\
&= \Phi_1^t(t; t + h, \sigma) + h D_Y \Phi_1^t(t; t + h, \sigma) \circ G(t, \sigma) + o(h).
\end{aligned}
$$

Now when h goes to zero $D_Y \Phi_1^t(t; t + h, \sigma) \to D_Y \Phi_1^t(t; t, \sigma) = Id$ since $\Phi_1^t(t; t, Y) = Y$. Finally, we have $T(h) \to -G(t, \sigma)$, thus $\partial_\tau \Phi_1^t(t; t, \sigma) = -G(t, \sigma)$ and $\partial_\tau \Phi_1^t \wedge \partial_\sigma \Phi_1^t(t; t, \sigma) = -G(t, \sigma) \wedge \sigma' = G(t, \sigma) \cdot \nu(\sigma)$. Solving the differential equation between times τ and t and taking the absolute value then gives the formula (6).

- *Globally, Φ_1^t is bilipschitz.* It is possible to show that $|||D\Phi_1^t|||_{L^\infty([0,t] \times \partial\Omega)} \leq e^{t|||DG|||_{L^\infty([0,T] \times \overline{\Omega})}}$. Using the formula $(D\Phi_1^t)^{-1} = J_1^{-1} \, {}^t Com(D\Phi_1^t)$ and the fact that from (6) J_1^{-1} is bounded on $\overline{\Omega}_1^t$ thanks to the assumption (3) we have $|||(D\Phi_1^t)^{-1}|||_{L^\infty(\overline{\Omega}_1^t)} < \infty$. Thus Φ_1^t and $(\Phi_1^t)^{-1}$ are Lipschitz on $[0, t] \times \partial\Omega \setminus \chi$ and $\Omega_1^t \setminus \chi_t$ respectively, and they are both globally continuous on $[0, t] \times \partial\Omega$ and $\overline{\Omega}_1^t$. Hence they are globally Lipschitz.

Remark 5.29. *Using the same technique than in the previous proof, we can calculate the derivative of $\Phi_1(t; \tau, \sigma)$ in the τ direction. Indeed we compute, for all t, τ, σ*

$$
\begin{aligned}
\Phi_1(t; \tau, \sigma) &= \Phi_1(t; \tau + h, \Phi_1(\tau + h; \tau, \sigma)) \\
&= \Phi_1(t; \tau + h, \sigma) + D_Y \Phi_1(t; \tau + h, \sigma)(\Phi_1(\tau + h; \tau, \sigma) - \Phi_1(\tau; \tau, \sigma)) + o(h) \\
&= \Phi_1(t; \tau + h, \sigma) + h D_Y \Phi_1(t; \tau + h, \sigma) \circ G(\tau, \sigma) + o(h)
\end{aligned}
$$

which gives

$$
\partial_\tau \Phi_1(t; \tau, \sigma) = \lim_{h \to 0} \frac{\Phi_1(t; \tau + h, \sigma) - \Phi_1(t; \tau, \sigma)}{h} = -D_Y \Phi_1(t; \tau, \sigma) \circ G(\tau, \sigma). \tag{42}
$$

Chapter 6

2D-1D Limit

In this chapter, we prove the convergence of a family of solutions to our model for the evolution of a population of metastases. We show that when the data of the repartition along the boundary tends to a dirac mass then the solution of the associated problem converges and we derive a simple expression for the limit in term of the solution of a 1D equation. This result permits to improve the computational time needed to simulate the model.

We formulate the biological assumption that the metastases are all born with size 1 and an angiogenic capacity close to a given value θ_0. This is a simplification hypothesis which reduces the complexity of the model and thus its computational cost (see the section 6.2 for numerical illustrations) and we hope that it doesn't impoverishes too much the model and that this one will still be able to describe the metastatic process. In this case, we would like to know if we can replace the function N by a Dirac mass centered in σ_0, in the equation (2). This is translated in the model by considering a density N (repartition along the boundary) very concentrated around the value $(1, \theta_0)$, for instance

$$N^\varepsilon(\sigma) = \frac{1}{2\varepsilon}\mathbf{1}_{\{\sigma=(1,\theta);\ \theta\in[\theta_0-\varepsilon,\theta_0+\varepsilon]\}} \tag{1}$$

with ε being a small parameter. The model then writes

$$\begin{cases} \partial_t\rho^\varepsilon(t,X) + \mathrm{div}(\rho^\varepsilon(t,X)G(X)) = 0, & (t,X)\in]0,T[\times\Omega \\ -G\cdot\nu(\sigma)\rho^\varepsilon(t,\sigma) = N^\varepsilon(\sigma)\left\{\int_\Omega \beta(X)\rho^\varepsilon(t,X)dX + f(t)\right\}, & (t,\sigma)\in]0,T[\times\partial\Omega \\ \rho^\varepsilon(0,X) = 0, & X\in\Omega. \end{cases} \tag{2}$$

In this chapter, we demonstrate that the family of solutions $\{\rho^\varepsilon\}_\varepsilon$ to the problem (2) converges when ε goes to zero, to the measure solution $\rho(t,dX)$ of the equation

$$\begin{cases} \partial_t\rho(t,X) + \mathrm{div}(\rho(t,X)G(X)) = 0, & (t,X)\in]0,T[\times\Omega \\ -G\cdot\nu(\sigma)\rho(t,\sigma) = \delta_{\sigma=(1,\theta_0)}\left\{\int_\Omega \beta(X)\rho(t,X)dX + f(t)\right\}, & (t,\sigma)\in]0,T[\times\partial\Omega \\ \rho(0,X) = 0, & X\in\Omega. \end{cases} \tag{3}$$

Moreover, we derive a simple expression for $\rho(t,dX)$ involving the solution of a one-dimensional renewal equation. This permits to simulate in practice only the 1D equation rather than the 2D one and greatly improves the computational times.

1   Statement and proof of the theorem
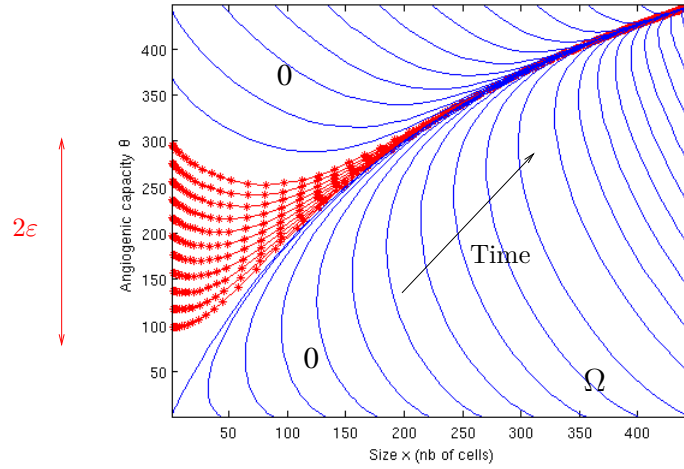
Figure 1: Trajectories for the growth field $G(X)$. The solution of (2) is zero out of the stared characteristics coming from points of the boundary $(1, \theta)$ with $\theta \in [\theta_0 - \varepsilon, \theta_0 + \varepsilon]$. The values of the parameters are chosen for illustrative purposes and are not realistic ones : $a = 2$, $c = 5.85$, $d = 0.1$, $\theta_0 = 200$, $\varepsilon = 100$.

For $\mathcal{O} = \Omega$, $\partial\Omega$ or $]0, T[\times\partial\Omega$, we will denote $\mathcal{M}(\mathcal{O}) := \mathcal{C}'_b(\mathcal{O})$ the set of continuous linear forms on the Banach space of bounded continuous functions on $\mathcal{O}$. We denote $\mathcal{C}([0, T]; * - \mathcal{M}(\mathcal{O}))$ the set of continuous functions with values in $\mathcal{M}(\mathcal{O})$, the continuity being taken in the sense of the weak-$*$ topology. We give now the definition of weak solution to the problem

$$\begin{cases} \partial_t \rho(t, X) + \mathrm{div}(\rho(t, X)G(X)) = 0, & (t, X) \in]0, T[\times\Omega \\ -G \cdot \nu(\sigma)\rho(t, \sigma) = N(\sigma)\left\{\int_\Omega \beta(X)\rho(t, X)dX + f(t)\right\}, & (t, \sigma) \in]0, T[\times\partial\Omega \\ \rho(0, X) = 0, & X \in \Omega. \end{cases} \quad (4)$$

when N is a measure on $\partial\Omega$.

Definition 6.1. *(Weak solution) Let $N(d\sigma) \in \mathcal{M}(\partial\Omega)$. We say that $\rho(t, dX) \in \mathcal{C}([0, T]; \mathcal{M}(\Omega))$ is a weak solution of the problem* (4) *if for all $\psi \in \mathcal{C}^1([0, T] \times \overline{\Omega})$ with $\psi(T, \cdot) = 0$*

$$\int_0^T < \rho(t, \cdot), \partial_t\psi + G \cdot \nabla\psi > dt + \int_0^T < N, \{B(t, \rho) + f(t)\}\psi_{|\partial\Omega}(t, \cdot) > dt = 0 \quad (5)$$

where $B(t, \rho) = < \rho(t, \cdot), \beta >$ and $< \cdot, \cdot >$ denote the duality brackets between a measure space and its associated space of continuous functions.

The proof of the theorem requires the following technical lemma.

Lemma 6.2. *Let $\{\varepsilon_k\}_{k\in\mathbb{N}}$ be a sequence going to zero, $N^k(\sigma) = N^{\varepsilon_k}(\sigma)$ and $\left\{n^k(t, \tau)\right\}_{k\in\mathbb{N}}$ be a sequence of functions of $\mathcal{C}([0, T]; L^1(]0, T[)$ such that $n^k \xrightarrow[k\to\infty]{\mathcal{C}([0,T];L^1(]0,T[)} n$. Then*

$$N^k n^k \rightharpoonup \delta_{\sigma=\sigma_0} \otimes n(t, \tau)d\tau, \quad in \ \mathcal{C}([0, T]; * - \mathcal{M}(]0, T[\times\partial\Omega)).$$

Proof. We compute, for $t \in [0, T]$ and $\psi \in \mathcal{C}_b(]0, T[\times \partial\Omega)$:

$$\left| \int_0^T n^k(t, \tau) \int_{\partial\Omega} N^k(\sigma)\psi(\tau, \sigma)d\sigma - n(t, \tau)\psi(\tau, \sigma_0)d\tau dt \right| \leq$$

$$\int_0^T \int_{\partial\Omega} \left| N^k(\sigma)\psi(\tau, \sigma)d\sigma \right| \left| n^k(t, \tau) - n(t, \tau) \right| d\tau$$

$$+ \int_0^T |n(t, \tau)| \left| \int_{\partial\Omega} N^k(\sigma)(\psi(\tau, \sigma) - \psi(\tau, \sigma_0))d\sigma \right| d\tau$$

$$\leq ||\psi||_{L^\infty(]0,T[\times\partial\Omega)} ||n^k(t, \cdot) - n(t, \cdot)||_{L^1(]0,T[)}$$

$$+ ||n(t, \cdot)||_{L^1(]0,T[)} \sup_{\tau \in [0,T]} \sup_{\sigma \in [\sigma_0 - \varepsilon_k, \sigma_0 + \varepsilon_k]} |\psi(\tau, \sigma) - \psi(\tau, \sigma_0)|.$$

Taking the supremum in t and passing to the limit $k \to \infty$ gives the result. $\qquad\square$

We can now state the theorem.

Theorem 6.3. *(Convergence) Let* $G(x, \theta) = \begin{pmatrix} ax \ln\left(\frac{\theta}{x}\right) \\ cx - dx^{2/3}\theta \end{pmatrix}$, $\beta \in \mathcal{C}(\Omega)$, $f \in L^1(]0, T[)$ *and* N^ε *given by* (1). *Let* ρ^ε *be the weak solution of the equation* (2). *Then*

$$\rho^\varepsilon \rightharpoonup \rho \in \mathcal{C}([0, T]; \mathcal{M}(\Omega)),$$

the convergence being in $\mathcal{C}([0, T]; * - \mathcal{M}(\Omega))$ *for all* $T > 0$. *The expression of* ρ *is given by : for all* $\psi \in \mathcal{C}_b(\Omega)$

$$< \rho(t, \cdot), \psi >= \int_0^\infty \psi(\Phi_\tau(\sigma_0))n(t, \tau)d\tau \tag{6}$$

with $\Phi_\tau(\sigma)$ *the solution of the differential equation* $\frac{dX}{d\tau} = G(X)$ *with initial condition* σ *and* n *the solution of the following 1D problem*

$$\begin{cases} \partial_t n + \partial_\tau n = 0, & t > 0, \tau > 0 \\ n(t, 0) = \int_0^\infty \beta(\Phi_\tau(\sigma_0))n(t, \tau) + f(t), & t \geq 0 \\ n(0, \tau) = 0, & \tau \geq 0 \end{cases} \tag{7}$$

Moreover, the measure ρ *is the weak solution of* (3).

Proof.
• *Step 1. Simplification of the problem.* Let $\{\varepsilon_k\}_{k\in\mathbb{N}}$ be a sequence going to zero, $T > 0$ and let $\rho^k := \rho^{\varepsilon_k}$. We suppose for now that $f \in \mathcal{C}^1$ and $f(0) = 0$ in order to have regular solutions $\rho^k \in \mathcal{C}^1([0, \infty[; L^1(\Omega)) \cap \mathcal{C}([0, \infty[; W_{\text{div}}(\Omega))$ to the problem (2) (see chapter 4), where $W_{\text{div}}(\Omega) = \left\{ V \in L^1(\Omega); \text{div}(GV) \in L^1(\Omega) \right\}$. We define

$$\tilde{\rho}^k(t, \tau, \sigma) = \rho^k(t, \Phi_\tau(\sigma))|J_\Phi|$$

where $\Phi_\tau(\sigma)$ is the solution of the differential equation $\frac{dX}{d\tau} = G(X)$ with initial condition σ. As proved in the chapter 4, this application is a locally bilipschitz homeomorphism between Ω and $]0, T[\times \partial\Omega \setminus (b, b)$ and hence can be used as a change of variable. We denote $J_\Phi = \det(D\Phi)$ the jacobian of Φ which verifies $\partial_\tau |J_\Phi| = \text{div}(G)|J_\Phi|$. Then $\tilde{\rho}^k$ solves the equation

$$\begin{cases} \partial_t \tilde{\rho}^k + \partial_\tau \tilde{\rho}^k = 0 \\ \tilde{\rho}^k(t, 0, \sigma) = N^k(\sigma) \left\{ \int_0^\infty \int_{\partial\Omega} \tilde{\beta}(\tau, \sigma)\tilde{\rho}^k(t, \tau, \sigma)d\tau d\sigma + f(t) \right\} \\ \tilde{\rho}^k(0) = 0 \end{cases} \tag{8}$$

set for $(t, \tau, \sigma) \in \mathbb{R}^+ \times \mathbb{R}^+ \times \partial\Omega$ and where $\widetilde{\beta}(\tau, \sigma) = \beta(\Phi_\tau(\sigma))$.

• *Step 2. Convergence for the sequence $\widetilde{\rho}^k$.* From the expression of the solutions given by the method of characteristics we have :

$$\widetilde{\rho}^k(t, \tau, \sigma) = N^k(\sigma) \left\{ \int_0^\infty \int_{\partial\Omega} \widetilde{\beta}(\tau', \sigma') \widetilde{\rho}^k(t - \tau, \tau', \sigma') d\tau' d\sigma' + f(t - \tau) \right\}, \tag{9}$$

where $N^k = N^{\varepsilon_k}$. Now we define

$$n^k(t, \tau) = \int_0^\infty \int_{\partial\Omega} \widetilde{\beta}(\tau', \sigma') \widetilde{\rho}^k(t - \tau, \tau', \sigma') d\tau' d\sigma' + f(t - \tau) \tag{10}$$

which we recognize being the solution of the following 1D problem :

$$\begin{cases} \partial_t n^k + \partial_\tau n^k = 0 & t > 0, \tau > 0 \\ n^k(t, 0) = \int_0^\infty B^k(\tau) n^k(t, \tau) d\tau + f(t) & t \geq 0 \\ n^k(0, \tau) = 0 & \tau \geq 0 \end{cases}, \tag{11}$$

with $B^k(\tau) = \int_{\partial\Omega} N^k(\sigma) \widetilde{\beta}(\tau, \sigma) d\sigma$. Indeed, the partial differential equation comes from differentiating the expression of n^k and the boundary condition follows from

$$\begin{aligned} n^k(t, 0) &= \int_0^\infty \int_{\partial\Omega} \widetilde{\beta}(\tau', \sigma') \widetilde{\rho}^k(t, \tau', \sigma') d\tau' d\sigma' + f(t) \\ &= \int_0^\infty \int_{\partial\Omega} \widetilde{\beta}(\tau', \sigma') N^k(\sigma') n^k(t, \tau') d\tau' d\sigma' + f(t) \end{aligned}$$

where we used $\widetilde{\rho}^k(t, \tau', \sigma') = N^k(\sigma') n^k(t, \tau')$ from (9). Now we have that since the data f is regular and satisfies the compatibility condition, $n^k \in \mathcal{C}^1([0, T]; L^1(]0, T[)) \cap \mathcal{C}([0, T]; W^{1,1}(]0, T[))$, and the following bound stands :

$$||n^k(t, \cdot)||_{L^1} \leq e^{t||B^k||_\infty} \int_0^t e^{-s||B^k||_\infty} |f(s)| ds \leq e^{t||\beta||_\infty} \int_0^t |f(s)| ds, \ \forall k \tag{12}$$

where we used that $||B^k||_\infty \leq ||\beta||_\infty$ for all k. Differentiating in time the equation (legitimate since the solution is regular), we also have bounds on the derivatives :

$$||\partial_t n^k(t, \cdot)||_{L^1} \leq e^{t||\beta||_\infty} \int_0^t |f'(s)| ds, \ ||\partial_\tau n^k(t, \cdot)||_{L^1} \leq e^{t||\beta||_\infty} \int_0^t |f'(s)| ds.$$

Using the compact embedding of $W^{1,1}(]0, T[)$ into $L^1(]0, T[)$, we obtain that for each t, the sequence $n^k(t, \cdot)$ is relatively compact in $L^1(]0, T[)$ and then, since $\partial_t n^k$ is bounded in $\mathcal{C}([0, T]; L^1(]0, T[))$ the Ascoli theorem proves that there exists a subsequence which converges in $\mathcal{C}([0, T]; L^1(]0, T[))$ to a function n. Now we pass to the limit in the expression $n^k(t, \tau) = \int_0^t B^k(\tau') n^k(t - \tau, \tau') d\tau' + f(t - \tau)$ to see that n satisfies

$$n(t, \tau) = \int_0^t \beta(\Phi_{\tau'}(\sigma_0)) n(t - \tau, \tau') d\tau' + f(t - \tau)$$

that is, $n \in \mathcal{C}([0, T]; L^1(]0, T[))$ is the solution of

$$\begin{cases} \partial_t n + \partial_\tau n = 0 & t > 0, \tau > 0 \\ n(t, 0) = \int_0^\infty \beta(\Phi_\tau(\sigma_0)) n(t, \tau) d\tau + f(t) & t \geq 0 \\ n(0, \tau) = 0 & \tau \geq 0 \end{cases} \tag{13}$$

By uniqueness of the solution to this equation, we obtain that the whole sequence n^k converges to n. Now, from $\widetilde{\rho}^k(t, \tau, \sigma) = N^k(\sigma)n^k(t, \tau)$, using the lemma 6.2, we get

$$\widetilde{\rho}^k(t, \tau, \sigma) \rightharpoonup \widetilde{\rho}(t, \tau, d\sigma) = \delta_{\sigma=\sigma_0} \otimes n(t, \tau)d\tau, \text{ in } \mathcal{C}([0, T], *-\mathcal{M}(]0, T[\times\partial\Omega)). \tag{14}$$

We remark from its expression that we have $\widetilde{\rho} \in \mathcal{C}([0, T]; \mathcal{M}(]0, T[\times\partial\Omega))$ as well as the following bound :

$$||\widetilde{\rho}(t, \cdot)||_{\mathcal{M}(]0, T[\times\partial\Omega)} \leq e^{t||\beta||_\infty} \int_0^t |f(s)|ds. \tag{15}$$

• *Step 3. Back to weak solutions.* For a general data $f \in L^1(]0, T[)$, we consider a regularized sequence $f_m \in \mathcal{C}^1([0, T])$ with $f_m(0) = 0$ which converges to f in $L^1(]0, T[)$, and define $\widetilde{\rho}_m^k$ the associated solution. For each m, the previous step gives a measure $\widetilde{\rho}_m = \delta_{\sigma=\sigma_0} \otimes n_m(t, \tau)d\tau$, with n_m the solution of the problem (13) with data f_m. The bound (15) shows that the sequence $\widetilde{\rho}_m$ is a Cauchy one, thus it converges in $\mathcal{C}([0, T]; \mathcal{M}(]0, T[\times\partial\Omega))$ to a measure $\widetilde{\rho} \in \mathcal{C}([0, T]; \mathcal{M}(]0, T[\times\partial\Omega))$. Then we can write, for $\psi \in \mathcal{C}_b(]0, T[\times\partial\Omega)$:

$$|| < \widetilde{\rho}^k - \widetilde{\rho}, \psi > ||_\infty \leq || < \widetilde{\rho}^k - \widetilde{\rho}_m^k, \psi > ||_\infty + || < \widetilde{\rho}_m^k - \widetilde{\rho}_m, \psi > ||_\infty + || < \widetilde{\rho}_m - \widetilde{\rho}, \psi > ||_\infty.$$

Thus for all m we have, using that $||\widetilde{\rho}^k(t, \cdot) - \widetilde{\rho}_m^k(t, \cdot)||_{L^1} \leq C||f - f_m||_{L^1}$ (see proposition 5.9 of chapter 5 for a similar bound as (12) in the two-dimensional case of the equation (2))

$$\limsup_{k\to\infty}|| < \widetilde{\rho}^k - \widetilde{\rho}, \psi > ||_\infty \leq C||f - f_m||_{L^1}||\psi||_\infty + || < \widetilde{\rho}_m - \widetilde{\rho}, \psi > ||_\infty.$$

Choosing now m large enough shows that $\widetilde{\rho}^k \rightharpoonup \widetilde{\rho}$ in $\mathcal{C}([0, T], *-\mathcal{M}(]0, T[\times\partial\Omega))$. Passing to the limit in the expression of $\widetilde{\rho}_m$, we see that the expression (14) is still valid.

• *Step 4. Back to ρ^k.* Denoting also ρ^k the measure on Ω with density ρ^k and in the same way $\widetilde{\rho}^k$ the measure on $]0, \infty[\times\partial\Omega$ with density $\widetilde{\rho}^k$, we observe from the following identity, where Φ is the map $]0, +\infty[\times\partial\Omega \to \Omega, (\tau, \sigma) \mapsto \Phi_\tau(\sigma)$

$$\int_A \rho^k = \int_A \rho^k(t, x, \theta)dxd\theta = \int_{\Phi^{-1}(A)} \rho^k(t, \Phi_\tau(\sigma))|J_\Phi|d\tau d\sigma = \int_{\Phi^{-1}(A)} \widetilde{\rho}^k, \quad \forall A \subset \Omega$$

that ρ^k is the push-forward of the measure $\widetilde{\rho}^k$ by Φ, that we denote $\widetilde{\rho}_{\sharp\Phi}^k$. Thus we have $\rho^k = \widetilde{\rho}_{\sharp\Phi}^k \underset{k\to\infty}{\rightharpoonup} \widetilde{\rho}_{\sharp\Phi} := \rho$, the convergence being in $\mathcal{C}([0, T], *-\mathcal{M}(\Omega))$. The measure $\rho(t, dX)$ is given by : for all $t > 0$ and all $\psi \in \mathcal{C}_b(\Omega)$

$$< \rho(t, \cdot), \psi >= \int_0^\infty \psi(\Phi_\tau(\sigma_0))n(t, \tau)d\tau.$$

Direct computations with this expression in the weak formulation of solutions to the equation (3) (or passing to the limit in the weak formulation of solutions to the equation (2)) shows that ρ solves the problem (3). $\qquad\square$

Remark 6.4. *(Uniqueness for (3)) In the proof of the previous theorem, we didn't need to address the question of uniqueness of solutions to the problem (3). However, there is uniqueness and it can be proved by the standard method of establishing existence of regular solutions to the adjoint problem. Indeed here the adjoint problem for a measure data $N \in \mathcal{M}(\partial\Omega)$ and a source term in $S \in \mathcal{C}_c^1(]0, T[\times\Omega)$ writes*

$$\partial_t\psi + G \cdot \nabla\psi + \beta < N, \psi_{|\partial\Omega}(t, \cdot) >= S.$$

It can be shown using the method of characteristics and a fixed point argument that this equation admits a regular solution $\psi \in \mathcal{C}^1([0,T] \times \overline{\Omega})$, with $\psi(T,\cdot) = 0$. Using this solution in the weak formulation (5) for a null boundary data gives that $\int_0^T < \rho(t,\cdot), S > dt = 0$. This identity being true for all $S \in \mathcal{C}_c^1(]0,T[\times\Omega)$ gives the result.

Remark 6.5. *(Linear density) To model directly the situation where all the metastases are born with the same angiogenic capacity θ_0, we could consider that the metastases evolve on the one-dimensional curve $\gamma := \{\Phi_\tau(\sigma_0); \tau \geq 0\}$ and model the number of metastases via a linear density $\rho_1 : [0,T] \times \gamma \to \mathbb{R}$. Then the number of metastases on the curve between the points $X_1 = \Phi_{\tau_1}(\sigma_0)$ and $X_2 = \Phi_{\tau_2}(\sigma_0)$ would be given by $\int_{\tau_1}^{\tau_2} \rho_1(t, \Phi_\tau(\sigma_0))|G(\Phi_\tau(\sigma_0))|d\tau$, since $\partial_\tau \Phi_\tau(\sigma_0) = G(\Phi_\tau(\sigma_0))$. Comparing this approach to the previous one where, after passing to the limit $\varepsilon \to 0$, the number of metastases between X_1 and X_2 is $\int_{\tau_1}^{\tau_2} n(t,\tau)d\tau$ (from formula (6)), the analogy would be to identify $n(t,\tau) = \rho_1(t, \Phi_\tau(\sigma_0))|G(\Phi_\tau(\sigma_0))|$ and thus this last quantity would solve the problem (13). In the linear density approach, it would yet not be possible to derive a simple equation on ρ_1 since $\partial_\tau |G(\Phi_\tau(\sigma_0))|$ has not a simple expression comparing to $\partial_\tau |J_\Phi| = \mathrm{div}(G)|J_\Phi|$ which gives the equation (2) in the 2D modeling approach.*

2   Numerical illustration

In the chapter 5, we developed a numerical scheme to simulate the problem (2). It is a Lagrangian scheme based on the method of characteristics which consists in discretizing the boundary with M points and simulating the equation along each characteristic curve coming from the boundary, after having straightened it. Remark that since the initial condition is zero, the solution only lives in the red part of the figure 1 and we only have to discretize the red part of the boundary $[\theta_0 - \varepsilon, \theta_0 + \varepsilon]$. We choose as a good approximation the values $dt = 0.1$ and $M = 10$ for the discretization parameters (see the section 5.3.3 for numerical illustrations of the convergence of the scheme).

Because the equation is two-dimensional simulating it can have an elevated computational cost, especially for large times (see table 1). Thanks to the theorem 6.3 if we make the biological assumption that all the metastases are born with an angiogenic capacity close to the value θ_0, then the metastasis density ρ^ε is close to ρ and the total number of metastases at time t is close to $\int_\Omega \rho(t, dX) = \int_0^t n(t,\tau)d\tau$, with n being the solution of (7), by applying the formula (6) with the test function $\psi = \mathbf{1}$ to obtain the total mass of the measure $\rho(t,\cdot)$. Thus we only have to simulate the equation (7), which with our scheme consists in simulating along the only characteristic coming from the point $(1,\theta_0)$. The convergence stated in theorem (6.3) is illustrated in the figure 2. It is plotted the relative difference for the total number of metastases at the end of the simulation, between the simulation in 1D and the one in 2D for various values of ε. That is, if T is the end time of the simulation :

$$\text{Relative Error} = \left| \frac{\int_0^T n(T,\tau)d\tau - \int_\Omega \rho^\varepsilon(T,X)dX}{\int_0^T n(T,\tau)d\tau} \right|.$$

We see that it decreases to zero as ε goes to zero. In the figure 2.A, we observe that, as can be expected, the convergence deteriorates when T is bigger. The figure 2.B shows that the convergence in ε does not depend on the number of discretization points of the boundary M,
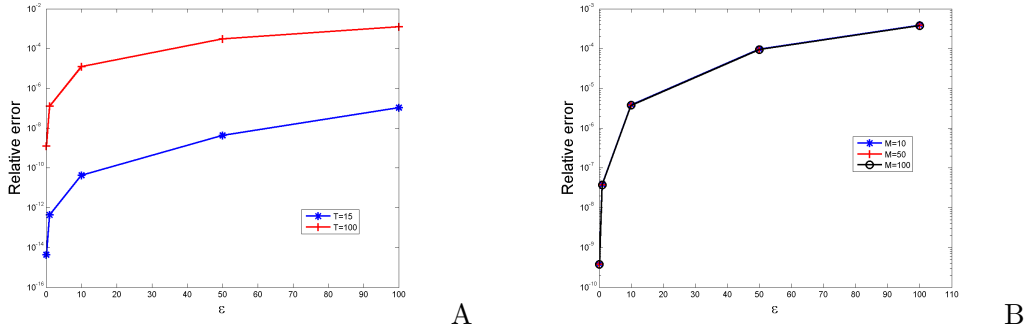
Figure 2: Relative difference between the 1D simulation and the 2D one, for 5 values of ε : 100, 50, 10, 1 and 0.1. The values of the parameters for the growth velocity field G are from [HPFH99] and correspond to mice data : $a = 0.192$, $c = 5.85$, $d = 0.00873$, $\theta_0 = 625$. For the metastases parameters, we used : $m = 0.001$ and $\alpha = 2/3$. The used timestep is $dt = 0.1$. A. Convergence when ε goes to zero, for $T = 15$ and $T = 100$. The value of M used for the 2D simulations is $M = 10$. B. Convergence when ε goes to zero, with respect to M ($M = 10, 50, 100$), for $T = 50$. The three curves are almost all the same.

for $M \geq 10$. This is coherent with the fact that the convergence of the scheme does not depend a lot on M, as explained and illustrated in the chapter 5, section 5.3.3.

In the table 1 are given various computational times on a personal computer for the simulation in 2D and in 1D. The simulations were performed with the same parameters as in the figure 2 and for the 2D simulations we used $\varepsilon = 0.1$ and $M = 10$ points of discretization of the boundary.

	2D	1D
T=15 days, dt=0.1	67 sec	10.69 sec
T=15 days, dt=0.01	1h42 min	11 min
T=100 days, dt=0.1	46 min	4.7 min

Table 1: Computational times on a personal computer of various simulations in 1D and 2D.

We observe that simulating in 1D improves greatly the computational times, especially for the large time simulations. Since the evolution of a cancer disease can be very slow, it is important to be able to simulate the model for large times (say, more than a year in the human case). Here the times are in days and we see that thanks to the convergence of the theorem 6.3, the numerical method for simulating the model is improved in terms of the computational cost, which was necessary when looking at the prohibitive costs in 2D.

Part III

Applications médicales

Chapter 7

Simulation results

In this chapter, we illustrate by numerical simulations of the model the potential use of the model as an helpful tool for sharper diagnosis and therapy decision in the clinic. All along, we try to use as much as possible parameters coming from data fits and will focus on the impact of the *scheduling* of the drugs.

We first present simulations without treatment and study the dependance on the metastatic parameters m and α, showing that identifying these parameters in a clinical setting could lead to a more precise classification of the cancer disease than the existing ones like TNM (Tumor Nodule Metastases), by describing more accurately the metastatic state of the patient, especially the micrometastases.

As our model was build up to integrate the effect of anti-angiogenic (AA) therapy, we investigate *in silico* the effect of these drugs with a particular focus on the difference of the effect on primary tumor evolution and metastases.

Then, we interest ourselves to a surprising phenomenon of metastatic acceleration after AA therapy recently reported in the literature. We adapt the model based on a biological hypothesis, in order to qualitatively reproduce these results, investigate the impact of scheduling in this framework and perform some predictions with the model.

As AA drugs are neither administrated alone in the clinic but rather in combination with cytotoxic (CT) drugs (usually refered as chemotherapies), we integrate the combination of these two drugs in the model and turn our interest on the order of administration.

Eventually, we use the model to perform interesting simulations about the emerging concept of *metronomic chemotherapies* which consists in administrating CT agents at low dose as continuously as possible. We integrate resistances to the CT in the model and show that the hypothesis of an AA action of the CT drug could explain the large-time benefit of these new ways of administrating the chemotherapy.

All the simulations are performed using the scheme developed in chapter 5, in the 1D approximation explained in the chapter 6. This work was accepted for publication [BAB$^+$11].

1 Without treatment

An interesting application of the model would be to help designing a predictive tool for the total number of metastases present in the organism of the patient. In this perspective, in the same way as what is done in [BBHV09] we define a metastatic index as the integral of ρ on Ω :

$$MI(t) := \int_\Omega \rho(t, X)dX.$$

We will also focus on two other quantities of interest

$$\text{Visible metastases} = \int_\Omega \mathbf{1}_{x \geq x_{vis}}(x, \theta)\rho(t, x, \theta)dx\, d\theta, \quad \text{Metastatic mass} = \int_\Omega x\rho(t, x, \theta)dx\, d\theta.$$

with x_{vis} being the minimal visible size at imagery for a tumor (10^7 - 10^8 cells). The size (= volume) is expressed in mm^3 though until now it was thought as the number of cells. The conversion rule we use is $1\ mm^3 \simeq 10^6$ cells.

1.1 Parameter values

Mice The values of the parameters for the tumoral growth in the mice case are taken from [HPFH99], where they were fitted from mice data bearing Lewis lung carcinoma. Following [IKN00] and [BBHV09], we take $\alpha = 2/3$ and fix the value of m arbitrarily (see (**??**) for the definition of these parameters). The values of the parameters (without the treatment) are gathered in the table 1, where (x_0, θ_0) are the initial traits of a metastasis.

a	c	d	x_0	θ_0	m	α
(day^{-1})	(day^{-1})	$(day^{-1}vol^{-2/3})$	(vol)	(vol)	$(Nb\,of\,meta)(day^{-1})(vol^{-\alpha})$	
0.192	5.85	8.73×10^{-3}	10^{-6}	625	10^{-3}	$2/3$

Table 1: Values of the growth and metastatic parameters for mice. Parameters a, c and d where fitted on mice data in [HPFH99].

Human In the paper of Iwata et al. [IKN00] where the growth rate was a Gompertz, parameters where identified from data on a hepatocellular carcinoma. To determine realistic parameters for human situations, we fix values of the parameters for the model of Hahnfeldt et al. reproducing the gompertzian growth curve of Iwata et al., keeping the carrying capacity from [IKN00] equal to $\left(\frac{c}{d}\right)^{3/2}$ and fixing θ_0 as being rescaled from the value of [HPFH99] by the ratio of the maximal reachable sizes from the two papers. We use the same value for α and adapt the value of m to a size unit in mm^3 : in [IKN00] $m = 5.3 \cdot 10^{-8}$(Number of metastases)·(cell$^{-\alpha}$)·day^{-1} gives $m = 5.3 \cdot 10^{-8} \cdot 10^{6\alpha}$·(Number of metastases)·(mm$^{-3\alpha}$)·day^{-1}. Comparison of the tumoral growth between the Gompertz with parameters from [IKN00] and the model of Hahnfeldt et al. with the parameters from table 2 is given in the Figure 1.

a	c	d	θ_0	m	α
0.0042	1	$5.7251 \cdot 10^{-4}$	2630.14	$5.3 \cdot 10^{-4}$	2/3
day^{-1}	day^{-1}	$\mathrm{day}^{-1}\mathrm{mm}^{-2}$	mm^3	Nb of meta$\cdot\mathrm{day}^{-1}\cdot\mathrm{mm}^{-3\alpha}$	

Table 2: Values of the growth and metastatic parameters for human. a, m and α are from [IKN00].
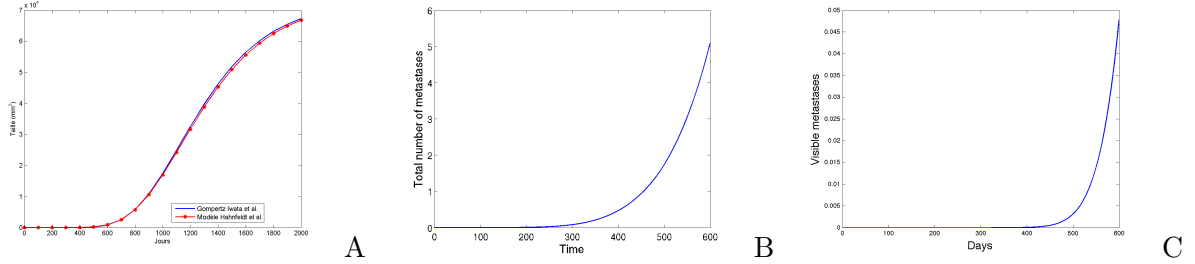
Figure 1: A. Tumoral evolution. Comparison between the Gompertz used in [IKN00] (parameters $a = 0.00286\ day^{-1}$, $\theta = 7.3 \cdot 10^{10}\ cells = 7.3 \cdot 10^4\ mm^3$) and the model of Hahnfeldt et al. with the growth parameters from table 2. B. Total number of metastases. C. Visible metastases ($x_{vis} = 10^7$).

1.2   Visible metastases. Metastases emitted by the primary tumor

A very important issue for clinicians is to determine the number of metastases which are not visible with medical imaging techniques (micro-metastases). Having a model for the density of metastases structured in size allows us to compute the number of visible and non-visible metastases. We take as threshold for a metastasis to be visible a size of 10^8 cells, that is $100\ mm^3$. In the Figure 2, we plotted the result of a simulation showing both the total number of metastases as well as only the visible ones.
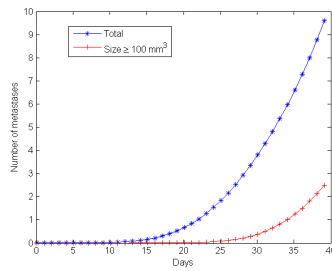
Figure 2: Evolution of the total number of metastases and of the number of visible metastases, that is whose size is bigger than $100\,mm^3 (\simeq 10^8\ cells)$.

We observe that at day 20 the model predicts approximately one metastasis though it is not visible. At the end of the simulation, the total number of metastases is much bigger than the number of visible ones.

In the Figure 3, we compare the influence of the metastases emitted by the primary tumor (first generation) and the number of metastases emitted by the metastases themselves (secondary generations).
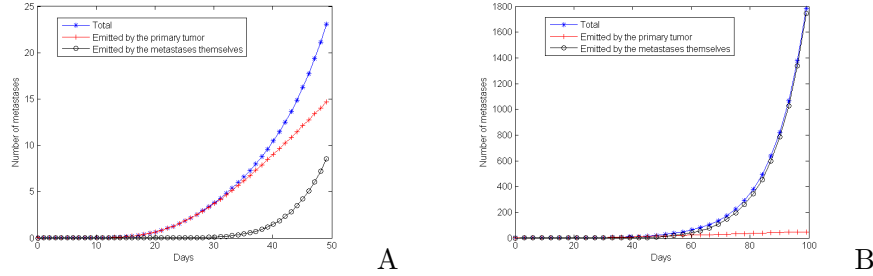
Figure 3: Number of metastases emitted by the primary tumour and by the metastases themselves. A. T=50. B. T=100

We observe that times less than 50 the first generation is the most important in the total number, while for larger times the secondary generations haver greater importance. Indeed, in the model this last quantity is exponential in time whereas the first one results from a source term. The life time of a mice is of the order of 50 days and thus, with the metastatic parameters that we arbitrarily fixed, the metastases at death of the animal are composed of about two thirds of first generation tumors and one third of secondary tumors.

1.3 Dependance on the metastatic parameters m and α

Dependance on m

The metastatic index dependance relatively to the metastatic aggressiveness parameter m is shown in the table 3. Of course, the larger m, the larger the metastatic index. The values of the growth parameters are those from [HPFH99], that is

$$a = 0.192, \quad c = 5.85, \quad d = 0.00873 \tag{1}$$

the value of α is constant equal to $\frac{2}{3}$, the initial values for the primary tumor are $(x_{p,0}, \theta_{p,0}) = (10^{-6}, 625)$ and the same for the metastases. In this table, we remark that at least for times less

	$MI(1.5)$	$MI(7.5)$	$MI(15)$
$m = 10^{-4}$	5.80×10^{-3}	6.60×10^{-2}	2.79×10^{-1}
$m = 10^{-3}$	5.80×10^{-2}	6.60×10^{-1}	2.81
$m = 10^{-2}$	5.80×10^{-1}	6.62	30.1

Table 3: Variation of the number of metastases with respect to m.

than 15 days, it seems that the metastatic index is linear in m. Indeed, this can be explained by the fact that at the beginning, most of the metastases come from the primary tumour and not by the metastases themselves. This means that the renewal term in the boundary condition

of the equation could be neglected for small times and that the solution of this problem is close to the one of

$$
\begin{cases}
\partial_t \rho + \operatorname{div}(\rho G) = 0 \\
-G \cdot \nu \rho(t, \sigma) = N(\sigma)\beta(X_p(t)) \\
\rho^0(X) = 0.
\end{cases}
$$

But then, integrating the equation on Ω gives $MI(t) = \int_0^t \beta(X_p(s))ds = m\int_0^t x_p(s)^\alpha ds$, where $X_p(s) = (x_p(s), \theta_p(s))$ represents the primary tumour and solves the system $\dot{X}_p(s) = G(X_p(s))$ with initial condition $(x_{0,p}, \theta_{0,p})$. For larger times, the metastatic index for large time is then not anymore linear in m, neither exponential nor following a power law, as illustrated in the figure 4 where is the plotted the number of metastases at time $T = 100$ versus m.

A

B
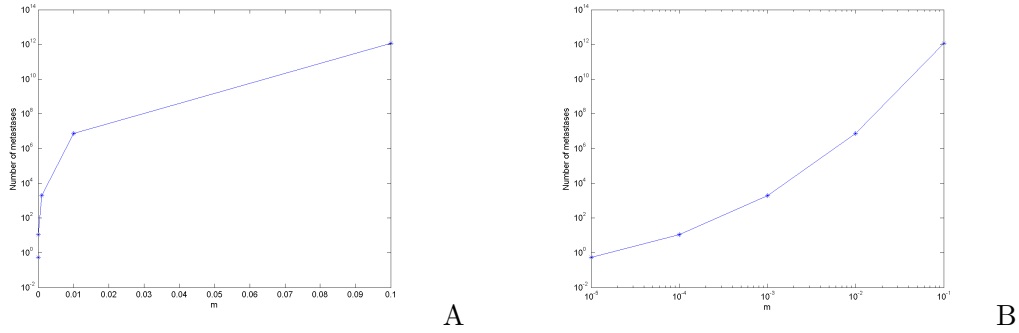
Figure 4: Number of metastases at the end of the simulation with $T = 100$ in log and log-log scales.

Dependance on α

For the dependance in α, things are more intricate. Indeed, if we think as x being bigger than 1 (for instance if x is expressed in number of cells), then $\alpha \mapsto mx^\alpha$ is an increasing function and we expect the total number of metastases being increasing relatively to α. But if we rather think to x as a volume (expressed in mm^3 for instance) and allow its value to be lower than 1, by taking as initial values for the size of the metastases $x_0 = 10^{-6}mm^3 \simeq 1$ cell, the other initial values being $\theta_0 = 10^{-5}mm^3$, $(x_{p,0}, \theta_{p,0}) = (1, 10^{-5})$, then the dependance in α is not so clear, resulting from a balance between small tumors for which decreasing α raises their importance and bigger ones which have the opposite behavior. The simulation results presented in the figure 5 indeed prove that we can have two opposite behaviors of the total number of metastases versus α, depending on the value of m : a small (and more realistic) value of m ($m = 10^{-3}$) exhibits an increasing curve of $MI(T)$ versus α whereas the opposite happends with $m = 10^4$. We also notice that for m small, the dependance of $MI(T)$ on α looks exponential, but we have no theoretical explanation to provide for this fact.

$$m = 10^{-3} \qquad\qquad\qquad m = 10^4$$
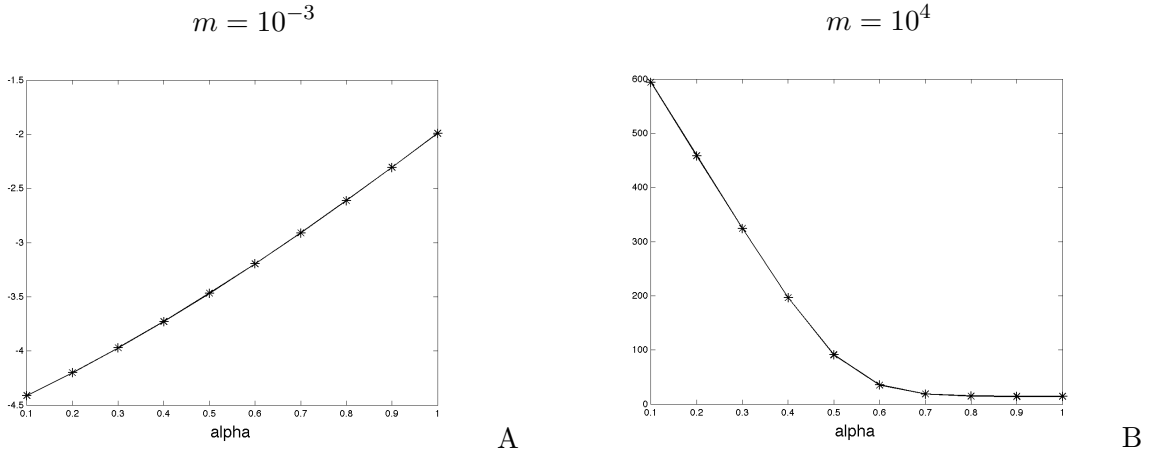
Figure 5: Total number of metastases at $T = 10$ versus the parameter α (in log scale) for two different values of m. The values of the growth parameters are those of [HPFH99] .

2 Anti-angiogenic therapy

2.1 Mice parameters

We present various simulations of anti-angiogenic (AA) treatments, in order to investigate the difference in effectiveness of various drugs regarding to their pharmacokinetic/pharmacodynamic parameters. The first result shown in Figure 6 takes the three drugs which were used in [HPFH99] where only the effect on tumor growth was investigated, and simulates the effect on the metastases. The three drugs are TNP-470, endostatin and angiostatin and each drug is characterized by two parameters in the model : its efficacy e and its clearance rate clr_A. The first one appears in the growth rate of each tumor, that we recall here

$$G(t, x, \theta) = \begin{pmatrix} ax \ln\left(\frac{\theta}{x}\right) \\ cx - dx^{2/3} - eA(t)(\theta - x_0)^+ \end{pmatrix}$$

where we took the size of one cell as minimal vascular capacity for the therapy to be active. The second parameter appears in the one-compartmental pharmacokinetics model for the concentration $A(t)$:

$$A(t) = D \sum_{i=1}^{N} e^{-clr(t-t_i)} \mathbf{1}_{t \geq t_i}, \tag{2}$$

where D is the administrated dose which is given at times t_i. These parameters were retrieved in [HPFH99] by fitting the model to mice data under AA therapy. The administration protocols are the same for endostatin and angiostatin (20 mg every day) but for TNP-470 the drug is administrated with a dose of 30 mg every two days.

We observe that TNP-470 seems to have the poorest efficacy, both on tumoral growth, vascular capacity and total number of metastases, due to its large clearance. As noticed in [HPFH99],

A

B

C
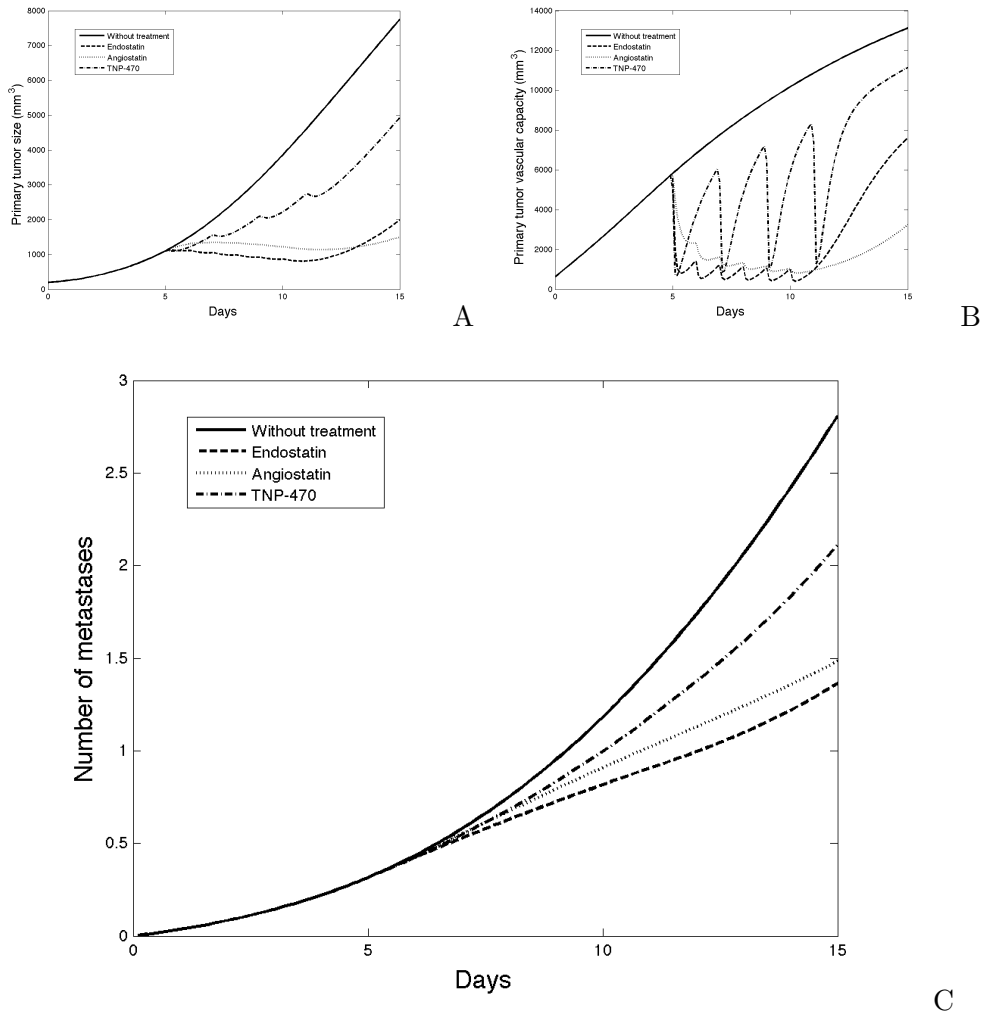
Figure 6: Effect of the three drugs from [HPFH99]. The treatment is administrated from days 5 to 10. Endostatin ($e = 0.66$, $clr_A = 1.7$) 20 mg every day, TNP-470 ($e = 1.3$, $clr_A = 10.1$) 30 mg every two days and Angiostatine ($e = 0.15$, $clr_A = 0.38$) 20 mg every day. A : tumor size. B : Angiogenic capacity. C : Number of metastases.

the ratio e/clr_A should govern the efficacy of the drug and its value is 0.13 for TNP-470 and 0.39 for both endostatin and angiostatin. The model we developed is now able to simulate efficacy of the drugs on the metastatic evolution (figure 6.C). Interestingly, the drug which seems to be more efficient regarding to the tumor size at the end of the simulation (day 15), namely angio-statin, is not the one which gives the best result on the metastases. Indeed, the lower efficacy of endostatin regarding to ultimate size is due to a relatively high clearance provoking a quite fast rebound of the angiogenic capacity once the treatment stops. But since the tumor size was lower for longer time, the metastatic evolution was better contained. This shows that the model could be a helpful tool for the clinician since the response to a treatment can differ from the primary tumor to metastases, but the clinician has no data about micro-metastases which are

not visible with imagery techniques.

In the figure 7, we investigate the influence of the AA dose (parameter D) on tumoral, vascular and metastatic evolution. We observe that the model is consistent since it exhibits a monotonous response to variation of the dose.
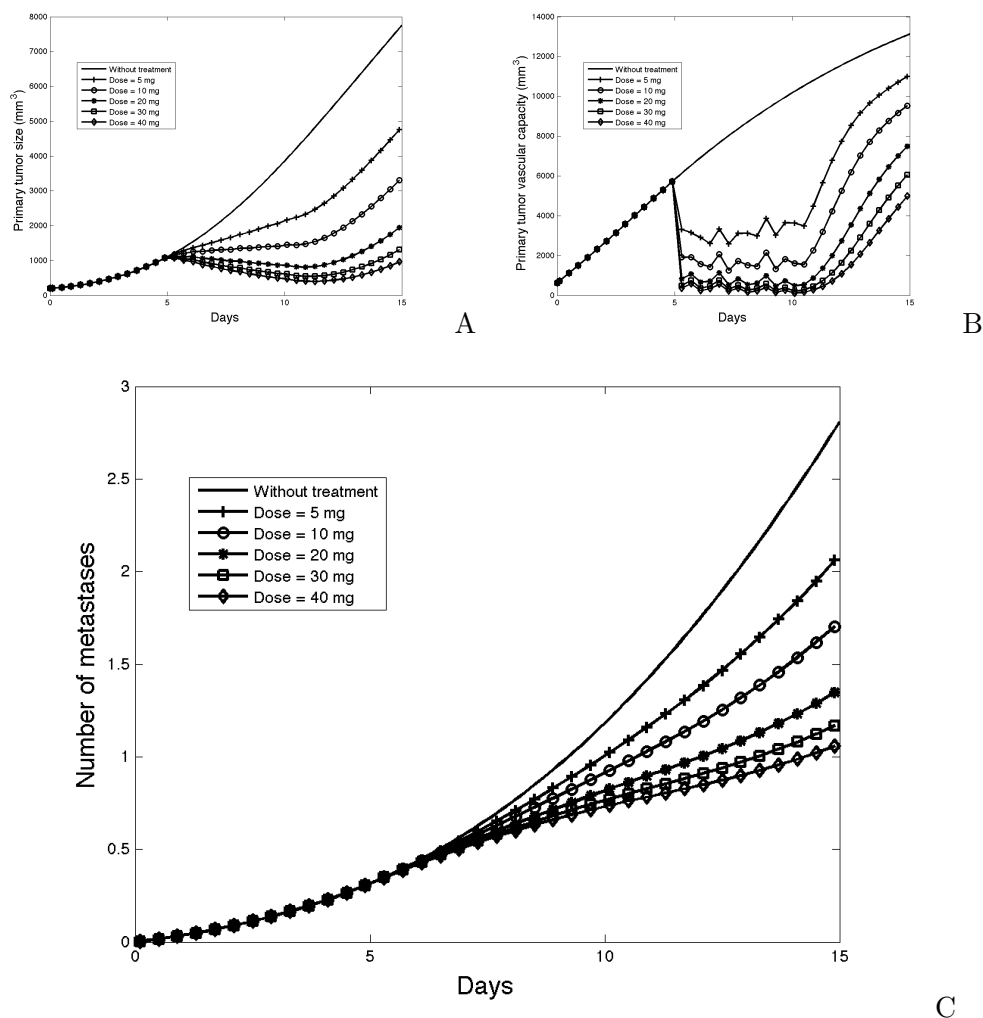
Figure 7: Effect of the variation of the dose for endostatin. A : tumor size. B : Angiogenic capacity. C : Number of metastases.

Influence of the scheduling

One of our main postulate in the treatment of cancer is that for a given drug, the effect can vary regarding to the temporal administration protocol of the drug, due to the combination of the pharmacokinetic of the drug and the intrinsic dynamic of tumoral and metastatic growth. To investigate the effect of varying the administration schedule of the drug, we simulated various administration protocols for the same drug (endostatin). The results are presented in figure

8. We gave the same dose and the same number of administrations of the drug but either uniformly distributed during 10 days (endostatin 2), concentrated in 5 days (endostatin 1) or in 2 days and a half (endostatin 3). We observe that the tumor is better stabilized with a uniform
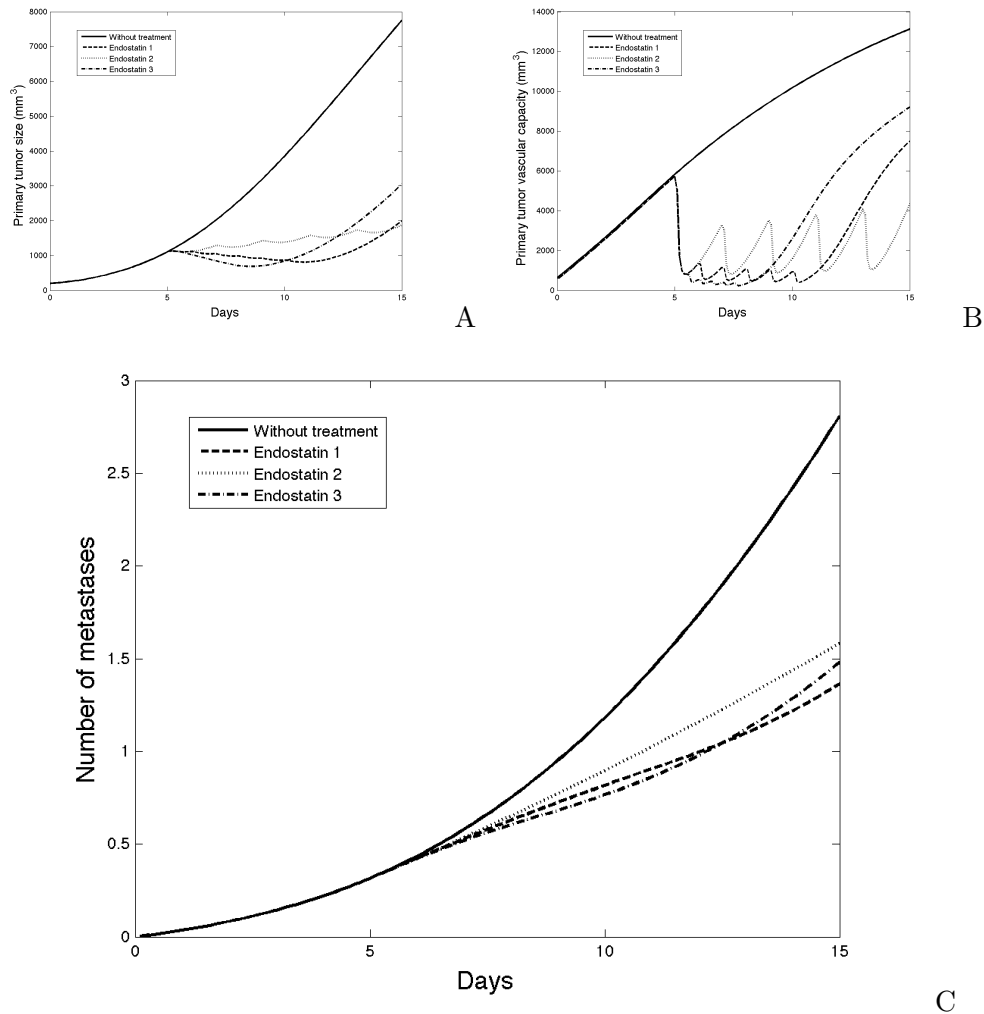
Figure 8: Three different temporal administration protocols for the same drug (Endostatin). Same dose (20 mg) and number of administrations (6) but more or less concentrated at the beginning of the treatment. Endostatin 1 : each day from day 5 to 10. Endostatin 2 : every two days from day 5 to 15. Endostatin 3 : twice a day from day 5 to 7.5. A : tumor size. B : Angiogenic capacity. C : Number of metastases.

administration of the drug (endostatin 2) but the number of metastases is better reduced with the intermediate protocol (endostatin 1). It is interesting to notice that again if we look at the effects at the end of the simulation, the results are different for the tumor size and for the metastases. The two protocols endostatin 1 and endostatin 2 give the same size at the end, but not the same number of metastases. Moreover, the best protocol regarding to minimization of the final number of metastases (endostatin 1) is neither the one which provoked the largest

regression of the tumor during the treatment (endostatin 3) nor the one with the most stable tumor dynamic (endostatin 2).

To investigate further the scheduling dependance of the administration of AA drugs such as endostatin, and motivated by various preclinical studies [KBP$^+$01, DBRR$^+$00] as well as phase I studies [HBvdH$^+$05, ESC$^+$02], A. d'Onofrio, A. Gandolfi and A. Rocca used in [dGR09] the Hahnfeldt - Folkman model of tumoral growth to assay low-dose, time-dense protocols in comparison with high-dose, time-sparse protocols. In Figure 9.A, we reproduce one of the result obtained in [dGR09] (Figure 5 of this paper, where the differences with our simulation are the values of e, changed from 0.66 to 1.3 in [dGR09] and the values of the doses), and then observe what happens on the total number of metastases and the metastatic mass, this last one being defined by $\int_\Omega x\rho(t,x,\theta)dxd\theta$, on Figures 9.B and 9.C. Two schedulings are considered for endostatin (noticed that the same global dose is administrated in both cases) :

Protocol 1 : 15 mg/kg, every day,   Protocol 2 : 30 mg/kg, every two days.

and simulations are run to compare their effects on the disease's evolution. We observe that in
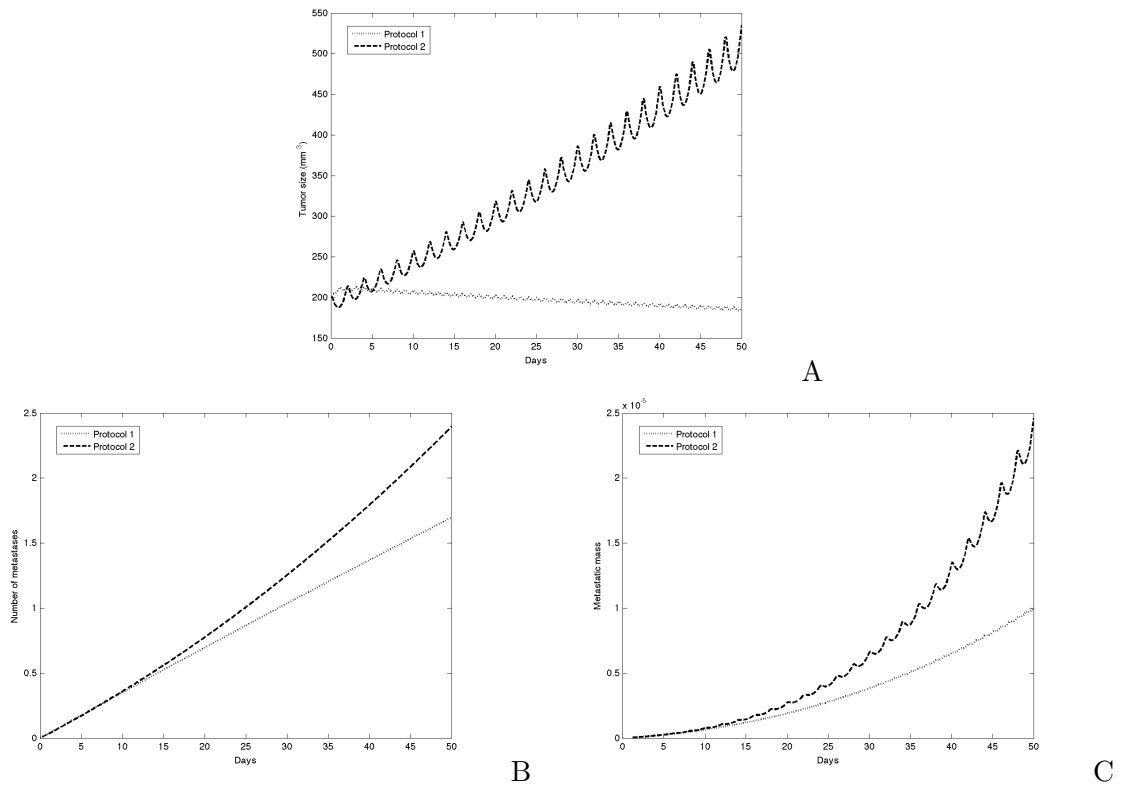
Figure 9: Two different schedulings for endostatin. Protocol 1 : 15 mg/kg, every day and Protocol 2 : 30 mg/kg, every two days. A. Tumor size. B. Number of metastases. C. Metastatic mass.

the case of protocol 1, the tumoral evolution is contained and eventually the therapy achieves tumor eradication whereas protocol 2 does not induce tumor reduction and leads to unbounded

growth. The same happens on the number of metastases and the metastatic mass. Notice that, if the tumoral growth model would have been linear with a log-kill term due to the therapy, both protocols would give the same results. This result emphasizes the good sensitivity of the Hahnfeldt-Folkman model which is able to distinguish between different schedulings of the same drug, with constant total administrated dose. According to this result and consistently with the aforementioned preclinical studies, endostatin would achieve better efficacy when administrated as continuous as possible.

2.2   Human parameters. Bevacizumab

Despite the great hope which succeeded the discovery of tumoral neo-angiogenesis process in the 1970's and the achievement of AA drugs in the 1990's and the beginning of the 21st century, only a few AA drugs obtained a full market approval for clinical use. One of the most famous is a monoclonal antibody, Bevacizumab (commercial name : Avastin). For the the PK of this drug, we base ourselves on the publication [LBE$^+$08] which shows that the PK can be described by a two-compartmental model :

$$\begin{cases} \frac{dc_1(t)}{dt} = -(k_{10} + k_{12})c_1(t) + k_{21}\frac{V_2}{V_1}A(t) + \frac{I_A(t)}{V_1} \\ \frac{dA(t)}{dt} = -(k_{20} + k_{21})A(t) + k_{12}\frac{V_1}{V_2}c_1(t). \end{cases} \tag{3}$$

with $I_A(t)$ having the same expression as in (16) with injection duration τ_A. The parameters were estimated from patients data in [LBE$^+$08] and their values can be found in the table 4. In the Figure 10, we compare three protocols used in clinical situations [LBE$^+$08] : 5 mg/kg/2

Parameter	V_1	V_2	k_{10}	k_{20}	k_{12}	k_{21}	τ_A	e
Value	2.66	2.66	0.0779	0	0.223	0.215	90	0.01
Unit	L	L	day^{-1}	day^{-1}	day^{-1}	day^{-1}	min	L·mg^{-1}· day^{-1}

Table 4: Parameter values for the PK model for Bevacizumab. All parameters except e are from [LBE$^+$08].

weeks, 7.5 mg/kg/3 weeks and an additional one : 2.5 mg/kg/week. See also [OB08] for other examples of protocols (15mg/kg/week). We consider that injections of the drug last 90 minutes. We take as non-zero initial condition the traits $(x_{0,p}, \theta_{0,p}) = (17112, 44849)$ corresponding to the values reached after 1000 days when starting with one cell and the parameters from table 2, except $m = 1$. We also take the corresponding value of $\rho(600)$ as ρ^0.

We observe that the response of the model again differs for the three considered schedulings, the best one being 7.5 mg/3 weeks for all the quantities plotted. Hence, according to these simulations and probably due to the large half-life of Bevacizumab it appears better to give a strong dose of the drug, with large periods without administration. These results contrast with the previous ones on mice data for endostatin, which advocate small dose/ time dense administration of the drug in this case, due to higher clearance of the drug. These results enhance the importance of pharmacokinetics in deciding the scheduling of a given drug. We also remark in Figure 10 that the overall behavior of the number of visible metastases is quite similar to the one of the primary tumor size. Indeed, large tumors are stabilized and thus the number of visible ones remains almost constant.
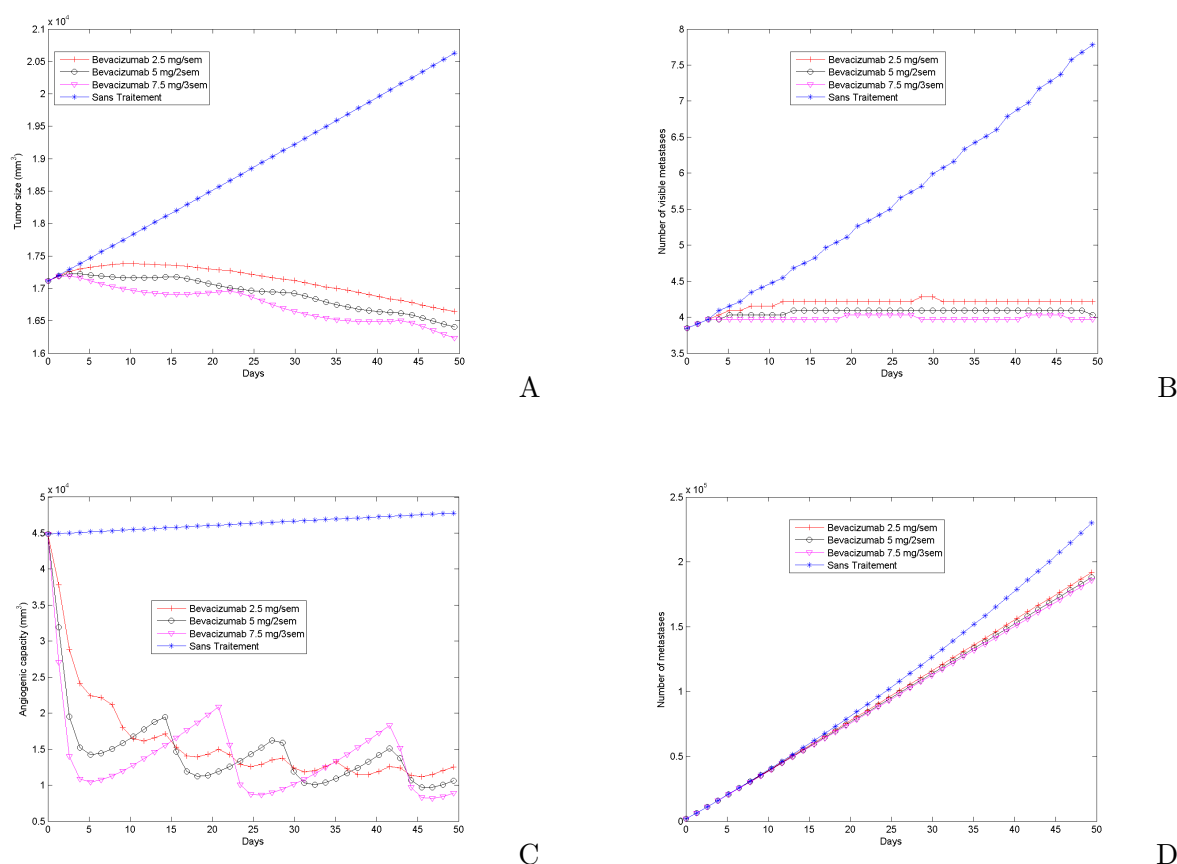
Figure 10: Comparison of clinically used protocols for Bevacizumab. A. Primary tumor size. B. Visible metastases. C. Vascular capacity. D. Total number of metastases.

3   Metastatic acceleration after anti-angiogenic therapy

In a recent paper [ELCM$^+$09], Ebos et al. obtained surprising results after AA therapy with Sunitinib (a tyrosine kinase inhibitor of VEGFR, a VEGF receptor) : the treatment could induce metastatic acceleration in mice, while substantially inhibiting primary tumor growth. They used two different experimental protocols to assay this phenomenon, on mice : by intravenous injection of cancerous cells or by orthotopic implantation of a tumor in the mammary fat pad and then removal of the primary tumor. In both cases, they obtained acceleration of the metastatic mass in groups treated by the AA drug, compared to an untreated group. In the Figure 11, we reproduce the Figure 2A from [ELCM$^+$09].

However, on the primary tumor, the effect of the treatment was beneficial, as shown in the Figure 12 which is Figure 4A from [ELCM$^+$09]. Moreover, sustained therapy at 60 mg/kg/day exhibited better tumor slowdown than a temporal protocol of 120 mg/kg/day during 7 days, starting the day after tumor implantation.
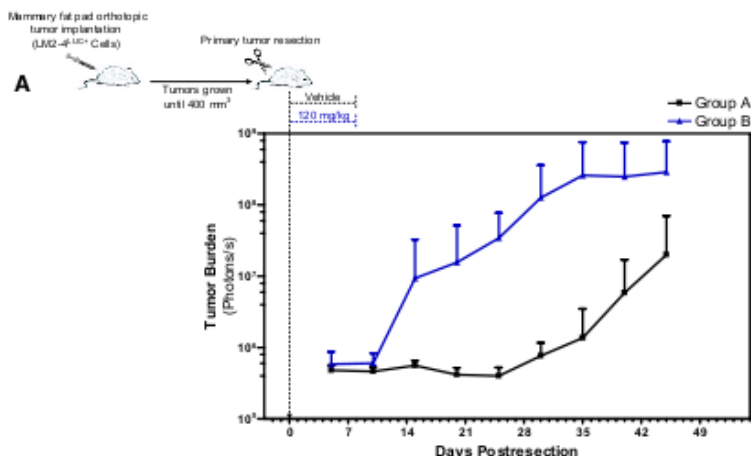
Figure 11: Figure 2A from Ebos et al. [ELCM$^+$09]. Both groups had orthotopically grown tumors which were surgically removed and then Group A were treated by Sunitinib therapy whereas Group B received only the vehicle.
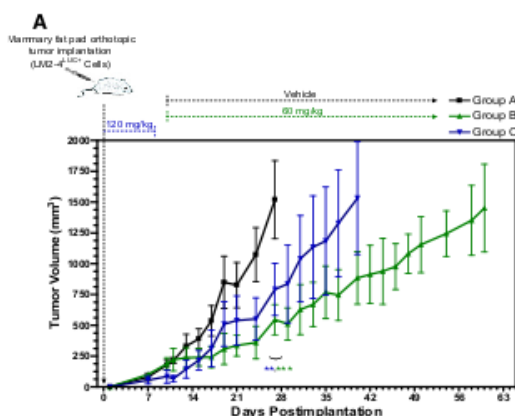
Figure 12: Figure 4A from Ebos et al. [ELCM$^+$09] showing the effect of the AA therapy on the primary tumor evolution, for two different schedules of the drug : Group B received 60 mg/kg/day when tumor size reached 200 mm^3 and Group C 120 mg/kg/day during 7 days, starting the first day after tumor implantation.

These results were corroborated by another paper of Paez-Ribes et. al [PRAH$^+$09] in the same issue of the journal.

3.1 Model

In this section, we modify our model in order to qualitatively reproduce these results, in a first attempt to have a theoretical tool aiming at controlling this paradoxical metastatic acceleration effect. In [ELCM$^+$09], the authors propose as possible explanation for the phenomenon an upregulation of proangiogenic factors :

« Our results present a [..] possibility [...] that involves microenvironmental changes in mouse organs. [...] A number of potential mechanisms alone or in combination could play a role. One is the [...] induced upregulation of multiple circulating proangiogenic cytokines and growth factors in response to treatment, including osteopontin, G-CSF, and SDF1α (Ebos et al., 2007) - all of which have been implicated in angiogenesis and/or metastasis (McAllister et al., 2008; Ben Baruch, 2008; Wai and Kuo, 2008; Natori et al., 2002; Zhang et al., 2000). Second, and likely related to such molecular changes, the mobilization of bone marrow-derived cells may facilitate an enhanced "premetastatic niche," including circulating endothelial (Okazaki et al., 2006) and myeloid progenitors (Shojaei et al., 2008), CXCR4$^+$ recruited bone marrow circulating cells (Grunewald et al., 2006), and circulating VEGFR1$^+$ bone marrow cells (Kaplan et al., 2005).»

To integrate this feature in the model, we propose to modify the angiogenesis stimulation parameter c of the tumoral growth model of Hahnfeldt - Folkman, only for the growth of metastases, by making it dependent of the AA drug concentration $A(t)$, with an increased value $c_M \gg c$ when the AA concentration is above a threshold A_τ :

$$c(A(t)) = \left\{ \begin{array}{ll} c_M & \text{if } A(t) \geq A_\tau \\ c & \text{if } A(t) < A_\tau \end{array} \right.$$

See Figure 13 for an illustration. Our model is thus designed to take into account for the possible
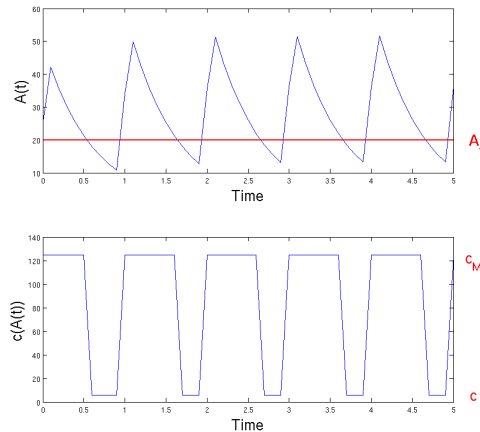
Figure 13: Illustration of the activation of the "boost" effect.

counter-attack of tumor cells towards AA therapy, as suggested by [ELCM$^+$09] and shown in [CFF$^+$10]. Indeed, in this last paper the authors demonstrate an increase of VEGF tumoral expression after erlotinib therapy in an *in vitro* experiment.

The equation for the dynamics of the vasculature of the metastases during the therapy thus becomes

$$\frac{d\theta}{dt} = c(A(t))x - dx^{2/3}\theta - eA(t)(\theta - \theta_{min})^+. \tag{4}$$

and we see that the effect of the treatment is balanced between this "boost" effect and the natural anti-angiogenic effect of the drug.

We justify the fact that this angiogenic "boost" effect only occurs on the metastases and not on the primary tumor in view of the following arguments :

1. The primary tumor is big and relatively stable regarding to angiogenesis, having already established a vascular network and thus it is less active regarding to this process. On the contrary, metastases are small and fully active, passing through the angiogenic switch. Hence they are more reactive to an external assault. We could be more accurate by making c_M dependent on the size of the tumor. In first approximation though, we don't do so.

2. Metastases are known to be genetically more aggressive, as the detaching cells which give rise to a malignant secondary tumor must have survived to various adverse events (intravasation into blood vessels, extravasation, settling in a new environment...). Thus they could have a stronger phenotype regarding to the AA drug injury.

In absence of pharmacokinetics data for the Sunitinib, we perform the simulations in the case of one-compartmental PK model (equation (2)), with clearance equal to 1.7 (endostatin in [HPFH99]).

3.2   Simulations

Metastatic acceleration

To perform the simulations, we used the tumoral growth parameters of table 1 (except for θ_0). For the other parameters, we used

$$e = 0.2, \quad clr_A = 1.7, \quad c_M = 50, \quad \theta_0 = 10^{-5}. \tag{5}$$

Of course, to obtain metastatic acceleration, we have to consider small value of the threshold A_τ, which can be approximated by taking $A_\tau = 0$ (immediate "boost" effect). In the Figure 14 are presented simulation results in this situation, which qualitatively reproduce the results of Figure 11. We simulated the model without therapy, with initial primary tumor values $(x_{0,p}, \theta_{0,p}) = (1, 10^{-5})$, virtually performed resection of the primary tumor on day 14.5 (which consists in removing the source term in the PDE for the metastatic density) and then administrated the AA drug starting day 15, during 6 days. The temporal administration protocol that we used for the drug is 20mg/day.

This result shows that for the parameter values (5), the model is able to reproduce metastatic acceleration, the balance between the anti-angiogenic effect and the "boost" effect in equation (4) being in favor of the second one.

Figure 14: Metastatic acceleration for $A_\tau = 0$. A. Total number of metastases, only from day 15 to day 30. B. Metastatic mass

In the Figure 15, we reproduced *in silico* the situation of Figure 12 by not performing resection of the primary tumor and testing two different temporal protocols for the AA drug : protocol 1 consists in giving the drug at 20mg/day during 7 days and protocol 2 administrates half of the dose, 10mg/kg, but during a larger time, from day 13 (which is the time for which the tumor reaches 200mm^3 in the model) until the end. We also used $A_\tau = 0$ in this simulation.

We observe good qualitative agreement between Figure 15.A, showing the primary tumor growth, and the Figure 12. Indeed, since the primary tumor is not subjected to the "boost" effect in the model, the AA drug induces inhibition of the growth. We also retrieve the fact that better results are obtained with sustained therapy (protocol 2). In the Figures 15.B, C and D we show some metastatic quantities, respectively the total number of metastases, the metastatic mass and the number of visible metastases (size exceeding 10^8 cells $=$ 100 mm^3) . It is interesting to notice that for both protocol, the total number of metastases is reduced compared to the situation without treatment whereas for the metastatic mass and the visible metastases, the effect depends on the protocol. While protocol 1 induces increased metastatic mass and number of visible metastases, protocol 2 has a positive effect, being even able to avoid apparition of visible metastases whereas protocol 1 provokes the presence of almost two visible metastases at the end of the simulation. It would be interesting to compare these *in silico* predictions to the metastatic data corresponding to Figure 12 from [ELCM$^+$09] (unfortunately not available in the paper).

We could imagine that the threshold value A_τ is a parameter which depends on the AA drug considered, or on the patient. Identification of its value would then be of fundamental importance since metastatic acceleration can occur or not depending on this value, as illustrated in Figure 16 where we performed the same numerical experiment as in Figure 14, but with $A_\tau = 20$, and observe reduction of the total number of metastases and of the metastatic mass.

Influence of the scheduling

In the Figure 17 we compare two protocols regarding to the metastatic acceleration phenomenon. Protocol 1 consists in giving the drug every day at dose 20 mg and Protocol 2 administrates the double dose every two days, each one being administrated from day 15 to 42 and with $A_\tau = 7$.
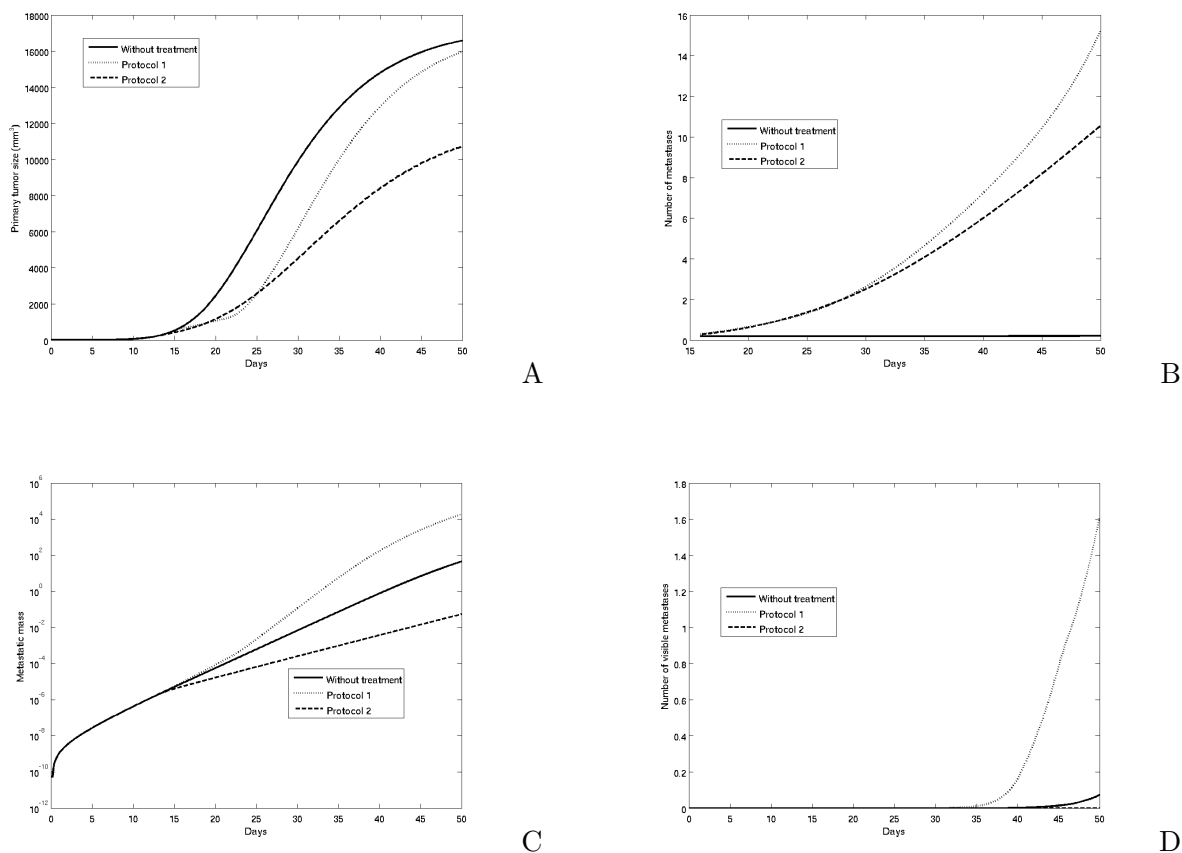
Figure 15: Without resection. Protocol 1 : 20mg/day from day 15 to day 21. 10mg/day from day 13 until the end A. Primary tumor. B. Total number of metastases, from day 15 until the end. C. Metastatic mass (log scale). D. Visible metastases
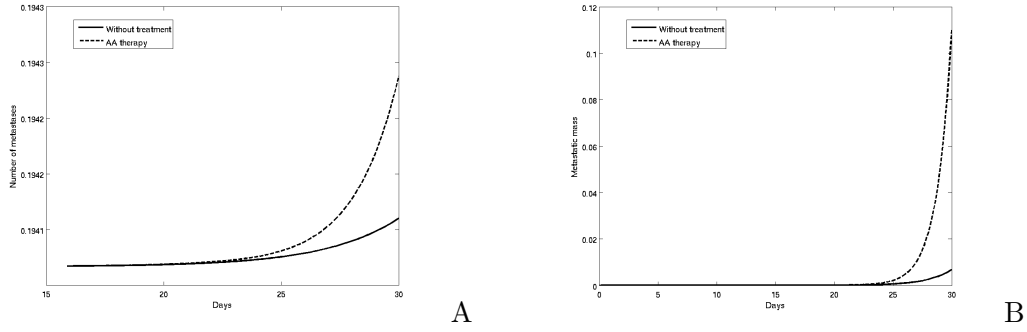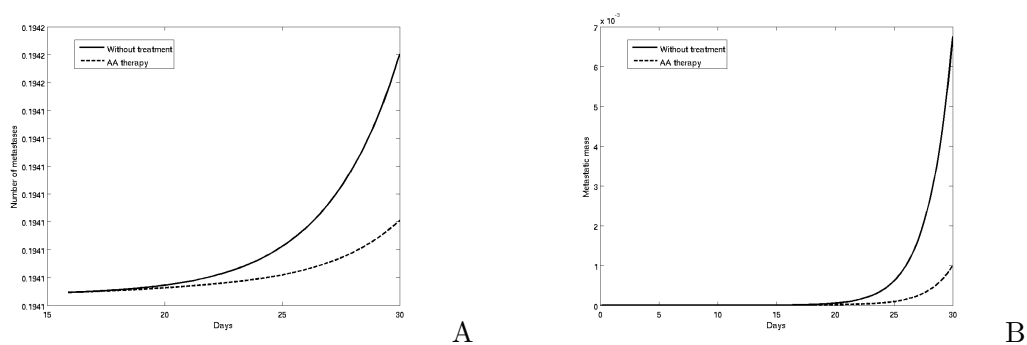

Figure 16: No metastatic acceleration for $A_\tau = 20$. A. Total number of metastases, only from day 15 to day 30. B. Metastatic mass
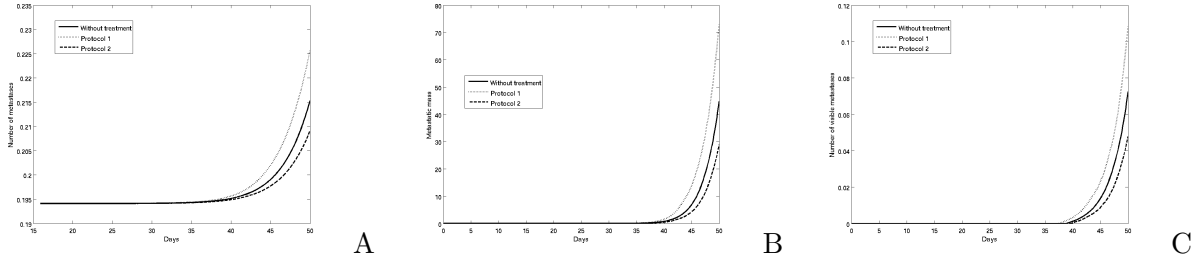
Figure 17: Influence of the scheduling. $A_\tau = 7$. Protocol 1 : 20 mg/day. Protocol 2 : 40 mg/2 days. A. Total number of metastases. B. Metastatic mass. C. Visible metastases

The two protocols have different implications : protocol 1 implies metastatic acceleration while protocol 2 results in deceleration of metastatic growth. These results are to be compared with the Figure 9.A from section 7.2.1.0 concerning primary tumor evolution, where the equivalent protocols give the opposite qualitative results, namely a better effect of protocol 1. Of course, what we observe here in the metastatic acceleration context (i.e., using equation (4) for the vascular dynamics of the metastases) is totally related to the PK of the drug. In comparing two schedulings, the one resulting in larger "boost" effect will be the one for which the total time above A_τ in the drug concentration time profile will be the largest (see Figure 13).

Again, the result depends on the value of the parameter A_τ, as shown in Figure 18 where we performed the same simulation with $A_\tau = 20$ and obtained the opposite result : protocol 1 is better than protocol 2.
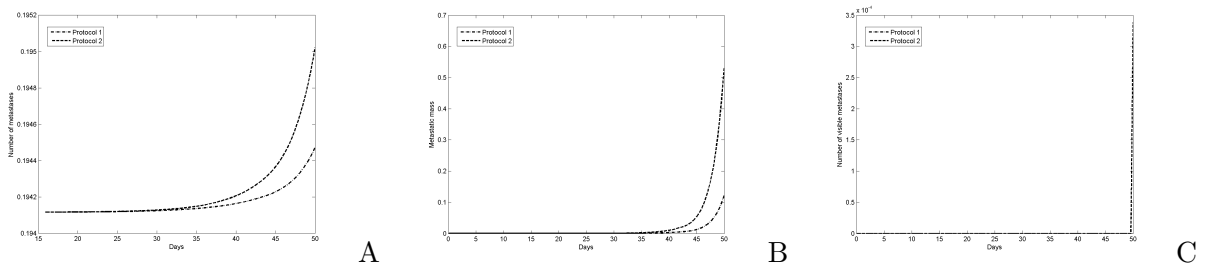
Figure 18: Influence of the scheduling. $A_\tau = 20$. Protocol 1 : 20 mg/day. Protocol 2 : 40 mg/2 days. A. Total number of metastases. B. Metastatic mass. C. Visible metastases

3.3 Perspectives

In this section, we proposed a modeling for describing metastatic acceleration after Sunitinib therapy observed in [ELCM$^+$09]. We based ourselves on a biological assumption these authors formulate. This assumption is an upregulation of pro-angiogenic factors which we translated in the model by an increase of the angiogenesis stimulation parameter c in response to the treatment, thus in the tumoral growth part of the model. However, other biological hypotheses can be formulated to explain this phenomenon :

1. In [PRAH$^+$09], mice experiments show an increased invasive phenotype and increased metastasis after AA therapy. One of their hypothesis is that this phenotypic change would be driven by hypoxia (lack of oxygen). The primary tumor cells, lacking of oxygen due to the action of the AA drug, would change their phenotype in order to escape the tumor area, which could enhance metastasis.

2. In another paper of Qu & al. [QGML10], entitled : "Antiangiogenesis therapy might have the unintended effect of promoting tumor metastasis by increasing an alternative circulatory system", the authors propose an hypothesis also related to hypoxia. When tumoral cells lack of oxygen, they would provoke formation of a parallel circulatory system through a phenomenon called vasculogenic mimicry [GCL$^+$07, LAL$^+$07].

These hypotheses of adaptive response of cancer cells to the treatment suggest to model the phenomenon by modification of the metastatic parameter m. An idea for a future work is to make this parameter depend on the vascular density of the tumor represented by $\delta = \frac{\theta}{x}$, thus changing β into

$$\beta(x, \theta) = m \left(\frac{\theta}{x} \right).$$

The shape to give to the function $\delta \mapsto m(\delta)$ is still to be defined. We can think to a unimodal function having one maximal value in δ^*. A very low value of δ should imply low metastasis since when there are no blood vessels detaching cells cannot escape. When δ is too high, vasculature is known not to be efficient and hence metastatic aggressiveness is not zero, but lower than in a hypoxia situation where it is enhanced due to development of vasculogenic mimicry. But other arguments may lead to a different shape for $\delta \mapsto m(\delta)$ as high vascular density seems to lead also to higher permeability of the vessels, more permissive for intravasation of cancerous cells.

Simulations of this model with anti-angiogenic therapy seems very interesting to perform.

4   Cytotoxic and anti-angiogenic drugs combination

An important problem in clinical oncology is to determine how to combine a cytotoxic drug (CT) that kills the proliferative cells and an anti-angiogenic (AA) drug which acts on the angiogenic process, either by blocking the angiogenic factors like VEGF (monoclonal antibodies, e.g. Bevacizumab) or by inhibiting the receptors to this molecule. The AA drugs are classified as part of the cytostatic drugs as they aim at stabilizing the disease. Two questions are still open : which drug should come before the other and then what is the best temporal repartition for each drug? Here, we perform a brief *in silico* study of the first question.

The treatments impact by reducing the tumoral growth rate. Following the log-kill assumption for chemotherapy which says that cytotoxic drugs kill a constant fraction of the tumoral cells (and not a constant number of them), the growth rate has the following expression

$$G(t, x, \theta) = \begin{pmatrix} ax \ln \left(\frac{\theta}{x} \right) - fC(t)(x - x_0)^+ \\ cx - dx^{2/3} - eA(t)(\theta - x_0)^+ \end{pmatrix}.$$

4.1 Mice parameters

Since we don't have real parameters for the cytotoxic drug we consider a one-compartmental PK model with expression (2), but with parameters clr_C and D_C that we arbitrarily fix to 1, as well as f. For the AA drug, we take the endostatin parameters from [HPFH99]. We perform simulations of the model to investigate combination of the CT and the AA. In Figure 19, we present the results of two simulations : one giving the AA before the CT (Fig. 19.A) and the other one doing the opposite (Fig. 19.B).
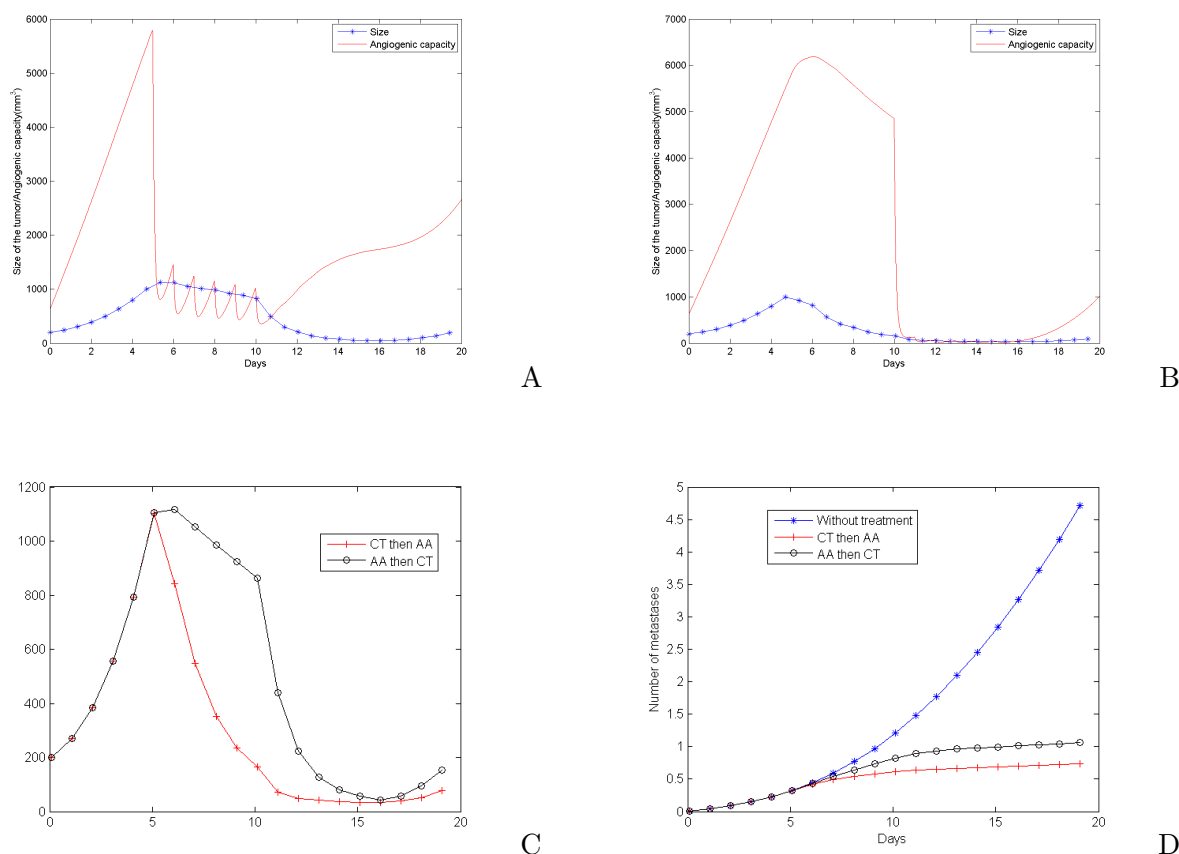
Figure 19: Combination of an anti-angiogenic drug (AA) : endostatin, with dose 20 mg and a cytotoxic one (CT). A. AA from day 5 to 10 then CT from day 10 to 15, every day. Tumor growth and vascular capacity. B. CT from day 5 to 10 then AA from day 10 to 15, every day. Tumor growth and vascular capacity. C : Comparison between both combinations on the tumor growth. D : Comparison between both combinations on the metastatic evolution.

Although in both cases the effect on the metastases is very good since the growth seems stopped (Fig. 19.D), it appears that the qualitative behaviors of the tumoral and metastatic responses are different regarding to the order of administration of the drugs (Fig. 19.C and 19.D). According to the model, it would be better to administrate first the CT in order to reduce the tumor burden and then use the AA to stabilize the disease. Indeed, the number of

metastasis at the end of the simulation is lower when the CT is applied first than in the opposite case. Of course, this conclusion depends on the tumoral growth and drugs parameters but this simulation shows that the model is able to exhibit different responses regarding to the order of administration between CT and AA drugs.

4.2   Human parameters. Etoposide + Bevacizumab

IConsidering a clinical setting, we evaluate the combination between Etoposide, which is a CT agent used in wide variety of cancers (lung, testicle cancers, lymphoma, leukemia...) and Bevacizumab (monoclonal antibody targeting Vascular Endothelial Growth Factor, used mainly in colorectal and breast cancers). Several recent clinical trials have been evaluating the combination of both drugs in lung cancers and glioblastoma, with mixed results [CBB$^+$11, STW$^+$11, RDP$^+$11, JWV$^+$10, FDM$^+$10]. The PK model and parameters for the CT drug are from [BFCI03] and for Bevacizumab we use the same values as in section 7.2.2. The PK model for Etoposide is two-compartmental with equations similar to (3) and parameter values are in table 5, with τ_C the infusion duration. As in section 7.2.2 we consider non-zero initial condition corresponding

Parameter	V_1	V_2	k_{10}	k_{20}	k_{12}	k_{21}	τ_C	f
Value	25	15	1.6	9.36	0.4	0	24	25
Unit	L	L	day^{-1}	day^{-1}	day^{-1}	day^{-1}	h	L·g^{-1}· day^{-1}

Table 5: Parameter values for the PK model for Etoposide. All parameters except f are from [BFCI03].

to the final state of the untreated system at time 1000 days.

In the Figure 20 we compare each monotherapy case to the combined treatment with the two drugs. The administration protocol for Bevacizumab is 5 mg/kg/2 weeks [LBE$^+$08] (with a virtual patient of 70 kg) and the Etoposide one is 0.5 g/m^2 at day 1 of the cycle [BFCI03] (virtual patient with a Body Surface Area of 1.75 m^2). We observe that, with the efficacity parameter e and f that we chose, the effect of the AA drug is to stabilize tumoral growth as well as the number of visible metastases. The CT has an important reduction effect and combination of both is strictly better than the two monotherapy cases since it allows to reduce the tumor burden and then stabilize it to a low level.

We ask now the question whether administrating the CT drug before or after the AA one. In the Figure 21 we simulated the two situations with one administration of each drug : either Bevacizumab at day 0 and Etoposide at day 8 or the opposite.

An interesting fact to observe is that the best way of combining both regarding to the tumor size, namely AA first and then CT is not the best for the total number of metastases, which rather suggests that the best is the CT first and then the AA. Although the difference between both is very low we still have qualitatively different answers for primary tumor size and metastases, for the problem of the order of administration.

As expressed several times all along this thesis, an actual important clinical problem is to know how to administrate anti-angiogenic (AA) and chemotherapies (CT) in combination. In
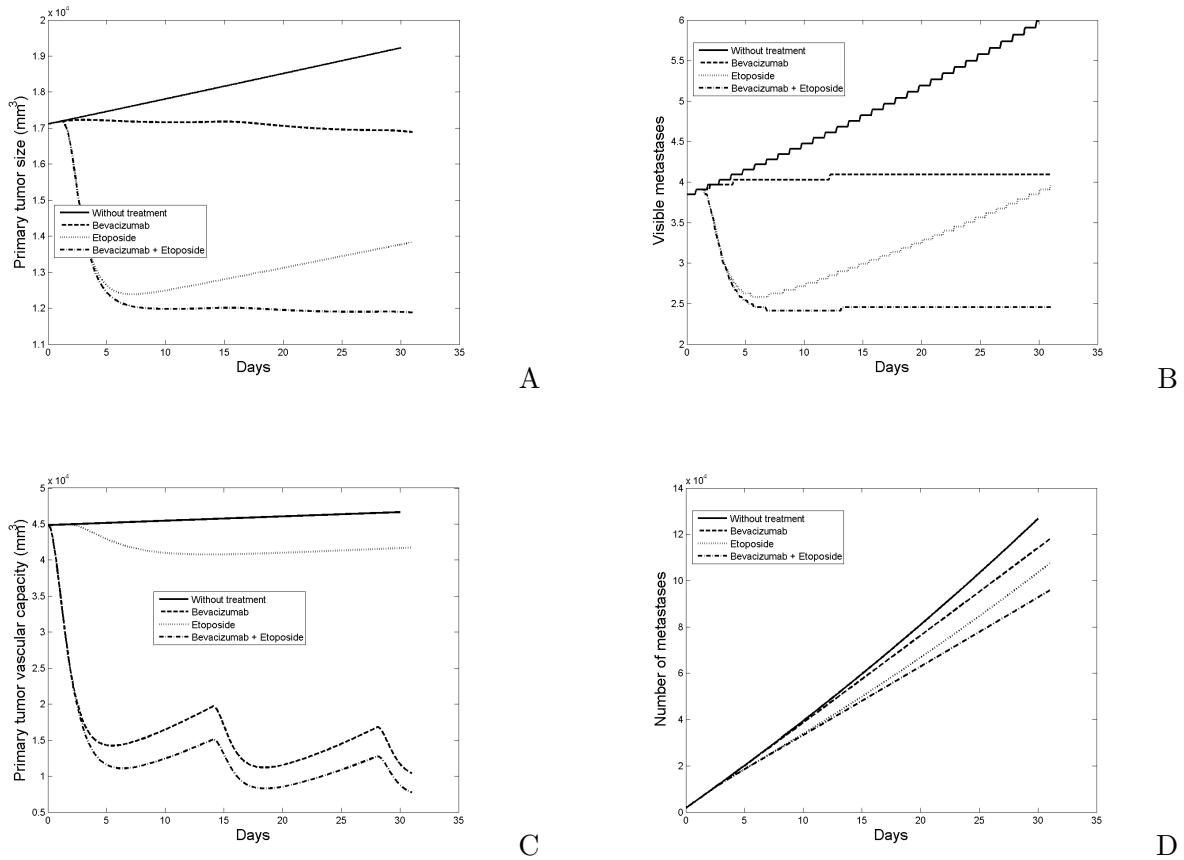
Figure 20: Comparison between the two monotherapy cases and the combined therapy. A : Primary tumor size. B : Visible metastases. C : Angiogenic capacity. D : Total number of metastases.

section 7.4 we performed simulations about this problem without integrating complex interactions between the AA and the CT (although interactions still are present, but implicitly). In particular, we did not explicitly take into account for the fact that delivery of the drug is achieved through the vascular system and thus the amount of drug reaching the tumor should depend on its vasculature. Moreover, the normalization effect of AA therapy [Jai01], also called "vascular pruning", which says that AA therapy is able to improve quality of the vasculature, should be taken into account.

In the publication [dG10a], d'Onofrio and Gandolfi enriched the Hahnfeldt - Folkman model by adding a term $\gamma\left(\frac{\theta}{x}\right)$ in front of the log-kill term for action of the CT. When using a unimodal function for γ in order to take into account for vascular pruning, it is possible to generate multistability under therapy in the ODE system. This could phenomenologically explain synergistic effects between the two drugs and also why therapy is ineffective in some cases. Furthermore, introducing stochastic effects yields to noise-induced transitions, studied in [dG10b], where the authors propose these transitions as explanation for fast relapse of the cancer disease. In the

Figure 21: Administer the CT before or after the AA? A : Primary tumor size. B : Visible metastases. C : Angiogenic capacity. D : Total number of metastases. These figures are part of the submitted publication [BBB⁺11].

chapter 2 of this thesis, we used a mechanistic model of vascular tumor growth in order to integrate this feature of angiogenesis through definition of a quality of the vasculature. We obtained numerical results suggesting an optimal delay between administration of the AA and the CT.

In this section, we present some current work on this problem, at intermediate level between the mechanistic model of chapter 2 and the complete phenomenological one from [dG10a].

Idea : model the biological fact that during angiogenesis, there is a **maturation process** of the vessels. They go from sprouts which are not effective to mature vessels able to deliver nutrients and drugs to the tumor.

4.3   Discrete structure of maturation

This subsection is some current work in collaboration with G. Chapuisat, J. Ciccolini, A. Erlinger and F. Hubert. We divide the carrying capacity K from the model of Hahnfeldt - Folkman,

supposed to be related to the tumoral vasculature, between two compartments : immature and mature vessels. We denote :

- V = tumoral volume (number of cells)

- I = immature vessels

- M = mature vessels

- A = effective concentration of anti-angiogenic (AA) agent

- C = effective concentration of chemotherapy (CT) agent

For the dynamics of the vasculature, we assume

1. Only mature vessels supply nutrients

2. Only immature vessels are subjected to stimulatory and inhibitory signals coming from the tumoral compartment, which are taken to be the one of Hahnfeldt - Folkman

3. Immature vessels maturate with a constant rate denoted by χ and mature vessels are subjected to natural apoptosis (rate τ).

For the dynamics of the therapy we assume :

4. The AA acts as a vessel-disruptive agent, only on the immature vessels.

5. The cytotoxic action of the chemotherapy is a modification of the classical log-kill term to take into account the balance of the two following effects :

   - When the effective vasculature (M) is low there is less delivery of the drug.
   - The "quality" of the tumor induced neo-vasculature is bad due to misorganisation of the vessels, resulting in a worse supply of the drug. This misorganisation is partially reolved by the "normalisation" effect/ vascular pruning of the AA drug.

   These considerations lead to model the effect of the drug as

$$ f\left(\frac{I}{V}\right) g(M)C(t) \tag{6} $$

with f a decreasing function of the immature vessels density and g an increasing function, such that $g(0) = 0$.

Remark 7.1. *Another possibility would be to take the function g depending on the mature vascular density $\frac{M}{V}$ since a very large tumor weakly vascularized should be less affected by the drug than a smaller one with the same amount of vessels. But this point remains unclear since in the log-kill assumption that an amount of drug kills a constant fraction of cells what is important is the total amount present at the tumor site. Assuming to be uniformly distributed gives expression (10).*

The complete set of equations writes

$$\dot{V} = aV \ln\left(\frac{M}{V}\right) - f\left(\frac{I}{V}\right) g(M)C \tag{7}$$

$$\dot{I} = bV - cV^{\frac{2}{3}}I - \chi I - \eta A \tag{8}$$

$$\dot{M} = \chi I - \tau M \tag{9}$$

Remark 7.2. *What we model for the delivery of the CT should also apply to the delivery of nutrients and thus maybe we should also modify the equation on the tumor evolution and replace M by $f\left(\frac{I}{V}\right) g(M)$ in $\ln\left(\frac{M}{V}\right)$.*

Simulations of this ODE model under action of Etoposide (CT) and Bevacizumab (AA) reveal an optimal delay between administration of the AA and the CT, as shown in Figure 23 (where, however, relative variation is quite low). The simulation corresponding to this Figure consists in one administration of first Bevacizumab, then Etoposide after some delay and to observe the size of the tumor at the end of the simulation, plotted against the delay.

Figure 22: Final size of the tumor plotted against the delay between administration of the AA and the CT

Interesting questions to be investigated can be

1. Theoretical study the behavior of the dynamical system in the case of constant infusion therapy. In particular, is there multistability?

2. In the case of multistability, investigate the possible effects of noise induce transitions.

3. Introduce a delay in the death of the vessels and study the resulting dynamical behavior in the parameter space.

4. More generally, look further at the various timescales involved.

5. Study an optimal control problem with this model and compare the structure of optimal solutions to previous study of CT/AA combination [dLMS09] which did not integrate for vascular pruning.

4.4 Continuous structure of maturation

This idea of possible future work is in collaboration with A. Gandolfi. In order to model more deeply the maturation process of the vessels, the idea is to structure the vessel population by maturity thus considering $n(t, x)$ the density of vessels with maturity $x \in [0, 1]$. Given some weighting functions $w_1(x) \leq 1$ and $w_2(x) \leq 1$ we define

$$\nu_1(t) = \int w_1(x)n(t, x)dx$$

and

$$\nu_2(t) = \int w_2(x)n(t, x)dx$$

representing respectively the inefficient and efficient ("immature" and "mature") vasculature. Note that $\nu_1 + \nu_2$ is not necessarily equal to $\int n(t, x)dx$, the sum can be greater due to some overlapping.

The equations write

$$\begin{cases} \dot{V} = aV \ln\left(\frac{\nu_2}{V}\right) - f\left(\frac{\nu_1}{V}\right) g\left(\nu_2\right) C \\ \partial_t n(t, x) + \partial_x(G(\int_0^1 n(t, x)dx)n(t, x)) = \delta(x, n) \\ G(0, \int_0^1 n(t, x)dx)n(t, 0) = b_1 V(t) + b_2(V) \int w_3(x)n(t, x)dx \end{cases}$$

with the maturity velocity $G(x, \int_0^1 n(t, x)dx)$ possibly depending on the total number of vessels, making the PDE nonlinear. An idea for the shape of G could be

$$G = \frac{1}{T_m(\int n)}$$

with T_m the time needed to maturate given by

$$T_m = r + \alpha \frac{\int n}{V}.$$

The boundary condition expresses that the input of endothelial cells results from stimulation by the primary tumor and proliferation, with $w_3(x) \leq w_1(x)$. In first approximation, $b_2(V)$ can be simply constant. Some biological insights about the maturation process have to be further studied, starting with the work of Yenkopoulos (in particular about angiopoïetins Ang1 - Ang2).
The death term $d(x, n)$ has to be clarified and should be inspired from the inhibition term of Hahnfeldt-Folkman. An expression which would allow to recover the model of Hahnfeldt - Folkman as a particular case is $\delta(x, n) = -dV^{\frac{2}{3}}M(t)\mathbf{1}_{x \in]0.5, 1[}$ but it seems irrelevant that inhibition acts on mature vessels. It should more probably act on immature vessels.

Interesting questions/problems in this framework could be

1. Perform simulations and look at the shape of the maturity distribution, without drug.

2. Perform mathematical analysis of the equations

4.5   Perspectives

In this section we performed simulations about CT/AA combination without integrating complex interactions between the AA and the CT (although interactions still are present, but implicitly). In particular, we did not explicitly take into account for the fact that delivery of the drug is achieved through the vascular system and thus the amount of drug reaching the tumor should depend on its vasculature. Moreover, the normalization effect of AA therapy [Jai01], also called "vascular pruning", which says that AA therapy is able to improve quality of the vasculature, should be taken into account.

In the publication [dG10a], d'Onofrio and Gandolfi enriched the Hahnfeldt - Folkman model by adding a term $\gamma\left(\frac{\theta}{x}\right)$ in front of the log-kill term for action of the CT. When using a unimodal function for γ in order to take into account for vascular pruning, it is possible to generate multi-stability under therapy in the ODE system. This could phenomenologically explain synergistic effects between the two drugs and also why therapy is ineffective in some cases. Furthermore, introducing stochastic effects yields to noise-induced transitions, studied in [dG10b], where the authors propose these transitions as explanation for fast relapse of the cancer disease. In the chapter 2 of this thesis, we used a mechanistic model of vascular tumor growth in order to integrate this feature of angiogenesis through definition of a quality of the vasculature. We obtained numerical results suggesting an optimal delay between administration of the AA and the CT.

We present now some current work on this problem, at intermediate level between the mechanistic model of chapter 2 and the complete phenomenological one from [dG10a].

Idea : model the biological fact that during angiogenesis, there is a **maturation process** of the vessels. They go from sprouts which are not effective to mature vessels able to deliver nutrients and drugs to the tumor.

Discrete structure of maturation

This subsection is some current work in collaboration with G. Chapuisat, J. Ciccolini, A. Erlinger and F. Hubert. We divide the carrying capacity K from the model of Hahnfeldt - Folkman, supposed to be related to the tumoral vasculature, between two compartments : immature and mature vessels. We denote :

- V = tumoral volume (number of cells)

- I = immature vessels

- M = mature vessels

- A = effective concentration of anti-angiogenic (AA) agent

- C = effective concentration of chemotherapy (CT) agent

For the dynamics of the vasculature, we assume

1. Only mature vessels supply nutrients

2. Only immature vessels are subjected to stimulatory and inhibitory signals coming from the tumoral compartment, which are taken to be the one of Hahnfeldt - Folkman

3. Immature vessels maturate with a constant rate denoted by χ and mature vessels are subjected to natural apoptosis (rate τ).

For the dynamics of the therapy we assume :

4. The AA acts as a vessel-disruptive agent, only on the immature vessels.

5. The cytotoxic action of the chemotherapy is a modification of the classical log-kill term to take into account the balance of the two following effects :

   • When the effective vasculature (M) is low there is less delivery of the drug.
   • The "quality" of the tumor induced neo-vasculature is bad due to misorganisation of the vessels, resulting in a worse supply of the drug. This misorganisation is partially reolved by the "normalisation" effect/ vascular pruning of the AA drug.

These considerations lead to model the effect of the drug as

$$f\left(\frac{I}{V}\right)g(M)C(t) \tag{10}$$

with f a decreasing function of the immature vessels density and g an increasing function, such that $g(0) = 0$.

Remark 7.3. *Another possibility would be to take the function g depending on the mature vascular density $\frac{M}{V}$ since a very large tumor weakly vascularized should be less affected by the drug than a smaller one with the same amount of vessels. But this point remains unclear since in the log-kill assumption that an amount of drug kills a constant fraction of cells what is important is the total amount present at the tumor site. Assuming to be uniformly distributed gives expression (10).*

The complete set of equations writes

$$\dot{V} = aV \ln\left(\frac{M}{V}\right) - f\left(\frac{I}{V}\right)g(M)C \tag{11}$$

$$\dot{I} = bV - cV^{\frac{2}{3}}I - \chi I - \eta A \tag{12}$$

$$\dot{M} = \chi I - \tau M \tag{13}$$

Remark 7.4. *What we model for the delivery of the CT should also apply to the delivery of nutrients and thus maybe we should also modify the equation on the tumor evolution and replace M by $f\left(\frac{I}{V}\right)g(M)$ in $\ln\left(\frac{M}{V}\right)$.*

Simulations of this ODE model under action of Etoposide (CT) and Bevacizumab (AA) reveal an optimal delay between administration of the AA and the CT, as shown in Figure 23 (where, however, relative variation is quite low). The simulation corresponding to this Figure consists in one administration of first Bevacizumab, then Etoposide after some delay and to observe the size of the tumor at the end of the simulation, plotted against the delay.

Interesting questions to be investigated can be
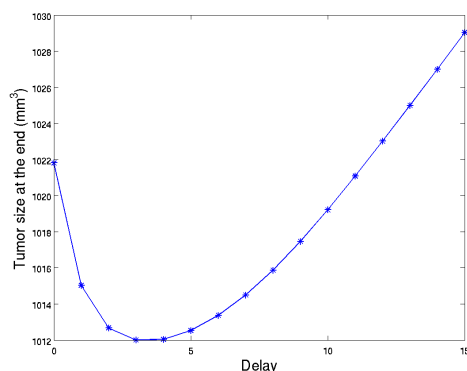
Figure 23: Final size of the tumor plotted against the delay between administration of the AA and the CT

1. Theoretical study the behavior of the dynamical system in the case of constant infusion therapy. In particular, is there multistability?

2. In the case of multistability, investigate the possible effects of noise induce transitions.

3. Introduce a delay in the death of the vessels and study the resulting dynamical behavior in the parameter space.

4. More generally, look further at the various timescales involved.

5. Study an optimal control problem with this model and compare the structure of optimal solutions to previous study of CT/AA combination [dLMS09] which did not integrate for vascular pruning.

Continuous structure of maturation

This idea of possible future work is in collaboration with A. Gandolfi. In order to model more deeply the maturation process of the vessels, the idea is to structure the vessel population by maturity thus considering $n(t,x)$ the density of vessels with maturity $x \in [0,1]$. Given some weighting functions $w_1(x) \leq 1$ and $w_2(x) \leq 1$ we define

$$\nu_1(t) = \int w_1(x)n(t,x)dx$$

and

$$\nu_2(t) = \int w_2(x)n(t,x)dx$$

representing respectively the inefficient and efficient ("immature" and "mature") vasculature. Note that $\nu_1 + \nu_2$ is not necessarily equal to $\int n(t,x)dx$, the sum can be greater due to some overlapping.

The equations write

$$\begin{cases} \dot{V} = aV \ln\left(\frac{\nu_2}{V}\right) - f\left(\frac{\nu_1}{V}\right) g\left(\nu_2\right) C \\ \partial_t n(t,x) + \partial_x (G(\int_0^1 n(t,x)dx)n(t,x)) = \delta(x,n) \\ G(0, \int_0^1 n(t,x)dx)n(t,0) = b_1 V(t) + b_2(V) \int w_3(x)n(t,x)dx \end{cases}$$

with the maturity velocity $G(x, \int_0^1 n(t,x)dx)$ possibly depending on the total number of vessels, making the PDE nonlinear. An idea for the shape of G could be

$$G = \frac{1}{T_m(\int n)}$$

with T_m the time needed to maturate given by

$$T_m = r + \alpha \frac{\int n}{V}.$$

The boundary condition expresses that the input of endothelial cells results from stimulation by the primary tumor and proliferation, with $w_3(x) \leq w_1(x)$. In first approximation, $b_2(V)$ can be simply constant. Some biological insights about the maturation process have to be further studied, starting with the work of Yenkopoulos (in particular about angiopoïetins Ang1 - Ang2).

The death term $d(x,n)$ has to be clarified and should be inspired from the inhibition term of Hahnfeldt-Folkman. An expression which would allow to recover the model of Hahnfeldt - Folkman as a particular case is $\delta(x,n) = -dV^{\frac{2}{3}}M(t)\mathbf{1}_{x\in]0.5,1[}$ but it seems irrelevant that inhibition acts on mature vessels. It should more probably act on immature vessels.

Interesting questions/problems in this framework could be

1. Perform simulations and look at the shape of the maturity distribution, without drug.

2. Perform mathematical analysis of the equations

5 Metronomic chemotherapy

During the last decade, a novel therapeutic approach called *metronomic chemotherapy* (also named low dose antiangiogenic therapy [BBK$^+$00]) appeared. Various Phase I studies have been performed [ARC$^+$08, BDH$^+$06, CFB$^+$04, SGH$^+$06, CRK$^+$08, KTR$^+$05, SVM$^+$06] using this new way of administrating cytotoxic agents which consists in giving the drug at low dose but as continuously as possible, whereas classical protocols administrate the Maximum Tolerate Dose (MTD) at the beginning of the therapy cycle, during a short time period followed by a large period without treatment dedicated to patient's recovery from severe toxicities, especially hematologial ones. Indeed, this scheduling of the drug is believed to have better efficacy, one argument being that it would generate less resistances in the cancerous cells population. However, metronomic schedules are now thought to be potentially more efficient while reducing the toxicities according to the paradigm that this low dose/time dense scheduling of the drug would

have important anti-angiogenic effect [KK04, HFH03]. Indeed, the endothelial cells which are proliferating during tumoral neo-angiogenesis are also targeted by the cytotoxic agent, while developping less resistances as they are genetically more stable than malignant cells. Moreover, the *dynamical* effect of metronomic schedules would be higher than the one of MTD protocoles. In this context, the open clinical problematic that physicians are facing is :

What is the best metronomic scheduling for chemotherapeutic agents?

In this section, we aim at using the Hahnfeldt - Folkman model to give insights on this issue, and observe the effect of metronomic schedules on the metastases population. As expressed above, one of the main ingredients explaining the benefit of metronomic schedules compared to MTD ones are the resistances, which we shall thus introduce in the model. We place ourselves in the context of breast cancer and will first consider a monotherapy situation with Docetaxel as the CT drug, and then combination of Docetaxel with Bevacizumab (monoclonal antibody targeting Vascular Endothelial Growth Factor).

5.1   Model

The main assumptions underlying our modeling of the metronomic paradigm are the following :

1. The CT has an anti-angiogenic effect by killing proliferative endothelial cells.

2. Cancerous cells develop resistances to the CT whereas endothelial cells don't.

3. The killing action of the drug is stronger on the endothelial compartment than on the tumoral one.

We start from the Hahnfeldt - Folkman, in which we integrate anti-angiogenic effect of a chemotherapy (assumption 1). We consider that the CT drug acts in both compartment : on the tumoral compartment x (classical cytotoxic effect) and on the vasculature θ (anti-angiogenic effect due to the killing of proliferative endothelial cells). The expression of the growth rate G is

$$G(t, X) = \left(\begin{array}{c} ax \ln \left(\frac{\theta}{x} \right) - C_1(t)(x - x_{min})^+ \\ cx - dx^{2/3}\theta - (eA(t) + C_2(t))(\theta - \theta_{min})^+ \end{array} \right) \tag{14}$$

where C_1 and C_2 are the exposures of the drug respectively on the tumoral cells and on the vascular compartment, defined from the output $C(t)$ of the PK model for Docetaxel expressed in mg· L^{-1}.

The PK model for Docetaxel is a three-compartmental model, coming from [BVV$^+$96]. Although it was initially designed as a model for hematotoxicity, we use the interface model from [MIB$^+$08] as PD model. All together, the equations are

$$\begin{cases} \dot{c}_1(t) = -k_e c_1(t) + k_{12}(c_1(t) - c_2(t)) - k_{13}(c_1(t) - c_3(t)) + \frac{I(t)}{V} \\ \dot{c}_2(t) = k_{21}(c_1(t) - c_2(t)) \\ \dot{c}_3(t) = k_{31}(c_1(t) - c_3(t)) \\ \dot{C}(t) = -\alpha_I e^{-\beta_I C(t)} C(t) + c_1(t) \end{cases} \tag{15}$$

The last equation is the interface model introduced in [MIB$^+$08] to model the effect (exposure) of the drug. It is intended to have more flexibility than just considering the area under the curve (which is obtained by taking $\alpha_I = 0$) or an effect compartment ($\beta_I = 0$). The term I stands for the drug input and writes

$$I(t) = \sum_{i=1}^{M} D_i \mathbf{1}_{t_i \leq t \leq t_i + \tau} \tag{16}$$

where $\{t_i; \ i = 1, .., M\}$ are the administration times of the drug, $\{D_i; \ i = 1, .., M\}$ the administrated doses and τ the injection duration. The parameter values used for the PK model can be found in table 6.

Parameter	V	k_{12}	k_{13}	k_e	k_{21}	k_{31}
Value	7.4	25.44	30.24	123.8	36.24	2.016
Unit	L	day^{-1}	day^{-1}	day^{-1}	day^{-1}	day^{-1}

Table 6: Parameter values of the PK model for Docetaxel [BVV$^+$96].

We take into account for the resistances (assumption 2) by assuming that each cell has probability $RC(t)$ to become resistant at time t. The probability of being resistant at time t is then exponentially distributed and we set

$$C_1(t) = \alpha_1 e^{-R \int_0^t C(s)ds} C(t), \quad C_2(t) = \alpha_2 C(t).$$

We transpose assumption 3 by taking $\alpha_2 > \alpha_1$. The parameter values for the PD model are in table 7.

Parameter	α_I	β_I	α_1	α_2	R	τ
Value	0.75	25	0.5	5	5	60
Unit	day^{-1}	L·mg^{-1}	L·mg^{-1}·day^{-1}	L·mg^{-1}·day^{-1}	L·mg^{-1}·day^{-1}	min

Table 7: Parameter values for the PD model for Docetaxel. Values α_I and β_I come from [MIB$^+$08]. Parameters α_1, α_2 and R were fixed arbitrarily.

The tumoral growth and metastatic parameters used in the simulations are those in table 2, coming from [IKN00] where they were fitted to data of a hepatocellular carcinoma. We take as non-zero initial condition the traits $(x_{0,p}, \theta_{0,p}) = (902.28, 15401)$ corresponding to the values reached by the primary tumor after 600 days when starting with one cell and the parameters from Table 2. We also take the corresponding value of $\rho(600)$ as ρ^0.

5.2 Simulation results

Metronomic Docetaxel In the publication [BDH$^+$06], for pediatric brain cancers, the authors compared a classical and a metronomic protocol. During 49-days therapy cycles, the classical protocol delivers 200 mg/m^2 of Temozolomide per day during the first 5 days whereas

the metronomic protocol gives 85 mg/m^2 per day during 42 days followed by a 7-day rest period. The total amount of drug delivered during a cycle are respectively 1000 mg/m^2 and 3570 mg/m^2, the second one being thus able to give more than 3.5 fold the total dose of the first one. We wish now to mimic this situation in the case of breast cancer with Docetaxel as CT and compare the two following schedules, based on a 21-day long therapy cycle :

1. MTD schedule : 100 mg at day 0, as considered in [MIB$^+$08].

2. Metronomic schedule : 10 mg/day every day, without resting period.

The total dose administrated during one cycle are respectively 100 mg and 210 mg. The simulation results for the tumoral evolution and the metastases are presented in Figure 24.

A

B

C

D
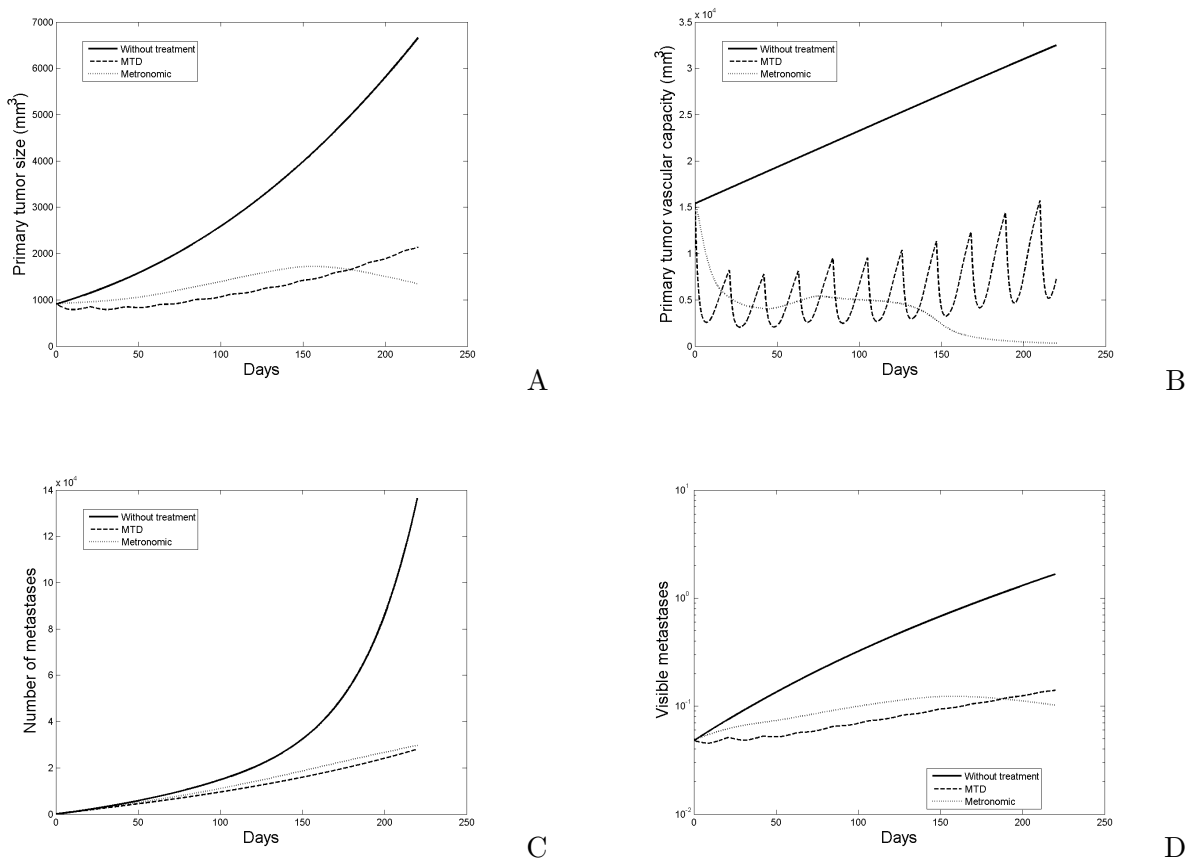
Figure 24: Comparison between MTD and metronomic schedules for Docetaxel. A. Primary tumor size. B. Primary tumor vascular capacity. C. Number of visible metastases.

We observe in Figure 24 that, at the beginning, the MTD schedule induces better tumoral reduction than the metronomic one, which exhibits only limited regression and even regrowth of the tumor. This could be misleading in practical situations since one could decide to stop the therapy when observing the regrowth. However, due to resistances the MTD schedule gets

worse and eventually doesn't contain regrowth of the primary tumor. On the opposite, for large times the metronomic schedule gives better results, being able to overcome the resistance phenomenon, and eventually leading to stable tumoral reduction, which still persists for times bigger than 220 days (simulation not shown). The explanation of this fact can be understood by looking at Figure 24.B representing the effect of the drug on the vascular capacity. While the MTD schedule doesn't provoke overall decrease of the vascular capacity on large time scale, the metronomic one ensures more deep and stable effect on the vasculature, which in the end explains the large time tumor decrease. Hence, the overall superiority of the metronomic schedule is explained in the model by the anti-angiogenic action of the drug. The MTD schedule does also exhibit anti-angiogenic effect but, combined with the intrinsic dynamic of the vasculature, it is not asymptotically efficient because the large rest period lets time for the vasculature to recover. The metronomic schedule on the contrary does not let time for vascular recovery and, since endothelial cells are not subjected to resistances to the drug, it is more efficient on large time scale.

On the metastases, we observe the same behavior on the number of visible metastases (Figure 24.D). While the untreated curve leads to apparition of one visible metastasis at the end of the simulation, both protocols don't. But the MTD schedule asymptotically has growing number of visible tumors whereas the metronomic one is able to decrease it and keep it under control. On the total number of metastases the MTD schedule is slightly better but we can suspect that for larger times both curves will cross since, according to Figure 24.A, all tumors will eventually decrease, thus leading to less emission of neo-metastases.

If the dose used in the metronomic schedule is too low, then it is not efficient, as shown in Figure 25 where the same metronomic schedule is simulated, but using a dose of 8 mg/day.
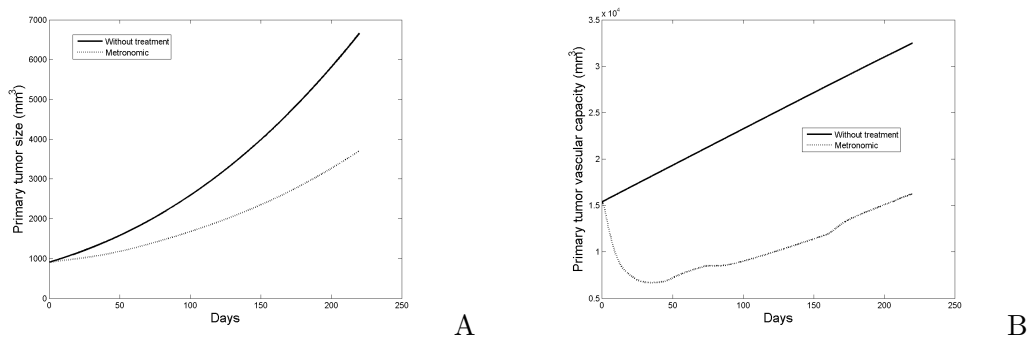
Figure 25: Metronomic schedule for Docetaxel with dose 8 mg/day. A. Tumor size. B. Vascular capacity

This result suggests that there is an optimal dose to use for metronomic schedules, and a mathematical model can be helpful in determining this optimum (see [BB11] for an optimal control problem for the scheduling). Integrating the toxicity issue in the model should help to further optimize the optimization of metronomic scheduling.

Metronomic Docetaxel + Bevacizumab We perform now the same comparison between metronomic schedule and classical one, but we add action of Bevacizumab. The scheduling that

we use for this last drug comes from [LBE$^+$08] and is 7.5 mg/kg every three weeks (Bevacizumab has a large half-life). We consider a virtual patient of 70 kg. The simulation results are plotted in Figure 26.
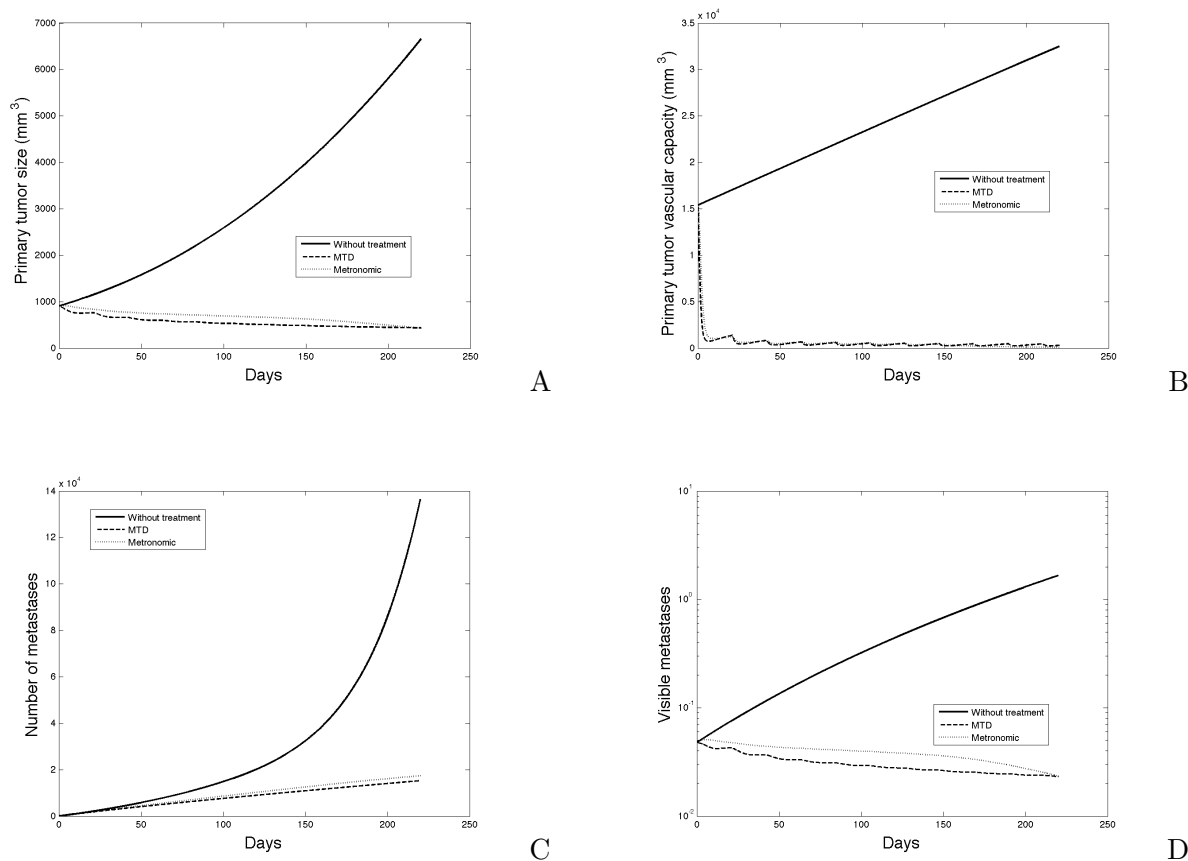
Figure 26: Comparison between MTD and metronomic schedules for Docetaxel in combination with Bevacizumab. A. Primary tumor size. B. Primary tumor vascular capacity. C. Total number of metastases. D. Number of visible metastases (log scale).

We observe that the two scheduling efficiently reduce the tumor size and control explosion of the total number of metastases and of the visible ones. If we look at evolution during the whole simulation time interval, the classical schedule is better than the metronomic one. Indeed, as shown in Figure 26.B when comparing it with Figure 24.B, addition of the AA drug ensures large reduction of the vasculature leading to tumor suffocation. This happens independently from the temporal administration protocol of the CT drug. Our model suggests thus no benefit of the metronomic schedule on the classical one in the case of combination therapy with AA drugs.

Chapter 8

An optimal control problem for the metastases

Although optimal control theory has been used for optimizing administration of anti-cancerous drugs with the aim of reducing primary tumor size, as far as we know metastases are never taken into account. In this chapter, we use our model for metastatic evolution to define optimal control problems at the scale of the entire organism of the patient. A theoretical study of the optimization problem written on the partial differential equation proves existence of a solution and derives a first order optimality system. Then we compare numerically in a simplified situation minimization criteria defined on the primary tumor and criteria on the metastases.

1 Optimal control of tumoral growth and metastases

1.1 Tumoral growth

Optimal control of tumoral growth by therapies has been the subject of various investigation, starting with administration of the chemotherapy (CT) (see for instance the work of Swan [Swa90, Swa88] and more recently the papers of Ledzewicz and Schättler [LS05, LS06]). The Model 1 project [BFCI03, MIB⁺08, BI01, IB00, IB94] drove a Phase I study by a mathematical model focused on hematotoxicity of the chemotherapies. The optimization schedule computed by the model allowed densification of a standard protocol while dynamically controlling the toxicities.

In the case of the tumoral growth described by the model of Hahnfeldt - Folkman [HPFH99] (see also section 1.3), optimal control problems have also been widely investigated, since the model allows for integration of anti-angiogenic (AA) therapy. Optimal schedules for AA treatments alone have been studied by Ledzewicz and Schättler in [LMS09, LMMS10, LS07, LLS09]. The combination of radiotherapy and AA treatment is studied in [ECW03], using a simplification of the Hahnfeldt - Folkman model. Recently, combination of CT and AA therapy has been considered in [dLMS09]. However, these model do not integrate the metastatic process.

Concerning the primary tumor, we will assume that its dynamics is given by the Hahnfeldt - Folkman model modified by the action of a therapy : denoting $X_p(t) = (x_p(t), \theta_p(t))$ the primary tumor state, $u(t) = \begin{pmatrix} u^1(t) \\ u^2(t) \end{pmatrix}$ with $u^1(t)$ and $u^2(t)$ the dose rates of CT and AA drugs respectively, we have

$$\dot{X}_p = \overline{G}(X_p; u), \quad \overline{G}(X; u) = G(X) - B(X)u(t), \quad G(X) = G(x, \theta) = \begin{pmatrix} ax \ln\left(\frac{\theta}{x}\right) \\ cx - dx^{2/3}\theta \end{pmatrix}, \quad (1)$$

with $B(X) \in \mathcal{L}(\mathbb{R}^2, \mathbb{R}^2)$, $B(X) \geq 0$ describing how does the treatment acts on the tumor. For example $B(X) = \begin{pmatrix} 0 & 0 \\ 0 & e\theta \end{pmatrix}$ for an AA drug alone.

Remark 8.1. *We assume in a first approximation that the input flow of the drug is the same than the efficient concentration acting on the tumor, thus neglecting the (important) role of pharmacokinetics and pharmacodynamics. This could be integrated by replacing $u(t)$ by $c(t, u(t))$ with c being a (possibly nonlinear) function describing the efficient concentration in function of the dose rate u.*

We will consider two criterions to be minimized for tumoral growth : the tumor size at the end time T and the maximal tumor reduction during the time interval $[0, T]$ and we denote

$$J_T(u) = x_p(T; u) \quad \text{and} \quad J_m(u) = \min_{t \in [0T]} x_p(t; u). \quad (2)$$

A minimization problem on the primary tumor (studied in [dLMS09]) then writes

Optimal control problem 1. *Find $\overline{u} \in \mathcal{U}_{ad}$ such that*

$$J_T(\overline{u}) = \min_{u \in \mathcal{U}_{ad}} J_T(u) \quad (3)$$

with $\mathcal{U}_{ad}$ being the space of admissible controls integrating toxicity constraints (see below for its expression). Changing J_T for J_m leads to the

Optimal control problem 2. *Find $\overline{u} \in \mathcal{U}_{ad}$ such that*

$$J_m(\overline{u}) = \min_{u \in \mathcal{U}_{ad}} J_m(u). \tag{4}$$

The same kind of criteria is used in the Model 1 project.

1.2   Formulation of an optimal control problem for the metastases.

Although the problem of best reduction of the primary tumor size is of great relevance for clinicians, the metastatic state cannot be neglected due to its importance in a cancer disease and its implication in the possibility of relapse. Two practical examples of clinical problematics that can lead to formulation of an optimal control problem for the metastases are given by :

1. In the case of metastatic breast cancer, after primary tumor resection. The clinician wants to control the number of metastases above a given size, for large time. He wants to give a combined CT - AA treatment such that in the next 20 years no visible metastasis appears.

2. In the context of metronomic CT (see section 7.5) that have the advantage to induce weaker hematological toxicities and thus don't require intricate modeling for this matter as in Model 1 [BFCI03]. The time horizon is then of the order of one year and resistances developed by cancerous cells have to be taken into account. The number of metastases and their sizes have to be kept under control.

However, in a first attempt to theoretically study the involved dynamics and for computational commodity as well as comparison with previous work on the primary tumor (in particular [LMMS10]), we will rather place ourselves in a framework where the time span is thought as being a therapy cycle, thus of the order of weeks.

The evolution of the metastases density $\rho(t, X; u)$ is given by

$$\begin{cases} \partial_t \rho(t, X; u) + \mathrm{div}(\rho(t, X; u)\overline{G}(X; u)) = 0 \\ -\overline{G}(t, \sigma; u) \cdot \nu(\sigma)\rho(t, \sigma; u) = N(\sigma) \left\{ \int_\Omega \beta(X)\rho(t, X; u)dX + \beta(X_p(t; u)) \right\} \\ \rho(0, X; u) = \rho^0(X) \end{cases} \tag{5}$$

Toxicity is now dealt by imposing constraints on u. We don't include a precise description of hematological toxicities. The common toxicities (like renal ones, for instance) are integrated by imposing, similarly as [dLMS09] :

1. Maximal local values for $u^1(t)$ and $u^2(t)$ denoted by u_{max} and v_{max}, respectively, which are non-negative constants.

2. Maximal total amounts of drug delivered (corresponding to the clinical Area Under the Curve (AUC)) : A_{max} for the AA and C_{max} for the CT, A_{max} and C_{max} being non-negative constants.

We consider thus the following space of admissible controls :

$$\mathcal{U}_{ad} = \left\{ u \in (L^\infty(0,T))^2; \begin{pmatrix} 0 \\ 0 \end{pmatrix} \leq u(t) \leq \begin{pmatrix} v_{max} \\ u_{max} \end{pmatrix} \ \forall t \text{ and } \int_0^T u(t)dt \leq \begin{pmatrix} C_{max} \\ A_{max} \end{pmatrix} \right\}.$$

Remark 8.2. *An easy way to integrate the resistances in the model would be to impose an exponential decrease of the effectiveness of the CT treatment and thus replacing the constraint on u^1 by : $0 \leq u^1(t) \leq e^{-Rt}v_{max}$, with $R > 0$.*

We will consider two criteria subjected to minimization for the metastases, given by

$$J(u) = \int_\Omega a(X)\rho(T,X;u)dX \quad \text{and } j(u) = \int_0^T \int_\Omega a(X)\rho(t,X;u)dXdt \tag{6}$$

with $a \geq 0$. Three examples of interest for a correspond to :

- the total number of metastases : $a_1(x,\theta) = 1$.

- the number of visible metastases : $a_2(x,\theta) = \mathbf{1}_{\{x \geq x_{min}\}}$, with x_{min} the minimal visible size (about 10^7 cells).

- the metastatic mass : $a_3(x,\theta) = x$.

The optimal control problem that we will consider is the following

Optimal control problem 3. *Find $\overline{u} \in \mathcal{U}_{ad}$ such that*

$$J(\overline{u}) = \min_{u \in \mathcal{U}_{ad}} J(u)$$

with possibly considering j instead of J.

2 Theoretical study

We define $Q :=]0,T[\times \Omega$ and do the following assumptions on the data 0

$$\beta \in W^{1,\infty}(\Omega), \ \rho^0 \in W^{1,\infty}(Q), \ \rho^0 \geq 0, \ N \in W^{1,\infty}(\partial\Omega), \ N \geq 0, \ \int_{\partial\Omega} N(\sigma)d\sigma = 1, \ a \in \mathcal{C}^\infty(\overline{\Omega}). \tag{7}$$

In the case of $a_2(x,\theta) = \mathbf{1}_{\{x \geq x_{min}\}}(x,\theta) \notin \mathcal{C}^\infty(\overline{\Omega})$ we take a as being a regularization of this function. Defining $\Sigma = \{(1,\theta); \ 1 < \theta < b\}$ we also assume that there exists $\delta > 0$ such that

$$\text{supp}N \subset \Sigma, \quad -\overline{G}(t,\sigma) \cdot \nu(\sigma) \geq \delta > 0, \ a.e.(t,\sigma) \in [0,T] \times \Sigma. \tag{8}$$

Finally, we assume the following compatibility condition for regularity issues, although in the case of our model it is not true

$$-\overline{G}(t,\sigma) \cdot \nu(\sigma)\rho^0(\sigma) = N(\sigma) \left\{ \int_\Omega \beta(X)\rho^0(X)dX + \beta(X_p(0)) \right\}. \tag{9}$$

2.1   Existence of an optimal solution

We first prove existence of a solution to the optimal control problem 3 (the following proposition as well as its proof still holds *verbatim* for j).

Theorem 8.3. *Under the assumptions* (7), (8) *and* (9) *there exists* $u^* \in \mathcal{U}_{ad}$ *such that*

$$J(u^*) \leq J(u), \quad \forall u \in \mathcal{U}_{ad}.$$

The proof of the theorem is based on the following proposition establishing $W^{1,\infty}$ bounds on the solution ρ of (5).

Proposition 8.4. *Under the assumptions* (7), (8) *and* (9) *if* $\rho(u)$ *is the solution of* (5), *then* $\rho(u) \in W^{1,\infty}(Q)$ *and there exists a continuous function* C *which can be explicited in terms of* $||\beta||_{W^{1,\infty}(\Omega)}$, $||N||_{W^{1,\infty}(\partial\Omega)}$, $||G||_{L^\infty(\Omega)}$ *and* $||B||_{L^\infty(\Omega)}$ *such that, for all* $u \in \mathcal{U}_{ad}$

$$||\rho(u)||_{W^{1,\infty}(Q)} \leq C(||u||_{L^\infty(Q)}). \tag{10}$$

Proof. For $u \in \mathcal{U}_{ad}$, let $\rho(u) = \rho(t, X; u)$ be the solution of (5). Following the method of the chapter 5, we use the flow $\Phi(t, \tau, \sigma; u)$ associated to the EDO $\frac{d}{dt}\Phi = \overline{G}(\Phi; u)$, that is $\Phi(t, \tau, \sigma; u)$ is the solution of this ODE being in σ at time τ. We consider the entrance time $\tau^t(X)$ and entrance point $\sigma^t(X)$ for a point $X \in \Omega$ given by

$$\tau^t(X) := \inf\{0 \leq \tau \leq t; \ \Phi(\tau; t, X) \in \Omega\}, \ \sigma^t(X) := \Phi(\tau^t(X); t, X).$$

and introduce the sets

$$\Omega_1^t = \{X \in \Omega; \ \tau^t(X) > 0\}, \ \Omega_2^t = \{X \in \Omega; \ \tau^t(X) = 0\}$$

as well as

$$Q_1 := \{(t, X) \in [0, T] \times \overline{\Omega}; \ X \in \overline{\Omega}_1^t\}, \ Q_2 := \{(t, X) \in [0, T] \times \overline{\Omega}; \ X \in \overline{\Omega}_2^t\}$$

and also define $\widetilde{Q_1} := \{(t, \tau, \sigma); \ 0 \leq \tau \leq t \leq T, \ \sigma \in \partial\Omega\} = \Phi^{-1}(Q_1)$. We define the two following changes of variables

$$\Phi_1 : \begin{array}{ccc} \widetilde{Q}_1 & \to & Q_1 \\ (t, \tau, \sigma) & \mapsto & (t, \Phi(t; \tau, \sigma; u)) \end{array} \quad \text{and } \Phi_2 : \begin{array}{ccc} [0, T] \times \overline{\Omega} & \to & Q_2 \\ (t, Y) & \mapsto & (t, \Phi(t; 0, Y; u)) \end{array}$$

and set

$$\widetilde{\rho}_1(t, \tau, \sigma; u) := \rho(\Phi_1(t; \tau, \sigma; u))J_1(t; \tau, \sigma; u) \text{ and } \widetilde{\rho}_2(t, Y; u) := \rho(\Phi_2(t, 0, Y; u))J_2(t, Y; u) \tag{11}$$

with

$$J_1(t, \tau, \sigma; u) = |\overline{G}(\tau, \sigma) \cdot \nu(\sigma)|e^{\int_\tau^t \text{div}\,\overline{G}(s, \Phi(\tau, \sigma; u))ds} \text{ and } J_2(t, Y; u) = e^{\int_0^t \text{div}\,\overline{G}(\Phi(s, 0, Y; u))ds}. \tag{12}$$

We have

$$\rho(t, X; u) := \widetilde{\rho}_1(\Phi_1^{-1}(t, X; u))J_1^{-1}(\Phi_1^{-1}(t, X; u))\mathbf{1}_{(t,X)\in Q_1} + \widetilde{\rho}_2(\Phi_2^{-1}(t, X; u))J_2^{-1}(\Phi_2^{-1}(t, X; u))\mathbf{1}_{(t,X)\in Q_2} \tag{13}$$

with $(\tilde{\rho}_1, \tilde{\rho}_2)$ solving the problems

$$
\begin{cases}
\partial_t \tilde{\rho}_1(t, \tau, \sigma; u) = 0 & 0 < \tau \le t < T, \ \sigma \in \partial\Omega \\
\tilde{\rho}_1(\tau, \tau, \sigma; u) = N(\sigma)\left\{\widetilde{B}(\tau, \tilde{\rho}_1, \tilde{\rho}_2) + \beta(X_p(\tau; u))\right\} & 0 < \tau < T, \ \sigma \in \partial\Omega
\end{cases}
\tag{14}
$$

where we denoted

$$
\widetilde{B}(\tau, \tilde{\rho}_1, \tilde{\rho}_2) = \int_0^\tau \int_{\partial\Omega} \beta(\Phi(\tau; s, \sigma; u))\tilde{\rho}_1(\tau, s, \sigma; u)d\sigma ds + \int_\Omega \beta(\Phi(\tau; 0, Y; u))\tilde{\rho}_2(\tau, Y; u)dY,
$$

and

$$
\begin{cases}
\partial_t \tilde{\rho}_2(t, Y; u) = 0 & t > 0, \ Y \in \Omega \\
\tilde{\rho}_2(0, Y; u) = \rho^0(Y) & Y \in \Omega.
\end{cases}
\tag{15}
$$

We have the following lemma on the regularity of $\tilde{\rho}_1$ solving (14).

Lemma 8.5. *Let F, $\beta \in W^{1,\infty}(\widetilde{Q}_1)$, $N \in W^{1,\infty}(\partial\Omega)$, $T > 0$ and $\rho \in L^\infty(\widetilde{Q}_1)$ be the solution of the following problem*

$$
\begin{cases}
\partial_t \rho = 0 & \widetilde{Q} \\
\rho(\tau, \tau, \sigma) = N(\sigma)\int_0^\tau \int_{\partial\Omega} \beta(\tau, \tau', \sigma')\rho(\tau, \tau', \sigma')d\tau d\sigma' + F(\tau, \sigma) & [0, T] \times \partial\Omega
\end{cases}
\tag{16}
$$

We also assume $\mathrm{supp}N$, $\mathrm{supp}_\sigma F \subset \Sigma$. Then $\rho \in W^{1,\infty}(\widetilde{Q}_1)$, with support in $R := \{(t, \tau, \sigma) \in \widetilde{Q}; \ \sigma \in \Sigma\}$ and

$$
||\rho||_{W^{1,\infty}} \le C(||\beta||_{L^\infty}, ||\partial_t\beta||_{L^\infty}, ||N||_{W^{1,\infty}}, ||F||_{W^{1,\infty}})
$$

with C being a continuous function which can be explicited.

Proof. From the equation, we have $\partial_t\rho \in L^\infty(\widetilde{Q}_1)$. Then, the solution of (16) is given by, for almost every $(t, \tau, \sigma) \in \widetilde{Q}_1$

$$
\rho(t, \tau, \sigma) = N(\sigma)\int_0^\tau \int_{\partial\Omega} \beta(\tau, s, \sigma')\rho(\tau, s, \sigma')ds d\sigma' + F(\tau, \sigma)
\tag{17}
$$

from which we get, in the distribution sense

$$
\partial_\tau \rho(t, \tau, \sigma) = N(\sigma)\Big\{\int_{\partial\Omega} \beta(\tau, \tau, \sigma')N(\sigma')\int_0^\tau \int_{\partial\Omega} \beta(\tau, s, \sigma'')\rho(\tau, s, \sigma'')ds d\sigma'' + F(\tau, \sigma')
$$

$$
+ \int_0^\tau \int_{\partial\Omega} \partial_\tau\beta(\tau, s, \sigma')\rho(\tau, s, \sigma') + \beta(\tau, s, \sigma')\partial_t\rho(\tau, s, \sigma')ds d\sigma'\Big\} + \partial_\tau F(\tau, \sigma)
$$

as well as

$$
\partial_\sigma \rho(t, \tau, \sigma) = \partial_\sigma N(\sigma)\int_0^\tau \int_{\partial\Omega} \beta(\tau, s, \sigma')\rho(\tau, s, \sigma')ds d\sigma' + \partial_\sigma F(\tau, \sigma)
$$

and prove that $\rho \in W^{1,\infty}(\widetilde{Q}_1)$. Formula (17) also proves the assertion on the support of ρ.

The $W^{1,\infty}$ bound (10) comes from the above explicit expressions and the following L^1 bound : for all $t \in [0, T]$

$$
\int_0^t \int_{\partial\Omega} |\rho(t, s, \sigma)|\, ds d\sigma \le \int_0^t e^{(t-s)||\beta||_{L^\infty}} \int_{\partial\Omega} |F(s, \sigma)|\, ds d\sigma.
$$

It is derived by applying a Gronwall lemma to the following inequality, obtained from equation (16)

$$
\frac{d}{dt}\int_0^t \int_{\partial\Omega} |\rho(t, \tau, \sigma)|\, d\sigma d\tau \le ||\beta||_{L^\infty}\int_0^t \int_{\partial\Omega} |\rho(t, \tau, \sigma)|\, d\sigma d\tau + \int_{\partial\Omega} |F(t, \sigma)|\, d\sigma.
$$

$\square$

We apply the previous lemma to $\widetilde{\rho}_1$ solving (14) by using $\widetilde{\beta}(t,\tau,\sigma) = \beta(\Phi(t,\tau,\sigma;u))$ and

$$F(\tau,\sigma) = N(\sigma)\left\{\int_\Omega \beta(\Phi(\tau,0,Y;u)\widetilde{\rho}_2(\tau,Y)dY + \beta(X_p(\tau))\right\}$$
$$= N(\sigma)\left\{\int_\Omega \beta(\Phi(\tau,0,Y;u)\rho^0(\tau,Y)dY + \beta(X_p(\tau))\right\}.$$

We observe that $||\widetilde{\beta}||_{L^\infty(\widetilde{Q})} = ||\beta||_{L^\infty(\Omega)}$ and

$$\partial_t\widetilde{\beta} = \nabla\beta \cdot \partial_t\Phi = \nabla\beta \cdot G(X) - \nabla\beta \cdot Bu$$

so

$$||\partial_t\beta||_{L^\infty(\widetilde{Q})} \leq ||\nabla\beta||_{L^\infty(\Omega)}\left\{||G||_{L^\infty(\Omega)} + ||B||_{L^\infty(\Omega)}||u||_{L^\infty(0,T)}\right\}.$$

Thus we have, since the $W^{1,\infty}$ norm of F is controlled by the $W^{1,\infty}$ norms of N, β and ρ^0 that

$$||\widetilde{\rho}_1(u)||_{W^{1,\infty}(\widetilde{Q}_1)} \leq C(||u||_{L^\infty(0,T)})$$

with C a continuous function.

We wish now to end the proof by recovering regularity on ρ using formula (13).

- From the assumption (8), we have that Φ_1 is an homeomorphism bilipschitz on R. Hence the chain rule applies on R and $\widetilde{\rho}_1 \circ \Phi_1^{-1} \in W^{1,\infty}(\Phi_1(R))$ and also

$$\rho_1 := \widetilde{\rho}_1 \circ \Phi_1^{-1}J_1^{-1} \in W^{1,\infty}(\Phi_1(R)).$$

- Since $\mathrm{supp}\widetilde{\rho}_1 \subset R$, then $\widetilde{\rho}_1 \circ \Phi_1^{-1}J_1^{-1} = \widetilde{\rho}_1 \circ \Phi_1^{-1}J_1^{-1}\mathbf{1}_{\{\Phi_1(R)\}} \in W^{1,\infty}(Q_1)$

- Φ_2 is always bilipschitz thus $\rho_2 := \widetilde{\rho}_2 \circ \Phi_2^{-1}J_2^{-1} \in W^{1,\infty}(Q_2)$.

Now we rewrite formula (13) as $\rho = \rho_1\mathbf{1}_{\{Q_1\}} + \rho_2\mathbf{1}_{\{Q_2\}}$. Since $Q_1 \cap Q_2 = \{\Phi(t,0,\sigma;u),;\ t \in [0,T], \sigma \in \partial\Omega\}$, we compute

$$\rho_1(t,\Phi(t,0,\sigma;u)) = -\left(\overline{G}(0,\sigma)\cdot\nu(\sigma)\right)^{-1}\widetilde{\rho}_1(t,0,\sigma)e^{-\int_0^t \mathrm{div}\,\overline{G}(s,\Phi(s,\tau,\sigma;u))ds}$$
$$= \left(\overline{G}(0,\sigma)\cdot\nu(\sigma)\right)^{-1}N(\sigma)\left\{\int_\Omega \beta(\Phi(\tau,0,Y;u)\rho^0(\tau,Y)dY + \beta(X_p(\tau))\right\}e^{-\int_0^t \mathrm{div}\,\overline{G}(s,\Phi(s,\tau,\sigma;u))ds}$$

and

$$\rho_2(t,\Phi(t,0,\sigma;u)) = \widetilde{\rho}_2(t,\sigma)e^{-\int_0^t \mathrm{div}\,\overline{G}(s,\Phi(s,\tau,\sigma;u))ds} = \rho^0(\sigma)e^{-\int_0^t \mathrm{div}\,\overline{G}(s,\Phi(s,\tau,\sigma;u))ds}.$$

Hence, using the compatibility condition (9) we obtain that $\rho \in \mathcal{C}(Q)$ which, combined with $\rho_{|Q_1} \in W^{1,\infty}(Q_1)$ and $\rho_{|Q_2} \in W^{1,\infty}(Q_2)$ gives $\rho \in W^{1,\infty}(Q)$. The $W^{1,\infty}$ bound (10) follows from formula (13), the $W^{1,\infty}$ bounds on $\widetilde{\rho}_1$ and on $\widetilde{\rho}_2$ (this last one coming from explicit solution of (15)), the chain rule and $W^{1,\infty}$ estimates on $\Phi_{1|\Phi(R)}^{-1}$ (using assumption (8)) as well as on Φ_2^{-1}, J_1^{-1} and J_2^{-1}. $\square$

Since $\{J(u);\ u \in \mathcal{U}_{ad}\}$ is bounded by zero by below from the positivity of the solution it has a finite lower bound and there exists a sequence u_n in $\mathcal{U}_{ad}$ such that

$$J(u_n) \xrightarrow[n \to \infty]{} \inf_{u \in \mathcal{U}_{ad}} J(u). \tag{18}$$

Since $\mathcal{U}_{ad}$ is bounded, from the estimate (10) we obtain that the family $\rho(u_n)$ is bounded in $W^{1,\infty}(Q)$. Using Ascoli-Arzela theorem there exists $\rho^* \in \mathcal{C}(Q)$ and a subsequence still denoted $\rho(u_n)$ such that $\rho(u_n) \xrightarrow[n \to \infty]{\mathcal{C}(Q)} \rho^*$. The weak formulation of the problem (5) writes : for all $\phi \in \mathcal{C}_c^1([0,T[\times\overline{\Omega})$

$$\int_0^T \int_\Omega \rho(t,X;u_n)\left[\partial_t\phi(t,X) + G(X)\cdot\nabla\phi(t,X) - u_n(t)B(X)\cdot\nabla\phi(t,X)\right]dtdX +$$

$$\int_\Omega \rho^0(X)\phi(0,X)dX + \int_0^T \int_{\partial\Omega} \phi(t,\sigma)N(\sigma)\left\{\int_\Omega \beta(X)\rho(t,X;u_n)dX + \beta(Xp(t;u_n))\right\}d\sigma dt = 0$$

and thus the convergence of $\rho(u_n)$ in $\mathcal{C}(Q)$ and the $*$- weak L^∞ convergence of u_n are sufficient to pass to the limit in order to obtain, using uniqueness of the solution to the problem (5) (see section 5.1.2), that $\rho^* = \rho(u^*)$. Now

$$J(u_n) = \int_\Omega a(X)\rho(T,X;u_n)dX \xrightarrow[n \to \infty]{} \int_\Omega a(X)\rho(T,X;u^*)dX = J(u^*)$$

Using (18) we get $J(u^*) = \inf_{u \in \mathcal{U}_{ad}} J(u)$, which ends the proof of the theorem.

2.2 Optimality system

In this section, we neglect the source term in the boundary condition of (5) and take it equal to zero.

Case $J(u) = \int_Q a(X)\rho(t,X;u)dtdX$.

If u^* is a solution of the optimal control problem 3, we have

$$J'(u^*)\cdot(v - u^*) \geq 0, \quad \forall v \in \mathcal{U}_{ad}.$$

Here we have, for all $u,\ v \in L^2(Q)$

$$J'(u)\cdot(v - u) = \int_Q a(X)z(t,X;\rho^*,u^*,v)\,dX\,dt.$$

where $z = z(\rho^*,u^*,v) = D_u\rho(u^*)\cdot(v - u^*)$ and $\rho^* = \rho(u^*)$. Thus

$$\int_Q a\,z(\rho^*,u^*,v)\,dX\,dt \geq 0, \quad \forall v \in \mathcal{U}_{ad}, \tag{19}$$

Notice that $z \in \mathcal{X}$ and that it satisfies

$$\begin{cases} \partial_t z + \operatorname{div}(z\overline{G}(X,u^*)) = \operatorname{div}(\rho^*B(X)\cdot(v - u^*)) \\ -G\cdot\nu(t,\sigma;u^*)z(t,\sigma;u^*) = N(\sigma)\left\{\int_\Omega \beta(X)z(t,X;u^*)dX + \nabla\beta(X_p(t;u^*))\cdot D_uX_p(t;u^*)\cdot(v - u^*)\right\} \\ z(0,X;u^*) = 0. \end{cases} \tag{20}$$

We will also need the Cauchy problem solved by $Y(t; u^*) := D_u X_p(t; u^*) \cdot (v - u^*) \in \mathbb{R}^2$ which is

$$\begin{cases} \dot{Y}(t; u^*) = D_X \overline{G}(X_p(t; u^*)) Y(t; u^*) - B(X_p(t; u^*))(v - u^*) \\ Y(0; u^*) = 0 \end{cases} \tag{21}$$

In order to simplify the optimality condition (19), we introduce the adjoint problem of (20). Let $p^* \in H^1(Q)$ solving

$$\begin{cases} -\partial_t p^*(t, X; u^*) - \overline{G}(X; u^*) \nabla p^*(t, X; u^*) - \beta(X) \int_{\partial \Omega} N(\sigma) p^*(t, \sigma) d\sigma = -a \\ \qquad\qquad\qquad\qquad\qquad p^*(T) = 0. \end{cases} \tag{22}$$

Such a p^* exists thanks to the following proposition 8.6. We introduce also the adjoint $\xi^*(t; u) \in \mathbb{R}^2$ of the problem (21) with a particular source term

$$\begin{cases} \dot{\xi}(t; u^*) = -\left(D_X \overline{G}\right)^T (t, X_p^*(t; u^*)) \xi(t; u^*) - \nabla \beta(X_p^*(t; u^*)) \int_{\partial \Omega} N(\sigma) p^*(t, \sigma; u^*) d\sigma \\ \xi(T) = 0 \end{cases}$$

We replace a from the first equation of (22) into (19) to obtain

$$\int_Q (-\partial_t p^*(t, X; u^*) - \overline{G}(X; u^*) \nabla p^*(t, X; u^*) - \beta(X) \int_{\partial \Omega} N(\sigma) p(t, \sigma) d\sigma) z \, dx \, dt \leq 0, \quad \forall v \in \mathcal{U}_{ad}.$$

By integration by part (valid since p^* is in a suitable space and $z \in \mathcal{X}$) we have

$$\int_0^T \int_\Omega p^* \operatorname{div}(\rho^* B(v - u^*)) \, dX - \left[\dot{\xi} + \left(D_X \overline{G}\right)^T \xi \right] \cdot Y \, dt \leq 0 \quad \forall v \in \mathcal{U}_{ad}$$

and another integration by part in time yields

$$\int_0^T \int_\Omega p^* \operatorname{div}(\rho^* B(v - u^*)) \, dX - \xi B(X_p(u^*))(v - u^*) \, dt \leq 0 \quad \forall v \in \mathcal{U}_{ad}$$

We deduce the following optimality system :

$$\begin{cases} \partial_t \rho^* + \operatorname{div}(\rho^* \overline{G}(u^*)) = 0 \\ -G \cdot \nu(t, \sigma; u^*) \rho^*(t, \sigma; u^*) = N(\sigma) \left\{ \int_\Omega \beta(X) \rho^*(t, X; u^*) dX + \beta(X_p(t; u^*)) \right\} \\ \rho^*(0, X; u^*) = \rho^0 \\ \dot{X}_p(t; u^*) = \overline{G}(t, X_p(t; u^*); u^*) \\ X_p(0; u^*) = 0 \\ -\partial_t p^*(t, X; u^*) - \overline{G}(X; u^*) \nabla p^*(t, X; u^*) - \beta(X) \int_{\partial \Omega} N(\sigma) p^*(t, \sigma) d\sigma = -a \\ p^*(T) = 0 \\ \dot{\xi}(t; u^*) = -\left(D_X \overline{G}\right)^T (t, X_p^*(t; u^*)) \xi(t; u^*) - \nabla \beta(X_p^*(t; u^*)) \int_{\partial \Omega} N(\sigma) p^*(t, \sigma; u^*) d\sigma \\ \xi(T) = 0 \\ < \int_\Omega \operatorname{div}(B \rho^*) p^* \, dX - \xi B(X_p(u^*)), (v - u^*) >_{L^2(0,T)^2} \leq 0, \quad \forall v \in \mathcal{U}_{ad}. \end{cases} \tag{23}$$

where $\operatorname{div}(\rho^* B)$ stands for the vector $\left(\operatorname{div}(\rho^* B^1), \operatorname{div}(\rho^* B^2) \right)$ with B^1, B^2 being the columns of B. We prove now the well-posedness, regularity and negativity of the adjoint problem (22).

Proposition 8.6. *Assume that $\beta \in \mathcal{C}^2(\Omega)$. There exists a unique solution $p \in \mathcal{C}^2(Q)$ to the problem (22). Moreover, if $\beta(X) > 0$ for all $X \in \Omega$ then*

$$p(t, X) < 0, \quad \forall (t, X) \in Q.$$

Proof. Using the method of characteristics, if a solution exists we have the following formula :

$$p(t, \Phi(t; T, z)) = \int_t^T \beta(\Phi(s; T, z)) \int_{\partial\Omega} N(\sigma)p(t, \sigma)d\sigma ds - \int_t^T a(\Phi(s; T, y))ds,$$

where $\Phi(t; T, z) = \Phi(t, T, z; u^*)$ is the characteristic being in z at time T, namely it is the solution of

$$\frac{d}{dt}\Phi(t; T, z) = \overline{G}(\Phi(t; T, z), u^*) \quad \Phi(T; T, z) = z.$$

If we set $\widetilde{p}(t, z) = p(t, \Phi(t; T, z))$, $\widetilde{\beta}(z) = \beta(\Phi(s; T, z))$ and $\widetilde{a}(t, z) = a(\Phi(t; T, z))$, we can rewrite it

$$\widetilde{p}(t, z) = -\int_t^T \widetilde{a}(s, z)ds + \int_t^T \widetilde{\beta}(s, z) \int_{\partial\Omega} N(\sigma)p_{|\partial\Omega}(s, \sigma)d\sigma, \quad \forall z \in \Omega. \tag{24}$$

We need the following compatibility condition on $p(t, \sigma)$ for $\sigma \in \partial\Omega$, using that $\sigma = \Phi(t; T, z) \Leftrightarrow z = \Phi(T; t, \sigma)$ and defining $z(t, \sigma) = \Phi(T; t, \sigma)$, $f(t, \sigma) := p(t, \Phi(T; t, \sigma))$:

$$f(t, \sigma) = -\int_t^T \widetilde{a}(s, z(t, \sigma))ds + \int_t^T \widetilde{\beta}(s, z(t, \sigma)) \int_{\partial\Omega} N(\sigma)f(s, \sigma)d\sigma ds. \tag{25}$$

The following lemma solves this fixed point problem.

Lemma 8.7. *Let $\beta \in \mathcal{C}^1(\Omega)$. There exists a unique solution $\overline{f} \in \mathcal{C}^1([0, T]; \mathcal{C}(\partial\Omega))$ to the integral equation* (25). *Moreover*

$$\overline{f}(t, \sigma) < 0, \quad \forall t \in [0, T], \ \sigma \in \partial\Omega.$$

Proof. Let $T_1 \in [0, T[$ and define the following operator :

$$\mathcal{T} : \begin{array}{ccc} \mathcal{C}([T_1, T] \times \partial\Omega) & \to & \mathcal{C}([T_1, T] \times \partial\Omega) \\ f & \mapsto & \int_t^T \widetilde{\beta}(s, z(t, \sigma)) \int_{\partial\Omega} N(\sigma)f(s, \sigma)d\sigma ds - \int_t^T \widetilde{a}(s, z)ds \end{array}$$

Then $\mathcal{T}$ is well defined in the claimed spaces and is a contraction if $(T - T_1)\|\beta\|_\infty \|N\|_{L^1} < 1$. A Banach fixed point theorem and a bootstrap argument prove existence and uniqueness of a solution $\overline{f}$ to (25). Moreover, let $0 < \varepsilon < T - T_1$ be fixed. On $[T_1, T - \varepsilon]$, $\overline{f} = \lim_{n \to \infty} \mathcal{T}^n f_0$, for any f_0 in $\mathcal{C}([T_1, T - \varepsilon] \times \partial\Omega)$. Direct computations, using the non-negativity of a, show that the set $\{f \in \mathcal{C}([T_1, T - \varepsilon] \times \partial\Omega); \ f(t, \sigma) \leq -\varepsilon, \ \forall t, \sigma\}$ is stable by $\mathcal{T}$ and since it is also closed, the unique fixed point belongs to it. The same argument can be applied on each interval used for the bootstrapp and thus we have proven that $\overline{f}(t, \sigma) < 0$. The announced regularity comes from formula (25). Indeed, we can compute

$$\partial_t f(t, \sigma) = \widetilde{a}(t, z(t, \sigma)) - \int_t^T \partial_z \widetilde{a}(s, z(t, \sigma))\partial_t z(t, \sigma)ds - \widetilde{\beta}(t, z(t, \sigma)) \int_{\partial\Omega} N(\sigma)f(t, \sigma)d\sigma$$

$$+ \int_t^T \partial_z \widetilde{\beta}(s, z(t, \sigma))\partial_t z(t, \sigma) \int_{\partial\Omega} N(\sigma)f(s, \sigma)d\sigma ds. \tag{26}$$

$\square$

The formula (24) gives the function $\widetilde{p}$ and we also see that we have $\widetilde{p}(T, \cdot) = 0$ and $\widetilde{p} \in \mathcal{C}^2([0, T] \times \Omega)$. Now, using the reverse change of variables $p(t, X) = \widetilde{p}(t, \Phi(T; t, X))$, we get the regularity on p since for each $t > 0$, $X \mapsto \Phi(T; t, X)$ is a diffeomorphism. We also deduce from formula (24) and the non-negativity of a that if $\beta > 0$ then, since $p(t, \sigma) < 0$ for all (t, σ) from lemma 8.7, we have $p(t, X) < 0$ for all $(t, X) \in Q$. $\square$

Case $j(u) = \int_\Omega \rho(T, X; u)dX$.

Here we consider the following functional

$$j(u) = \int_\Omega a(X)\rho(T, X; u)dX.$$

In a minimum u^* we still have

$$\int_\Omega a(X)z(T; \rho^*, u^*, v)\, dx\, d\theta \geq 0, \quad \forall v \in U_{ad}.$$

Let $p^* \in H^1(Q)$ solving

$$\begin{cases} -\partial_t p^*(t, X; u^*) - \overline{G}(X; u^*)\nabla p^*(t, X; u^*) + \beta(X)\int_{\partial\Omega} N(\sigma)p(t, \sigma)d\sigma = 0 \\ \qquad\qquad\qquad p^*(T) = -a(X). \end{cases} \tag{27}$$

The same calculations as above lead to

$$\begin{cases} \partial_t \rho^* + \mathrm{div}(\rho^* \overline{G}(u^*)) = F \\ -G \cdot \nu(t, \sigma; u^*)\rho^*(t, \sigma; u^*) = N(\sigma)\int_\Omega \beta(X)\rho^*(t, X; u^*)dX \\ \rho^*(0, X; u^*) = \rho^0 \\ -\partial_t p^*(t, X; u^*) - \overline{G}(X; u^*)\nabla p^*(t, X; u^*) + \beta(X)\int_{\partial\Omega} N(\sigma)p(t, \sigma)d\sigma = 0 \\ p^*(T) = -a \\ -(\int_\Omega \mathrm{div}(B(X))\rho^*)p^*\, dX, (v - u^*))_{L^2(0,T)^2} \geq 0, \quad \forall\, v \in \mathcal{U}_{ad}. \end{cases} \tag{28}$$

Remark 8.8. *The proposition 8.6 still holds in this case, its proof being adaptable to the new adjoint problem.*

3   Numerical simulations in a two-dimensional case

A natural question is to know if the optimal control problems 3 (with $a(X) = 1$) and 1 or 2 are really different, that is :

Is the best control for tumor reduction, the best one for metastases reduction?

The answer to this question seems to be no, as illustrated by numerical simulations in this section. Heuristically it makes sense since one can imagine a scenario having different effects on the growth of each tumor and on the total number of metastases at the end : if we let tumoral growth being important during a large time and give a large amount of drug at the end, the tumors can be largely reduced whereas the total number of metastases is still high since during the whole time where growth is important there is more metastases emission and the final decrease of tumors sizes doesn't impact a lot.

For example, in the Figure 6 of the chapter 7 where three AA drugs and protocols are compared, we observe that results differ on the primary tumor and on the metastases. For criterion J_T, the best drug is angiostatin whereas criterion J would recommend endostatin. Notice that this last one corresponds to the best drug regarding to the primary tumor criterion

J_m. On the Figure 21 concerning comparison of two schedulings for combination of AA and CT, although the difference of the total number of metastases is weak, J recommends to administrate the CT before the AA whereas J_T and J_m suggest the opposite. We also remark that on these two examples, the best control for J seems to correlate with the control presenting the smallest area under the curve of the primary tumor evolution curves, in agreement that the number of secondary tumors emitted by the primary one at time t is $m \int_0^t x_p(s)^\alpha ds$. However, depending on the influence of metastases emitted by metastases, it is not clear whether this will always be the case (see in particular Figure 6 below).

As suggested in Ledzewicz et al. [LMMS10], an easy-to-handle but nevertheless clinically interesting question is to look at optimality in a two-dimensional framework where the problem is to administrate total given amounts of agents (C_{max}, A_{max}) from time 0 to times (t_v, t_u) at constant rates $V = \frac{C_{max}}{t_v}$ and $U = \frac{A_{max}}{t_u}$. This means that the set of admissible controls is

$$\mathcal{U}_{ad} = \{u \in (L^\infty(0,T))^2; u^1(t) = V\mathbf{1}_{[0,t_v]}(t),\ u^2(t) = U\mathbf{1}_{[0,t_u]}(t),$$
$$(V,U) = \left(\frac{C_{max}}{t_v}, \frac{A_{max}}{t_u}\right) \le (v_{max}, u_{max})\}. \quad (29)$$

In this context, we will slightly abuse the notation and write $J(t_v, t_u)$, $J_T(t_v, t_u)$ and $J_m(t_v, t_u)$ for $J(v,u)$, $J_T(v,u)$ and $J_m(v,u)$ and, in the monotherapy cases, forget the dependence on the other drug. We consider J as being the total number of metastases and thus take $a(X) = 1$ in the expression (6). The metastatic mass $(a(x,\theta) = x$ for J in (6)) is also investigated and will be denoted by J_M. The problem is the following

Is the best anti-cancer efficacy achieved by the most brief but intense protocol or rather by the longer but weaker delivery of the drug? Is there a non-trivial optimum between these two situations?

We place ourselves in the context of Ledzewicz et al. [LMMS10] which was for an AA therapy alone (i.e. $v_{max} = 0$). Our aim here is to extend this approach by looking at the behavior on the metastases and also in the context of combination of CT and AA therapy. The values of the parameters that we use are the same as [LMMS10] for the tumoral growth

$$a = 0.0084, \quad \lambda = -0.02, \quad c = 5.85, \quad d = 0.00873$$

and for the effect of the treatments we take

$$B(X) = \begin{pmatrix} \gamma(x - x_0) & 0 \\ 0 & \phi(\theta - x_0) \end{pmatrix}, \quad \gamma = 0.15, \quad \phi = 0.1.$$

For the emission parameters we use most often $m = 10^{-3}$ and $\alpha = 2/3$. Concerning the initial conditions, except for the Figure 2 where we use values from [LMMS10], we take the ones corresponding to the simulation of the model after 40 days starting with an initial tumor of size $10^{-6}\,mm^3$ (= 1 cell) and vascular capacity 625 (value taken from [HPFH99]). This gives, for the primary tumor, $(x_{0,p}, \theta_{0,p}) = (1015, 6142)$ and some non-zero initial condition ρ^0. For the newly created metastases we take $(x_0, \theta_0) = (10^{-6}, 625)$. We run the simulations during a total time $T = 10$ days and take $A_{max} = 300$ (consistently with the order of the total doses administrated in [HPFH99]) as well as $C_{max} = 30$.

In all the presented Figures, the scale is only valid for one criterion (most of the time, J_m) and the other curves have been rescaled.

Anti-angiogenic therapy alone

We first investigate the case of AA monotherapy and so take $v_{max} = 0$. For comparison with the results of [LMMS10], we first investigate the case $(x_{0,p}, \theta_{0,p}) = (12000, 15000)$ and zero-initial condition for the metastatic density. We first look at the two extreme situations of giving the whole dose during a small time ($t_u = 4$) or rather during a large time ($t_u = 10$), on the tumoral evolution. The results are plotted in the Figure 1 and we observe that the two strategies have a complete different result concerning the tumor size at the end of the simulation. One of the
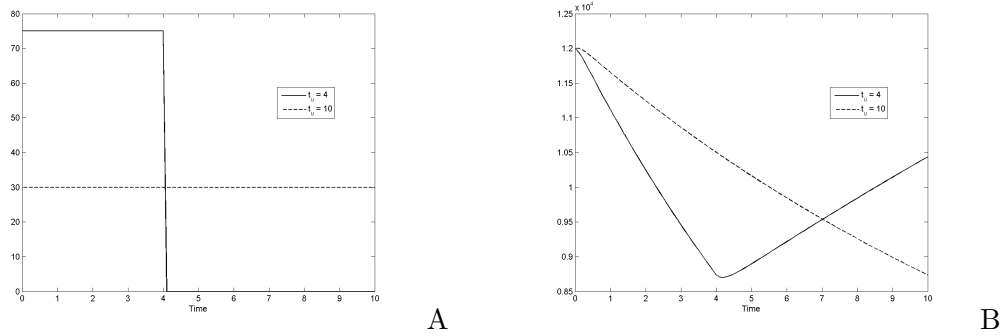

Figure 1: Two extreme examples of delivery of the AA drug on the tumor evolution. A. Drug profile. B. Tumor size

interesting results obtained in [LMMS10] is that the function $t_u \mapsto J_m(t_u)$ is convex on the interval $[4, 10]$, having thus a nontrivial minimum. This result is reproduced in the Figure 2 as well as the graphs of J_T, J and J. We observe that J is also a convex function but interestingly it does not have the same minimizer than J_m, indicating that the best therapeutic strategy is not the same for the primary tumor than for the number of metastases. A possible way of comnbining reduction of tumors burdens and number of metastases is to use the metastatic mass J_M as a criterion. This index as well as J_T suggests that the best strategy for AA drug is to deliver it at low doses during a long time, consistently with the results obtained in [dGR09, HBvdH$^+$05, KBP$^+$01, ESC$^+$02].

In the Figure 3 are plotted the same simulation results, but with initial conditions $(x_{0,p}, \theta_{0,p}) = (1015, 6142)$ and non-zero ρ^0, corresponding to a 40 days old tumor. The qualitative behavior of J_T and J_M are almost the same than in the previous case, but J_m is now an increasing function (with a plateau at the end, meaning that for the last values of t_u there was no tumoral reduction during the simulation time) and the optimal value minimizing J has deplaced to the right.

Cytotoxic therapy alone

We investigate now the problem in the case of a CT therapy alone (that is, $u_{max} = 0$ in (29)). We deliver a total dose C_{max} during a time t_v. We first illustrate the behavior for the two extreme situations on the tumor size, in the Figure 4. Regarding to the tumor size at the end of the simulation, delivering the CT drug during a large time at low dose is better. We notice that with the criteria of the minimal value reached during $[0, T]$, the other way is better. The

Figure 2: For $(x_{0,p}, \theta_{0,p}) = (12000, 15000)$. Two functionals on metastases : total number of metastases J, the metastatic mass J_M and two functionals on the primary tumor : tumor size at the end J_T and minimal tumor size J_m, in function of t_u (the scale is valid only for J_m).

question, again is : is there a monotonic behavior with respect to t_v? Is it the same behavior on the tumor size and on the metastases?

In the Figure 5 are plotted the total number of metastases $J(t_v)$, the primary tumor size at the end time $J_T(t_v)$, the minimal tumor size $J_m(t_v)$ and the metastatic mass $J_M(t_v)$.

We observe the following :

- The curve for J_m is increasing whereas J_T is almost monotonous but with opposite monotonicity.

- The curve for J has a nontrivial minimum.

- The curve of the metastatic mass is non-monotonous and concave.

Thus, it seems that to reduce the best the tumor it is better to give a low-dose but continuous infusion of the drug, the opposite (a bolus of the whole dose at the beginning) if the obejctive is minimizing the minimal tumor size and for the metastases a nontrivial minimum exists for t_v. Again, a way to synthetize tumoral and metastatic evolution in a unique criterion could be the metastatic mass J_M for which the low-dose/large time appears to be the best strategy.

With the value of m chosen here and such a small end time, almost all the metastases were emitted by the primary tumor, this amount being given by $\int_0^T \beta(x_p(t))dt = m \int_0^T x_p(t)^\alpha dt$. In Figure 6, we compare the metastatic criteria as well as this last integral for two different values of m. For these simulations, we did not consider any initial condition for the metastases and took
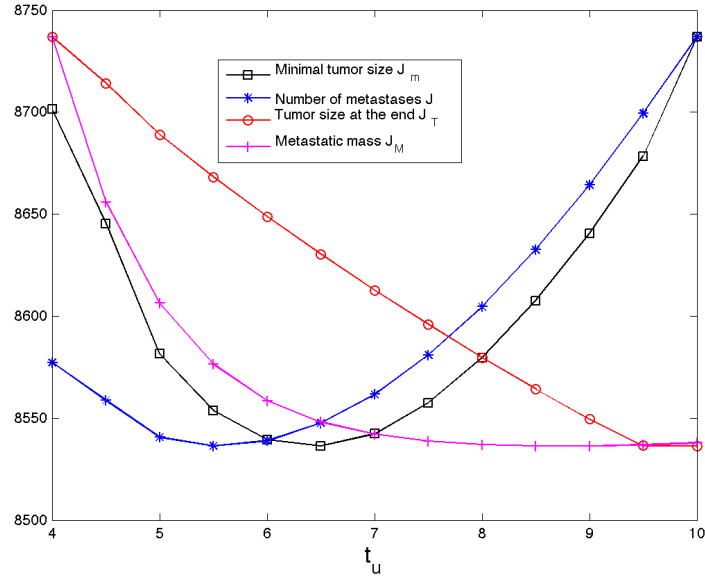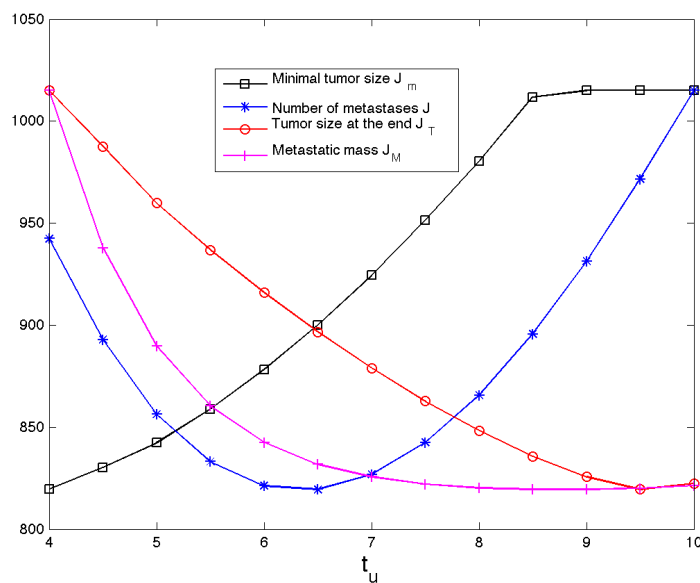
Figure 3: For $(x_{0,p}, \theta_{0,p}) = (1015, 6142)$. Two functionals on metastases : total number of metastases J, the metastatic mass J_M and two functionals on the primary tumor : tumor size at the end J_T and minimal tumor size J_m, in function of t_u (the scale is valid only for J_m).
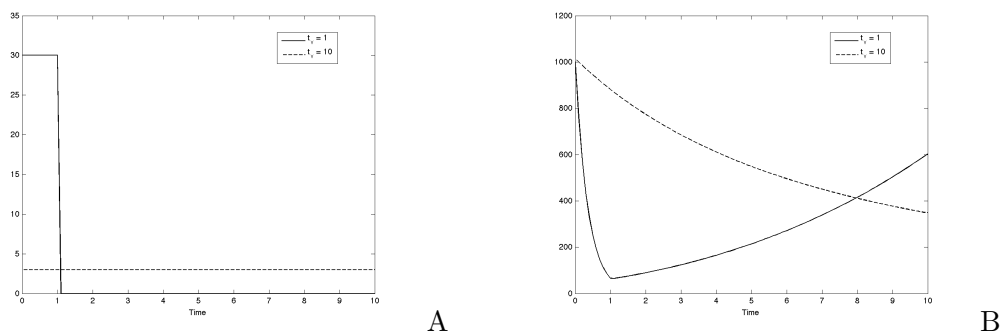
Figure 4: Two extreme examples of delivery of the CT drug on the tumor evolution. A. Drug profile. B. Tumor size

$\rho^0 = 0$. In Figure 6.A, we observe that the curves for J and $\int_0^T \beta(x_p(t))dt$ are almost identical and could conclude that the scheduling reducing the best the metastases is the one reducing the best $m \int_0^T x_p(t)^\alpha dt$. But for large values of m this is not so clear since the metastases curve has a different shape, as illustrated in the Figure 6.B (however, the two curves have the same minimizer).

We observe that changing the value of m, while changing the shape of the curve for J, did not affect much the one of the metastatic mass.
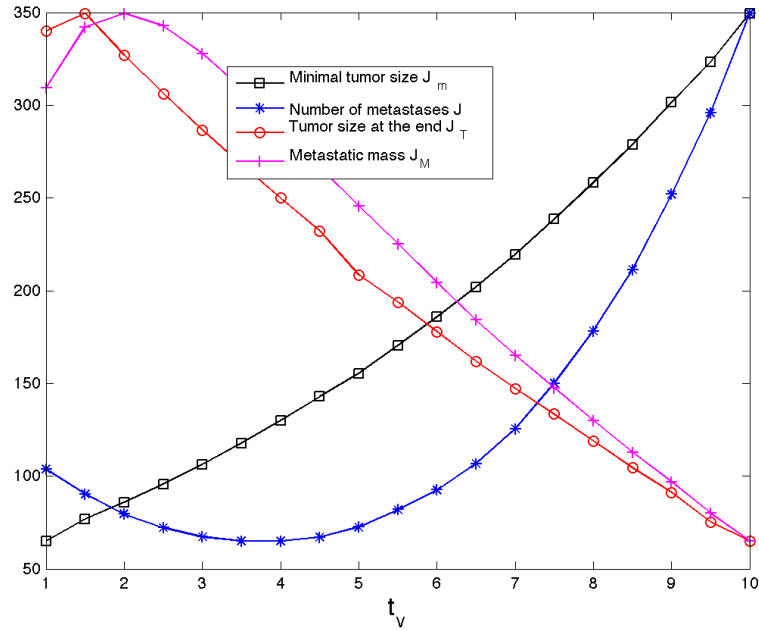
Figure 5: Cytotoxic drug alone. Total dose $C_{max} = 30$. Scale only valid for minimal tumor size.

$m = 0.001$ $m = 100$
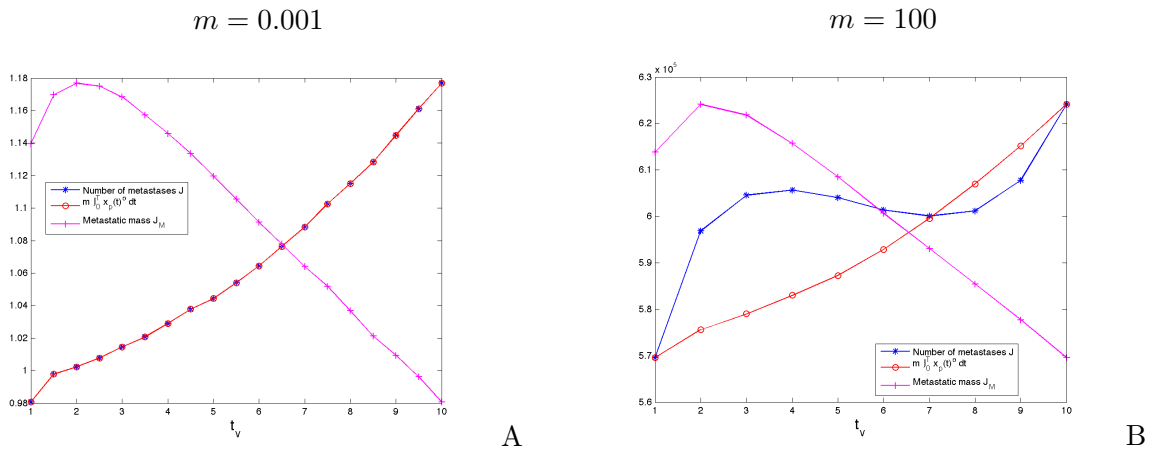
Figure 6: Variation of the parameter m. For theses simulations, we took $\rho^0 = 0$. For $m = 0.001$, the curves for J and $m \int_0^T x_p(t)^\alpha dt$ are identical.

CT-AA combination

We address now the problem in the case of combination of an AA and a CT drug. The optimization problem is two-dimensional and the corresponding surfaces are shown in the Figure 7.
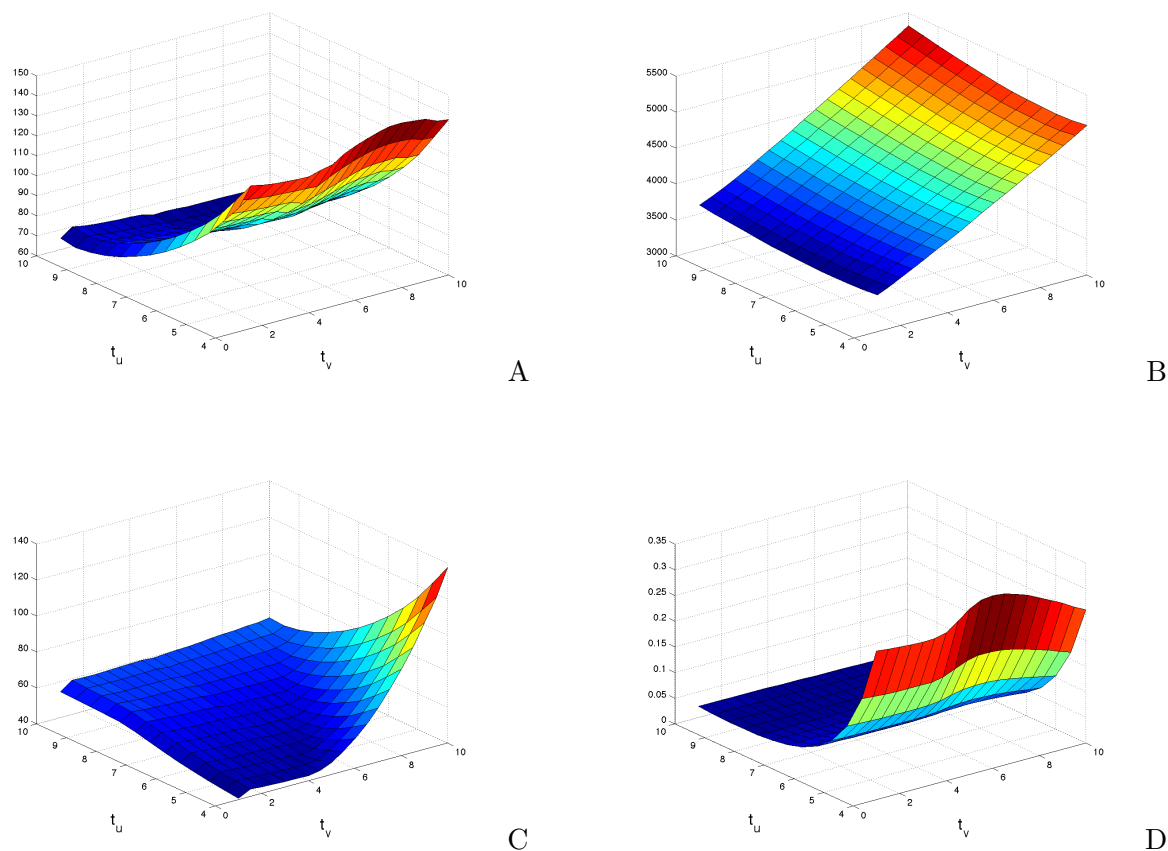
Figure 7: Combination of a CT and an AA drug. A. Primary tumor size at the end J_T. B. Number of metastases J . C. Minimal tumor size J_m. D. Metastatic mass J_M.

The optimal minimizer (t_v^*, t_u^*) as well as the optimal values for the various criteria are given in the table 1.

Criterion	End tumor size J_T	Minimal tumor size J_m	Nb of meta J	Metast. mass J_M
(t_v^*, t_u^*)	$(9.5, 9.5)$	$(1, 4)$	$(1, 5.5)$	$(10, 9)$
Optimal value	62.7	40.8	3478	0.015

Table 1: Minimizer (t_u^*, t_v^*) and optimal values for various criterions.

We observe two opposite behaviors for the tumoral criteria J_T and J_m and also opposite behaviors on the metastatic criteria J and J_M. Concerning the values of the optima, we notice that for each criterion, almost the same strategy is best for the AA and the CT. For example, in the case of J_m, the best would be to deliver shortly the whole dose at the beginning for both the AA and the CT drugs, consistently with what happens in the Figures 4 and 5. The two opposite strategies appear as optima and we can regroup criteria J_m and J under the strong

dose/short time strategy whereas J_T and J_M have the opposite low dose/large time strategy as optimum.

However, looking more precisely at what happens shows a large variability in the optimal solutions. The evolution of the minimizer on t_u for a fixed value of t_v and conversely are plotted in the Figure 8.
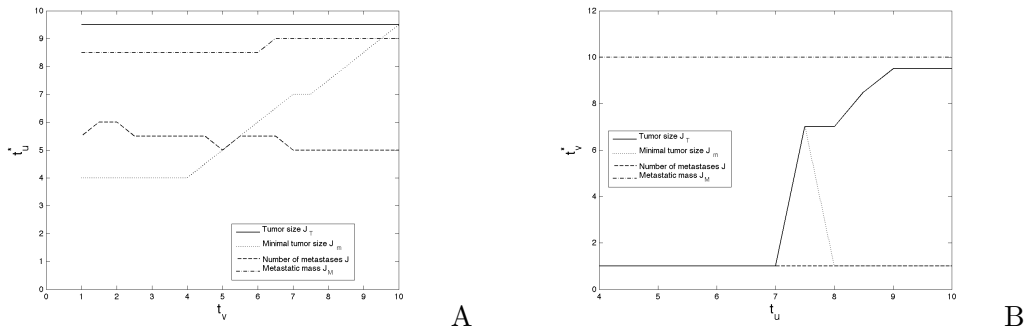
Figure 8: A. Graphs of the applications $t_v \mapsto \underset{t_u}{\mathrm{argmin}}\, J(t_u, t_v)$, $t_v \mapsto \underset{t_u}{\mathrm{argmin}}\, J_T(t_u, t_v)$, $t_v \mapsto \underset{t_u}{\mathrm{argmin}}\, J_m(t_u, t_v)$ and $t_v \mapsto \underset{t_u}{\mathrm{argmin}}\, J_M(t_u, t_v)$. B. Graphs of the applications $t_u \mapsto \underset{t_v}{\mathrm{argmin}}\, J(t_u, t_v)$, $t_u \mapsto \underset{t_v}{\mathrm{argmin}}\, J_T(t_u, t_v)$, $t_u \mapsto \underset{t_v}{\mathrm{argmin}}\, J_m(t_u, t_v)$ and $t_u \mapsto \underset{t_v}{\mathrm{argmin}}\, J_M(t_u, t_v)$.

In this Figure, we observe a relative small variability of the optima t_v^* and t_u^* when respectively t_u and t_v vary, for the criteria J_T, J and J_M whereas the criterion for the J_m the optimal value tends to increase. This interesting fact suggests that both drugs should be "synchronised" in the sense that they should be given in the same way. If the protocol is strong dose/short time for one drug, then so should be the protocol for the other drug and similarly in the opposite case.

The projection of the surfaces in Figure 7 on the planes $t_v = 1$ and $t_v = 10$ are plotted in the Figure 9.

In the Figures 9.A and B, we observe that the qualitative shape of the criteria J, J_T and J_M are almost identical in the two opposite cases for t_v and the same as Figure 3. Only the criterion J_m drastically changes, passing from an increasing function to a decreasing one (notice that the curves for J_T and J_m are identical in Figure 9.B, indicating that the minimal size on $[0T]$ is reached at the end time), in coherence with Figure 8.

Surprisingly, things are much more tumultuous concerning evolution of the dependance in t_v as illustrated in Figure 9.C and D. All the criteria are deeply affected by the adjunction of an AA drug, since the behaviors differ to the monotherapy situation of Figure 3. For example, the number of metastases J becomes an increasing function and does not present any interior minimum anymore. The monotinicity if J_T and J_M is also greatly affected. Variation of the administration protocol from $t_u = 4$ to $t_u = 10$ implies important changes in the shape of J_T and J_M.

$t_v = 1$

$t_v = 10$

A

B

$t_u = 4$

$t_u = 10$

C

D
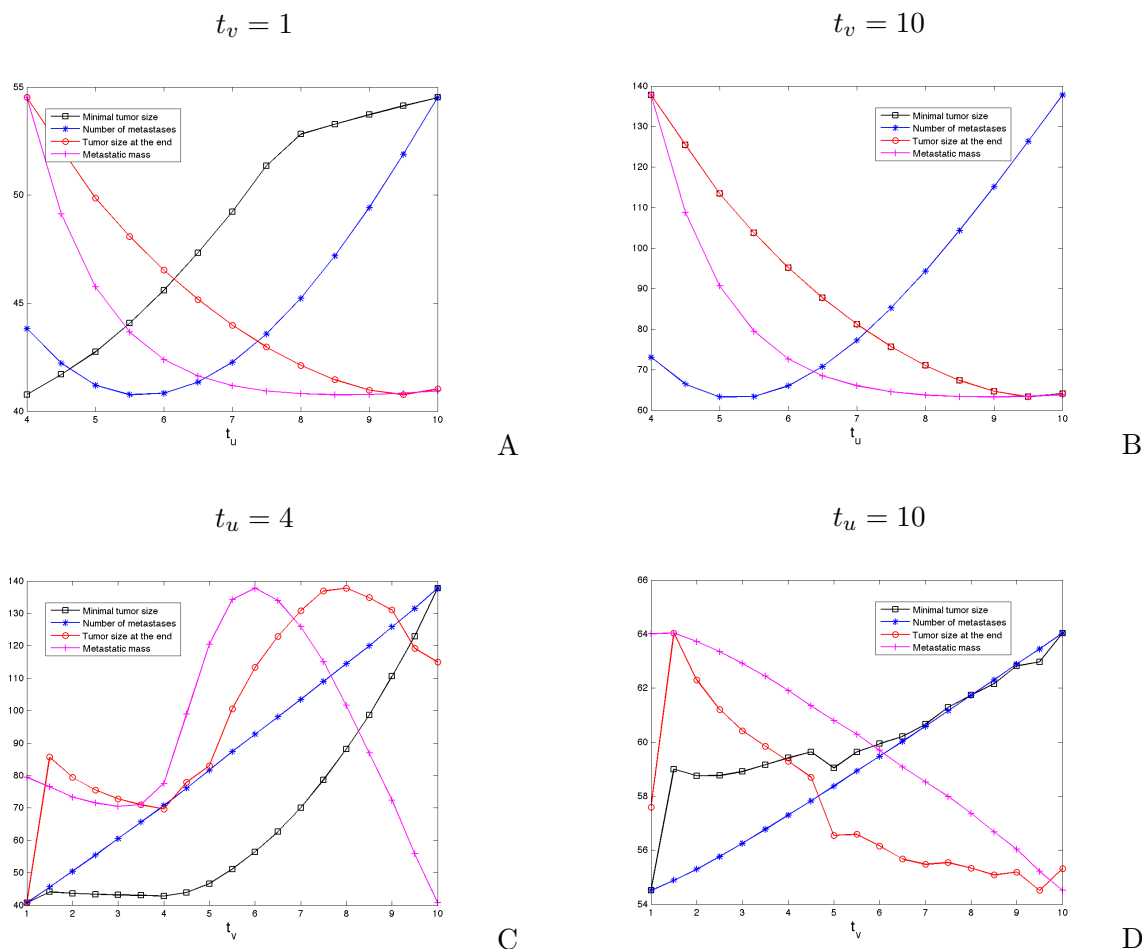
Figure 9: Projections of the surface in the Figure 7 on the extremal planes.

4   Conclusion - Future work

The problem of optimizing the scheduling of the drugs in an anti-cancer therapy is of fundamental importance in the clinic. While reduction of the primary tumor size is the first main target of therapy, the number and size of the metastases have to be taken into account. Using our phenomenological model for evolution of the metastases population, we have set an optimal control problem, proved existence of a solution to this problem and derived a first order optimality system for the optimal control. We then have numerically studied the problem in a subsequently simplified case which is two-dimensional, but still relevant.

We compared two criteria on the primary tumor size J_T and J_m and two criteria on the metastases J and J_M in the AA and CT monotherapy cases, as well as in combination. We obtained a great difference of the qualitative behavior of the criteria, passing through a wide range of possibilities : increasing function, decreasing one, non-monotonous convex function, non-monotonous concave function... In the monotherapy cases, the criterion J was never found

to correlate with J_T nor J_m, thus emphasizing the relevance of adding a metastatic component in the optimal control problem of the drugs scheduling. Since all the criteria have different (and sometimes even opposite) behaviors, the natural question that raises is : which one has to be chosen? Maybe some suitable weighting of the criteria can be done. Another way of integrating both tumoral size and number of metastases is to consider the metastatic mass J_M. For most of the cases, this criterion has the same minimizer than J_T : in the monotherapy cases, for both the AA and the CT drug, it suggests to deliver the drug at low level for a large time.

In the combined therapy case, the qualitative behavior of the criteria are all different again, but we can regroup J and J_m together, as well as J_T and J_M, regarding to the optimal value that they generate. The first ones advocate a strong and short delivery of the two drugs whereas the second ones suggest the opposite. In some cases, the minimizer value is different for J_T and J_M (see for example Figure 9.C).

Although the two-dimensional situation studied here is already rich and complex, we should now address the numerical resolution of the complete infinite-dimensional optimal control problem on the number of metastases. The problem (3) is not linear but rather bilinear in (u, ρ). Hence, resolution of the minimization problem is not standard. The first thing we could do is to implement a gradient method, since the derivative of $\rho(u)$ in some direction solves a partial differential that we can compute. A question that arises in this approach is : should we first take the gradient in the continuous formulation and then discretize or rather consider from the beginning the discretized version of equation (5) from the numerical scheme developed in chapter 5 and take the gradient in the scheme?

Without resolving the complete problem, we could also investigate situations slightly more elaborated than the one of section 8.3 but still simple to compute, for example by dividing the time interval in two and applying what we did on the whole interval to each sub interval.

On the modeling part, the optimal control problem that we defined is not completely clinically relevant since the metastatic problem typically arises on larger time scales, for example in determining the best way to avoid relapse after surgery. Since it is not numerically neither clinically tractable to compute/administrate a continuous control on a large time interval, we should impose some periodic structure which remains to be precise. If we still focus on optimizing metastatic emission and growth on the time scale of a therapy cycle (for example, 28 days), then we should integrate more complex modeling of hematotoxicities of the chemotherapy, as done in the MODEL I project [BFCI03, MIB⁺08].

Conclusion et perspectives

We elaborated and mathematically analyzed a model for metastatic evolution, able to take into account for the effect of chemotherapies and anti-angiogenic treatments. An adapted numerical scheme was also introduced. This allowed us to study *in silico* clinically open problems in cancer therapy. An optimal control problem was also formulated for which a first study was performed. Four axes of further research seem interesting to perform : validation of the model by comparison with experiments, biological understanding and quantification of metastatic emission from primary tumor informations, further optimal control and systemic modeling of a cancer disease.

Validation of the model A crucial step on the way to concrete application of the model is confrontation to data. Indeed, in this thesis we established well-posedness of the mathematical problem and illustrated the potential of the model but all of this is now conditioned to comparison with *in vivo* data. Both models from Iwata & al. and Hahnfeldt & al., the combination of which gave birth to our model, were compared to data and exhibited good agreement. In the ANR project MEMOREX-PK, we are currently performing mice experiments in order to assess the validity of our metastatic model. Confrontation of these to the upcoming data promise to be very interesting. On the mathematical part, this raises problems of identifiability of the parameters which consists in establishing (or prove false) uniqueness of the parameters resulting in a given observation.

Biological understanding and quantification of metastatic emission from primary tumor informations A necessary further step on the way to concrete clinical application of the model developed in this thesis consists in being able to estimate the metastatic parameters, especially metastatic aggressiveness m, *from data on the primary tumor*. Indeed, as tumors in patients are visible with imaging techniques only with large size ($\geq 10^7$ - 10^8 cells), it is not possible to wait for data on the metastatic colonies to identify the parameters of the model and decide a therapeutic strategy, since war against the patient's cancer would already be lost. Hence, within our model's framework, we are forced to find a way to estimate m and α from : images on the primary tumor coming from imaging devices and histological data.

Optimal control The study of an optimal control problem involving the metastatic state of the patient raised questions about the minimization criteria to use for optimizing the drug scheduling. We want to follow in this direction, by a further study of implications of the primer

order optimality system and development of a numerical method to solve the infinite-dimensional optimal control problem.

Systemic modeling of cancer   The model that we developed in this thesis considers the cancer at the scale of the organism. This systemic approach of the disease is able to integrate primary tumor/metastasis interactions and metastasis/metastasis interactions. Chemical agents such as chemotherapies and anti-angiogenic drugs act systemically, as the blood network conveys them in the whole organism. We believe that our model could could give insights about the clinical observation of metastatic acceleration after resection of the primary tumor. This work is in collaboration with Alberto Gandolfi from the Instituto di Analisi dei Sistemi ed Informatica "Antonio Ruberti" of the Consiglio Nazionale delle Ricerche in Rome and Alberto d'Onofrio from the European Institute of Oncology in Milan.

The idea is to integrate in the model a systemic angiogenesis inhibition. Indeed, vasculature inhibitors produced by the various tumors (both the primary and the metastases) are released in the central blood circulation and affect the neo-angiogenesis of all the metastatic population. One of the rational to assume so is the claimed slow elimination rate of these molecules in the paper of Hahnfeldt & al., together with references [Pre93, OHS$^+$94] (which have to be checked and whose validity has to be confirmed regarding to their age). In the equation that they derive for the concentration of the inhibitor outside the tumor, this concentration is proportional to the tumoral volume. We assume that the contribution of each tumor to the rate of production in some central compartment is proportional to its volume. Regarding to each tumor's behavior, the angiogenesis inhibition term is the sum of a local term and a "systemic" term which we denote by $s(t)$. The equations write

$$\begin{cases} \dot{x} = axF\left(\frac{\theta}{x}\right) \\ \dot{\theta} = bx - \left(\gamma s + dx^{2/3}\right)\theta \end{cases}$$

where F is the tumoral growth rate, together with

$$\dot{s} = c\left(x_p + \int_\Omega x\rho(t,X)dX\right) - \delta s$$

and the population of metastases has now a velocity $G(X,s)$

$$\begin{cases} \partial_t \rho + \mathrm{div}(G(X,s)\rho) = 0 \\ -G \cdot \nu\rho(\sigma,t) = N(\sigma)\left\{\int_\Omega \beta(X)\rho(t,X)dX + \beta(X_p(t))\right\} \\ \rho(X,0) = \rho^0(X) \end{cases}$$

In this model, surgery removing the primary tumor would thus remove an important source of angiogenic inhibitors which could lead to accelerated growth of metastases.

Mathematical analysis of this new model seems challenging since it presents an original nonlinear term which stands in the velocity coefficient of the transport equation. In particular, well-posedness of the problem should be established and analysis of the regularity of the solutions seems an interesting problem. Also, observing the resulting dynamics by numerical simulations is an interesting perspective. Interactions of this model with various therapies could lead to valuable clinical applications. In particular, the following problematics could be investigated :

When to perform surgery? How to efficiently combine surgery with anti-angiogenic and cytotoxic therapies in order to avoid accelerated growth of the secondary tumors?

Bibliographie

Bibliographie

[AC03]   M. Adimy and F. Crauste. Un modèle non-linéaire de prolifération cellulaire :
            extinction des cellules et invariance. *C. R. Math. Acad. Sci. Paris*, 336(7) :559–
            564, 2003.

[AF03]   Robert A. Adams and John J. F. Fournier. *Sobolev spaces*, volume 140 of *Pure and
            Applied Mathematics (Amsterdam)*. Elsevier/Academic Press, Amsterdam, second
            edition, 2003.

[ALM99]   Oscar Angulo and J. C. López-Marcos. Numerical schemes for size-structured po-
            pulation equations. *Math. Biosci.*, 157(1-2) :169–188, 1999. Deterministic models
            with applications in population dynamics and other fields of biology (Sofia, 1997).

[AM04]   R. P. Araujo and D. L. S. McElwain. A history of the study of solid tumour growth :
            the contribution of mathematical modelling. *Bull. Math. Biol.*, 66(5) :1039–1091,
            2004.

[AP02]   D. Ambrosi and L. Preziosi. On the closure of mass balance models for tumor
            growth. *Math. Models Method A Appl. Sci.*, 12 :737–754, 2002.

[ARC+08]   N. André, A. Rome, C. Coze, L. Padovani, E. Pasquier, L. Camoin, and J.-C.
            Gentet. Metronomic etoposide/cyclophosphamide/celecoxib regimen to children
            and adolescents with refractory cancer : a preliminary monocentric study. *Clin.
            Therapeutics*, 30(7) :1336–1340, 2008.

[BAB+11]   S. Benzekry, N. André, A. Benabdallah, S. Benzekry, J. Ciccolini, C. Faivre, F. Hu-
            bert, and D. Barbolosi. Modelling the impact of anticancer agents on metastatic
            spreading. *to appear in Mathematical Modeling of Natural Phenomena*, 2011.

[Bar70]   C. Bardos. Problèmes aux limites pour les équations aux dérivées partielles du pre-
            mier ordre à coefficients réels ; théorèmes d'approximation ; application à l'équation
            de transport. *Ann. Sci. École Norm. Sup. (4)*, 3 :185–233, 1970.

[BB11]   S. Benzekry and A. Benabdallah. An optimal control problem for anti-cancer
            therapies in a model for metastatic evolution. *in preparation.*, 2011.

[BBB+11]   D. Barbolosi, A. Benabdallah, S. Benzekry, J. Ciccolini, C. Faivre, F. Hubert,
            F. Verga, and B. You. A mathematical model for growing metastases on oncolo-
            gist's service. *submitted*, 2011.

[BBCRP08]   Fadia Bekkal Brikci, Jean Clairambault, Benjamin Ribba, and Benoît Perthame. An age-and-cyclin-structured cell population model for healthy and tumoral tissues. *J. Math. Biol.*, 57(1) :91–110, 2008.

[BBHV09]   D. Barbolosi, A. Benabdallah, F. Hubert, and F. Verga. Mathematical and numerical analysis for a model of growing metastatic tumors. *Math. Biosci.*, 218(1) :1–14, 2009.

[BBK+00]   T. Browder, C. E. Butterfield, B. M. Kraling, B. Shi, B. Marshall, M. S. O'Reilly, and J. Folkman. Antiangiogenic scheduling of chemotherapy improves efficacy against experimental drug-resistant cancer. *Cancer Res.*, 60 :1878–1886, Apr 2000.

[BCG+10]   Didier Bresch, Thierry Colin, Emmanuel Grenier, Benjamin Ribba, and Olivier Saut. Computational modeling of solid tumor growth : the avascular stage. *SIAM J. Sci. Comput.*, 32(4) :2321–2344, 2010.

[BDH+06]   S. Baruchel, M. Diezi, D. Hargrave, D. Stempak, J. Gammon, A. Moghrabi, MJ. Coppes, C.V. Fernandez, and E. Bouffet. Safety and pharmacokinetics of temozolomide using a dose-escalation, metronomic schedule in recurrent paediatric brain tumours. *Eur. J. Cancer*, 42 :2335–2342, 2006.

[Ben11a]   S. Benzekry. Mathematical analysis of a two-dimensional population model of metastatic growth including angiogenesis. *J. Evol. Equ.*, 11(1) :187–213, 2011.

[Ben11b]   S. Benzekry. Mathematical and numerical analysis of a model for anti-angiogenic therapy in metastatic cancers. *to appear in M2AN*, 2011.

[Ben11c]   S. Benzekry. Passing to the limit 2D-1D in a model for metastatic growth. *to appear in J. Biol. Dyn.*, 2011.

[BF06]   Franck Boyer and Pierre Fabrie. *Éléments d'analyse pour l'étude de quelques modèles d'écoulements de fluides visqueux incompressibles*, volume 52 of *Mathématiques & Applications (Berlin) [Mathematics & Applications]*. Springer-Verlag, Berlin, 2006.

[BFCI03]   D. Barbolosi, G. Freyer, J. Ciccolini, and A. Iliadis. Optimisation de la posologie et des modalités d'administration des agents cytotoxiques à l'aide d'un modèle mathématique. *Bulletin du Cancer*, 90(2) :167–175, 2003.

[BFGS08]   Alessandro Bertuzzi, Antonio Fasano, Alberto Gandolfi, and Carmela Sinisgalli. Tumour cords and their response to anticancer agents. In *Selected topics in cancer modeling*, Model. Simul. Sci. Eng. Technol., pages 183–206. Birkhäuser Boston, Boston, MA, 2008.

[BG00]   A. Bertuzzi and A. Gandolfi. Cell kinetics in a tumour cord. *J. Theor. Biol.*, 204 :587–599, Jun 2000.

[BI01]   D. Barbolosi and A. Iliadis. Optimizing drug regimens in cancer chemotherapy : a simulation study using a pk–pd model. *Comput. Biol. Med.*, 31 :157–172, 2001.

[Bil09]   F. Billy. *Modélisation mathématique multi-échelle de l'angiogenèse tumorale. Analyse de la réponse tumorale aux traitements anti-angiogéniques.* PhD thesis, Université Claude Bernard - Lyon 1, 2009.

[BK89]   H. T. Banks and F. Kappel. Transformation semigroups and L^1-approximation for size structured population models. *Semigroup Forum*, 38(2) :141–155, 1989. Semigroups and differential operators (Oberwolfach, 1988).

[Boy05]   Franck Boyer. Trace theorems and spatial continuity properties for the solutions of the transport equation. *Differential Integral Equations*, 18(8) :891–934, 2005.

[BP87]   R. Beals and V. Protopopescu. Abstract time-dependent transport equations. *J. Math. Anal. Appl.*, 121(2) :370–405, 1987.

[Bre83]   H. Brezis. *Analyse fonctionnelle.* Collection Mathématiques Appliquées pour la Maîtrise. [Collection of Applied Mathematics for the Master's Degree]. Masson, Paris, 1983. Théorie et applications. [Theory and applications].

[BRS+09]   F. Billy, B. Ribba, O. Saut, H. Morre-Trouilhet, T. Colin, D. Bresch, J-P. Boissel, E. Grenier, and J-P. Flandrois. A pharmacologically based multiscale mathematical model of angiogenesis and its use in investigating the efficacy of a new cancer treatment strategy. *J. Theor. Biol.*, 260(4) :545–62, 2009.

[BvLO+08] Helen M. Byrne, I. M. M. van Leeuwen, Markus R. Owen, Tomás Alarcón, and Philip K. Maini. Multiscale modelling of solid tumour growth. In *Selected topics in cancer modeling*, Model. Simul. Sci. Eng. Technol., pages 449–473. Birkhäuser Boston, Boston, MA, 2008.

[BVV+96]   R. Bruno, N. Vivier, J. C. Vergniol, S. L. De Phillips, G. Montay, and L. B. Sheiner. A population pharmacokinetic model for docetaxel (Taxotere) : model building and validation. *J Pharmacokinet Biopharm*, 24 :153–172, Apr 1996.

[CBB+11]   P. Correale, C. Botta, A. Basile, M. Pagliuchi, A. Licchetta, I. Martellucci, E. Bestoso, S. Apollinari, R. Addeo, G. Misso, O. Romano, A. Abbruzzese, M. Lamberti, L. Luzzi, G. Gotti, M. S. Rotundo, M. Caraglia, and P. Tagliaferri. Phase II trial of bevacizumab and dose/dense chemotherapy with cisplatin and metronomic daily oral etoposide in advanced non-small-cell-lung cancer patients. *Cancer Biol Ther*, 12, Jul 2011.

[Ces84]   M. Cessenat. Théorèmes de trace L^p pour des espaces de fonctions de la neutronique. *C. R. Acad. Sci. Paris Sér. I Math.*, 299(16) :831–834, 1984.

[Ces85]   M. Cessenat. Théorèmes de trace pour des espaces de fonctions de la neutronique. *C. R. Acad. Sci. Paris Sér. I Math.*, 300(3) :89–92, 1985.

[CFB+04]   M. Casanova, A. Ferrari, G. Bisogno, J. H. Merks, G. L. De Salvo, C. Meazza, K. Tettoni, M. Provenzi, I. Mazzarino, and M. Carli. Vinorelbine and low-dose cyclophosphamide in the treatment of pediatric sarcomas : pilot study for the upcoming European Rhabdomyosarcoma Protocol. *Cancer*, 101 :1664–1671, Oct 2004.

[CFF+10] M. Chefrour, J. L. Fischel, P. Formento, S. Giacometti, R. M. Ferri-Dessens, H. Marouani, M. Francoual, N. Renee, C. Mercier, G. Milano, and J. Ciccolini. Erlotinib in combination with capecitabine (5'dFUR) in resistant pancreatic cancer cell lines. *J Chemother*, 22 :129–133, Apr 2010.

[CNM11] E. Comen, L. Norton, and J. Massague. Clinical implications of cancer self-seeding. *Nat Rev Clin Oncol*, 8 :369–377, Jun 2011.

[CRK+08] L. M. Choi, B. Rood, N. Kamani, D. La Fond, R. J. Packer, M. R. Santi, and T. J. Macdonald. Feasibility of metronomic maintenance chemotherapy following high-dose chemotherapy for malignant central nervous system tumors. *Pediatr Blood Cancer*, 50 :970–975, May 2008.

[DBRR+00] T. A. Drixler, I. H. Borel Rinkes, E. D. Ritchie, T. J. van Vroonhoven, M. F. Gebbink, and E. E. Voest. Continuous administration of angiostatin inhibits accelerated growth of colorectal liver metastases after partial hepatectomy. *Cancer Res.*, 60 :1761–1765, Mar 2000.

[DD07] Françoise Demengel and Gilbert Demengel. *Espaces fonctionnels.* Savoirs Actuels (Les Ulis). [Current Scholarship (Les Ulis)]. EDP Sciences, Les Ulis, 2007. Utilisation dans la résolution des équations aux dérivées partielles. [Application to the solution of partial differential equations].

[Dem96] J-P. Demailly. *Numerical analysis and differential equations. (Analyse numérique et équations différentielles.) Nouvelle éd.* Grenoble : Presses Univ. de Grenoble. 309 p. , 1996.

[DFH00] RF. De Vore, Rs. Fehrenbacher, and RS. Herbst. A randomized phase ii trial comparing rhumab vegf (recombinant humanized monoclonal antibody to vascular endothelial cell growth factor) plus carboplatin/paclitaxel (cp) to cp alone in patients with stage iiib/iv nsclc. *Proc Am Soc Clin Oncol*, 19(485a), 2000.

[dG04] A. d'Onofrio and A. Gandolfi. Tumour eradication by antiangiogenic therapy : analysis and extensions of the model by Hahnfeldt et al. (1999). *Math. Biosci.*, 191(2) :159–184, 2004.

[dG10a] A. d'Onofrio and A. Gandolfi. Chemotherapy of vascularised tumours : role of vessel density and the effect of vascular "pruning". *J. Theor. Biol.*, 264 :253–265, May 2010.

[dG10b] A. d'Onofrio and A. Gandolfi. Resistance to antitumor chemotherapy due to bounded-noise-induced transitions. *Phys Rev E Stat Nonlin Soft Matter Phys*, 82 :061901, Dec 2010.

[DGL09] A. Devys, T. Goudon, and P. Laffitte. A model describing the growth and the size distribution of multiple metastatic tumors. *Discret. and contin. dyn. syst. series B*, 12(4) :731–767, 2009.

[dGR09] A. d'Onofrio, A. Gandolfi, and A. Rocca. The dynamics of tumour-vasculature interaction suggests low-dose, time-dense anti-angiogenic schedulings. *Cell Prolif.*, 42 :317–329, Jun 2009.

[DL89]   R. J. DiPerna and P.-L. Lions. Ordinary differential equations, transport theory and Sobolev spaces. *Invent. Math.*, 98(3) :511–547, 1989.

[dLMS09]   Alberto d'Onofrio, Urszula Ledzewicz, Helmut Maurer, and Heinz Schättler. On optimal delivery of combination therapy for tumors. *Math. Biosci.*, 222(1) :13–26, 2009.

[Dos53]   F.H. Dost. Der blütspiegel-kinetic der konzentrationsablaüfe in der frieslaufflüssigkeit. *G. Thieme, Leipzig*, page 244, 1953.

[Dou07]   M. Doumic. Analysis of a population model structured by the cells molecular content. *Math. Model. Nat. Phenom.*, 2(3) :121–152, 2007.

[Dro01a]   J. Droniou. Intégration et espaces de sobolev à valeurs vectorielles. 2001.

[Dro01b]   J. Droniou. Quelques résultats sur les espaces de sobolev. 2001.

[EAC+09]   H. Enderling, A. R. Anderson, M. A. Chaplain, A. Beheshti, L. Hlatky, and P. Hahnfeldt. Paradoxical dependencies of tumor dormancy and progression on basic cell kinetics. *Cancer Res.*, 69 :8814–8821, Nov 2009.

[ECW03]   A. Ergun, K. Camphausen, and L. M. Wein. Optimal scheduling of radiotherapy and angiogenic inhibitors. *Bull. Math. Biol.*, 65 :407–424, May 2003.

[ELCM+09] J. M.L. Ebos, C. R. Lee, W. Crus-Munoz, G. A. Bjarnason, and J. G. Christensen. Accelerated metastasis after short-term treatment with a potent inhibitor of tumor angiogenesis. *Cancer Cell*, 15 :232–239, 2009.

[EMSC05]   N. Echenim, D. Monniaux, M. Sorine, and F. Clément. Multi-scale modeling of the follicle selection process in the ovary. *Math. Biosci.*, 198(1) :57–79, 2005.

[EN00]   K-J Engel and R. Nagel. *One-parameter semigroups for linear evolution equations*, volume 194 of *Graduate Texts in Mathematics*. Springer-Verlag, New York, 2000. With contributions by S. Brendle, M. Campiti, T. Hahn, G. Metafune, G. Nickel, D. Pallara, C. Perazzoli, A. Rhandi, S. Romanelli and R. Schnaubelt.

[ESC+02]   J. P. Eder, J. G. Supko, J. W. Clark, T. A. Puchalski, R. Garcia-Carbonero, D. P. Ryan, L. N. Shulman, J. Proper, M. Kirvan, B. Rattner, S. Connors, M. T. Keogan, M. J. Janicek, W. E. Fogler, L. Schnipper, N. Kinchla, C. Sidor, E. Phillips, J. Folkman, and D. W. Kufe. Phase I clinical trial of recombinant human endostatin administered as a short intravenous infusion repeated daily. *J. Clin. Oncol.*, 20 :3772–3784, Sep 2002.

[FDM+10]   A. B. Francesconi, S. Dupre, M. Matos, D. Martin, B. G. Hughes, D. K. Wyld, and J. D. Lickliter. Carboplatin and etoposide combined with bevacizumab for the treatment of recurrent glioblastoma multiforme. *J Clin Neurosci*, 17 :970–974, Aug 2010.

[FGG11]   A. Fasano, M. Gabrielli, and A. Gandolfi. Investigating the steady state of multicellular spheroids by revisiting the two-fluid model. *Math. Biosci. Eng.*, 8 :239–252, 2011.

[Fol72]   J. Folkman. Antiangiogenesis : new concept for therapy of solid tumors. *Ann. Surg.*, 175 :409–416, 1972.

[Fri04]   Avner Friedman. A hierarchy of cancer models and their mathematical challenges. *Discrete Contin. Dyn. Syst. Ser. B*, 4(1) :147–159, 2004. Mathematical models in cancer (Nashville, TN, 2002).

[GCL$^+$07] G. Guzman, S. J. Cotler, A. Y. Lin, A. J. Maniotis, and R. Folberg. A pilot study of vasculogenic mimicry immunohistochemical expression in hepatocellular carcinoma. *Arch. Pathol. Lab. Med.*, 131 :1776–1781, Dec 2007.

[GG96]   R. A. Gatenby and E. T. Gawlinski. A reaction-diffusion model of cancer invasion. *Cancer Res.*, 56 :5745–5753, Dec 1996.

[GHM$^+$04] G. Giaccone, R. S. Herbst, C. Manegold, G. Scagliotti, R. Rosell, and V. et al. Miller. Gefitinib in combination with gemcitabine and cisplatin in advanced non-small-cell lung cancer : a phase iii trial–intact 1. *J. Clin. Oncol.*, 22(5) :777–784, 2004.

[GLFT05]   G. Gasparini, R. Longo, M. Fanelli, and B. A. Teicher. Combination of antiangiogenic therapy with other anticancer therapies : Results, challenges, and open questions. *Journal of Clinical Oncology*, 23(6) :1295–1311, 2005.

[GM03]   R. A. Gatenby and P. K. Maini. Mathematical oncology : cancer summed up. *Nature*, 421 :321, Jan 2003.

[GM06]   G. P. Gupta and J. Massagué. Cancer metastasis : Building a framework. *Cell*, 127 :679–695, 2006.

[Gom25]   B. Gompertz. On the nature of the function expressive of the law of human mortality and on a new mode of determining the nature of life contingencier. *Letter to Francis Baily*, pages 513–585, 1825.

[GR79]   V. Girault and P.-A. Raviart. *Finite element approximation of the Navier-Stokes equations*, volume 749 of *Lecture Notes in Mathematics*. Springer-Verlag, Berlin, 1979.

[Gre72]   H.P. Greenspan. Models for the growth of a solid tumor by diffusion. *Studies in Applied Mathematics*, 52 :317–340, 1972.

[GW89]   M. Gyllenberg and G. F. Webb. Quiescence as an explanation of gompertzian tumor growth. *Growth, Development and Aging*, 53 :25–33, 1989.

[HBvdH$^+$05] A. H. Hansma, H. J. Broxterman, I. van der Horst, Y. Yuana, E. Boven, G. Giaccone, H. M. Pinedo, and K. Hoekman. Recombinant human endostatin administered as a 28-day continuous intravenous infusion, followed by daily subcutaneous injections : a phase I and pharmacokinetic study in patients with advanced cancer. *Ann. Oncol.*, 16 :1695–1701, Oct 2005.

[HFH03]   P. Hahnfeldt, J. Folkman, and L. Hlatky. Minimizing long-term tumor burden : the logic for metronomic chemotherapeutic dosing and its antiangiogenic basis. *J. Theor. Biol.*, 220 :545–554, 2003.

[HFN⁺04]   H. Hurwitz, L. Fehrenbacher, W. Novotny, T. Cartwright, J. Hainsworth, W. Heim, J. Berlin, A. Baron, S. Griffing, E. Holmgren, N. Ferrara, G. Fyfe, B. Rogers, R. Ross, and F. Kabbinavar. Bevacizumab plus irinotecan, fluorouracil, and leucovorin for metastatic colorectal cancer. *N. Engl. J. Med.*, 350 :2335–2342, Jun 2004.

[HGM⁺09]   Peter Hinow, Philip Gerlee, Lisa J. McCawley, Vito Quaranta, Madalina Ciobanu, Shizhen Wang, Jason M. Graham, Bruce P. Ayati, Jonathan Claridge, Kristin R. Swanson, Mary Loveless, and Alexander R. A. Anderson. A spatial model of tumor-host interaction : application of chemotherapy. *Math. Biosci. Eng.*, 6(3) :521–546, 2009.

[HGS⁺05]   R. S. Herbst, G. Giaccone, J. H. Schiller, R. B. Natale, V. Miller, and Manegold et al. et al. Tribute : a phase iii trial of erlotinib hydrochloride (osi-774) combined with carboplatin and paclitaxel chemotherapy in advanced non-small-cell lung cancer. *J. Clin. Oncol.*, 23(25) :5892–5899, 2005.

[HKN⁺03]   M. Hatakeyama, S. Kimura, T. Naka, T. Kawasaki, N. Yumoto, M. Ichikawa, J. H. Kim, K. Saito, M. Saeki, M. Shirouzu, S. Yokoyama, and A. Konagaya. A computational model on the modulation of mitogen-activated protein kinase (MAPK) and Akt pathways in heregulin-induced ErbB signalling. *Biochem. J.*, 373 :451–463, Jul 2003.

[HPFH99]   P. Hahnfeldt, D. Panigraphy, J. Folkman, and L. Hlatky. Tumor development under angiogenic signaling : a dynamical theory of tumor growth, treatment, response and postvascular dormancy. *Cancer Research*, 59 :4770–4775, 1999.

[HPH⁺04]   R. S. Herbst, D. Prager, R. Hermann, L. Fehrenbacher, B.E. Johnson, and Sandler et al. et al. Gefitinib in combination with paclitaxel and carboplatin in advanced non-small-cell lung cancer : a phase iii trial–intact 2. *J. Clin. Oncol.*, 22(5) :785–794, 2004.

[HW00]   Douglas Hanahan and Robert A. Weinberg. The hallmarks of cancer. *Cell*, 100(1) :57–70, 2000.

[Ian95]   M. Ianelli. *Mathematical theory of age-structured population dynamics*. Applied Mathematical Monographs, C.N.R.I. Giardini Editori e Stampatori, Pisa, Pisa, 1995.

[IB94]   A. Iliadis and D. Barbolosi. Dosage regimen calculations with optimal control theory. *Int. J. Biomed. Comput.*, 36 :87–93, Jun 1994.

[IB00]   A. Iliadis and D. Barbolosi. Optimizing drug regimens in cancer chemotherapy by an efficacy-toxicity mathematical model. *Comput. Biomed. Res.*, 33 :211–226, Jun 2000.

[IKN00]   K. Iwata, K. Kawasaki, and Shigesada N. A dynamical model for the growth and size distribution of multiple metastatic tumors. *J. Theor. Biol.*, 203 :177–186, 2000.

[Jai01]   R. K. Jain. Normalizing tumor vasculature with anti-angiogenic therapy : A new paradigm for combination therapy. *Nature Medicine*, 7 :987–989, 2001.

[JDCL05]   R. K. Jain, D.G. Duda, J. W. Clark, and J. S. Loeffler. Lessons from phase iii clinical trials on anti-vegf therapy for cancer. *Nature Clin. Practice Oncology*, 3(1) :24–40, 2005.

[JWV+10]   K. Jordan, H. H. Wolf, W. Voigt, T. Kegel, L. P. Mueller, T. Behlendorf, C. Sippel, D. Arnold, and H. J. Schmoll. Bevacizumab in combination with sequential high-dose chemotherapy in solid cancer, a feasibility study. *Bone Marrow Transplant.*, 45 :1704–1709, Dec 2010.

[KBP+01]   O. Kisker, C. M. Becker, D. Prox, M. Fannon, R. D'Amato, E. Flynn, W. E. Fogler, B. K. Sim, E. N. Allred, S. R. Pirie-Shepherd, and J. Folkman. Continuous administration of endostatin by intraperitoneally implanted osmotic pump improves the efficacy and potency of therapy in a mouse xenograft tumor model. *Cancer Res.*, 61 :7669–7674, Oct 2001.

[Kho00]   B. N. Kholodenko. Negative feedback and ultrasensitivity can bring about oscillations in the mitogen-activated protein kinase cascades. *Eur. J. Biochem.*, 267 :1583–1588, Mar 2000.

[KK04]   R.S. Kerbel and B.A. Kamen. The anti-angiogenic basis of metronomic chemotherapy. *Nature Reviews Cancer*, 4 :423–436, 2004.

[KSKK98]   L. A. Kunz-Schughart, M. Kreutz, and R. Knuechel. Multicellular spheroids : a three-dimensional in vitro culture system to study tumour biology. *Int J Exp Pathol*, 79 :1–23, Feb 1998.

[KTR+05]   M. W. Kieran, C. D. Turner, J. B. Rubin, S.N. Chi, M.A. Zimmerman, C. Chordas, G. Klement, A. Laforme, A. Gordon, A. Thomas, D. Neuber, T. Browder, and J. Folkman. A feasibility trial of antiangiogenic (metronomic) chemotherapy in pediatric patients with recurrent or progressive cancer. *J. Pediatr. Hematol. Oncol.*, 27(11) :573–581, 2005.

[Lai64]   A. K. Laird. Dynamics of tumor growth. *Br. J. Cancer*, 13 :490–502, 1964.

[LAL+07]   A. Y. Lin, Z. Ai, S. C. Lee, P. Bajcsy, J. Pe'er, L. Leach, A. J. Maniotis, and R. Folberg. Comparing vasculogenic mimicry with endothelial cell-lined vessels : techniques for 3D reconstruction and quantitative analysis of tissue components from archival paraffin blocks. *Appl. Immunohistochem. Mol. Morphol.*, 15 :113–119, Mar 2007.

[LBE+08]   J. F. Lu, R. Bruno, S. Eppler, W. Novotny, B. Lum, and J. Gaudreault. Clinical pharmacokinetics of bevacizumab in patients with solid tumors. *Cancer Chemother. Pharmacol.*, 62 :779–786, Oct 2008.

[LFJ+10]   J. S. Lowengrub, H. B. Frieboes, F. Jin, Y.-L. Chuang, X Li, P. Macklin, S. M. Wise, and V. Cristini. Nonlinear modelling of cancer : bridging the gap between cells and tumours. *Nonlinearity*, 23(1) :R1–R91, 2010.

[LKS74]   L. A. Liotta, J. Kleinerman, and G. M. Saidel. Quantitative relationships of intravascular tumor cells, tumor vessels, and pulmonary metastases following tumor implantation. *Cancer Res.*, 34 :997–1004, May 1974.

[LLS09]   Urszula Ledzewicz, Yi Liu, and Heinz Schättler. The effect of pharmacokinetics on optimal protocols for a mathematical model of tumor anti-angiogenic therapy. In *Proceedings of the 2009 conference on American Control Conference*, ACC'09, pages 1060–1065, Piscataway, NJ, USA, 2009. IEEE Press.

[LMMS10]   Urszula Ledzewicz, John Marriott, Helmut Maurer, and Heinz Schättler. Realizable protocols for optimal administration of drugs in mathematical models for anti-angiogenic treatment. *Math. Med. Biol.*, 27(2) :157–179, 2010.

[LMS09]   Urszula Ledzewicz, James Munden, and Heinz Schättler. Scheduling of angiogenic inhibitors for Gompertzian and logistic tumor growth models. *Discrete Contin. Dyn. Syst. Ser. B*, 12(2) :415–438, 2009.

[LS05]   Urszula Ledzewicz and Heinz Schättler. The influence of pk/pd on the structure of optimal controls in cancer chemotherapy models. *Math. Biosci. Eng.*, 2(3) :561–578, 2005.

[LS06]   Urszula Ledzewicz and Heinz Schättler. Drug resistance in cancer chemotherapy as an optimal control problem. *Discrete Contin. Dyn. Syst. Ser. B*, 6(1) :129–150, 2006.

[LS07]   Urszula Ledzewicz and Heinz Schättler. Antiangiogenic therapy in cancer treatment as an optimal control problem. *SIAM J. Control Optim.*, 46(3) :1052–1079, 2007.

[LSK76]   L. A. Liotta, G. M. Saidel, and J. Kleinerman. Stochastic model of metastases formation. *Biometrics*, 32 :535–550, Sep 1976.

[MCH+05]   K. D. Miller, L. I. Chap, F. A. Holmes, M. A. Cobleigh, P. K. Marcom, L. Fehrenbacher, M. Dickler, B. A. Overmoyer, J. D. Reimann, A. P. Sing, V. Langmuir, and H. S. Rugo. Randomized phase III trial of capecitabine compared with bevacizumab plus capecitabine in patients with previously treated metastatic breast cancer. *J. Clin. Oncol.*, 23 :792–799, Feb 2005.

[McK26]   A.G. McKendrick. Applications of mathematics to medical problems. *Proc. Edin. Math. Soc.*, 44 :98–130, 1926.

[MD86]   J. A. J. Metz and O. Diekmann, editors. *The dynamics of physiologically structured populations*, volume 68 of *Lecture Notes in Biomathematics*. Springer-Verlag, Berlin, 1986. Papers from the colloquium held in Amsterdam, 1983.

[MIB⁺08]   C. Meille, A. Iliadis, D. Barbolosi, N. Frances, and G. Freyer. An interface model for dosage adjustment connects hematotoxicity to pharmacokinetics. *J Pharmacokinet Pharmacodyn*, 35 :619–633, Dec 2008.

[MM13]   L. Michaelis and M.L. Menten. Die kinetik der invertinwirking. *Biochem. Z.*, 49 :333–369, 1913.

[MMP05]   P. Michel, S. Mischler, and B. Perthame. General relative entropy inequality : an illustration on growth models. *J. Math. Pures Appl. (9)*, 84(9) :1235–1260, 2005.

[MWO04]   Nikos V. Mantzaris, Steve Webb, and Hans G. Othmer. Mathematical modeling of tumor-induced angiogenesis. *J. Math. Biol.*, 49(2) :111–187, 2004.

[OAMB09]   Markus R. Owen, Tomás Alarcón, Philip K. Maini, and Helen M. Byrne. Angiogenesis and vascular remodelling in normal and cancerous tissues. *J. Math. Biol.*, 58(4-5) :689–721, 2009.

[OB08]   J.A. O'Shaughnessy and A. Brufsky. Ribbon 1 and ribbon 2 : Phase iii trials of bevacizumab with standard chemotherapy for metastatic breast cancer. *Clin. Breast Cancer*, 8(4) :370–373, 2008.

[OHS⁺94]   M. S. O'Reilly, L. Holmgren, Y. Shing, C. Chen, R. A. Rosenthal, M. Moses, W. S. Lane, Y. Cao, E. H. Sage, and J. Folkman. Angiostatin : a novel angiogenesis inhibitor that mediates the suppression of metastases by a Lewis lung carcinoma. *Cell*, 79 :315–328, Oct 1994.

[Per01]   L. Perko. *Differential equations and dynamical systems*, volume 7 of *Texts in Applied Mathematics*. Springer-Verlag, New York, third edition, 2001.

[Per07]   B. Perthame. *Transport equations in biology*. Frontiers in Mathematics. Birkhäuser Verlag, Basel, 2007.

[PKG⁺03]   J. C. Panetta, M. N. Kirstein, A. Gajjar, G. Nair, M. Fouladi, R. L. Heideman, M. Wilkinson, and C. F. Stewart. Population pharmacokinetics of temozolomide and metabolites in infants and children with primary central nervous system tumors. *Cancer Chemother. Pharmacol.*, 52 :435–441, Dec 2003.

[PRAH⁺09]   M. Paez-Ribes, E. Allen, J. Hudock, T. Takeda, H. Okuyama, F. Vinals, M. Inoue, G. Bergers, D. Hanahan, and O. Casanovas. Antiangiogenic therapy elicits malignant progression of tumors to increased local invasion and distant metastasis. *Cancer Cell*, 15 :220–231, 2009.

[Pre93]   R. T. Prehn. Two competing influences that may explain concomitant tumor resistance. *Cancer Res.*, 53 :3266–3269, Jul 1993.

[PT08]   B. Perthame and S. K. Tumuluri. Nonlinear renewal equations. In *Selected topics in cancer modeling*, Model. Simul. Sci. Eng. Technol., pages 65–96. Birkhäuser Boston, Boston, MA, 2008.

[QGML10]   B. Qu, L. Guo, J. Ma, and Y. Lv. Antiangiogenesis therapy might have the unintended effect of promoting tumor metastasis by increasing an alternative circulatory system. *Med. Hypotheses*, 74 :360–361, Feb 2010.

[RCS10]   B. Ribba, T. Colin, and S. Schnell. A multiscale mathematical model of cancer, and its use in analyzing irradiation therapies. theoretical biology and medical modelling. *Theoretical Biology and Medical Modelling*, 3(7), 2010.

[RDG+11]   N. J. Robert, V. Dieras, J. Glaspy, A. M. Brufsky, I. Bondarenko, O. N. Lipatov, E. A. Perez, D. A. Yardley, S. Y. Chan, X. Zhou, S. C. Phan, and J. O'Shaughnessy. RIBBON-1 : Randomized, Double-Blind, Placebo-Controlled, Phase III Trial of Chemotherapy With or Without Bevacizumab for First-Line Treatment of Human Epidermal Growth Factor Receptor 2-Negative, Locally Recurrent or Metastatic Breast Cancer. *J Clin Oncol*, Mar 2011.

[RDP+11]   D. A. Reardon, A. Desjardins, K. Peters, S. Gururangan, J. Sampson, J. N. Rich, R. McLendon, J. E. Herndon, J. Marcello, S. Threatt, A. H. Friedman, J. J. Vredenburgh, and H. S. Friedman. Phase II study of metronomic chemotherapy with bevacizumab for recurrent glioblastoma after progression on bevacizumab therapy. *J. Neurooncol.*, 103 :371–379, Jun 2011.

[Rey10]   A. R. Reynolds. Potential relevance of bell-shaped and u-shaped dose-responses for the therapeutic targeting of angiogenesis in cancer. *Dose-Response*, 8 :253–284, 2010.

[RRK+09]   G. J. Riely, N. A. Rizvi, M. G. Kris, D. T. Milton, D. B. Solit, N. Rosen, E. Senturk, C. G. Azzoli, J. R. Brahmer, F. M. Sirotnak, V. E. Seshan, M. Fogle, M. Ginsberg, Miller V. A., and C. M. Rudin. Randomized phase ii study of pulse erlotinib before or after carboplatin and paclitaxel in current or former smokers with advanced non-small-cell lung cancer. *J. Clin. Oncol.*, 27(2) :264–270, 2009.

[RSC+06]   B. Ribba, O. Saut, T. Colin, D. Bresch, E. Grenier, and J. P. Boissel. A multiscale mathematical model of avascular tumor growth to investigate the therapeutic benefit of anti-invasive agents. *J. Theor. Biol.*, 243(4) :532–541, 2006.

[SGH+06]   D. Stempak, J. Gammon, J. Halton, A. Moghrabi, G. Koren, and S. Baruchel. A pilot pharmacokinetic and antiangiogenic biomarker study of celecoxib and low-dose metronomic vinblastine or cyclophosphamide in pediatric recurrent solid tumors. *J. Pediatr. Hematol. Oncol.*, 28 :720–728, Nov 2006.

[Ske86]   P. Skehan. On the normality of growth dynamics of neoplasms *in vivo* : a data base analysis. *Growth*, 50 :496–515, 1986.

[SL11]   F.R. Sharpe and F.R. Lotka. A problem in age distribution. *Phil. Mag.*, 21 :435–438, 1911.

[SLK76]   G. M. Saidel, L. A. Liotta, and J. Kleinerman. System dynamics of metastatic process from an implanted tumor. *J. Theor. Biol.*, 56 :417–434, Feb 1976.

[SMC$^+$04]   M. Simeoni, P. Magni, C. Cammia, G. De Nicolao, V. Croci, E. Pesenti, M. Germani, I. Poggesi, and M. Rocchetti. Predictive pharmacokinetic-pharmacodynamic modeling of tumor growth kinetics in xenograft models after administration of anticancer agents. *Cancer Res.*, 64 :1094–1101, Feb 2004.

[SMS96]   J. S. Spratt, J. S. Meyer, and J. A. Spratt. Rates of growth of human neoplasms : part ii. *J. Surg. Oncol.*, 61 :143–150, 1996.

[SNV$^+$10]   G. Scagliotti, S. Novello, P.J. Von, M. Reck, J.R. Pereira, and M. et al. Thomas. Phase iii study of carboplatin and paclitaxel alone or with sorafenib in advanced non-small-cell lung cancer. *J. Clin. Oncol.*, 28(11) :1835–1842, 2010.

[STW$^+$11]   D. R. Spigel, P. M. Townley, D. M. Waterhouse, L. Fang, I. Adiguzel, J. E. Huang, D. A. Karlin, L. Faoro, F. A. Scappaticci, and M. A. Socinski. Randomized Phase II Study of Bevacizumab in Combination With Chemotherapy in Previously Untreated Extensive-Stage Small-Cell Lung Cancer : Results From the SALUTE Trial. *J. Clin. Oncol.*, 29 :2215–2222, Jun 2011.

[SV69]   J. Serrin and D. E. Varberg. A general chain rule for derivatives and the change of variables formula for the Lebesgue integral. *Amer. Math. Monthly*, 76 :514–520, 1969.

[SVM$^+$06]   J. Sterba, D. Valik, P. Mudry, T. Kepak, Z. Pavelka, V. Bajciova, K. Zitterbart, V. Kadlecova, and P. Mazanek. Combined biodifferentiating and antiangiogenic oral metronomic therapy is feasible and effective in relapsed solid tumors in children : single-center pilot study. *Onkologie*, 29 :308–313, Jul 2006.

[Swa88]   G. W. Swan. General applications of optimal control theory in cancer chemotherapy. *IMA J. Math. Appl. Med. Biol.*, 5(4) :303–316, 1988.

[Swa90]   G. W. Swan. Applications of optimal control theory in biomedicine. *Math. Biosc.*, 101 :237–284, 1990.

[Tar07]   L. Tartar. *An introduction to Sobolev spaces and interpolation spaces*, volume 3 of *Lecture Notes of the Unione Matematica Italiana*. Springer, Berlin, 2007.

[TZ88]   S. L. Tucker and S. O. Zimmerman. A nonlinear model of population dynamics containing an arbitrary number of continuous structure variables. *SIAM J. Appl. Math.*, 48(3) :549–591, 1988.

[Ver45]   P. F. Verhulst. Recherches mathématiques sur la loi d'accroissement de la population. *Nouveaux mémoires de l'Académie royale de Bruxelles*, 18 :1–42, 1845.

[Ver10]   F. Verga. *Modélisation mathématique de processus métastatiques*. PhD thesis, Université de Provence, 2010.

[Wag81]   J. G. Wagner. History of pharmacokinetics. *Pharmac. Theor.*, 12 :537–562, 1981.

[Web85]   G. F. Webb. *Theory of nonlinear age-dependent population dynamics*, volume 89 of *Monographs and Textbooks in Pure and Applied Mathematics*. Marcel Dekker Inc., New York, 1985.

[Wei07]   R. Weinberg. *The Biology of Cancer*. New York : Garland Science, 2007.

[WT24]   E. Widmark and J. Tandberg. Über die bedingungen für die akkumulation indifferenter narkoliken theoretische bereckerunger. *Biochem Z.*, 3 :358–369, 1924.

Résumé

Nous introduisons un modèle mathématique d'évolution d'une maladie cancéreuse à l'échelle de l'organisme, prenant en compte les métastases ainsi que leur taille et permettant de simuler l'action de plusieurs thérapies telles que la chirurgie, la chimiothérapie ou les traitements anti-angiogéniques.

Le problème mathématique est une équation de renouvellement structurée en dimension deux. Son analyse mathématique ainsi que l'analyse fonctionnelle d'un espace de Sobolev sous-jacent sont effectuées. Existence, unicité, régularité et comportement asymptotique des solutions sont établis dans le cas autonome. Un schéma numérique lagrangien est introduit et analysé, permettant de prouver l'existence de solutions dans le cas non-autonome. L'effet de la concentration de la donnée au bord en une masse de Dirac est aussi envisagé.

Le potentiel du modèle est ensuite illustré pour des problématiques cliniques telles que l'échec des anti-angiogéniques, les protocoles temporels d'administration pour la combinaison d'une chimiothérapie et d'un anti-angiogénique et les chimiothérapies métronomiques. Pour tenter d'apporter des réponses mathématiques à ces problèmes cliniques, un problème de contrôle optimal est formulé, analysé et simulé.

Mots-clés : Métastases, Modélisation du cancer, Anti-angiogéniques, Dynamique de populations structurées, Contrôle optimal.

Abstract

We introduce a mathematical model for the evolution of a cancer disease at the organism scale, taking into account for the metastases and their sizes as well as action of several therapies such as primary tumor surgery, chemotherapy and anti-angiogenic therapy.

The mathematical problem is a renewal equation with bi-dimensional structuring variable. Mathematical analysis and functional analysis of an underlying Sobolev space are performed. Existence, uniqueness, regularity and asymptotic behavior of the solutions are proven in the autonomous case. A lagrangian numerical scheme is introduced and analyzed. Convergence of this scheme proves existence in the non-autonomous case. The effect of concentration of the boundary data into a Dirac mass is also investigated.

Possible applications of the model are numerically illustrated for clinical issues such as the failure of anti-angiogenic monotherapies, scheduling of combined cytotoxic and anti-angiogenic therapies and metronomic chemotherapies. In order to give mathematical answers to these clinical problems an optimal control problem is formulated, analyzed and simulated.

Keywords: Metastases, Cancer modeling, Anti-angiogenic therapy, Structured population dynamics, Optimal control.